Contents

Preface

> A doctrine of nature can only contain so much science proper as there is in it of applied mathematics.
>
> *Immanuel Kant*

In 1945 Pablo Picasso created a celebrated ensemble of 11 lithographs known as *Bull*, which rapidly became a milestone in the manner in which the abstract arts synthesize the observable world by reducing its complexity, such that the structure of the subjects may emerge. In the artwork in Figure 1, each plate is a successive stage used to find the spirit of the beast. In other words, Picasso visually dissects step by step the initial representation of a full bull to demonstrate the way in which its essential presence is given only by reproduction and fighting.

This suite of drawings clearly exemplifies how mathematics move from observable phenomena to their artificial synthesis. The strength of mathematical modeling relies, in fact, on a reduction of physical reality, which contains all the ingredients for making the model realistic, even though it is not real. Hence, the importance of a sound mathematical model goes hand in hand with the necessity to reproduce and predict the behavior of the phenomena under investigation.

Among others, the development of mathematical tools for the description of emerging collective phenomena in interacting systems may be viewed as the scientific counterpart of the dictates of abstract art. In fact, in the modeling of many complex systems composed of a large number of agents, a rather common assumption lies in considering the entire population to be formed by indistinguishable particles. These are endowed with a finite set of characteristic variables determining their coordinates, which do not need to be defined in the geometrical space, but may be a location in the velocity space as well as in the social structure of the population. Hence, it is of paramount importance to identify the fundamental factors that generate an observable experiment, quantifying their impact.

The intriguing world of these self–organizing systems has gained increasing

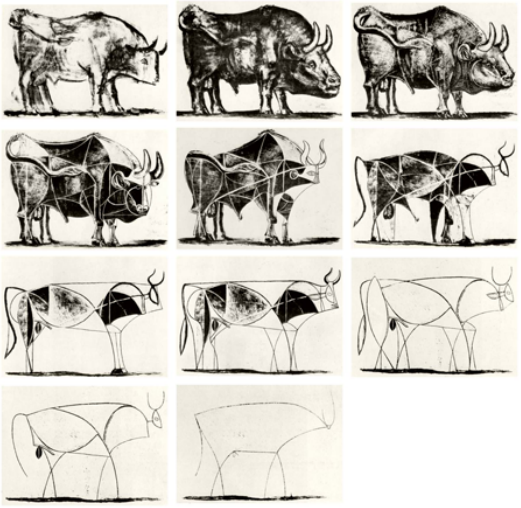

Figure 1: Pablo Picasso *Bull* (1945–1946).

interest in heterogeneous research communities in biology, robotics, sociology, and economics. Classical examples of such systems are groups of animals or humans with the tendency to herd, stockbrokers working in a financial market, and potential voters during elections.

To study the evolution in time of this active matter, the dynamics must be defined for the set of detected variables. Realistic models start from the definition of rationally simple interaction rules, defined for each agent of the system. Hence, it is often possible to observe the emergence of global patterns and structures, also called collective phenomena. From the mathematical viewpoint, this level of description is usually known as microscopic and is achieved by considering systems of ordinary differential equations (ODEs). The resulting differential problem for the general N-body system follows:

$$\dot{\mathbf{x}}_i = \sum_{j=1}^{N} w_j P(\mathbf{x}_i, \mathbf{x}_j), \qquad i = 1, \dots, N,$$

where $\mathbf{x}_i$ denotes the set of evolving variables, w_j denotes a weight function, and $P(\cdot, \cdot)$ denotes a pairwise interaction term depending on the whole set of variables characterizing the ith and jth particle. At the computational level, the introduced general dynamics is related to a considerable computational complexity of the order of $O(N^2)$, due to the summation term. Then we highlight how the microscopic description level induces unaffordable numerical costs for a system composed of a very large number of particles.

The key idea behind the reduction in complexity of the introduced modeling is through a change of scale in the description of the phenomena, implying the derivation of the so-called mesoscopic and macroscopic models. The main tools rely on a statistical description based on the kinetic theory, where the

particle density distribution in the phase space is studied. The new equations are derived in the limit of a large number of agents from the microscopic modeling. This mesoscopic level of description leads to partial differential equations describing the evolution of density functions.

Kinetic modeling gained an increased interest in the community studying the collective behavior of interacting systems owing to strong analogies between these models and classical kinetic theory of rarefied gases described by the Boltzmann equation [10, 83, 165]. Analytical methods allow the explicit computation of the stationary states of the whole system [92, 146, 164, 165] and a minimal energy state [169, 99].

Rigorous derivation of mean–field models from microscopic equations is a deeply fascinating issue that may pose nontrivial questions. There exist several approaches for first- or second-order systems of ODEs such as the BBGKY hierarchy [63, 109], mean–field limit [31, 53, 90], as well as the binary interaction approximation of the dynamics [66, 83, 145, 164]. In any case, the transition to chaos remains an indispensable ansatz to deduce the new mesoscopic model. This latter issue is definitely significant in mathematical terms, involving the proof of the propagation in time of chaos [122].

Finally, the macroscopic level of description of the dynamics may be deduced from the mesoscopic level by the extrapolation of thermodynamic quantities through the definition of the moment equations. The resulting continuous equations are also called hydrodynamic equations and generally require a closure.

Once a sound mathematical model is available, the reflection of our ultimate understanding of a complex system relies on the possibility of controlling its evolution. The scientific keyword comes in this case from the engineering literature: with the aim of minimizing the cost of the required interventions to steer the dynamics toward the prescribed state we introduce the optimal control problems. The control mechanisms of self–organized systems have been investigated as follow–up questions to the progress in the mathematical modeling and simulation. The control of emergent patterns has been studied on the level of microscopic particles as well on the level of kinetic or fluid dynamics equations.

Fundamental to the construction of more realistic models is the introduction of uncertainty in the dynamics, reflecting a wide range of possible perturbations and mimicking our imperfect knowledge of the phenomena. These errors are due to the random effects of a wide range of uncontrollable phenomena such as the influence of weather during an experiment, temperature variations, or even human carelessness. This is particularly relevant in many problems in the natural and socio-economic sciences, where the interaction rules are based on observations and empirical evidence and not on physical laws. In such cases, we can have at most statistical information on the modeling parameters. Therefore, statistical errors become ineradicable from any quantitative representation. To fully understand simulation results

and produce predictions, it is of utmost importance to incorporate uncertainty from the beginning of the modeling. The introduction of randomness in kinetic and mean-field equations is central to many practical applications of these deeply studied results with an interest in physical and engineering sciences.

From the numerical point of view, the implementation of accurate numerical methods is fundamental to quantify the impact of uncertainty in the overall dynamics. Among the most efficient methods in uncertainty quantification (UQ) for partial differential equations, generalized polynomial chaos (gPC) and stochastic Galerkin (SG) methods are very attractive thanks to their property of spectral convergence in the probability space, see [176, 177], representing an important step forward from the classic Monte Carlo technique, whose convergence is extremely slow. Despite its accuracy, the intrusive SG–gPC formulation may significantly modify the original problem. One the most evident and significant losses affects systems of hyperbolic equations [77, 151].

The aim of the present manuscript is to investigate a novel perspective in the modeling and control of complex system both in the deterministic and stochastic case, with particular attention to numerical methods, control methodologies and uncertainty quantification. Each chapter is designed to be self-consistent, starting from a general framework of the treated problem in the introduction and then moving through results and conclusions. In particular, each chapter refers to a previously published research article, manuscript under the revision process in a peer-reviewed journal, or ongoing research.

In Chapter 1 the research addressed in [11] is presented. In this work, we applied the techniques developed in [6] for the Boltzmann-type control of a consensus dynamics to the case of a hierarchical opinion model in the presence of different populations: the first composed by the so–called followers which are influenced by a second group, i.e. the leader group, controlled by external agents. Based on a microscopic model we design a Boltzmann-type optimal control thanks to the model predictive control (MPC) approach in the case of an instantaneous control. MPC utilizes the assumption that agents optimize their cost functional not necessarily over an infinite time horizon, instead they determine their locally best action by minimizing their cost over a short time interval which recedes as time evolves. We formulated a control strategy by embedding the control action in the binary interaction dynamics, thereby deriving the kinetic formulation of the problem. The main advantages lie in the efficiency of the instantaneous controls, which can be explicitly embedded in the dynamics, and the Boltzmann binary approximation applied to an MPC of an interacting system of N agents with computational cost $O(N)$, instead of $O(N^2)$ of the standard dynamics which must be solved forward–backward in time. In the quasi–invariant limit [91, 164] the corresponding Fokker–Planck formulation has been derived and explicit expressions of the

steady states have been computed.

A fruitful application of the MPC methodology has been applied in the context of complex networks in Chapter 2, where a control acts over a minimum set of nodes/agents influencing the dynamics of the whole network. There exists an incredible number of applications of control strategies on graphs: from pure social–marketing purposes, to national security reasons for the fastest spreading of information. Even if the introduced problem is *a priori* of a difficult solution, a first attempt to deal with the problem from a microscopic point of view has been made in [12], where the mathematical model is formulated as a coupling of an opinion alignment system with a probabilistic description of the graph. Let us consider the optimal control problem for opinions on the complex network $\mathcal{G}_N(t)$

$$\min_{u\in\mathcal{U}} \frac{1}{2}\int_{t_0}^{t_f}\left[\frac{1}{N}\sum_{j=1}^{N}(w_j - w_d)^2 + \nu u^2\right] ds$$

subject to

$$\dot{w}_i = \frac{1}{c_i}\sum_{j\in S_i} P(w_i, w_j; \mathcal{G}_N)(w_j - w_i) + u\chi(c_i \geq c^*), \qquad w_i(0) = w_{i,0}$$

for each $i = 1, \dots, N$. We adopted the notation $(w_i)_{i=1}^N \in I = [-1, 1]$ and $(c_i)_{i=1}^N = \{0, \dots, c_{\max}\}$ for the opinions and the number of connections of the ith agent, $w_d \in I$ is the desired opinion of the system, and $\nu > 0$ is a regularization parameter. As before, $P(\cdot, \cdot; \cdot)$ is an interaction potential which weights the opinion w_i on the subgraph S_i of the agents connected with the ith agent. It depends, in general, on the opinions and on the statistical properties of $\mathcal{G}_N$. Observe the way in which the action of the control u is weighted by an indicator function $\chi(\cdot)$, therefore the control is active only on the nodes with a degree of connection $c_i \geq c^*$, for a certain threshold c^*. The evolution of the network is coherent with a preferential attachment mechanism, see Figure 2. The introduction of a suitable selective control depending on the connection degree of each node is capable of driving the overall opinion towards consensus.

In Chapter 3, where we present joint research published with Professor Michael Herty [117], the mean–field formulation of kinetic under control actions is investigated. In particular, we consider a control formulated through an MPC strategy with varying horizon focusing on the relation between the (usually hard to compute) optimal control and the MPC approach in the mean-field case. We have established a computable and provable bound on the difference in the cost functional for MPC-controlled and optimally controlled dynamics in the case of a large number of agents. The derived estimates yield performance bounds for general symmetric multiagent dynamics with applications to swarming dynamics, consensus modeling, or economics. Numerical examples confirm the theoretical analysis.

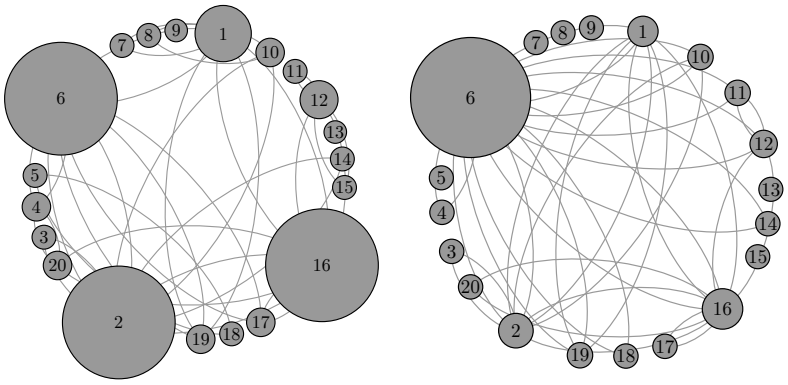

Figure 2: Evolution of a graph with density of connectivity $\gamma = 5$ through a rewiring process with preferential attachment. The diameter of each node is proportional to its connection.

The development of numerical schemes for the mean-field equation for collective behavior is the subject of Chapter 4. The presented results are a joint research with my advisor Professor Lorenzo Pareschi and refer to [149, 148], . The developed schemes are based on a generalization of the classical Chang–Cooper approach and capable of preserving the structural properties of the systems: non-negativity of the solution, physical conservation laws, entropy dissipation, and stationary solutions. In this work, we considered the following class of nonlinear Fokker–Planck equations

$$\partial_t f + \mathcal{L}[f] = \nabla_w \cdot \left[\mathcal{B}[f] f + \nabla_w (Df)\right],$$

with $f = f(x, w, t)$ depending on $x \in \mathbb{R}^{d_x}$ and $w \in \mathbb{R}^{d_w}$, where $d_x, d_w \geq 1$, $\mathcal{L}[\cdot]$ is an operator for the agents' dynamics with respect to the x variable, $\mathcal{B}[\cdot]$ is an alignment operator, and $D = D(x, w) \geq 0$ is a diffusion function. The presented equation describes a wide class of models for the collective behavior such as the mean–field *Cucker–Smale* model [8, 53, 71], for which

$$\mathcal{L}[f] = w \cdot \nabla_x f, \qquad \mathcal{B}[f] = \int_{\mathbb{R}^{d_x} \times \mathbb{R}^{d_w}} H(x, y)(w - v) f(y, v, t)\, dy\, dv,$$

with

$$H(x, y) = \frac{1}{(1 + |x - y|^2)^\gamma}, \qquad D(x, w) = D \in \mathbb{R}^+,$$

or the non–homogeneous mean–field *Cordier–Pareschi–Toscani* model for

wealth distribution [66, 146], where

$$\mathcal{L}[f] = \phi(x,w)\nabla_x f, \qquad \mathcal{B}[f] = \int_{\mathbb{R}^+} (w-v) f(y,v,t)\, dw, \qquad D(x,w) = \frac{\sigma^2}{2} w^2.$$

The proposed schemes have the property of being entropic and describing with arbitrary accuracy the steady-state solution of the mean–field problem.

In Chapter 5 we deal with opinion dynamics over a large network, where interactions depend on the opinion itself and on the discrete number of connections $c \in \mathcal{C} = \{0, \dots, c_{\max}\}$. The increasing capacity to produce data seems to be unavoidable in contemporary societies. This is mainly due to the rapid proliferation in the sources of data that the social media are able to capture: we are consumers as well as producers of data. The need to handle millions, and often billions, of vertices implies a considerable shift of interest to large–scale statistical properties of the network architectures.

Hence, the evolution of the distribution $f(w,c,t)$, given by the density of opinion and connections, obeys the introduced Fokker–Planck equation where the operator $\mathcal{L}[f]$ is now defined as follows

$$\begin{aligned}\mathcal{L}[f(w,c,t)] = &- \frac{2V_r(f;w)}{\gamma+\beta}\left[(c+1+\beta)f(w,c+1,t) - (c+\beta)f(w,c,t)\right] \\ &- \frac{2V_a(f;w)}{\gamma+\alpha}\left[(c-1+\alpha)f(w,c-1,t) - (c+\alpha)f(w,c,t)\right],\end{aligned}$$

where γ is the mean density of connectivity, $\alpha, \beta > 0$ are attraction coefficients, and $V_r(f;w) \geq 0$ and $V_a(f,w) \geq 0$ are characteristic rates of removal and addition, respectively. At the boundaries of $\mathcal{C}$ it is defined in such a way that the overall number of connections is conserved. The interaction operator is now defined as follows

$$\mathcal{B}[f](w,c,t) = \sum_{c_*=0}^{c_{\max}} \int_{[-1,1]} P(w,w_*;c,c_*)(w_*-w) f(w_*,c_*,t)\, dw_*,$$

where $P(\cdot,\cdot;\cdot,\cdot)$ is an interaction kernel depending on opinions and connections of the interacting dyads. It has been proven that for different choices of weights functions the introduced generator of the network may produce stationary scale-free degree distributions as well as uniform random graphs. Further, we observed that the presence of a small portion of highly connected agents may drive the overall dynamics towards their position, see Figure 3.

In Chapter 6, based on [147], we further investigate the proposed setting with a direct application to decision science. In particular, we introduce and discuss multivariate kinetic models describing the influence of competence in the evolution of decisions in a multiagent system. The exchange mechanism includes the role of the agents' tendency to behave in the same way as if they were as good, or as bad, as their partner: the so–called *equality bias*. The

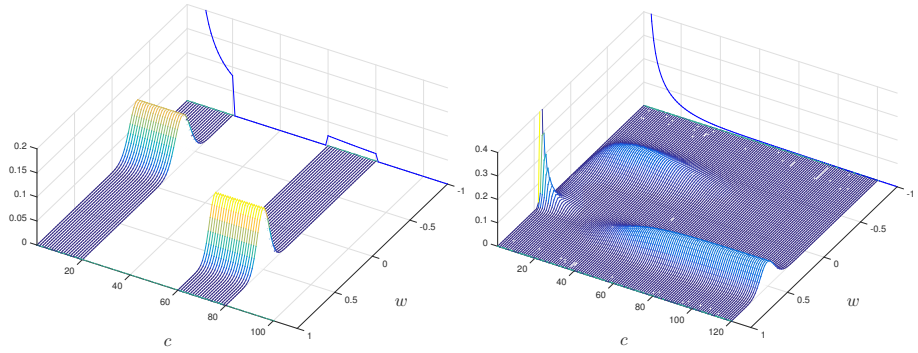

(a) $t = 0$ (b) $t = 2.5$

Figure 3: Evolution highlighting the way in which a small portion of agents with high connectivity can bias the majority of the evolution of the overall population.

presented modeling is inspired by real experiments [124, 131] and reproduces the empirical findings. Analytic and numerical results describe the way in which the equality bias leads the group to suboptimal collective decisions.

The role of stochastic quantities in the dynamics is investigated in Chapter 7, which refers to the article [13]. Here we analyze the effect of the uncertainty in the interaction parameter in a Cucker–Smale microscopic-type system using a gPC approach. Analytic evidence of threshold effects in the alignment dynamics, due to the presence of the random parameter, is given. In particular, the presence of negative tails in the distribution of the random inputs lead to the divergence of the expected velocities of the system of agents, even in the regimes of unconditional flocking. At the numerical level, we introduce in detail the SG–gPC numerical approach to the problem. We formalized a selective MPC approach to stabilize the dynamics and to steer the expected velocities toward the desired one, even in the divergence regimes.

Finally, in Chapter 8, we present the ongoing work in collaboration with Professor Josè Antonio Carrillo and Professor Lorenzo Pareschi [55]. Here, we investigate alignment models at the mesoscopic level of description depending on random inputs. The stochastic quantities act on the dynamics through perturbation of the initial conditions as well as typical modeling parameters. The derivation of mean–field models has been formally completed through the BBGKY hierarchy. The aim of this chapter is to develop positive preserving numerical schemes that maintain the spectral accuracy for the statistical quantities of interest. To this end, we have formulated a Monte Carlo SG–gPC method and numerical tests have been performed to prove the effectiveness of the algorithm.

Part I

Boltzmann–type and mean–field model predictive control

Chapter 1

Boltzmann-type control of opinion consensus

1.1 Introduction

Mean-field games and mean-field type control theory has raised a lot of interest in the recent years (see for example [27, 43, 76, 89, 128] and the references therein). The general setting consists in a control problem involving a very large number of agents where both the evolution of the state and the objective functional of each agent are influenced by the collective behavior of all other agents. Typical examples in socio-economical sciences, biology and engineering are represented by the problems of persuading voters to vote for a specific candidate, influencing buyers towards a given good or asset, forcing human crowds or group of animals to follow a specific path or to reach a desired zone, or optimizing the traffic flow in road networks and supply chains [9, 25, 43, 69, 82, 114, 115, 130, 132, 161].

In this paper we focus on control problems where the collective behaviour corresponds to the formation process of opinion consensus [26, 38, 94, 113, 139, 162, 164]. In particular, we consider models where the control strategy is based on hierarchical leadership. This concept of hierarchical leadership has been discussed in [82], where a population of leaders is considered giving rise to aggregate opinions and convergence towards specific patterns. Further, opinion dynamics in presence of different populations has been previously introduced in [34, 166, 173]. We mention here that control through leaders in self-organized flocking systems has been studied in [9, 161].

We introduce a hierarchical opinion formation dynamics where the leaders aim at controlling the followers through a suitable cost function which characterizes the leaders strategy in trying to influence the followers opinion. Based on this microscopic model, we develop a Boltzmann type optimal control approach following the ideas recently presented in [6]. The approach is closely related to model predictive and instantaneous control techniques

[44, 62, 110, 133]. We derive an explicit controller for the leader dynamics using an instantaneous binary control framework on the microscopic level and, similarly to the mean field control, study the related kinetic description for large number of agents. Thanks to this formulation, the minimization of the cost functional is embedded into the microscopic leaders interactions of the corresponding Boltzmann equation.

The rest of the manuscript is organized as follows. First in Section 1.2 we introduce the microscopic model of the leader strategy in the leader-follower interactions and derive the corresponding Boltzmann-type control formulation. The main properties of the kinetic model are studied in Section 1.3, in particular we show that that the leaders control strategy may lead the followers opinion towards the desired state. Explicit asymptotic opinion distributions are computed in Section 6.4 using an approximated Fokker-Planck description derived in the so-called quasi invariant opinion limit. Several numerical results confirm the theoretical analysis in Section 7.5.

1.2 Microscopic models of opinion control through leaders

A rather common assumption in opinion formations is that interactions are formed mainly by binary exchange of informations, see for example [38, 100, 145, 164]. Similar to [82] we are interested in the opinion formation process of a followers' population steered by the action of a leaders' group. The major novelty here is that the leaders' behaviour is driven by a suitable control strategy based on the interplay between the desire to force followers towards a given state and the necessity to keep a position close the the mean opinion of the followers in order to influence them. In the following we first generalize the approach of [6] starting from a differential system describing the evolution of the two populations of leaders and followers. In the second part we present a binary interaction model for the same dynamics showing how the two descriptions are related.

Microscopic modeling We assume to have two populations, one of followers and one of leaders. Each follower is mutually influenced by the other followers and by the leaders, whose target is to steer the followers' opinion to a desired configuration of consensus following some prescribed strategy. We consider the evolution of a population of N_L leaders and N_F followers, with opinions $w_i, \tilde{w}_k \in I = [-1, 1]$, for $i = 1, \dots, N_F$ and $k = 1, \dots, N_L$, evolving according to

$$\begin{aligned} \dot{w}_i &= \frac{1}{N_F} \sum_{j=1}^{N_F} P(w_i, w_j)(w_j - w_i) + \frac{1}{N_L} \sum_{h=1}^{N_L} S(w_i, \tilde{w}_h)(\tilde{w}_h - w_i), \\ w_i(0) &= w_{i,0}, \end{aligned} \tag{2.1}$$

$$\begin{aligned} \dot{\tilde{w}}_k &= \frac{1}{N_L}\sum_{h=1}^{N_L} R\left(\tilde{w}_k, \tilde{w}_h\right)\left(\tilde{w}_h - \tilde{w}_k\right) + u, \\ \tilde{w}_k\left(0\right) &= \tilde{w}_{k,0}, \end{aligned} \tag{2.2}$$

where $P(\cdot,\cdot), S(\cdot,\cdot)$ and $R(\cdot,\cdot)$ are given *compromise functions*, typically taking values in $[0,1]$, measuring the relative importance of the interacting agent in the consensus dynamics. The control term u characterizes the strategy of the leaders, and is given by the solution of the following optimal control problem

$$u = \operatorname{argmin}\left\{J(u, \underline{w}, \underline{\tilde{w}})\right\}, \tag{2.3}$$

where

$$J(u, \underline{w}, \underline{\tilde{w}}) = \frac{1}{2}\int_0^T \left\{ \frac{\psi}{N_L}\sum_{h=1}^{N_L}(\tilde{w}_h - w_d)^2 + \frac{\mu}{N_L}\sum_{h=1}^{N_L}(\tilde{w}_h - m_F)^2 \right\} ds + \int_0^T \frac{\nu}{2}u^2 ds. \tag{2.4}$$

In the latter equation $\underline{w}$ and $\underline{\tilde{w}}$ are the vectors with the followers and leaders opinions, T represents the final time horizon, w_d is the desired opinion and m_F is the average opinion of the followers group at time $t \geq 0$ defined as

$$m_F = \frac{1}{N_F}\sum_{j=1}^{N_F} w_j.$$

The parameter $\nu > 0$, as usual, is a regularization term representing the importance of the control u in the overall dynamics. More precisely, ν penalizes the action of the control u in such a way that for large values of ν the control action vanishes and viceversa.

The problem may also be formulated as constrained minimization problem for $u^n, \underline{w}^n, \underline{\tilde{w}}^n$ in the form

$$\begin{aligned} &\min J\left(u^n, \underline{w}^n, \underline{\tilde{w}}^n\right) \\ &\text{subject to} \quad (2.1) - (2.2). \end{aligned} \tag{2.5}$$

In general the solution of this problems is a difficult task, in particular for nonlinear constrains and non convex functional. In the following we assume sufficient regularity on the constrains of (2.5), in such a way that the minimizer fulfills the necessary first order optimality conditions. We refer to [129] for a detailed discussion of necessary and sufficient optimality conditions.

Thus the control strategy of the leaders' population is based on an interplay of two behaviours weighted by the nonnegative constants ψ and μ such that

$\psi + \mu = 1$. On one hand they aim at minimizing the distance with respect to the desired state w_d (*radical behaviour*) and on the other hand they aim at minimizing the distance with respect to the followers' mean opinion (*populistic behaviour*). Therefore, the leaders influence the followers opinion interacting through the function $S(\cdot,\cdot)$ and the followers influence the leaders strategy through their mean opinion in the cost functional (2.4).

The above optimization problem is approximated using the Boltzmann type optimal control approach recently presented in [6] which corresponds to a binary model predictive control of (2.1)-(2.3) in the case of a very large number of agents [133, 44].

Instantaneous binary control The main idea is to avoid the solution of the dynamics on the whole time interval and to consider a closed-loop strategy for the opinion model in the case of binary interactions. Hence, we split the time interval $[0, T]$ in M time intervals of length Δt and let $t^n = \Delta t\, n$ and solve sequentially the optimal control problem in each time interval. This approach is related to the receding horizon strategy, or instantaneous control in the engineering literature, which allows to express the control as a feedback of the state variables. In general, with respect to the associated optimal control problem (2.1)-(2.3) this technique furnishes a suboptimal solution. Rigorous results on the properties of u for a constrained quadratic cost functional are discussed, for example, in [133, 44].

More precisely, we approximate both (2.1) and (2.2) by the following discretized binary dynamics

$$\begin{cases} w_i^{n+1} = & w_i^n + \alpha P(w_i^n, w_j^n)(w_j^n - w_i^n) + \alpha S(w_i^n, \tilde{w}_l^n)(\tilde{w}_l^n - w_i^n) \\ w_j^{n+1} = & w_j^n + \alpha P(w_j^n, w_i^n)(w_i^n - w_j^n) + \alpha S(w_j^n, \tilde{w}_l^n)(\tilde{w}_l^n - w_j^n) \end{cases} \tag{2.6}$$

$$\begin{cases} \tilde{w}_k^{n+1} = & \tilde{w}_k^n + \alpha R(\tilde{w}_k^n, \tilde{w}_h^n)(\tilde{w}_h^n - \tilde{w}_k^n) + 2\alpha u^n \\ \tilde{w}_h^{n+1} = & \tilde{w}_h^n + \alpha R(\tilde{w}_h^n, \tilde{w}_k^n)(\tilde{w}_k^n - \tilde{w}_h^n) + 2\alpha u^n \end{cases} \tag{2.7}$$

where $\alpha = \Delta t/2$, i and j are the indexes of the two interacting followers, l the index of an arbitrary leader, h and k the indexes of the two interacting leaders. The control variable u is given by the solution of the following optimization problem

$$u^n = \text{argmin}\, \{J\,(u^n, \underline{w}^n, \underline{\tilde{w}}^n)\} \tag{2.8}$$

$$\begin{aligned} J\,(u^n, \underline{w}^n, \underline{\tilde{w}}^n) = \alpha \Bigg(& \frac{\psi}{2} \sum_{p=\{k,h\}} (\tilde{w}_p^n - w_d)^2 \\ & + \frac{\mu}{2} \sum_{p=\{k,h\}} (\tilde{w}_p^n - m_F^n)^2 + \nu (u^n)^2 \Bigg). \end{aligned} \tag{2.9}$$

In order to solve the minimization problem introduced in (2.8), we can proceed as in [6] using a standard Lagrange multipliers approach to compute explicitly u^n. In this way we obtain the feedback control

$$2\alpha u^n = -\sum_{p=\{k,h\}} \frac{2\alpha^2}{\nu}\left[\psi(\tilde{w}_p^{n+1} - w_d) + \mu(\tilde{w}_p^{n+1} - m_F^{n+1})\right]. \tag{2.10}$$

Note that since the feedback control u^n in (2.10) depends on the post interaction opinion the constrained binary interaction (2.7) is implicitly defined but it can be easily inverted. The explicit version of the control reads

$$\begin{aligned} 2\alpha u^n = &-\sum_{p=\{k,h\}} \frac{\beta}{2}\left[\psi(\tilde{w}_p^n - w_d) + \mu(\tilde{w}_p^n - m_F^n)\right] \\ &-\frac{\alpha\beta}{2}(R(\tilde{w}_k^n, \tilde{w}_h^n) - R(\tilde{w}_h^n, \tilde{w}_k^n))(\tilde{w}_h^n - \tilde{w}_k^n), \end{aligned} \tag{2.11}$$

where we further approximated m_F^{n+1} with m_F^n to have a fully explicit expression and introduced the parameter β defined as

$$\beta = \frac{4\alpha^2}{\nu + 4\alpha^2}. \tag{2.12}$$

1.3 Boltzmann-type control

In this section, we consider a Boltzmann dynamics corresponding to the above instantaneous control formulation. In order to derive a kinetic equation we introduce a density distribution of followers $f_F(w,t)$ and leaders $f_L(\tilde{w},t)$ depending on the opinion variables $w, \tilde{w} \in I$ and time $t \geq 0$. It is assumed that the followers' density is normalized to 1, that is

$$\int_I f_F(w,t)\, dw = 1,$$

whereas

$$\int_I f_L(\tilde{w},t)\, d\tilde{w} = \rho \leq 1.$$

The kinetic model can be derived by considering the change in time of $f_F(w,t)$ and $f_L(\tilde{w},t)$ depending on the interactions with the other individuals and the leaders' strategy. This change depends on the balance between the gain and loss due to the binary interactions.

Binary constrained interactions dynamics Let us consider the pairwise opinions (w,v) and $(\tilde{w},\tilde{v})$, respectively of two followers and two leaders, the corresponding post interaction opinions are computed according with three dynamics, the interaction between two followers, the interaction between follower and leader and finally between two leaders.

The post-interaction opinions $(\tilde{w}^*, \tilde{v}^*)$ of two leaders are given by

$$\begin{cases} \tilde{w}^* = \tilde{w} + \alpha R(\tilde{w}, \tilde{v})(\tilde{v} - \tilde{w}) + 2\alpha u + \tilde{\theta}_1 \tilde{D}(\tilde{w}) \\ \tilde{v}^* = \tilde{v} + \alpha R(\tilde{v}, \tilde{w})(\tilde{w} - \tilde{v}) + 2\alpha u + \tilde{\theta}_2 \tilde{D}(\tilde{v}), \end{cases} \tag{3.1}$$

where the feedback control is defined as

$$\begin{aligned} 2\alpha u = &- \frac{\beta}{2} \left[\psi \left((\tilde{w} - w_d) + (\tilde{v} - w_d) \right) + \mu \left((\tilde{w} - m_F) + (\tilde{v} - m_F) \right) \right] \\ &- \frac{\alpha\beta}{2} (R(\tilde{w}, \tilde{v}) - R(\tilde{v}, \tilde{w}))(\tilde{v} - \tilde{w}), \end{aligned} \tag{3.2}$$

and

$$m_F(t) = \int_I f_F(w, t) w \, dw. \tag{3.3}$$

Note that the control term is now embedded into the binary interaction and that we considered an additional noise component such that the diffusion variables $\tilde{\theta}_1, \tilde{\theta}_2$ are realizations of a random variable with zero mean and finite variance $\tilde{\sigma}^2$. Moreover the noise influence is weighted by the function $\tilde{D}(\cdot)$, representing the local relevance of diffusion for a given opinion, and such that $0 \leq \tilde{D}(\cdot) \leq 1$.

We assume that the opinions (w^*, v^*) in the follower-follower interactions are derived according to

$$\begin{cases} w^* = w + \alpha P(w, v)(v - w) + \theta_1 D(w), \\ v^* = v + \alpha P(v, w)(w - v) + \theta_2 D(v), \end{cases} \tag{3.4}$$

where the diffusion variables θ_1, θ_2 are again realizations of a random variable with zero mean, finite variance σ^2 and $0 \leq D(\cdot) \leq 1$. Finally the leader-follower interaction is described for every agents from the leaders' group, thus in general we have

$$\begin{cases} w^{**} = w + \alpha S(w, \tilde{v})(\tilde{v} - w) + \hat{\theta} \hat{D}(w) \\ \tilde{v}^{**} = \tilde{v} \end{cases} \tag{3.5}$$

where similar to the previous dynamics, $\hat{\theta}$ is a random variable with zero mean and finite variance $\hat{\sigma}^2$ and $0 \leq \hat{D}(\cdot) \leq 1$

Since we are dealing with a kinetic problem in which the variable belongs to a bounded domain, namely $I = [-1, 1]$, we must deal with additional mathematical difficulties in the definition of agents interactions. In fact, it is essential to consider only interactions that do not produce values outside the finite interval.

For the leaders' interaction if we consider the constrained binary interactions system (3.1)-(3.2), without diffusion we obtain that $|\tilde{w}^* - \tilde{v}^*|$ is a contraction if $\alpha \leq 1/2$

$$|\tilde{w}^* - \tilde{v}^*| = |(\tilde{w} - \tilde{v}) - \alpha(\tilde{w} - \tilde{v})(R(\tilde{w}, \tilde{v}) + R(\tilde{v}, \tilde{w}))| \leq |1 - 2\alpha||\tilde{w} - \tilde{v}|.$$

The following proposition gives sufficient conditions to preserve the bounds for the leaders' interactions (3.1).

Proposition 1.3.1. *Let r, d_+ and d_- be defined as follows*

$$r = \min_{\tilde{v},\tilde{w}\in I} \left[R(\tilde{v},\tilde{w})\right], \qquad d_\pm = \min_{\tilde{w}\in I} \left[\frac{1\mp\tilde{w}}{\tilde{D}(\tilde{w})}, \tilde{D}(\tilde{w}) \neq 0\right]. \tag{3.6}$$

If $\tilde{v}, \tilde{w} \in I$ then $\tilde{v}^*, \tilde{w}^* \in I$ if the following conditions hold

$$\alpha r \geq \frac{\beta}{2}, \qquad d_-\left(1-\frac{\beta}{2}\right) \leq \tilde{\theta}_i \leq d_+\left(1-\frac{\beta}{2}\right), \quad i = 1, 2. \tag{3.7}$$

The proof follows by the same arguments used in [6, 82] and we omit the details. On the other hand from the definition of binary interaction between followers (3.4), in absence of diffusion, the boundaries are never violated. Indeed since $|w| \leq 1$ it follows that $|v - w| \leq 1$ and being $0 \leq P(\cdot,\cdot) \leq 1$ it is easily seen that $w^*, v^* \in I$.

Finally, as shown in [82], the post-interaction opinion of followers w^{**}, in the leader-follower interaction (3.5), takes values in the reference interval I if the hypothesis of the following proposition are satisfied.

Proposition 1.3.2. *Let K_- and K_+ be defined as follows*

$$K_\pm = \min_{w\in I} \left[\frac{1\mp w}{\hat{D}(w)}, \hat{D}(w) \neq 0\right]. \tag{3.8}$$

If $w \in I$ then $w^{**} \in I$ if the following conditions hold

$$(1-\alpha)K_- \leq \hat{\theta} \leq (1-\alpha)K_+, \quad i = 1, 2. \tag{3.9}$$

Main properties Following the derivation in [145], for a suitable choice of test functions φ we can describe the evolution of $f_F(w,t)$ thanks to the integro-differential equation of Boltzmann type

$$\frac{d}{dt}\int_I \varphi(w) f_F(w,t)dw = (Q_F(f_F, f_F), \varphi) + (Q_{FL}(f_L, f_F), \varphi) \tag{3.10}$$

where

$$(Q_F(f_F, f_F), \varphi) = \left\langle \int_{I^2} B^F_{int}(\varphi(w^*) - \varphi(w)) f_F(w,t) f_F(v,t) dwdv \right\rangle \tag{3.11}$$

and

$$(Q_{FL}(f_F, f_L), \varphi) = \left\langle \int_{I^2} B^{FL}_{int}(\varphi(w^{**}) - \varphi(w)) f_F(w,t) f_L(\tilde{v},t) dwd\tilde{v} \right\rangle. \tag{3.12}$$

In (3.11) and (3.12) we used the notation $\langle \cdot \rangle$ to indicate the expectations with respect the random variables, respectively $\theta_i, i = 1, 2$ and $\hat{\theta}$, and the nonnegative interaction kernels B^F_{int}, B^{FL}_{int} are related to the probability of the microscopic interactions. The simplest choice of interaction kernels which guarantees that the post interaction opinions never violate the bounds is given by

$$\begin{aligned} B^F_{int} &= B^F_{int}(w, v, \theta_1, \theta_2) = \eta_F \chi(|w^*| \leq 1)\chi(|v^*| \leq 1) \\ B^{FL}_{int} &= B^{FL}_{int}(w, \tilde{v}, \hat{\theta}) = \eta_{FL} \chi(|w^{**}| \leq 1)\chi(|\hat{v}| \leq 1) \end{aligned} \tag{3.13}$$

where $\eta_F, \eta_{FL} > 0$ are constant relaxation rates and $\chi(\cdot)$ is the indicator function. If we now assume that the interaction parameters are such that $|w^*|, |w^{**}| \leq 1$ the Boltzmann operators can be written as

$$(Q_F(f_F, f_F), \varphi) = \eta_F \left\langle \int_{I^2} (\varphi(w^*) - \varphi(w)) f_F(w, t) f_F(v, t) dw dv \right\rangle \tag{3.14}$$

$$\begin{aligned} (Q_{FL}(f_F, f_L), \varphi) = \eta_{FL} \Bigg\langle \int_{I^2} (\varphi(w^{**}) \\ - \varphi(w)) f_F(w, t) f_L(\tilde{v}, t) dw d\tilde{v} \Bigg\rangle. \end{aligned} \tag{3.15}$$

In order to study the evolution of the average opinion $m_F(t)$, we take $\varphi(w) = w$ in (3.10). We have that the evolution of the average opinion of followers is

$$\begin{aligned} \frac{d}{dt} m_F(t) =& \frac{\eta_F}{2} \left[\int_{I^2} (w^* + v^* - w - v) f_F(w, t) f_F(v, t) dw dv \right] \\ &+ \eta_{FL} \int_{I^2} (w^{**} - w) f_F(w, t) f_L(\tilde{v}, t) dw d\tilde{v}, \end{aligned} \tag{3.16}$$

since the noise in (3.4) has zero mean. From the definition of binary interactions between followers (3.4) and the definition of interaction leader-follower (3.5) we have

$$\begin{aligned} \frac{d}{dt} m_F(t) =& \frac{\eta_F}{2} \alpha \int_{I^2} (v - w)(P(w, v) - P(v, w)) f_F(w, t) f_F(v, t) dw dv \\ &+ \eta_{FL} \alpha \int_{I^2} S(w, \tilde{v})(\tilde{v} - w) f_F(w, t) f_L(\tilde{v}, t) dw d\tilde{v}. \end{aligned} \tag{3.17}$$

Remark 1. *If we suppose P symmetric, that is $P(w, v) = P(v, w)$, and $S \equiv 1$ we obtain a simplified equation for the time evolution of m_F*

$$\frac{d}{dt} m_F(t) = \tilde{\eta}_{FL} \ \alpha(m_L(t) - m_F(t)) \tag{3.18}$$

where we introduced the notations $\tilde{\eta}_{FL} = \rho \ \eta_{FL}$ and $m_L(t) = \dfrac{1}{\rho} \displaystyle\int_I \tilde{w} f_L(\tilde{w}, t) d\tilde{w}$.

The evolution equation for $m_L(t)$ can be found thanks to similar arguments. We can describe the dynamics of $f_L(\tilde{w}, t)$ thanks to the following integro-differential equation of Boltzmann type in weak form

$$\frac{d}{dt}\int_I \varphi(\tilde{w}) f_L(\tilde{w}, t) d\tilde{w} = (Q_L(f_L, f_L), \varphi) \tag{3.19}$$

where

$$(Q_L(f_L, f_L), \varphi) = \left\langle \int_{I^2} B_{int}(\varphi(\tilde{w}^*) - \varphi(\tilde{w})) f_L(\tilde{w}, t) f_L(\tilde{v}, t) d\tilde{w} d\tilde{v} \right\rangle. \tag{3.20}$$

As before $\langle \cdot \rangle$ denotes the expectation taken with respect to the random variables $\tilde{\theta}_i, i = 1, 2$ and B_{int} is related to the probability of the microscopic interactions. A choice which preserves post interaction opinion bounds is

$$B_{int} = B_{int}(\tilde{w}, \tilde{v}, \tilde{\theta}_1, \tilde{\theta}_2) = \eta_L \chi(|\tilde{w}^*| \leq 1)\chi(|\tilde{v}^*| \leq 1) \tag{3.21}$$

where $\eta_L > 0$ is a constant rate and $\chi(\cdot)$ is the indicator function. Let us consider as test function $\varphi(\tilde{w}) = \tilde{w}$. Then equation (3.19) assumes the form

$$\frac{d}{dt}\int_I \tilde{w} f_L(\tilde{w}, t) d\tilde{w} = \eta_L \left\langle \int_{I^2} (\tilde{w}^* - \tilde{w}) f_L(\tilde{w}, t) f_L(\tilde{v}, t) d\tilde{w} d\tilde{v} \right\rangle, \tag{3.22}$$

which is equivalent to consider

$$\frac{d}{dt}\int_I \tilde{w} f_L(\tilde{w}, t) d\tilde{w} = \frac{\eta_L}{2} \left\langle \int_{I^2} (\tilde{v}^* + \tilde{w}^* - \tilde{v} - \tilde{w}) f_L(\tilde{w}, t) f_L(\tilde{v}, t) d\tilde{w} d\tilde{v} \right\rangle.$$

Then being the noise in (3.1) with zero mean we have

$$\begin{aligned} \frac{d}{dt} m_L(t) = & \\ & \eta_L \alpha (1 - \beta) \frac{1}{\rho} \int_{I^2} (R(\tilde{w}, \tilde{v}) - R(\tilde{v}, \tilde{w})) \tilde{v} f_L(\tilde{w}, t) f_L(\tilde{v}, t) d\tilde{w} d\tilde{v} \\ & + \tilde{\eta}_L \psi \beta (w_d - m_L(t)) + \tilde{\eta}_L \beta \mu (m_F(t) - m_L(t)), \end{aligned} \tag{3.23}$$

where $\tilde{\eta_L} = \rho \eta_L$.

Remark 2. *If $R(\tilde{w}, \tilde{v}) = R(\tilde{v}, \tilde{w})$ equation (3.23) becomes*

$$\frac{d}{dt} m_L(t) = \tilde{\eta}_L \psi \beta (w_d - m_L(t)) + \tilde{\eta}_L \mu \beta (m_F(t) - m_L(t)). \tag{3.24}$$

Moreover if the assumptions on P and S in Remark 1 hold we obtain the following closed system of differential equations for the mean opinions m_L and m_F

$$\begin{cases} \dfrac{d}{dt} m_L(t) = \tilde{\eta}_L \psi \beta (w_d - m_L(t)) + \tilde{\eta}_L \mu \beta (m_F(t) - m_L(t)) \\ \dfrac{d}{dt} m_F(t) = \tilde{\eta}_{FL} \alpha (m_L(t) - m_F(t)). \end{cases} \tag{3.25}$$

Straightforward computations show that the exact solution of the above system has the following structure

$$\begin{cases} m_L(t) = & C_1 \exp\{-|\lambda_1|t\} + C_2 \exp\{-|\lambda_2|t\} + w_d \\ m_F(t) = & C_1 \left(1 + \dfrac{\lambda_1}{\beta\mu\tilde{\eta}_L}\right) \exp\{-|\lambda_1|t\} \\ & + C_2 \left(1 + \frac{\lambda_2}{\beta\mu\tilde{\eta}_L}\right) \exp\{-|\lambda_2|t\} + w_d \end{cases} \tag{3.26}$$

where C_1, C_2 depend on the initial data $m_F(0), m_L(0)$ in the following way

$$C_1 = -\frac{1}{\lambda_1 - \lambda_2}\left((\beta\tilde{\eta}_L m_L(0) + \lambda_2)m_L(0) - \mu\beta\tilde{\eta}_L m_F(0) - (\lambda_2 + \beta\tilde{\eta}_L\psi)w_d\right) \tag{3.27}$$

$$C_2 = \frac{1}{\lambda_1 - \lambda_2}\left((\beta\tilde{\eta}_L m_L(0) + \lambda_1)m_L(0) - \mu\beta\tilde{\eta}_L m_F(0) - (\lambda_1 + \beta\tilde{\eta}_L\psi)w_d\right) \tag{3.28}$$

with

$$\lambda_{1,2} = -\frac{1}{2}\left(\alpha\tilde{\eta}_{FL} + \beta\tilde{\eta}_L\right) \pm \frac{1}{2}\sqrt{(\alpha\tilde{\eta}_{FL} + \beta\tilde{\eta}_L)^2 - 4\psi\alpha\beta\tilde{\eta}_L\tilde{\eta}_{FL}}. \tag{3.29}$$

Note that $\lambda_{1,2}$ are always negative, this assures that the contribution of the initial averages, $m_L(0), m_F(0)$, vanishes as soon as time increases and the mean opinions of leaders and followers converge towards the desired state w_d.

We now take into account the evolution of the second order moments

$$E_F(t) = \int_I w^2 f_F(w,t)\, dw, \qquad E_L(t) = \frac{1}{\rho}\int_I \tilde{w}^2 f_L(\tilde{w},t)\, d\tilde{w}.$$

First we analyze the followers group from equation (3.10) with test functions $\varphi(w) = w^2$, we have

$$\begin{aligned} \frac{d}{dt}E_F(t) = & \\ & \frac{\eta_F}{2}\left\langle \int_{I^2} \left((w^*)^2 + (v^*)^2 - w^2 - v^2\right) f_F(w,t) f_F(v,t) dw dv \right\rangle \\ & + \eta_{FL}\left\langle \int_{I^2} \left((w^{**})^2 - w^2\right) f_F(w,t) f_L(\tilde{v},t) dw d\tilde{v} \right\rangle. \end{aligned} \tag{3.30}$$

Thanks to (3.4) -(3.5), in the simplified case $P \equiv S \equiv 1$, we obtain

$$\begin{aligned}\frac{d}{dt}E_F(t) =& 2\eta_F\alpha(\alpha-1)(E_F(t)-m_F^2(t))\\ &+\tilde{\eta}_{FL}\alpha^2(E_L+E_F-2m_L(t)m_F(t))\\ &+2\alpha\tilde{\eta}_{FL}(m_F(t)m_L(t)-E_F(t))\\ &+\eta_F\sigma^2\int_I D^2(w)f_F(w,t)dw\\ &+\tilde{\eta}_{FL}\hat{\sigma}^2\int_I \hat{D}^2(w)f_F(w,t)dw.\end{aligned} \tag{3.31}$$

Finally, for the leaders group let us consider the function $\varphi(\tilde{w}) = \tilde{w}^2$ in (3.19) and the case $R \equiv 1$. Then thanks to equation (3.1) we obtain

$$\begin{aligned}\frac{d}{dt}E_L(t) =& \frac{\eta_L}{2}\frac{1}{\rho}\Big\langle\int_{I^2}((\tilde{w}^*)^2+(\tilde{v}^*)^2-\tilde{w}^2-\tilde{v}^2)\\ &f_L(\tilde{w},t)f_L(\tilde{v},t)d\tilde{w}d\tilde{v}\Big\rangle\\ =&\tilde{\eta}_L\Big[2\alpha(\alpha-1)(E_L(t)-m_L^2(t))\\ &-\frac{\beta}{2}(2-\beta)(E_L(t)+m_L^2(t))\\ &+2\beta(1-\beta)(\psi w_d+\mu m_F(t))m_L(t)+\beta^2(\psi w_d\\ &+\mu m_F(t))^2+\tilde{\sigma}^2\int_I\tilde{D}^2(\tilde{w})f_L(\tilde{w},t)d\tilde{w}\Big].\end{aligned} \tag{3.32}$$

In absence of diffusion, since $m_F(t), m_L(t) \to w_d$ as $t \to \infty$, it follows that $E_F(t), E_L(t)$ converge toward w_d^2. Then the quantities

$$\begin{aligned}\int_I f_F(w,t)(w-w_d)^2dw =& E_F(t)+w_d^2-2m_F(t)w_d\\ \frac{1}{\rho}\int_I f_L(\tilde{w},t)(\tilde{w}-w_d)^2d\tilde{w} =& E_L(t)+w_d^2-2m_L(t)w_d\end{aligned} \tag{3.33}$$

go to zero as $t \to \infty$, i.e. under the above assumptions the steady state solutions have the form of a Dirac delta centered in the target opinion w_d.

1.4 Fokker-Planck modeling

In the general case, it is quite difficult to obtain analytic results on the large time behaviour of the kinetic equation (3.10). A step towards the simplification of the analysis, is the derivation of asymptotic states of the Boltzmann model resulting in simplified Fokker-Planck type models, for which the study of the asymptotic properties is easier [145]. In order to obtain such simplification we will follow the approach usually referred as quasi–invariant opinion limit [145, 164], which is closely related to the so-called grazing collision limit of the Boltzmann equation (see [91, 168]).

Quasi invariant opinion limit The main idea is to rescale the interaction frequencies $\eta_L, \eta_F, \eta_{FL}$, the propensity strength α, the diffusion variances $\tilde{\sigma}^2, \sigma^2, \hat{\sigma}^2$ and the action of the control ν at the same time, in order to maintain, at level of the asymptotic procedure, memory of the microscopic interactions.

Let us introduce the parameter $\varepsilon > 0$, and consider the rescaling

$$\begin{aligned} &\alpha = \varepsilon, \qquad \nu = \varepsilon\kappa, \qquad \sigma^2 = \varepsilon\varsigma^2, \qquad \hat{\sigma}^2 = \varepsilon\hat{\varsigma}^2, \qquad \tilde{\sigma}^2 = \varepsilon\tilde{\varsigma}^2, \\ &\eta_F = \frac{1}{c_F\varepsilon}, \qquad \eta_{FL} = \frac{1}{c_{FL}\varepsilon}, \qquad \eta_L = \frac{1}{c_L\varepsilon}, \qquad \beta = \frac{4\varepsilon}{\kappa + 4\varepsilon}. \end{aligned} \tag{4.1}$$

This corresponds to the situation where the interaction operator concentrates on binary interactions which produce a very small change in the opinion of the agents. From a modeling viewpoint, we require that the scaling (3.1) in the limit $\varepsilon \to 0$ preserves the main macroscopic properties of the kinetic system. To this extent, let us consider the evolution of the scaled first two moments under the simplifying hypothesis P, R symmetric and $S \equiv 1$.

The evolution of the mean opinions described in the system (3.25) rescales as

$$\begin{cases} \dfrac{d}{dt}m_F(t) = \varepsilon\dfrac{1}{c_{FL}\varepsilon}(m_L(t) - m_F(t)) \\ \dfrac{d}{dt}m_L(t) = \dfrac{\psi}{c_L\varepsilon}\dfrac{4\varepsilon}{\kappa + 4\varepsilon}(w_d - m_L(t)) \\ \qquad\qquad + \dfrac{\mu}{c_L\varepsilon}\dfrac{4\varepsilon}{\kappa + 4\varepsilon}(m_F(t) - m_L(t)) \end{cases} \tag{4.2}$$

which as $\varepsilon \to 0$ yields

$$\begin{cases} \dfrac{d}{dt}m_F(t) = \dfrac{\rho}{c_{FL}}(m_L(t) - m_F(t)) \\ \dfrac{d}{dt}m_L(t) = \dfrac{4\rho}{c_L\kappa}\left[\psi(w_d - m_L(t)) + \mu(m_F(t) - m_L(t))\right]. \end{cases} \tag{4.3}$$

The second moment equations (3.31) and (3.32) are then scaled as follows

$$\begin{aligned} \frac{d}{dt}E_F(t) =& (\varepsilon - 1)\frac{2}{c_F}(E_F(t) - m_F^2(t)) \\ &+ \frac{\varepsilon\rho}{c_{FL}}(E_L(t) + E_F(t) - 2m_L(t)m_F(t)) \\ &+ \frac{2\rho}{c_{FL}}(m_F(t)m_L(t) - E_F(t)) + \frac{\varsigma^2}{c_F}\int_I D^2(w)f_F(w,t)dw \\ &+ \frac{\hat{\varsigma}^2\rho}{c_{FL}}\int_I \hat{D}^2(w)f_F(w,t)dw \end{aligned} \tag{4.4}$$

$$\begin{aligned}\frac{d}{dt}E_L(t) =&\frac{\rho}{c_L\varepsilon}\Big[2\varepsilon(\varepsilon-1)(E_L(t)-m_L^2(t))\\ &-\frac{2\varepsilon}{\kappa+4\varepsilon}(2-\frac{4\varepsilon}{\kappa+4\varepsilon})(E_L(t)+m_L^2(t))\\ &+\frac{8\varepsilon}{\kappa+4\varepsilon}(1-\frac{4\varepsilon}{\kappa+4\varepsilon})(\psi w_d+\mu m_F(t))m_L(t)\\ &+\left(\frac{4\varepsilon}{\kappa+4\varepsilon}\right)^2(\psi w_d+\mu m_F(t))^2\\ &+\tilde\sigma^2\int_I\tilde D^2(\tilde w)f_L(\tilde w,t)d\tilde w\Big]\end{aligned} \tag{4.5}$$

and as $\varepsilon\to 0$ we obtain

$$\begin{aligned}\frac{d}{dt}E_F(t) =&-\frac{2}{c_F}(E_F(t)-m_F^2(t))+\frac{2\rho}{c_{FL}}(m_F(t)m_L(t)-E_F(t))\\ &+\frac{\varsigma^2}{c_F}\int_I D^2(w)f_F(w,t)dw+\frac{\hat\varsigma^2\rho}{c_{FL}}\int_I\hat D^2(w)f_F(w,t)dw\\ \frac{d}{dt}E_L(t) =&-\frac{2\rho}{c_L}(E_L(t)-m_L^2(t))-\frac{4\rho}{c_L\kappa}(E_L(t)+m_L^2(t))\\ &+\frac{8\rho}{c_L\kappa}(\psi w_d+\mu m_F(t))m_L(t)+\frac{\tilde\varsigma^2\rho}{c_L}\int_I\tilde D^2(\tilde w)f_L(\tilde w,t)d\tilde w.\end{aligned} \tag{4.6}$$

Therefore the asymptotic scaling preserve the behaviour of the first two moments of the solution. We show how this approach leads to a constrained Fokker–Planck system for the description of the opinion distribution of leaders and followers. We present formal computation, following the same arguments in [145, 164] it is possible to give a rigorous mathematical basis of our derivation. Here we omit the details for the sake of brevity.

Fokker-Plank equations The scaled equation (3.10) reads

$$\begin{aligned}\frac{d}{dt}\int_I\varphi(w)f_F(w,t)dw =&\\ &\frac{1}{c_F\varepsilon}\left\langle\int_{I^2}(\varphi(w^*)-\varphi(w))f_F(w,t)f_F(v,t)dwdv\right\rangle\\ &+\frac{1}{c_{FL}\varepsilon}\left\langle\int_{I^2}(\varphi(w^{**})-\varphi(w))f_F(w,t)f_L(\tilde w,t)dwd\tilde w\right\rangle.\end{aligned} \tag{4.7}$$

Considering the second order Taylor expansion of φ around w we obtain

$$\begin{aligned}\varphi(w^*)-\varphi(w)&=(w^*-w)\varphi'(w)+\frac{1}{2}(w^*-w)^2\varphi''(\bar w)\\ \varphi(w^{**})-\varphi(w)&=(w^{**}-w)\varphi'(w)+\frac{1}{2}(w^{**}-w)^2\varphi''(\hat w)\end{aligned} \tag{4.8}$$

where for some $0 \leq \vartheta_1, \vartheta_2 \leq 1$

$$\bar{w} = \vartheta_1 w^* + (1-\vartheta_1)w, \qquad \hat{w} = \vartheta_2 w^{**} + (1-\vartheta_2)w.$$

Taking into account the binary interactions (3.4)-(3.5) in (4.8), and substituting in (4.7), we obtain a second order approximation of the dynamics. In the limit $\varepsilon \to 0$ the leading order is given by

$$\begin{aligned}
\frac{d}{dt}\int_I \varphi(w) f_F(w) dw = \\
&\frac{1}{c_F}\left[\int_{I^2} P(w,v)(v-w)\varphi'(w) f_F(w,t) f_F(v) dw dv\right] \\
&+ \frac{1}{c_{FL}}\left[\int_{I^2} S(w,\tilde{w})(\tilde{w}-w)\varphi'(w) f_F(w) f_L(\tilde{w}) dw d\tilde{w}\right] \\
&+ \frac{1}{2}\frac{\varsigma^2}{c_F}\int_I \varphi''(w) D^2(w) f_F(w,t) dw \\
&+ \frac{1}{2}\frac{\hat{\varsigma}^2\rho}{c_{FL}}\int_I \varphi''(w)\hat{D}^2(w) f_F(w,t) dw.
\end{aligned} \tag{4.9}$$

Integrating back by parts the last expression we obtain the Fokker-Planck equation for the followers' opinion distribution

$$\begin{aligned}
\frac{\partial f_F}{\partial t} + \frac{\partial}{\partial w}\left(\frac{1}{c_F}K_F[f_F](w) + \frac{1}{c_{FL}}K_{FL}[f_L](w)\right) f_F(w) = \\
\frac{1}{2}\frac{\partial^2}{\partial \tilde{w}^2}\left(\frac{\varsigma^2}{c_F}\tilde{D}^2(\tilde{w}) + \frac{\hat{\varsigma}^2\rho}{c_{FL}}\right) f_F(w),
\end{aligned} \tag{4.10}$$

where

$$\begin{aligned}
K_F[f_F](w) &= \int_I P(w,v)(v-w) f_F(v,t) dv, \\
K_{FL}[f_L](w) &= \int_I S(w,\tilde{w})(\tilde{w}-w) f_L(\tilde{w}) d\tilde{w}.
\end{aligned} \tag{4.11}$$

Following the same strategy we obtain the analogous result for the leaders' opinion distribution

$$\begin{aligned}
\frac{\partial f_L}{\partial t} + \frac{\partial}{\partial \tilde{w}}\left(\frac{\rho}{c_L}H[f_L](\tilde{w}) + \frac{1}{c_L}K_L[f_L](\tilde{w})\right) f_L(\tilde{w}) = \\
\frac{1}{2}\frac{\tilde{\varsigma}^2\rho}{c_L}\frac{\partial^2}{\partial \tilde{w}^2}\tilde{D}^2(\tilde{w}) f_L(\tilde{w})
\end{aligned} \tag{4.12}$$

where

$$K[f_L](\tilde{w}) = \int_I R(\tilde{w},\tilde{v})(\tilde{v}-\tilde{w}) f_L(\tilde{v},t) d\tilde{v} \tag{4.13}$$

and

$$H[f_L](\tilde{w}) = \frac{2\psi}{\kappa}\left(\tilde{w} + m_L(t) - 2w_d\right) + \frac{2\mu}{\kappa}\left(\tilde{w} + m_L(t) - 2m_F(t)\right). \tag{4.14}$$

Steady state solutions In this section we show that in some cases it is possible to find explicit stationary states of the Fokker-Planck system of equation described in (4.10) and (4.12). Here we restrict to the simplified situation where every interaction function is constant and unitary, i.e. $P \equiv S \equiv R \equiv 1$, and

$$D(w) = \tilde{D}(w) = \hat{D}(w) = 1 - w^2. \tag{4.15}$$

The steady state of equations (4.10) and (4.12) is solution of the following equations

$$\begin{aligned} \left(\frac{1}{c_F}(m_F - w) + \frac{\rho}{c_{FL}}(m_L - w)\right) f_{F,\infty} = \\ \frac{1}{2}\left(\frac{\varsigma^2}{c_F} + \frac{\hat{\varsigma}^2\rho}{c_{FL}}\right)\frac{\partial}{\partial w} D^2(w) f_{F,\infty}, \end{aligned} \tag{4.16}$$

and

$$\begin{aligned} \left(\frac{2\psi}{\kappa}[\tilde{w} - 2w_d - m_L] + \frac{2\mu}{\kappa}[\tilde{w} - 2m_F + m_L]\right) f_{L,\infty} = \\ \frac{1}{2}\frac{\tilde{\varsigma}^2\rho}{c_L}\frac{\partial}{\partial \tilde{w}} D^2(\tilde{w}) f_{L,\infty}. \end{aligned} \tag{4.17}$$

As soon as $t \to \infty$, thanks to equation (4.3), the followers and the leaders' mean opinion m_F and m_L relax to the desired opinion w_d. Then

$$\left(\frac{1}{c_F} + \frac{\rho}{c_{FL}}\right)(w_d - w) f_{F,\infty} = \frac{1}{2}\left(\frac{\varsigma^2}{c_F} + \frac{\hat{\varsigma}^2\rho}{c_{FL}}\right)\frac{\partial}{\partial w} D^2(w) f_{F,\infty}, \tag{4.18}$$

that is

$$\left(\frac{1}{c_F} + \frac{\rho}{c_{FL}}\right)(w_d - w)\frac{g_F}{D^2(w)} = \frac{1}{2}\left(\frac{\varsigma^2}{c_F} + \frac{\hat{\varsigma}^2\rho}{c_{FL}}\right)\frac{\partial}{\partial w} g_F \tag{4.19}$$

where $g_F = D^2(w) f_{F,\infty}$. This implies

$$g_{F,\infty} = a_F \exp\left\{-\frac{2}{b_F}\int_0^w \frac{z - w_d}{(1 - z^2)^2} dz\right\}, \qquad b_F = \frac{\varsigma^2 c_{FL} + \hat{\varsigma}^2 c_F \rho}{c_{FL} + c_F \rho}, \tag{4.20}$$

and a_F is a normalization constant such that $\int_I g_{F,\infty} dw = 1$. Finally we have

$$f_{F,\infty} = \frac{a_F}{(1 - w^2)^2} \exp\left\{-\frac{2}{b_F}\int_0^w \frac{z - w_d}{(1 - z^2)^2} dz\right\}. \tag{4.21}$$

Similarly we can find the steady state $f_{L,\infty}$ as a solution of the equation

$$-\left(\frac{2\psi}{\kappa} + \frac{2\mu}{\kappa}\right)(w_d - \tilde{w})\frac{g_{L,\infty}}{D^2(\tilde{w})} = \frac{1}{2}\frac{\tilde{\varsigma}^2\rho}{c_L}\frac{\partial}{\partial \tilde{w}} g_{L,\infty}, \tag{4.22}$$

where $g_{L,\infty} = f_{L,\infty} D^2(w)$. The solution of the differential equation (4.22) is given by

$$g_{L,\infty} = a_L \exp\left\{-\frac{2}{b_L}\int_0^{\tilde{w}} \left(\frac{z - w_d}{(1-z^2)^2}\right) dz\right\}, \qquad b_L = \frac{\bar{\varsigma}\rho\kappa}{2c_L(\psi+\mu)}, \quad (4.23)$$

and a_L is chosen such that the mass of $g_{L,\infty}$ is equal to ρ. Then the steady state is

$$f_{L,\infty} = \frac{a_L}{(1-\tilde{w}^2)^2} \exp\left\{-\frac{2}{b_L}\int_0^{\tilde{w}} \left(\frac{z - w_d}{(1-z^2)^2}\right) dz\right\}. \quad (4.24)$$

1.5 Numerical Simulation

In this section we present several numerical results concerning the numerical simulation of the Boltzmann type control model introduced in the previous paragraphs. All the results have been computed by a Monte Carlo method for the Boltzmann model (see [145] for more details) in the Fokker-Planck regime $\varepsilon = 0.01$ under the scaling (3.1). In the numerical tests we assume that the five per cent of the population is composed by opinion leaders, see for example [82]. Note that, for clarity, in all figures the leaders' profiles have been magnified by a factor 10. The regularization term in the control is fixed to $\nu = 1$. The random diffusion effects have been computed in the case (4.15) for a uniform random variable with scaled variance $\varsigma^2 = \tilde{\varsigma}^2 = \hat{\varsigma}^2 = 0.01$. It is easy to check that the above choices preserve the bounds in the numerical simulations. First we present some test cases with a single population of leaders as discussed in our theoretical analysis. Then we consider the case of multiple leaders' populations with different time-dependent strategies. This leads to more realistic applications of our arguments, introducing the concept of competition between leaders' populations. For the sake of simplicity we fix constant interaction functions $P(\cdot,\cdot) \equiv 1$ and $R(\cdot,\cdot) \equiv 1$ and the remaining scaled computational parameters have been summarized in Table 5.1.

Test	$S(\cdot,\cdot)$	c_F	$\hat{c}_{FL}$	$\hat{c}_L$	ρ	ψ	w_d					
1a	1	1	0.1	0.1	0.05	0.5	0.5					
1b	(5.3)	1	0.1	0.1	0.05	0.5	0.5					
	$S(\cdot,\cdot)$	c_F	$\hat{c}_{FL_1}$	$\hat{c}_{L_1}$	ρ_1	ψ_1	w_{d_1}	$\hat{c}_{FL_2}$	$\hat{c}_{L_2}$	ρ_2	ψ_2	w_{d_2}
2	1	1	0.1	0.1	0.05	0.5	0.5	0.1	0.1	0.05	0.5	-0.5
3	1	1	0.1	0.1	0.05	(5.7)	0.5	1	0.1	0.05	(5.7)	-0.5

Table 5.1: Computational parameters for the different test cases.

Test 1. Leaders driving followers In the first test case we consider a single population of leaders driving followers described by the following

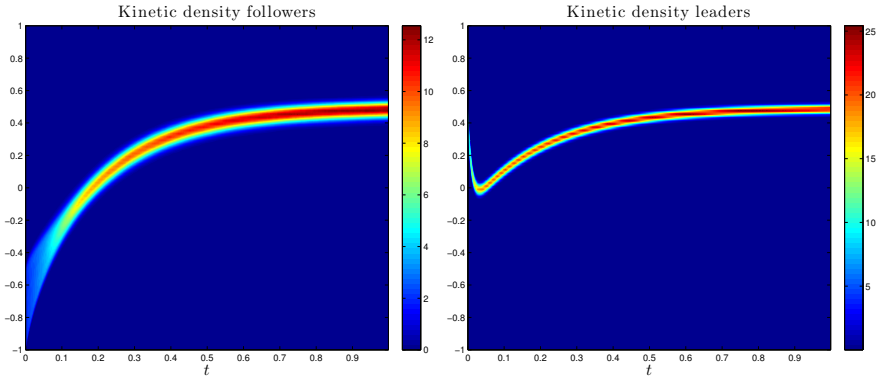

Figure 5.1: Test 1a: Kinetic densities evolution over the time interval $[0, 1]$ for a single population of leaders.

system of Boltzmann equations

$$\begin{cases} \dfrac{d}{dt}\displaystyle\int_I \varphi(w) f_F(w,t)dw = (Q_F(f_F, f_F), \varphi) + (Q_{FL}(f_F, f_L), \varphi) \\ \dfrac{d}{dt}\displaystyle\int_I \varphi(\tilde{w}) f_L(\tilde{w},t)d\tilde{w} = (Q_L(f_L, f_L), \varphi)\,. \end{cases} \tag{5.1}$$

Numerical experiments show that the optimal control problem is capable to introduce a non monotone behaviour of $m_L(t)$. We report the evolution, over the time interval $[0, 1]$, of the the kinetic densities $f_F(w, t)$ and $f_L(\tilde{w}, t)$ in Figure 5.1 for constant interaction functions P, R and S. The initial distributions $f_F \sim U([-1, -0.5])$ and $f_L \sim N(w_d, 0.05)$ where $U(\cdot)$ and $N(\cdot, \cdot)$ denote, as usual, the uniform and the normal distributions. We used the compact notations

$$\hat{c}_{FL} = c_{FL}/\rho, \qquad \hat{c}_L = c_L/\rho. \tag{5.2}$$

This non monotone behaviour shows that the leaders use a combination of populistic and radical strategy to drive the followers towards their desired state. In an electoral context, this is a characteristic which can be found in populistic radical parties, which typically include non-populist ideas and their leadership generates through a dense network of radical movements [140].

Next we consider a bounded confidence model for the leader-follower interaction with

$$S(w, \tilde{w}) = \chi(|w - \tilde{w}| \leq \Delta), \tag{5.3}$$

where $0 \leq \Delta \leq 2$. In the simulation we assume $\Delta = 0.5$ and use the same initial data of the previous case. It is interesting to observe how the model is capable to reproduce a realistic behavior where the leaders first are able to attract a small group of followers which subsequently are capable to drive the whole majority towards the desired state (see Figures 5.2 and 5.3).

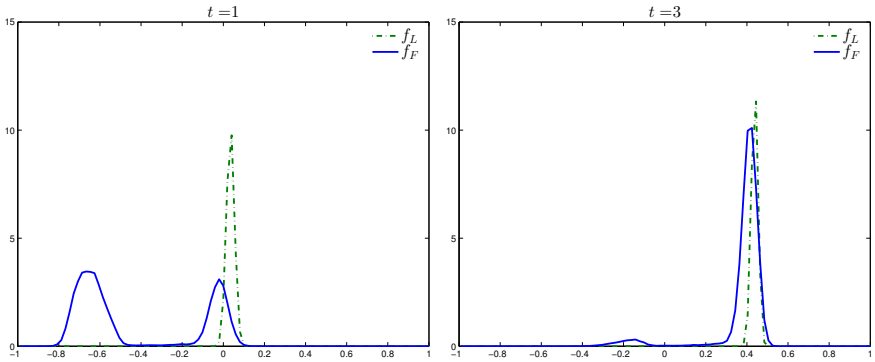

Figure 5.2: Test 1b: Kinetic densities at different times for a single population of leaders with bounded confidence interaction.

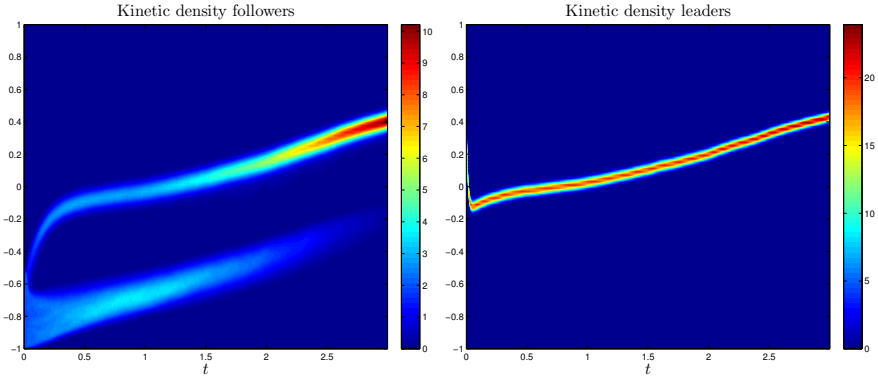

Figure 5.3: Test 1b: Kinetic densities evolution over the time interval $[0, 3]$ for a single population of leaders with bounded confidence interaction.

Test 2. The case of multiple leaders populations Similarly, if more than one population of leaders occurs, each one with a different strategy, we can describe the evolution of the kinetic density of the system through a Boltzmann approach. Let $M > 0$ be the number of families of leaders, each of them described by the density $f_{L_p}, p = 1, ..., M$ such that

$$\int_I f_{L_p}(\tilde{w}) d\tilde{w} = \rho_p. \tag{5.4}$$

If we suppose that an unique population of followers does exist, with density f_F, and that every follower interacts both with the others agents from the same population and with every leader of each p-th family, for a suitable test

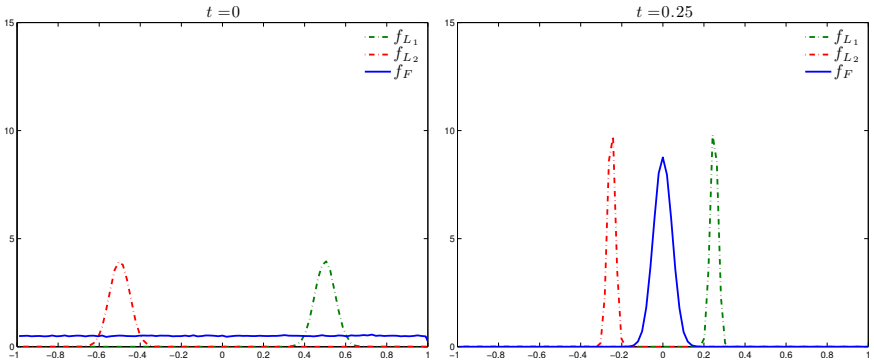

Figure 5.4: Test 2: Kinetic densities at different times reproducing a Hotelling-like model behaviour for two populations of leaders.

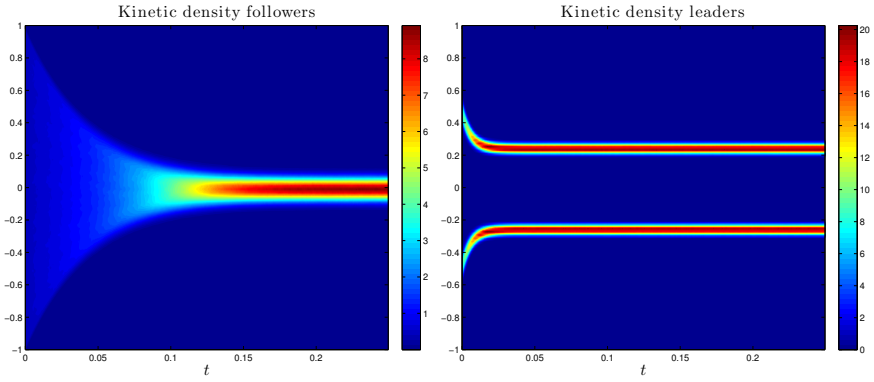

Figure 5.5: Test 2: Kinetic densities evolution over the time interval $[0, 0.25]$ reproducing a Hotelling-like model behaviour for two populations of leaders.

function φ we obtain the following system of Boltzmann equations

$$\begin{cases} \dfrac{d}{dt}\displaystyle\int_I \varphi(w) f_F(w,t)dw = (Q_F(f_F,f_F),\varphi) + \sum_{p=1}^{M} \big(Q_{FL}(f_{L_p},f_F),\varphi\big) \\ \dfrac{d}{dt}\displaystyle\int_I \varphi(\tilde{w}) f_{L_p}(\tilde{w},t)d\tilde{w} = (Q_L(f_{L_p},f_{L_p}),\varphi), \qquad p=1,\dots,M. \end{cases} \tag{5.5}$$

We assume that the leaders aim at minimising cost functionals of the type (2.8) and therefore the differences consist in two factors: the target opinions w_{d_p} and in the leaders' attitude towards a radical ($\psi_p \approx 1$) or populistic strategy ($\mu_p \approx 1$). We therefore introduce the analogous rescaling (3.1) and we define

$$\hat{c}_{FL_p} = c_{FL_p}/\rho_p, \quad \hat{c}_{L_p} = c_{L_p}/\rho_p, \quad p=1,\dots,M. \tag{5.6}$$

In the numerical test we establish a link between our arguments and a Hotelling's type model [118]. The model describes how two shop owners, which sell the same product at the same price in the same street, must locate their shops in order to reach the maximum number of customers, uniformly distributed along the street (in other words, in order to maximize their profits). Paradoxically the model yields that the equilibrium, without changing prices, is reached if they get closer. In the cited original paper electoral dynamics are placed in this context and it can be regarded as the reason why political parties' programs are often perceived as similar. We consider the case of two populations of leaders, described by the densities f_{L_1} and f_{L_2}, exercising different controls over a population of followers uniformly distributed within the interval $I=[-1,1]$. Initially the leaders are distributed as $f_{L_p} \sim N(w_{d_p}, 0.05)$, $p=1,2$. We can observe that the model leads to a centrist population of followers, whose opinion spreads in a range between leaders' mean opinions (see Figures 5.4 and 5.5).

Test 3. Two leaders populations with time-dependent strategies Finally we introduce a multi-population model for opinion formation with time-dependent coefficients. This approach leads to the concept of adaptive strategy for every family of leaders $p=1,...,M$. The coefficients ψ and μ which appear into the functional now evolve in time and are defined for every $t\in[0,T]$ as

$$\begin{aligned} \psi_p(t) =& \frac{1}{2}\int_{w_{d_p}-\delta}^{w_{d_p}+\delta} f_F(w)dw + \frac{1}{2}\int_{m_{L_p}-\bar{\delta}}^{m_{L_p}+\bar{\delta}} f_F(w)dw \\ \mu_p(t) =& 1-\psi_p(t) \end{aligned} \tag{5.7}$$

where both $\delta,\bar{\delta}\in[0,1]$ are fixed and m_{L_p} is the average opinion of the p-th leader. This choice of coefficients is equivalent to introduce a competition

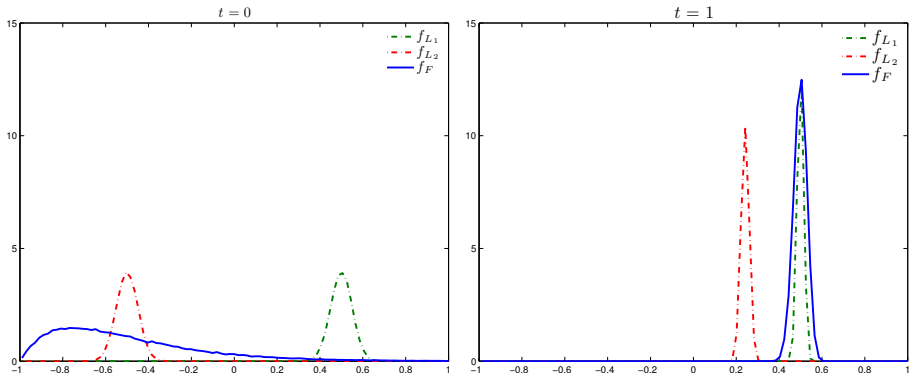

Figure 5.6: Test 3: Kinetic densities at different times for for a two populations of leaders model with time dependent strategies.

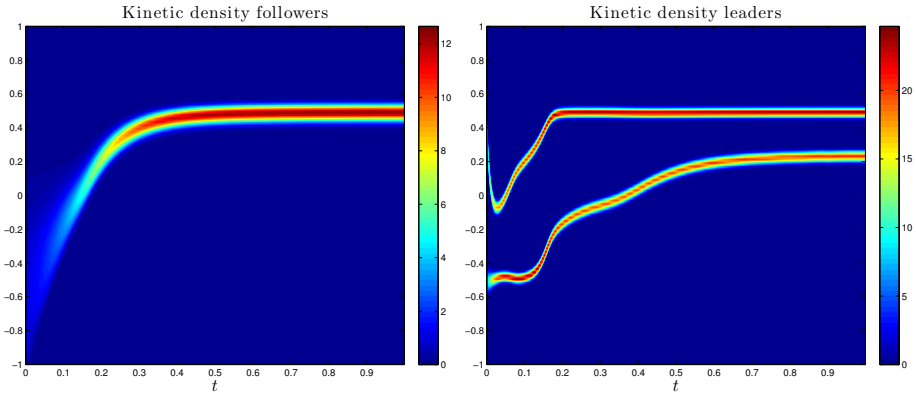

Figure 5.7: Test 3: Kinetic density evolution over the time interval $[0, 1]$ for a two populations of leaders model with time dependent strategies.

between the populations of leaders, where each leader try to adapt its populistic or radical attitude accordingly to the success of the strategy. Note also that the success of the strategy is based on the local perception of the followers.

In the numerical experiments reported in Figure 5.6 and Figure 5.7 we take into account two populations of leaders, initially normally distributed with mean values w_{d_1} and w_{d_2} and parameters $\delta = \bar{\delta} = 0.5$, respectively, and a single population of followers, represented by a skewed distribution $f_F \sim \Gamma(2, \frac{1}{4})$ over the interval $[-1, 1]$, where $\Gamma(\cdot, \cdot)$ is the Gamma distribution. Here the frequencies of interactions are assumed to be unbalanced since $\hat{c}_{FL_1} = 0.1$ and $\hat{c}_{FL_2} = 1$. In the test case we assume that the followers group has an initial natural inclination for a position represented by one leader but, thanks to communication strategies pursued by the minority leader, it is driven to different positions (see Figures 5.6 and 5.7). In a bipolar electoral

context, an example of the described behaviour would be a better use of the media in a coalition with respect to the opponents.

1.6 Conclusions

We introduced a Boltzmann type control for a hierarchical model of opinion formation where the leader behaviour is influenced both by the desire to achieve a prescribed opinion consensus and by the mean opinion of the followers. The main novelty of the method is that, thanks to an instantaneous binary control approximation, the control is explicitly incorporated in the resulting leader dynamics. The use of instantaneous control and the kinetic description permit to pass from an $O(N^2)$ dynamics, which must be solved forward-backward in time, to a much simpler forward $O(N)$ stochastic simulation. This is of paramount importance in view of possible applications of this kind of constrained opinion modeling. In the so-called quasi invariant opinion limit the corresponding Fokker-Planck descriptions have been derived and explicit expressions of their steady states computed. Several numerical examples illustrate the robustness of the controlled dynamics using various leaders strategies even in presence of different groups of competing leaders.

Chapter 2

Optimal control of opinion dynamics over complex networks

2.1 Introduction

Graph theory has emerged in recent years as one of the most active fields of research [3, 21, 24, 175]. In fact, the study of technological and communication networks earned a special attention thanks to a huge amount of data coming from empirical observations and more recently from online platforms like Facebook, Twitter, Instagram and many others. This fact offered a real laboratory for testing on a large-scale the collective behavior of large populations of agents [123, 159] and new challenges for the scientific research has emerged. In particular, the necessity to handle millions, and often billions, of vertices implied a substantial shift to large-scale statistical properties of graphs giving rise to the study of the so-called scale-free networks [21, 143, 175].

In this work, we will focus our attention on the modelling and control of opinion dynamics on a time evolving network. We consider a system of agents, each one belonging to a node of the network, interacting only if they are connected through the network. Each agent modifies his/her opinion through a compromise function which depends both on opinions and the network [6, 11, 13, 61, 72, 172]. At the same time new connections are created and removed from the network following a preferential attachment process. For simplicity here we restrict to non-growing network, that is a graph where the total number of nodes and the total number of edges are conserved in time. An optimal control problem is then introduced in order to drive the agents toward a desired opinion. The rest of the chapter is organized as follows. In Section 6.2 we describe the alignment model for opinions spreading on a non-growing network. In order to control the trajectories of the model we

introduce in Section 2.3 a general setting for a control technique weighted by a function on the number of connections. A numerical method based on model predictive control is then developed. Finally in Section 6.5 we perform numerical experiments showing the effectiveness of the present approach. Some conclusion are then reported in the last Section.

2.2 Modeling opinion dynamics on networks

In the model each agent $i = 1, \dots, N$ is characterized by two quantities $(w_i, c_i), i = 1, \dots, N$, representing the opinion and the number of connections of the agent ith respectively. This latter term is strictly related to the architecture of the social graph where each agent shares its opinion and influences the interaction between individuals. Each agent is seen here as a node of a time evolving graph $\mathcal{G}^N = \mathcal{G}^N(t), t \in [t_0, t_f]$ whose nodes are connected through a given set of edges. In the following we will indicates the density of connectivity the constant $\gamma \geq 0$.

2.2.1 Network evolution without nodes' growth

In the sequel we will consider a graph with both a fixed number of nodes N and a fixed number of edges E. In order to describe the network's evolution we take into account a preferential attachment probabilistic process. This mechanism, known also as Yule process or Matthew effect, has been used in the modeling of several phenomena in biology, economics and sociology, and it is strictly connected to the generation of power law distributions [21, 175]. The initial state of the network, $\mathcal{G}^N(0)$, is chosen randomly and, at each time step an edge is randomly selected and removed from the network. At the same time, a node is selected with probability

$$\Pi_\alpha(c_i) = \frac{c_i + \alpha}{\sum_{j=0}^{N}(c_j + \alpha)} = \frac{c_i + \alpha}{2E + N\alpha}, \qquad i = 1, \dots, N, \tag{2.1}$$

among all possible nodes of $\mathcal{G}^N$, with $\alpha > 0$ an attraction coefficient. Based on the probability (2.1) another node is chosen at time t and connected with the formerly selected one. The described process is repeated at each time step. In this way both the number of nodes and the total number of edges remains constant in the reference time interval. Let $p(c, t)$ indicates the probability that a node is endowed of degree the c at time t. We have

$$\sum_c p(c, t) = 1, \qquad \sum_c c\, p(c, t) = \gamma. \tag{2.2}$$

The described process may be described by the following master equation [14]

$$\begin{aligned}\frac{d}{dt}p(c,t) =& \frac{D}{E}\left[(c+1)p(c+1,t) - cp(c,t)\right] \\ &+ \frac{2D}{2E+N\alpha}\left[(c-1+\alpha)p(c-1,t) - (c+\alpha)p(c,t)\right],\end{aligned} \tag{2.3}$$

where $D > 0$ characterizes the relaxation velocity of the network toward an asymptotic degree distribution $p_\infty(c)$, the righthand side consists of four terms, the first and the third terms account the rate of gaining a node of degree c and respectively the second and fourth terms the rate of losing a node of degree c. The equation (2.22) holds in the interval $c \leq E$, whereas for each $c > E$ we set $p(c,t) = 0$. While most the random graphs models with fixed number of nodes and vertices produces unrealistic degree distributions like the Watts and Strogatz generation model, called small-world model [171], the main advantage of the graph generated through the described rewiring process stands in the possibility to recover the scale-free properties. Indeed we can easily show that if $\gamma = 2E/N \geq 1$ with attraction coefficient $\alpha \ll 1$ then the stationary degree distribution $p_\infty(c)$ obeys a power-law of the following form

$$p_\infty(c) = \left(\frac{\alpha}{\gamma}\right)^\alpha \frac{\alpha}{c}. \tag{2.4}$$

When $\alpha \gg 1$ we loose the features of the preferential attachment mechanism, in fact high degree nodes are selected approximately with the same probability of the nodes with low degree of connection. Then the selection occurs in a non preferential way and the asymptotic degree distribution obeys the Poisson distribution

$$p_\infty(c) = \frac{e^{-\gamma}}{c!}\gamma^c. \tag{2.5}$$

A simple graph is sketched in Figure 2.1 where we can observe how the initial degree of the nodes influences the evolution of the connections. In order to correctly observe the creation of the new links, that preferentially connect nodes with the highest connection degree, we marked each node with a number $i = 1, \ldots, 20$ and the nodes' diameters are proportional with their number of connections.

2.2.2 The opinion alignment dynamics

The opinion of the ith agent ranges in the closed set $I = [-1, 1]$, that is $w_i = w_i(t) \in I$ for each $t \in [t_0, t_f]$, and its opinion changes over time according to the following differential system

$$\dot{w}_i = \frac{1}{|S_i|}\sum_{j \in S_i} P_{ij}(w_j - w_i), \qquad i = 1, \ldots, N \tag{2.6}$$

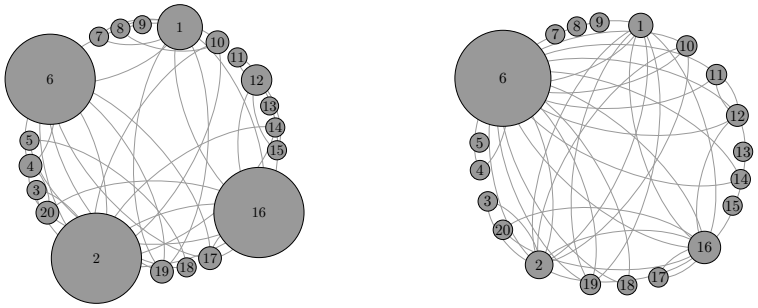

Figure 2.1: Left: initial configuration of the sample network $\mathcal{G}^{20}$ with density of connectivity $\gamma = 5$. Right: a simulation of the network $\mathcal{G}^{20}$ after 10 time steps of the preferential attachment process. The diameter of each node is proportional to its degree of connection.

where S_i indicates the set of vertex connected with the ith agent and reflects the architecture of the chosen network, whereas $c_i = |S_i| < N$ stands for the cardinality of the set S_i, also known as degree of vertex i. Note that the number of connections c_i evolves in time accordingly to the process described in Section 2.2.1. Furthermore we introduced the interaction function $P_{ij} \in [0, 1]$, depending on the opinions of the agents and the graph $\mathcal{G}^N$ which can be written as follows

$$P_{ij} = P(w_i, w_j; \mathcal{G}^N). \tag{2.7}$$

A possible choice for the interaction function is the following

$$P(w_i, w_j; \mathcal{G}^N) = H(w_i, w_j)K(\mathcal{G}^N), \tag{2.8}$$

where $H(\cdot, \cdot)$ represents the positive compromise propensity, and K a general function taking into account statistical properties of the graph $\mathcal{G}$. In what follows we will consider $K = K(c_i, c_j)$, a function depending on the vertices' connections.

2.3 Optimal control problem of the alignment model

In this section we introduce a control strategy which characterizes the action of an external agent with the aim of driving opinions toward a given target w_d. To this goal, we consider the evolution of the network $\mathcal{G}^N(t)$ and the opinion dynamics in the interval $[t_0, t_f]$. Therefore we introduce the

following optimal control problem

$$\min_{u\in\mathcal{U}} J(\mathbf{w},u) := \frac{1}{2}\int_{t_0}^{t_f}\Big\{\frac{1}{N}\sum_{j=1}^{N}(w_j(s)-w_d)^2+\nu u(s)^2\Big\}ds, \tag{3.1}$$

subject to

$$\dot{w}_i = \frac{1}{|S_i|}\sum_{j\in S_i} P_{ij}(w_j-w_i)+u\chi(c_i\geq c^*), \quad w_i(0)=w_i^0, \tag{3.2}$$

where we indicated with $\mathcal{U}$ the set of admissible controls, with $\nu>0$ a regularization parameter which expresses the strength of the control in the overall dynamics and $w_d\in[-1,1]$ the target opinion. Note that the action of the control u is weighted by an indicator function $\chi(\cdot)$, which is active only for the nodes with degree $c_i\geq c^*$. In general this selective control approach models an a-priori strategy of a policy maker, possibly acting under limited resources or unable to influence the whole ensemble of agents. For example we can consider a varying horizon control acting on a fixed portion of connected agents.

The solution of this kind of control problems is in general a difficult task, given that their direct solution is prohibitively expensive for a large number of agents. Different strategies have been developed for alignment modeling in order to obtain feedback controls or more general numerical control techniques [5, 6, 11, 13, 32, 174, 117]. To tackle numerically the described problem a standard strategy makes use of a model predictive control (MPC) approach, also referred as receding horizon strategy.

In general MPC strategies solves a finite horizon open-loop optimal control problem predicting the dynamic behavior over a predict horizon $t_p\leq t_f$, with initial state sampled at time t (initially $t=t_0$), and computing the control on a control horizon $t_c\leq t_p$. The optimization is computed introducing a new integral functional $J_p(\cdot,\cdot)$, which is an approximation of (3.1) on the time interval $[t,t+t_p]$, namely

$$J_p(\mathbf{w},\bar{u}) := \frac{1}{2}\int_{t}^{t+t_p}\Big\{\frac{1}{N}\sum_{j=1}^{N}(w_j(s)-w_d)^2+\nu_p\bar{u}(s)^2\Big\}ds \tag{3.3}$$

where the control, $\bar{u}:[t,t+t_p]\to\mathcal{U}$, is supposed to be an admissible control in the set of admissible control $\mathcal{U}$, subset of $\mathbb{R}$, and ν_p a possibly different penalization parameter with respect to the full optimal control problem. Thus the computed optimal open-loop control $\bar{u}(\cdot)$ is applied feedback to the system dynamics until the next sampling time $t+t_s$ is evaluated, with $t_s\leq t_c$, thereafter the procedure is repeated taking as initial state of the dynamics at time $t+t_s$ and shifting forward the prediction and control horizons, until the final time t_f is reached. This process generates a sub-optimal solution with respect to the solution of the full optimal control problem (3.1)-(3.2).

Let us consider now the full discretize problem, defining the time sequence $[t_0, t_1, \dots, t_M]$, where $t_n - t_{n-1} = t_s = \Delta t > 0$ and $t_M := M\Delta t = t_f$, for all $n = 1, \dots, M$, assuming furthermore that $t_c = t_p = p\Delta t$, with $p > 0$. Hence the linear MPC method look for a piecewise control on the time frame $[t_0, t_M]$, defined as follows

$$\bar{u}(t) = \sum_{n=0}^{M-1} \bar{u}^n \chi_{[t_n, t_{n+1}]}(t). \tag{3.4}$$

In order to discretize the evolution dynamics we consider a Runge-Kutta scheme, the full discretized optimal control problem on the time frame $[t_n, t_n + p\Delta t]$ reads

$$\min_{\bar{u}\in\mathcal{U}} J_p(\mathbf{w}, \bar{u}) := \frac{1}{2} \int_{t_n}^{t_n + p\Delta t} \Big\{ \frac{1}{N} \sum_{j=1}^{N} (w_j(s) - w_d)^2 + \nu_p \bar{u}^2 \Big\} ds \tag{3.5}$$

subject to

$$\begin{aligned} W_{i,l}^{(n)} &= w_i^n + \Delta t \sum_{k=1}^{s} a_{l,k} \left(F(t + \theta_k \Delta t, W_{i,k}^{(n)}) + \bar{U}_k^{(n)} Q_i(t + \theta_k \Delta t) \right), \\ w_i^{n+1} &= w_i^n + \Delta t \sum_{l=1}^{s} b_l \left(F(t + \theta_l \Delta t, W_{i,l}^{(n)}) + \bar{U}_l^{(n)} Q_i(t + \theta_l \Delta t) \right), \\ w_i^n &= w_i(t_n), \end{aligned} \tag{3.7}$$

for all $n = 1, \dots, p-1$; $l = 1, \dots, s$; $i, \dots, N$ and having defined the following functions

$$F(t, w_i) = \frac{1}{|S_i(t)|} \sum_{j \in S_i(t)} P_{ij}(w_j - w_i), \quad Q_i(t) = \chi(c_i(t) \geq c^*).$$

The coefficients $(a_{l,k})_{l,k}$, $(b_l)_l$ and $(\theta_l)_l$, with $l, k = 1, \dots, s$, define the Runge-Kutta method and $(\bar{U}^{(n)})_l, (W_{i,l}^{(n)})_l$ are the internal stages associated to $\bar{u}(t), w_i(t)$ on time frame $[t_n, t_{n+1}]$.

2.3.1 Instantaneous control

Let us restrict to the case of a single prediction horizon, $p = 1$, where we discretize the dynamics with an explicit Euler scheme ($a_{1,1} = \theta_1 = 0$ and $b_1 = 1$). Notice that since the control $\bar{u}$ is a constant value and assuming that the network, $\mathcal{G}^N$ remains fixed over the time interval $[t_n, t_n + \Delta t]$ the discrete optimal control problem (3.5) reduces to

$$\min_{\bar{u}\in\mathcal{U}} J_p(\mathbf{w}, \bar{u}^n) := \Delta t \Big\{ \frac{1}{N} \sum_{j=1}^{N} (w_j^{n+1}(\bar{u}^n) - w_d)^2 + \nu_p (\bar{u}^n)^2 \Big\} \tag{3.8}$$

with

$$w_i^{n+1} = w_i^n + \Delta t \left(F(t_n, w_i^n) + \bar{u}^n Q_i^n \right), \quad w_i^n = w_i(t_n). \tag{3.9}$$

In order to find the minima of (3.5) is sufficient to find the value $\bar{u}$ satisfying $\partial_{\bar{u}} J_p(\mathbf{w}, \bar{u}) = 0$, which can be computed by a straightforward calculation

$$\bar{u}^n = -\frac{1}{N\nu + \Delta t \sum_{j=1}^N (Q_j^n)^2} \left(\sum_{j=1}^N Q_j^n \left(w_j^n - w_d \right) + \Delta t \sum_{j=1}^N Q_j^n F(t_n, w_i^n) \right). \tag{3.10}$$

where we scaled the penalization parameter with $\nu_p = \Delta t \nu$.

2.4 Numerical results

In this section we present some numerical results in order to show the main features of the control introduced in the previous paragraphs. We considered a population of $N = 100$ agents, each of them representing a node of an undirected graph with density of connectivity $\gamma = 30$. The network $\mathcal{G}^{100}$ evolves in the time interval $[0, 50]$ with attraction coefficient $\alpha = 0.01$ and represents a single sample of the evolution of the master equation (2.22) with $D = 20$. The control problem is solved by the instantaneous control method described in Remark 2.3.1 with $\Delta t = 5\ 10^{-2}$. In Figure 4.3 we present the evolution over the reference time interval of the constrained opinion dynamics. The interaction terms have been chosen as follows

$$K(c_i, c_j) = e^{-\lambda c_i} \left(1 - e^{-\beta c_j} \right), \qquad H(w_i, w_j) = \chi(|w_i - w_j| \leq \Delta), \tag{4.1}$$

where the function $H(\cdot, \cdot)$ is a bounded confidence function with $\Delta = 0.4$, while $K(\cdot, \cdot)$ defines the interactions between the agents i and j taking into account that agents with a large number of connections are more difficult to influence and at the same time they have more influence over other agents. The action of the control is characterized by a parameter $\kappa = 0.1$ and target opinion $w_d = 0.8$. We present the resulting opinion dynamics for a choice of constants $\lambda = 1/100, \beta = 1$ in Figure 4.2. We report the evolution of the network and of the opinion in Figure 4.3, here the diameter of each node is proportional with its degree of connection whereas the color indicates its opinion. As a measure of consensus over the agents we introduce the quantity

$$V_{w_d} = \frac{1}{N-1} \sum_{i=1}^N (w_i(t_f) - w_d)^2, \tag{4.2}$$

where $w_i(t_f)$ is the opinion of the ith agent at the final time t_f. In Figure 4.4 we compare different values of V_{w_d} as a function of c^*. Here we calculated

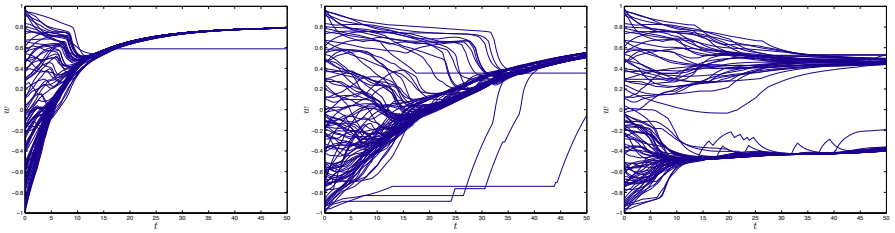

(a) $c^* = 10$ (b) $c^* = 20$ (c) $c^* = 30$

Figure 4.2: Evolution of the constrained opinion dynamics with uniform initial distribution of opinions over the time interval $[0, 50]$ for different values of $c^* = 10, 15, 30$ with target opinion $w_d = 0.8$, control parameter $\kappa = 0.1$, $\Delta t = 10^{-3}$ and confidence bound $\Delta = 0.4$.

the size of the controlled agents and the values of V_{w_d} both, starting from a given uniform initial opinion and the same graph with initial uniform degree distribution. It can be observed how the control is capable to drive the overall dynamics toward the desired state acting only on a portion of the nodes.

2.5 Conclusions and perspectives

In this short note we focus our attention on a control problem for the dynamic of opinion over a time evolving network. We show that the introduction of a suitable selective control depending on the connection degree of the agent's node is capable to drive the overall opinion toward consensus. In a related work we have considered this problem in a mean-field setting where the number of agents, and therefore nodes, is very large [14]. In future works we plan to concentrate on the model predictive control setting, where the evolution of the control is based on the evolution of the network, and on the case with varying prediction horizon acting on a given portion of the agents.

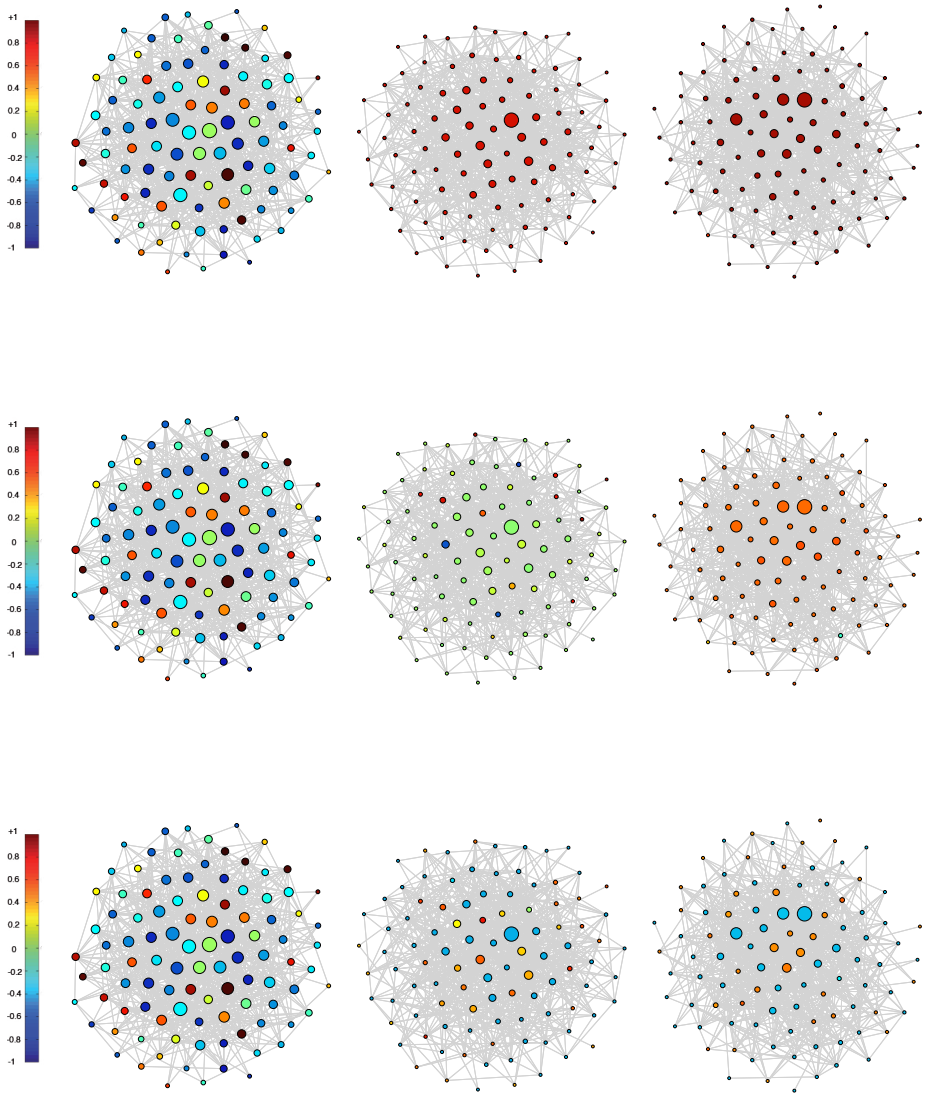

Figure 4.3: Evolution of opinion and connection degree of each node of the previously evolved graph $\mathcal{G}^{100}$. From left to right: graph at times $t = 0, 25, 50$. From the top: opinion dynamics for threshold values $c^* = 10, 20, 30$. The target opinion is set $w_d = 0.8$ and the control parameter $\kappa = 0.1$.

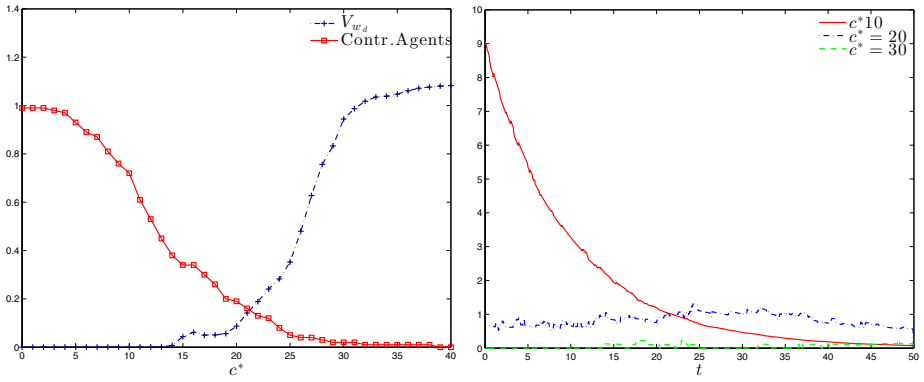

Figure 4.4: Left: the red squared plot indicates the size of the set of controlled agent at the final time t_f in dependence on c^* whereas the blue line indicates the mean square displacement V_{w_d}. Right: values of the control u at each time step for $c^* = 10, 20, 30$. In the numerical test we assumed $\Delta = 0.4, \Delta t = 5\ 10^{-2}, \kappa = 0.1$.

Chapter 3

Performance bounds for mean–field constrained dynamics

3.1 Introduction

In recent years many mathematical models of self-organized systems of interacting agents have been introduced in the literature, see for example [16, 19, 46, 67, 66, 68, 70, 71, 74, 94, 115, 119, 139, 145, 164] and the references therein. The general setting consists of a microscopic dynamics described by systems of ordinary differential equations where the evolution of the state of each agent is influenced by the collective behavior of all other agents. Examples in those microscopic interacting systems are frequently seen in the real world like: schools of fish, swarm of bees, herds of sheep, opinion formation in crowds and financial markets. Of interest is usually the case when the number of agents becomes very large. Here, the qualitative behavior is studied through a different level of description, i.e. through the introduction of distribution functions whose behavior is governed by kinetic (or fluid–dynamic) partial differential equations.

The control mechanisms of self–organized systems has been investigated recently as follow–up questions to the progress in mathematical modeling and simulation. The control of emergent behavior has been studied on the level of the microscopic agents [13, 33] as well as on the level of the kinetic [6, 11, 116] or fluid–dynamic equations [27, 65, 75, 89]. The contributions have to be further distinguished depending on the type of applied control. Without intending to review all literature we give some references on certain classes of control, e.g., sparse control [88], Nash equilibrium control [128], control using linearized dynamics and Riccati equations [115, 116] or control driven by other external dynamics [11, 82].

Here, we focus on a general method to construct a control mechanism,

called model predictive control (MPC). MPC utilizes the assumption that agents optimize their cost functional *not* necessarily over a large time horizon. Instead they determine their (locally best) action by minimizing their cost only over a short time interval which recedes as time evolves. The methodology of MPC is also called receding horizon control (or instantaneous control when the length of the horizon is equal to one). From the modeling point of view the fact that agents may be able to optimize strategically their trajectories over a small, but finite, interval of time opened several connections to socio–economic problems, where each agent, or a portion of them, is influenced in order to force the entire system toward specific patterns.

MPC has been used in the engineering community for over fifty years, see e.g. [134, 135, 136, 163] for an overview and further references. However, therein, only a small number of agents $M < \infty$ is considered and the optimization problems are then studied at the level of ODEs. The link between MPC on the level of agents and the MPC on the level of kinetic and fluid–dynamic equations has been subject to recent investigations [6, 75, 116], and also the relation between MPC and mean-field games [128] has been a subject to recent studies [73]. However, in *all* currently presented approaches on MPC in relation to mean-field limits the *special* case of a receding time horizon has been considered. While this is computationally advantageous, it is known to have some severe drawbacks: in the case of finitely many agents stability of the controlled system can expected only if the horizon is sufficiently *large*, the instability of the controlled system has been also observed numerically e.g. in [11]. Further, MPC leads to a control that is suboptimal compared with the theoretical optimal one, that is a control with infinite control horizon. Except for a very particular case [116] there is *no* result on the relation between the optimal control and the MPC approach in the mean-field limit.

In the case $M < \infty$ there has been recent progress on the relation between the time horizon for MPC and the stability as well as optimality estimates of MPC controls [105, 106, 107, 121]. In particular an estimate on the difference between MPC and optimal control has been given in [106, Corollary 4.5]. The theory therein covers finite and infinite dimensional phase spaces, but still requires the number M of agents to be *finite*.

The main purposes of the present work is to extend the theory presented in [106] to the limit case of infinitely many agents. The goal is to derive the corresponding mean-field results for the optimality estimates under the *same* assumptions as in the case $M < \infty$. While the presentation will cover a general dynamics we exemplify the results on a first–order alignment model, as an extension to models recently presented [6, 11].

The rest of the manuscript is organized as follows. First, in Section 3.2, we introduce some notations and results for an exemplified constrained model deriving its mean-field formulation and highlighting the main features

of the performance estimate for the MPC approach. In a more general setting, in Section 3.3, we define the objects of a mean-field optimal control problem subject to a given dynamics proving several estimates in relation to MPC. Here, an example is proposed with numerical results, in Section 3.4, confirming the theoretical analysis. In 5.6 we recall technical details.

3.2 Notation and motivating example

In this section, in order to clarify the notations and exemplify the aims of this work, we introduce a stylized problem which has been extensively investigated in several recent works on constrained alignment dynamics [5, 6, 13]. At the microscopic level, the mathematical description of collective motion is given by a nonlinear system of ordinary differential equations, from which the mean-field level may be obtained through specific assumptions [53, 66, 90]. Let us assume that $M > 0$ agents fulfill the dynamics in discretized form

$$x_{i,n+1} = x_{i,n} + \frac{\Delta t}{M} \sum_{j=1}^{M} P(x_{j,n} - x_{i,n}) + u_n \tag{2.1}$$

where $P \geq 0$ is a general interaction function that may also depend on variables $(x_{j,n})_{i=1}^{M}$ and $x_{i,n} = x_i(t^n) \in \mathcal{X} \subset \mathbb{R}$ is the state of the ith agent at time $t^n \geq 0$ with $t^n = n \in \mathbb{N}$. We denote by

$$X_n = (x_{i,n})_{i=1}^{M}, \qquad X_{-i,n} = (x_{j,n})_{j=1, j\neq i}^{M} \tag{2.2}$$

the state of the full system at time t^n and the state of the all agents except the ith agent, respectively. In the following we will drop the dependence on the time variable whenever the intention is clear. Moreover we assume that initial conditions $X(t^0) = X_0$ are given.

The control sequence $(u_n)_n$ is to be determined in order to minimize a given cost functional

$$J_\infty^u(X_0) := \sum_{n=0}^{\infty} \ell(X_n, u_n) \tag{2.3}$$

where X_n is the solution to (2.1) for the control $u_n \in U$, with $U \subset \mathbb{R}$ bounded, and initial datum $X(0) = X_0$. In (2.3) we introduce a general function $\ell : \mathbb{R}^M \times U \to \mathbb{R}$. Hence, the functional J depends on the initial datum X_0 as well as the choice of the control sequence $u = (u_n)_n$. The dependence of J on the time horizon is indicated by a subscript $+\infty$, whereas the dependence on the control by the superscript u. We assume here that there exists a solution u^* of the optimal control problem

$$u^* = \arg\min_u J_\infty^u(X_0). \tag{2.4}$$

From the computational point of view this approach is generally too expensive, therefore, a suboptimal approach named model predictive control (MPC) has been proposed. The leading idea of the MPC approach is to avoid the solution of the dynamics on the whole time interval by considering a closed-loop control for the considered model, see [44, 158] for an exhaustive introduction. In particular a control mechanism designed through a MPC might be interpreted as a strategy in the contest of the mean-field games [73].

(Single-step) MPC with receding time horizon N applies a control u of the type

$$u^{MPC}(t) = \sum_{n=0}^{\infty} u_n^{MPC} \chi_{[t^n, t^{n+1})}(t). \tag{2.5}$$

The unknown control actions $u_n^{MPC} \in \mathbb{R}$ are determined at each time t^n by

$$u_n^{MPC} = v_1 \tag{2.6}$$

where $(v_k)_{k=1}^N$ are the solutions of the following auxiliary minimization problem

$$(v_k)_{k=1,\dots,N} = \arg \min_{(v_k)_{k=1}^N} \Delta t \sum_{k=1}^{N} \ell(Y_k, v_k) \text{ subject to (2.8)}, \tag{2.7}$$

where the states Y_k, $k = 1, \dots, N$, are given by the dynamics (2.8) for an initial value X_n and a time horizon N, i.e., for each $k = 1, \dots, N$

$$y_{i,k+1} = y_{i,k} + \frac{\Delta t}{M} \sum_{j=1}^{M} P(y_{j,k} - y_{i,k}) + \Delta t v_k, \qquad y_{i,1} = x_{i,n}. \tag{2.8}$$

In the introduced notations, the case $N = 2$ corresponds to instantaneous-type control, which has been extensively investigate in the literature, see [6, 11, 73, 75].

A first obvious relation between the optimal control and the control introduced through a model predictive approach is the following

$$J_\infty^{u^{MPC}}(X_0) \geq J_\infty^{u*}(X_0). \tag{2.9}$$

Part of the investigation in [106] is related to a result to establish an *upper bound* on $J_\infty^{u^{MPC}}$ by a multiple of $J_\infty^{u^*}$, in particular the result [106, Theorem 4.2] proves that such a multiplicative factor can be obtained and depends in particular on the optimization horizon N and on the decay rate of the function $\ell(\cdot, \cdot)$. The result of the aforementioned work leads to an estimate at the ODE level of the type

$$\alpha_N J_\infty^{u^*}(X_0) \leq \alpha_N J_\infty^{u_N^{MPC}}(X_0) \leq J_\infty^{u^*}(X_0), \tag{2.10}$$

for some $0 < \alpha_N \leq 1$. Where we indicated the dependence of u^{MPC} on the time horizon in problem (2.7) by the subscript N on the control. Further, an estimate $\alpha_N J_\infty^{u_N^{MPC}}(X_0) \leq J_N^{u^*}(X_0)$ has been established as an additional result in [106, Corollary 4.5]. Here, $J_N^{u^*}$ is defined as in equation (2.3) but for a finite time horizon $T = N\Delta t$. An estimate on the crucial constant α_N is provided e.g. in [107].

We are interested in a corresponding result in the case of a large number of agents, that is in the limit $M \to \infty$. We sketch here the derivation of the semi discrete mean-field formulation of the constrained problem (2.1). Let us suppose that for each $n \geq 0$ the introduced MPC control u_n^{MPC} is symmetric with respect to each position of the system of agents at time t^n. We define the empirical measure

$$f_M(t^n) = f_{M,n} = \frac{1}{M}\sum_{i=1}^{M} \delta(x - x_{i,n}), \tag{2.11}$$

where δ is the Dirac delta, or localizing function, defined in the space of probability measures of $\mathbb{R}^d$, namely $\mathcal{P}(\mathbb{R}^d)$. For any test function function $\phi \in \mathcal{C}_0^1(\mathbb{R}^d)$ we have

$$\int_{\mathbb{R}} \phi(x) f_{M,n}(x) dx = \frac{1}{M}\sum_{i=1}^{M} \phi(x_{i,n}), \tag{2.12}$$

then through a first order Taylor expansion we obtain

$$\phi(x_{i,n+1}) - \phi(x_{i,n}) = \phi'(x_{i,n})(x_{i,n+1} - x_{i,n}) + O(\Delta t^2) \tag{2.13}$$

Now from the original dynamic (2.1) we can replace the quantity $x_{i,n+1} - x_{i,n}$ in (2.13), we have

$$\phi(x_{i,n+1}) - \phi(x_{i,n}) = \phi'(x_{i,n}) \left[\frac{\Delta t}{M} \sum_{j=1}^{M} P(x_{j,n} - x_{i,n}) + \Delta t u_n^{MPC} \right]. \tag{2.14}$$

If we consider not the sum over $i = 1, \ldots, M$ equation (2.14) assumes the following form

$$\begin{aligned} \frac{1}{M}\sum_{i=1}^{M} \phi(x_{i,n+1}) - \phi(x_{i,n}) = \\ \frac{1}{M}\sum_{i=1}^{M} \phi'(x_{i,n}) \left[\frac{\Delta t}{M} \sum_{j=1}^{M} P(x_{j,n} - x_{i,n}) + \Delta t u_n^{MPC} \right]. \end{aligned} \tag{2.15}$$

Given that $f_{M,n}$ is a probability measure in the space $\mathcal{P}(\mathbb{R}^d)$ with uniform support with respect to M, Prokhorov's theorem implies that the sequence

$(f_{M,n})_M$ is weakly-* relatively compact, i.e. there exists a subsequence $(f_{M_m,n})_m$ and a probability measure $f_n \in \mathcal{P}(\mathbb{R}^d)$ such that

$$f_{M_m,n} \rightharpoonup_{w*} f_n \tag{2.16}$$

in $\mathcal{P}(\mathbb{R}^d)$ pointwise in time. Recall that for the Cucker-Smale model the tightness hypothesis is in general satisfied if the initial distribution $f_{M,0}$ is compactly supported with respect to M. For a rigorous proof we refer to [53, 90].

As an example, consider the special function $\ell : \mathbb{R}^M \times U \to \mathbb{R}$

$$\ell(X,u) = \frac{1}{2}\left(\frac{1}{M}\sum_{j=1}^{M} x_j\right)^2 + \frac{\nu}{2}u^2, \tag{2.17}$$

for some regularization parameter $\nu > 0$. Then, the limit $M \to \infty$ of ℓ exists and is given by

$$\tilde{\ell}(f,u) = \frac{1}{2}\left(\int_{\mathbb{R}} y f(y) dy\right)^2 + \frac{\nu}{2}u^2 \tag{2.18}$$

with $\tilde{l} : \mathcal{P}(\mathbb{R}) \times U \to \mathbb{R}$, where $\mathcal{P}(\mathbb{R})$ denotes the probability measures on $\mathbb{R}$.

Let us consider the dynamics (2.8) and denote by $y \to f_k(y)$ the agent probability density at time t^k with $f_k(\cdot) \in \mathcal{P}(\mathbb{R})$ for $k = 1, \dots, N$. The limiting equation corresponding to the microscopic dynamics in (2.8) for $M \to \infty$ and a.e. $y \in \mathbb{R}$ reads

$$\begin{aligned} &f_{k+1}(y) = f_k(y) - \Delta t \partial_y \int_{\mathcal{X}} P(z-y) f_k(z) f_k(y) dz - \Delta t v_k \partial_y f_k(y), \\ &f_1(y) = h_n(y). \end{aligned} \tag{2.19}$$

The probability distribution $h_n(\cdot) \in \mathcal{P}(\mathbb{R})$ is the distribution $h(t_n)$ at time t^n obtained by propagation of the mean-field limit of the original dynamics (2.1), i.e. for each $n \geq 0$

$$h_{n+1}(x) - h_n(x) + \Delta t \partial_x \left(\int_{\mathcal{X}} P(z-x) h_n(z) h_n(x) dz - u_n h_n(x)\right) = 0 \tag{2.20}$$

In equation (2.20) $u(\cdot) = u^{MPC}(\cdot)$ is the control obtained by the MPC approximation (2.5) and (2.6). The initial state $h(t^0, 0) = h_0(x)$ is obtained as the probability distribution corresponding to the mean-field limit of the initial data to (2.1). The control $(v_k)_{k=1}^N$ in equation (2.6) is determined by solving the corresponding mean-field optimization problem, i.e.,

$$(v_k)_{k=1,\dots,N} = \arg\min_{(v_k)_{k=1}^N} \Delta t \sum_{k=1}^{N} \tilde{\ell}(f_k(\cdot), v_k), \text{ subject to (2.19)}. \tag{2.21}$$

As usual, the constrained initial discrete dynamics in the case of the introduced MPC control is recovered by substituting the discrete measure $f_{M,n}$, defined in (2.11), in the weak form of the equation (2.19). Again, we refer to [53, 90, 138] for rigorous results and more details on the mean-field limit. As an example, note that the mean-field limit $J^u_\infty : \mathcal{P}(\mathbb{R}) \to \mathbb{R}$ is

$$\tilde{J}^u_\infty(h_0) = \sum_{n=0}^{\infty} \tilde{\ell}(h_n(\cdot), u_n), \tag{2.22}$$

where h is determined by equation (2.20) with initial condition $h_0 \in \mathcal{P}(\mathbb{R})$. As before a horizon of $N = \infty$, corresponding to the optimal case, is desirable but computationally inefficient. In the sequel we want to establish the estimate (2.10) also for the mean-field cost functional $\tilde{J}^u$. Except for the assumptions required to derive the mean-field limit we only enforce the assumptions of [106, Theorem 4.2] and we will show how those are sufficient to derive the corresponding estimates. Also, we will justify by obtaining the suitable mean-field limits the previously outlined recipe for MPC mean-field control for a broader class of agent dynamics.

3.3 Optimality estimate for the mean-field cost functional using MPC approach

We will follow the approach described in [106, 107] with applications to the infinite dimensional mean-field case taking first into account a discretized system of ordinary differential equations.

Let us consider a homogeneous time discretization for a general problem $\dot{x}_i = g(x_i(t), X_{-i}(t)) + u(t)$ given by

$$x_{i,n+1} = x_{i,n} + \Delta t g\left(x_{i,n}, X_{-i,n}\right) + \Delta t u_n \tag{3.1}$$

where $g : \mathbb{R}^M \to \mathbb{R}$ is a general differentiable function that depends on the state of the ith agent and on the states of the other agents (2.2). Also, $\Delta t = t^{n+1} - t^n > 0$ and for simplicity we assume $\Delta t = 1$. Let us suppose that g fulfills the assumptions of [29, Section 4], see also 5.6. In order to pass to the mean-field limit we require that the trajectory of each agent $x_{i,n}$ belongs to a compact subset $\mathcal{X}$ of $\mathbb{R}$ for all time steps $n \geq 0$. Let U be a compact subset of $\mathbb{R}$. Then, we assume that for $x_{i,0} \in \mathcal{X}$ and $u_n \in U$ we have $x_{i,n} \in X$ for each $i = 1, \ldots, M$. Then, according to the result 3.5.1 there exists a function

$$G : \mathcal{X} \times \mathcal{P}(\mathcal{X}) \to \mathbb{R}$$

such that the sequence

$$G_M(x_{i,n}, m^M_{X_{-i,n}}) = g(x_{i,n}, X_{-i,n})$$

converges toward G in the limit $M \to \infty$. For the precise definition of $(G_M)_M$ with $G_M : \mathcal{X} \times \mathcal{P}(\mathcal{X}) \to \mathbb{R}$ we refer to equation (5.3). This allows to obtain that the particle density function $f_n \in \mathcal{P}(\mathcal{X})$ satisfies the semi–discrete partial differential equation in strong form

$$f_{n+1}(x) = f_n(x) - \partial_x[G(x, f_n(x))f_n(x)] - \partial_x[f_n(x)\, u_n], \tag{3.2}$$

for a given initial distribution $f_0 \in \mathcal{P}(\mathcal{X})$. We denote with $\mathcal{U}$ the set of admissible control sequences $(u_n)_{n\in\mathbb{N}_0}$, where $u_n \in U \subset \mathbb{R}$. In the following we will always assume that for any given initial distribution $f_0 \in \mathcal{P}(\mathcal{X})$ and control $u = (u_n)_n$, there exists a sequence of sufficiently regular functions $(f_n)_{n\in\mathbb{N}_0}, f_n \in \mathcal{P}(\mathcal{X})$, given by the dynamics described in (3.2). This sequence depends on the initial distribution f_0 and on the choice of the control sequence $u = (u_n)_n$. We observe how equation (3.2) is meaningful provided that f_n are absolute continuous, in the sense of Radon-Nikodym, with sufficiently smooth densities. The assumption is rather strong for the introduced dynamics $G(\cdot,\cdot)$ and it is not trivial that, for a general f_0, the distribution f_n for all $n > 0$ stays smooth.

The equation (3.2) is the discrete time counterpart of a non-local non-linear transport equation, see [64] and the references therein.

Definition 3.3.1. *The infinite horizon mean-field cost $J^u_\infty : \mathcal{P}(\mathcal{X}) \to \mathbb{R}^+_0$ is denoted by*

$$J^u_\infty(f_0) = \sum_{n=0}^{+\infty} \ell(f_n, u_n), \tag{3.3}$$

where $l : \mathcal{P}(\mathcal{X}) \times U \to \mathbb{R}^+_0$ is the running cost function and where $(f_n)_n, f_n : \mathcal{P}(\mathcal{X}) \to \mathbb{R}$, is the solution to equation (3.2) with initial distribution $f_0 \in \mathcal{P}(\mathcal{X})$ and given control sequence $u = (u_n)_n$.

Example 1. *Consider the discrete problem (2.8). Let the cost functional be given by a discretization of (2.3) with ℓ as in the previous section:*

$$\ell(X_n, u_n) = \frac{1}{2}\left(\frac{1}{M}\sum_{i=1}^{M} x_{i,n}\right)^2 + \frac{\nu}{2}u_n^2$$

for some fixed parameter $\nu > 0$. The function ℓ is symmetric in X_n. Provided that $x_{i,n} \in \mathcal{X}, u_n \in U$, we obtain that ℓ is uniformly bounded independently on M, i.e. $\|\ell(\cdot,\cdot)\|_\infty \le C_0$. Further, ℓ is locally Lipschitz-continuous in X_n as composition of locally Lipschitz continuous functions. In fact let $x_{i,n}, y_{i,n} \in \mathcal{X}$, then we can compute

$$\left|\frac{1}{2}\left(\frac{1}{M}\sum_{i=1}^{M} x_{i,n}\right)^2 + \frac{\nu}{2}{u_n}^2 - \frac{1}{2}\left(\frac{1}{M}\sum_{i=1}^{M} y_{i,n}\right)^2 - \frac{\nu}{2}{u_n}^2\right| \le \frac{2C_1}{M}\left|\sum_{i=1}^{M}(x_{i,n} - y_{i,n})\right|,$$

with $C_1 \geq 0$ the Lipschitz constant. Therefore, $\ell(\cdot,\cdot)$ fulfills as function of X the assumptions of Theorem 3.5.1 and its mean-field limit exists and is given by

$$\ell(f_n, u_n) = \frac{1}{2}\left(\int_{\mathcal{X}} x f_n(x) dx\right)^2 + \frac{\nu}{2} u_n^2. \tag{3.4}$$

The previous example shows that the cost functional (2.3) requires strong symmetry assumptions. This is fulfilled for example if it depends on functions of average quantities of the state of the particles. Under the symmetry assumption we expect to extend the results proposed in [106]. Therefore, we require in the following that the running cost ℓ is symmetric with respect to each agent, that the running costs are uniformly bounded and Lipschitz continuous with respect to the distance $\mathbf{d}_1$, defined in 5.6.

Let us now introduce the notion of optimal value-function, in the mean-field setting, and show a first result.

Definition 3.3.2. *We denote by $V_\infty : \mathcal{P}(\mathcal{X}) \to \mathbb{R}$ the* optimal value function *of the mean-field control problem (3.2) associated with the infinite horizon cost $J^u_\infty(f_0)$:*

$$V_\infty(f_0) = \inf_{u \in \mathcal{U}} J^u_\infty(f_0). \tag{3.5}$$

We define the approximate optimal cost $J^u_N : \mathcal{P}(\mathcal{X}) \to \mathbb{R}$ *with optimization horizon N as*

$$J^u_N(f_0) = \sum_{n=0}^{N-1} \ell(f_n, u_n). \tag{3.6}$$

The approximate value function $V_N(f_0) : \mathcal{P}(\mathcal{X}) \to \mathbb{R}$ in the case of receding horizon strategy is defined by

$$V_N(f_0) = \inf_{u \in \mathcal{U}} J^u_N(f_0, u). \tag{3.7}$$

Further we introduce the notion of a feedback law. A feedback law for M agents is a mapping $\mu_M : \mathcal{X}^M \to U$. A symmetric feedback law is a feedback law such that for all $X \in \mathcal{X}^M : \mu_M(X) = \mu_M((x_i)_{\sigma(i)})$ and any permutation $\sigma \in S_M$, with S_M the symmetric group of degree M

$$\sigma = \begin{pmatrix} 1 & 2 & \dots & M \\ \sigma(1) & \sigma(2) & \dots & \sigma(M) \end{pmatrix}. \tag{3.8}$$

As for the running cost ℓ, we further assume that the feedback law μ_M is symmetric, uniformly bounded and Lipschitz continuous with respect to $\mathbf{d}_1$.

We now establish an estimate of the type (2.10) in the mean-field case. Note that the result in [106] alreadys covers the case of a cost functional (3.3) and (3.2). Therefore, our purpose is to derive the estimate (2.10) starting from the finite discrete dynamics (3.1) and in the mean-field limit case $M \to \infty$.

Proposition 3.3.1. *Let us consider a set of M agents which evolve according to the microscopic dynamics (3.1) with known initial data $(x_{i,0})_{i=1}^M$. Consider the functions $\ell_M : \mathcal{X}^M \to \mathbb{R}$, and $\tilde{V}_M : \mathcal{X}^M \times \mathcal{U} \to \mathbb{R}$, and a symmetric feedback $\mu_M : \mathcal{X}^M \to U$, fulfilling the assertions of Theorem 3.5.1 and Definition 3.3.2.*

Assume furthermore that $\tilde{V}_M$ fulfills for all $X_0 \in \mathcal{X}^M$ the inequality

$$\begin{aligned}\tilde{V}_M(X_0) \geq &\tilde{V}_M\left((x_{0,i} + \Delta t\,(g(x_{i,n}, X_{-i,n}) + \mu_M(X_0)))_{i=1}^M\right) \\ &+ \alpha \ell_M(X_0, \mu_M(X_0))\end{aligned} \tag{3.9}$$

with $\alpha \in (0, 1]$. Then, there exists a function $\tilde{V} : \mathcal{P}(\mathcal{X}) \to \mathbb{R}$ as mean-field limit of $\tilde{V}_M$ for $M \to \infty$ such that for all $f \in \mathcal{P}(\mathcal{X})$ we obtain

$$\alpha V_\infty(f) \leq \alpha J_\infty^u(f) \leq \tilde{V}(f). \tag{3.10}$$

for $u = (u_n)_n, u_n = \mu(f_n)$, where μ is the mean-field limit of $(\mu_M)_M$.

Proof. Due to the assertion of Theorem 3.5.1 we have $\tilde{V}$, $\ell : \mathcal{P}(\mathcal{X}) \times U \to \mathbb{R}$ and $\mu : \mathcal{P}(\mathcal{X}) \to U$ exist. Further, we obtain for $f_0 \in \mathcal{P}(\mathcal{X})$ (as limit for $M \to \infty$ of the sequence $(m_{X_0}^M)_M$) the corresponding inequality for $\tilde{V}$

$$\tilde{V}(f_0) \geq \tilde{V}(f_0 - \partial_x[f_0 G(x, f_0)] - \partial_x[f_0\, \mu(f_0)]) + \alpha \ell(f_0, \mu(f_0)). \tag{3.11}$$

In fact for all $i = 1, \ldots, M$ and all M

$$x_{1,i} = x_{0,i} + \Delta t\; g(x_{i,n}, X_{-i,n}) + \Delta t\, \mu_M(X_0), \tag{3.12}$$

which corresponds in the mean-field limit to

$$f_1 = f_0 - \partial_x[f_0 G(x, f_0)] - \partial_x[f_0\, \mu(f_0)]. \tag{3.13}$$

The mean-field limit $\tilde{V}$ is obtained as limit of the sequence $\mathbf{V}_M : \mathcal{P}(\mathcal{X}) \to \mathbb{R}$ where

$$\mathbf{V}_M(f) = \inf_{X \in \mathcal{X}^M} \{V_M(X) + \omega(\mathbf{d}_1(m_X^M, f))\}, \tag{3.14}$$

see Theorem 3.5.1. We therefore have $\mathbf{V}_M(m_X^M) = V_M(X)$ and therefore for all $X_0 \in \mathcal{X}^M$

$$\mathbf{V}_M(m_{X_0}^M) \geq \mathbf{V}_M(m_{X_1}^M) + \alpha \ell_M(m_{X_0}^M, \mu_M(m_{X_0}^M)).$$

Further, $\mathbf{V}_M$ has modulus of continuity ω, i.e., $|\mathbf{V}_M(f) - \mathbf{V}_M(g)| \leq \omega(\mathbf{d}_1(f, g))$. Let $f_0 \in \mathcal{P}(\mathcal{X})$ be the limit of $m_{X_0}^M$ for $M \to \infty$. Note that the limit exists for metric $\mathbf{d}_1$ on the probability measures, since $\mathcal{X}$ is compact subset of $\mathbb{R}$ and therefore $m_{X_0}^M$ has finite 1–Wasserstein distance, i.e., $\int_{\mathcal{X}} |x| dm_{X_0}^M < C$ with C independent of M and X_0. Due to the dynamics (3.12) we have f_1 is then

the limit of $m^M_{X_1}$, X_1 given by (3.12). Since $\mathbf{V}_M$ has modulus of continuity ω, we obtain

$$\mathbf{V}_M(f_0) \geq \mathbf{V}_M(f_1) + \alpha \ell_M(f_0, \mu_M(f_0)).$$

Hence, we have

$$\tilde{V}(f_0) \geq \tilde{V}(f_1) + \alpha \ell(f_0, \mu(f_0)).$$

Define now $u_n = \mu(f_n)$ and consider the solution to (3.2). Since $X_0 \in \mathcal{X}^M$ is arbitrary we obtain that (3.11) holds for all $f_0 \in \mathcal{P}(\mathcal{X})$ and therefore

$$\tilde{V}(f_n) \geq \tilde{V}(f_{n+1}) + \alpha \ell(f_n, \mu(f_n)). \tag{3.15}$$

Summation over n yields

$$\alpha \sum_{n=0}^{K-1} \ell(f_n, u_n) \leq \tilde{V}(f_0) - \tilde{V}(f_K) \leq \tilde{V}(f_0). \tag{3.16}$$

Let now $K \to \infty$, then $\tilde{V}(f_0)$ is an upper bound for $J^u_\infty = \sum_{n=0}^\infty \ell(f_n, u_n)$ and where $u_n = \mu(f_n)$. Since u_n is an admissible control we obtain for all $f_0 \in \mathcal{P}(\mathcal{X})$

$$\alpha V_\infty(f_0) \leq \alpha J^u_\infty(f_0) \leq \tilde{V}(f_0), \tag{3.17}$$

our assertion as limit of discrete measures. □

The previous results hold for any family of functions $\tilde{V}_M$ and any symmetric feedback law. The idea is now to establish the inequality in (3.9) for a general MPC strategy and a family of functions $\tilde{V}_M$ given by the optimal running costs V_N as in Definition (3.3.2). In order to establish equation (3.9) for a broad class of running costs ℓ, the functions ρ, β have been introduced in Section 3 in [106]. We recall their definition and assertions in Definition 3.3.3 below. Under Assumption 1 we prove that $\mu = u_N^{MPC}$ and V_N fulfill the assertions of Proposition 8.2.3. The Assumption 1 is the mean-field analogous to the assumption imposed in [106, Assumption 3.1].

Definition 3.3.3. *We say that a function $\rho : \mathbb{R}^+ \to \mathbb{R}^+$ is of class $\mathcal{K}_\infty$ if*

(i) $\rho(0) = 0$,

(ii) $\rho(\cdot)$ *is strictly increasing*

(iii) $\rho(\cdot)$ *is unbounded.*

Moreover a continuous function $\beta : \mathbb{R}^+ \times \mathbb{R}^+ \to \mathbb{R}^+$ is of class $\mathcal{KL}_0$, if $\forall r > 0$ we have $\lim_{r \to +\infty} \beta(r, t) = 0$ and for each $t \geq 0$ we either have $\beta(\cdot, t) \in \mathcal{K}_\infty$ or (b) $\beta(\cdot, t) \equiv 0$.

We will denote by $\ell^*(f)$ the minimum of the mean-field running cost ℓ and as in [106] we assume it exists

$$\ell^*(f) = \min_{u \in \mathcal{U}} \ell(f, u). \tag{3.18}$$

Assumption 1. *We assume that $\ell^*(f)$ is well–defined for all $f \in \mathcal{P}(\mathcal{X})$. Further, for given $\beta \in \mathcal{KL}_0$ and each $f_0 \in \mathcal{P}(\mathcal{X})$,there exists a sequence of controls $(u_n)_n, u_n \in \mathcal{U}$ depending only on f_0 such that for each n we have*

$$\ell(f_n, u_n) \leq \beta(\ell^*(f_0), n). \tag{3.19}$$

In the following Lemma we prove that Assumption 1 is fulfilled provided that the finite–dimensional problem fulfills the corresponding assumption [106, Assumption 3.1]. We establish the proof in the special case of β given by

$$\beta(r, n) = C\sigma^n r, \tag{3.20}$$

where $C \geq 1$ is the overshoot constant and $\sigma \in (0, 1)$ the decay rate. Clearly, the particular choice $\beta(r, n) \in \mathcal{KL}_0$.

Lemma 3.3.2. *Let β be given by equation (3.20). Consider a dynamics with M agents given by the dynamics of equation (3.1) with a control sequence $(u_n)_n$ and $u_n \in \mathcal{U}$ and initial conditions $X_0 \in \mathcal{X}^M$. Assume $\ell_M : \mathcal{X}^M \times \mathcal{U} \to \mathbb{R}$ and $\ell_M^* : \mathcal{X}^M \to \mathbb{R}$ fulfill the assumptions of Proposition 8.2.3 for all M. Further, we assume that [106, Assumption 3.1] holds, that is for all M we have*

$$\ell_M(X_n, u_n) \leq \beta(\ell_M^*(X_0), n). \tag{3.21}$$

Then, the mean-field limit $(\ell_M)_M$ and $(\ell_M^*)_M$ exist and the limit $\ell : \mathcal{P}(\mathcal{X}) \times \mathcal{U} \to \mathbb{R}$ and $\ell^* : \mathcal{P}(\mathcal{X}) \to \mathbb{R}$, fulfills Assumption 1:

$$\ell(f_n, u_n) \leq \beta(\ell^*(f_0), n). \tag{3.22}$$

Proof. Due to the assumptions on the family $(\ell_M)_M$ given in Proposition 8.2.3 we have the existence of the mean-field limit ℓ according to Theorem 3.5.1. Consider the family of functions

$$\beta_M(X, n) := \beta(\ell_M^*(X), n).$$

Clearly, the function β_M is symmetric in $X \in \mathcal{X}^M$. Using the definition of β by equation (3.20) and the properties of ℓ_M^* we have that $\beta_M(X, n)$ is uniformly bounded with respect to X on the compact subset $\mathcal{X}^M$ by $C\sigma^n \|\ell_M^*(X)\|$. For each r_1, r_2 such that $|r_1 - r_2| < \delta$ we have

$$|\beta(r_1, n) - \beta(r_2, n)| \leq C\sigma^n |r_1 - r_2|.$$

Hence, for $\epsilon = C\sigma^n\delta$, we have uniform continuity of β_M due to the uniform continuity of ℓ_M^*. If $\omega(\cdot)$ is the modulus of continuity of ℓ_M^* then $C\sigma^{\tilde{n}}|\omega(\cdot)|$ is the modulus of continuity of β_M. Hence, for each fixed n there exists the mean-field limit β of $(\beta_M)_M$. Also, there exists the mean-field limit ℓ^* of (ℓ_M^*). Due to the Lipschitz continuity of β we also have that $\sup_X |\beta(\ell_{M_k}^*(X)) - \beta(\ell^*(m_X^{M_k})| \to 0$ for $(M_k)_k \to \infty$. Therefore, the mean-field limit $\beta(f, n) = \beta(\ell^*(f), n)$. Similarly to what we have proven in Proposition 8.2.3 it follows that the inequality (3.21) implies then (3.22). □

Example 2. *Consider the example of Section 3.2. The running cost has been given by*

$$\ell(f_n, u_n) = \frac{1}{2}\left(\int_{\mathcal{X}} x f_n(x) dx\right)^2 + \frac{\nu}{2} u_n^2. \tag{3.23}$$

The optimal running cost ℓ^* can be computed explicitly and is given by

$$\ell^*(f_n) = \frac{1}{2}\left(\int_{\mathcal{X}} x f_n(x) dx\right)^2. \tag{3.24}$$

From the mean-field dynamics for f_n are given by (2.19). Upon integration on $\mathcal{X}$ we obtain

$$\int_{\mathcal{X}} x f_{n+1}(x) dx = \int_{\mathcal{X}} x f_n(x) dx + \Delta t \; u_n. \tag{3.25}$$

In [6] the following feedback law $\mu : \mathcal{P}(\mathcal{X}) \to \mathcal{U}$ has been proposed as instantaneous MPC:

$$\mu(f_n) = \frac{1}{1+\nu} \int_{\mathcal{X}} x f_n(x) dx. \tag{3.26}$$

Using $\Delta t u_n := \mu(f_n)$ the optimal running cost $\ell^*(f_n)$ is expressed in terms of the initial cost $\ell^*(f_0)$ as

$$\ell^*(f_n) = \frac{1}{2}\left(1 - \frac{1}{1+\nu}\right)^2 \left(\int_{\Omega} x f_{n-1} dx\right)^2 = \left(1 - \frac{1}{1+\nu}\right)^{2n} \ell^*(f_0). \tag{3.27}$$

Therefore we have

$$\ell(f_n, u_n) = \left(1 + \frac{\nu}{(1+\nu)^2}\right)\left(1 - \frac{1}{1+\nu}\right)^{2n} \ell^*(f_0) = C\sigma^n \ell^*(f_0). \tag{3.28}$$

The overshoot constant C and the decay rate σ are computed explicitly for a given regularization $\nu > 0$ as

$$C = 1 + \frac{\nu}{(1+\nu)^2} \geq 1, \qquad \sigma = \left(1 - \frac{1}{1+\nu}\right)^2 \in (0, 1). \tag{3.29}$$

Consider the receeding horizon costs with length one as $\tilde{V} : \mathcal{P}(\mathcal{X}) \to \mathbb{R}$ defined as

$$\tilde{V}(f_0) := \sum_{n=0}^{1} \ell(f_n, \mu(f_n)). \tag{3.30}$$

Due to equation (3.28) we obtain the assertion of Proposition 8.2.3 is true by simple computation

$$\tilde{V}(f_0) \geq \tilde{V}(f_1) + \alpha \ell(f_0, \mu(f_0)) \tag{3.31}$$

provided that $\alpha := 1 - (C\sigma)^2$ fulfills $0 < \alpha$. This yields a bound on the regularization parameter ν. This estimate for α is only *valid in the case*

of the feedback law (3.26). The idea is to generalize the result to arbitrary symmetric running costs ℓ and different *control horizons. In the numerical results we then observe for large values of ν also a decay in the receeding horizon costs provided the control horizon is sufficiently large.*

The following Lemma is the analog to [106, Theorem 4.2]. The main idea is to establish the inequality (3.9) using Lemma 3.3.2 for a function $\tilde{V}$ given by the approximate value function (3.7). The discrete approximate optimal cost $J^u_{N,M} : \mathcal{X}^M \times \mathcal{U}^N \to \mathbb{R}$ with running cost $\ell_M : \mathcal{X}^M \times \mathcal{U} \to \mathbb{R}$ and corresponding approximate value function $V_{N,M} : \mathcal{X}^M \to \mathbb{R}$ are obtained by considering the discrete measure m^M_X for $X \in \mathcal{X}^M$ and fixed M :

$$\mathbf{V}_{N,M}(X_0) := V_N(m^M_{X_0}),\ \mathbf{J}^u_{N,M}(X_0,(u_n)_{n=0}^{N-1}) := \sum_{n=0}^{N-1} \ell_M(X_n,u_n). \tag{3.32}$$

where

$$\ell_M(X) = \ell(m^M_{X_n}, u_n). \tag{3.33}$$

Here, $X_n = (x_{i,n})_{i=0}^M$ fulfills the discrete dynamics (3.12) with initial data $x_i(0) = x_{i,0}$. We *assume* that the discrete functions fulfill the corresponding relation (3.7) for all $X \in \mathcal{X}^M$:

$$\mathbf{V}_{N,M}(X) = \min_{(u_n)\in\mathcal{U}^N} \mathbf{J}^u_{N,M}(X,(u_n)_{n=0}^{N-1}).$$

The symmetric feedback law μ is the MPC feedback introduced on the discrete level by equation (2.6) and equation (2.7), respectively.

Lemma 3.3.3. *Consider the discrete dynamics (3.1) with M agents and β given by equation (3.20) with $C \geq 1$ and $\sigma \in (0,1)$. Consider a model predictive control horizon of N. Assume the family $(\ell_M)_M, \ell_M : \mathcal{X}^M \times \mathcal{U} \to \mathbb{R}$ fulfill the assertions of Proposition 8.2.3. Assume assumption 1 holds true. Let $\mathbf{V}_{N,M}, \ell_M$ and $\mathbf{J}^u_{N,M}$ be given by equation (3.32). Given are sequences $\lambda_n > 0$, $n = 0,\dots,N-1$ and $\nu > 0$ such that*

$$\sum_{n=k}^{N-1} \lambda_n \leq C\lambda_k \frac{1-\sigma^{N-k}}{1-\sigma}, \qquad k = 0,\dots,N-2, \tag{3.34}$$

$$\nu \leq \sum_{n=0}^{j-1} \lambda_{n+1} + C\lambda_{j+1}\frac{1-\sigma^{N-j}}{1-\sigma}, \qquad j = 0,\dots,N. \tag{3.35}$$

holds true. Assume that then also

$$\sum_{n=0}^{N-1} \lambda_n - \nu \geq \lambda_0\alpha, \tag{3.36}$$

holds true for some $\alpha \in (0,1]$. *Then, for any* M *and any* $X_0 \in \mathcal{X}^M$ *and any running cost* ℓ_M *fulfilling* (3.21) *we obtain* (3.9) *for the MPC feedback law* μ_M *given by* (3.39) *and for the value function*

$$\tilde{V}_M := \mathbf{V}_{N,M}.$$

Provided that $(\mu_M)_M$ *is symmetric and fulfills the assertions of Theorem 3.5.1, we obtain for each* $f \in \mathcal{P}(\mathcal{X})$ *as limit of* $(m_X^M)_M, M \to \infty$, *the inequality*

$$\alpha V_\infty(f) \leq \alpha J_\infty^u(f) \leq V_N(f) \tag{3.37}$$

where $u = (u_n)_n, u_n = \mu(f_n)$ *and where* μ *is the mean-field limit of* $(\mu_M)_M$.

Sketch of the proof. The proof is analogous to the proof of [106, Theorem 4.2]. We recall that condition (3.36) is equivalent to the assertion [106, (4.3)]. For β given by equation (3.20) the assertions [106, (4.1),(4.2)] simplify to equation (3.35) and (3.34), respectively. Consider M agents with corresponding arbitrary initial condition $X_0 \in \mathcal{X}^M$. Consider the finite horizon problem of length N given by

$$(u_n^*)_{n=0}^{N-1} = \arg \min_{(u_n)_n \in \mathcal{U}^M} \mathbf{J}_{N,M}^u(X_0, (u_n)_{n=0}^{N-1}). \tag{3.38}$$

Then, we denote the corresponding optimal trajectory X_n^* obtained through the dynamics (3.1) for $u_n = u_n^*$. We define

$$\lambda_{n,M} = \ell_M(X_n^*, u_n^*),\ n = 0, \dots, N-1$$

and

$$\nu_M = \mathbf{V}_{N,M}(X_1^*).$$

Similarly to [106, Proposition 4.1] the values $\lambda_{n,M}$ and ν_M defined in the proof above fulfill equation (3.35) and equation (3.34). This result has been established in the case of finite number of agents in a sequence of auxiliary aftermaths that are not repeated here. Now, consider the MPC feedback law $\mu_M(X) = v_0$ where

$$(v_0)_{k=0,\dots,N-1} = \arg \min_{(v_k), v_k \in \mathcal{U}} \sum_{n=0}^{N-1} \ell_M(Y_n, v_k) \tag{3.39}$$

where $Y_n \in \mathcal{X}^M$ solves equation (3.1) with initial data $Y_0 = X$ and let $(X_n^\mu)_n$ be the trajectory obtained through (3.1) for initial data X_0 and for $u_n = \mu(X_n)$. We observe that $u_0^* = \mu(X_0)$ and $X_i^\mu = X_i^*$ for $i = 0$ and $i = 1$. Therefore, $\ell_M(X_0, u_0^*) = \ell_M(X_0, \mu(X_0))$. Therefore, we obtain for all M and any α from equation (3.36)

$$\begin{aligned}&\mathbf{V}_{N,M}(X_1^\mu) + \alpha \ell_M(X_0, \mu(X_0)) = \mathbf{V}_{N,M}(X_1^*) + \alpha \ell_M(X_0, u_0^*) \\ &= \nu_M + \alpha \lambda_{0,M} \leq \sum_{n=0}^{N-1} \lambda_{n,M} = \sum_{n=0}^{N-1} \ell_M(X_n^*, u_n^*) = \mathbf{V}_{N,M}(X_0).\end{aligned}$$

Therefore, $\mathbf{V}_{N,M}$ fulfills the assertion on $\tilde{V}_M$ of Proposition 8.2.3. The second assertion follows as a consequence of Proposition 8.2.3. This finishes the outline of the proof.

The assumption on existence of an optimal control (3.38) for $\mathbf{J}_{N,M}$ is also precisely as in the case of finitely many agents. Note that as in the finite dimensional case the optimal control might not exist. The previous result (3.37) gives a *performance bound* in the following sense: due to the definition of the approximate value function $V_N(f)$ and $V_\infty(f)$ we have

$$V_N(f) \leq V_\infty(f).$$

Therefore, we obtain the (usable) estimate on the suboptimality of the MPC μ as

$$J^u_\infty(f) \leq \frac{1}{\alpha} V_\infty(f). \tag{3.40}$$

This precisely tells the dependence of the MPC cost on the optimal expected cost V_∞ provided that α is known. The value of α is the effective degree of μ with respect to the (unknown) infinite horizon control. Clearly, the computation of α fulfilling inequality (3.36) is in general a difficult task requiring estimates on the value function and running costs. However, for β given by equation (3.20) we may estimate α solely based on the inequalities (3.34) and (3.35). This estimate is denoted by α_N. The corresponding result is independent of the mean-field limit and has been established in [107, Theorem 5.4].

Lemma 3.3.4. *Let β be given by equation (3.20) for some $C \geq 1$ and $\sigma \in (0,1)$. Let N be the prediction horizon N. Given is a sequence λ_n and $\nu > 0$ such that equation (3.34) and (3.35) holds true. Assume that*

$$\alpha_N = 1 - \frac{(\gamma_N - 1)\prod_{i=2}^{N}(\gamma_i - 1)}{\prod_{i=2}^{N}\gamma_i - \prod_{i=2}^{N}(\gamma_i - 1)} > 0 \tag{3.41}$$

holds with $\gamma_i = C\sum_{n=0}^{i-1}\sigma^n$. Then, for $\alpha = \alpha_N$ the inequality (3.36) is fulfilled.

Equation (3.41) is therefore called performance bound and may be computed a priori to estimate the distance of the optimal cost towards the MPC controlled problem. It solely depends on C and σ being the estimates on a the running cost ℓ. As already noted in [106] this estimate might give not necessarily optimal performance bounds.

3.4 Numerical Results

First, we investigate the performance bound (3.41). In the example 2 we have the following explicit values for C and σ:

$$C = 1 + \frac{\nu}{(1+\nu)^2}, \qquad \sigma = \left(1 - \frac{1}{1+\nu}\right)^2.$$

Estimations on the coefficient α_N allow to measure the quality of the MPC generated control sequence. We depict the value of α_N as a function of N and ν in Figure 4.1. The performance bound can only be used if $\alpha_N > 0$ and we indicate the line $\alpha_N = 0$ by a black line. We observe that the performance bound increases with respect to the MPC horizon as expected. The best bound is $\alpha_N = 1/2$. For large values of the regularization parameter ν we have to consider a sufficiently large MPC horizon N in order to use the theoretical results. Moreover, we observe that the result of Lemma 3.3.4 is consistent with the estimate derived in the special case of example 2 in the case $N = 2$. The numerical results below indicate that the bound is too pessimistic, similarly to what has been already observed in the finite dimensional case.

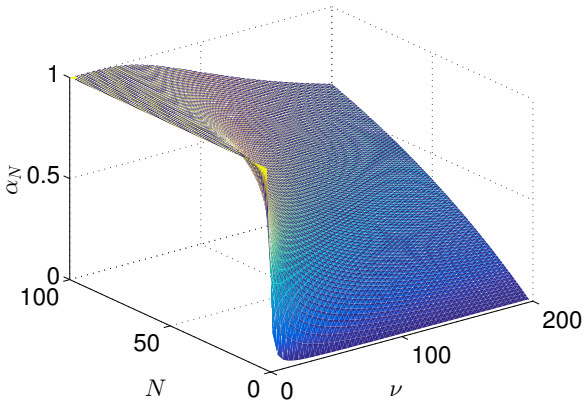

Figure 4.1: Computation of α_N for different values of the regularization parameter ν.

As a numerical example we propose the following discretization coherently with what we discussed in Section 3.3. This discretization reduces the N step MPC problem to again a discrete problem of M agents. We approximate the initial distribution $f_0 \in \mathcal{P}(\mathcal{X})$ by $f_{M,0}$ given by a sum of Dirac delta

$$f_{M,0} = \frac{1}{M} \sum_{i=1}^{M} \delta(x - x_{i,0}). \tag{4.1}$$

located at points $x_{i,0} \in \mathcal{X}$. Following this approach we recover the microscopic formulation of [106, 107] from which we started in Section 3.3. The continuous description is approximated in the large particle limit $M \to +\infty$. In particular the Example 2 we observe that if $f_0 = f_{M,0}$, then f_n is also composed of a sum of Dirac delta. We assume in the following that f_0 as well as f_n decays to zero at the boundaries $x \in \partial\mathcal{X}$. We observe that if $\int_{\mathcal{X}} f_0 dx = 1$ then we have $\int_{\mathcal{X}} f_n dx = 1$. An approach based on Dirac delta converges toward a continuous distribution function in the limit $M \to +\infty$, provided we have a considerably amount of particles centered in $x_{i,n} \in \mathcal{X}$. Within the described discretization we also recover the setting of [106, 107] as numerical scheme.

Thanks to the structure of example 2 further simplifications can be obtained. We recall the mean-field running cost $\ell(f_n.u_n) = \frac{1}{2}\left(\int_{\mathcal{X}} x f_n(x)dx\right)^2 + \frac{\nu}{2}u_n^2$. We consider the mean-field equation equivalent to the discretized dynamics of (2.1) for $P = 1$ and $\Delta t = 1$

$$f_{n+1}(x) = f_n(x) - \partial_x \int_{\mathcal{X}} (y - x) f_n(y) f_n(x) dy - \partial_x \left(u_n f_n(x)\right), \tag{4.2}$$

a detailed derivation is given in Section 3.3. Upon multiplicating by a general $x \in \mathcal{X}$ and integrating with respect dx we obtain

$$\int_{\mathcal{X}} x f_{n+1}(x)dx = \int_{\mathcal{X}} x f_n(x)dx + u_n. \tag{4.3}$$

If we introduce a new variable for the mean $Y_n := \int_{\mathcal{X}} x f^n(x)dx$ the problem simplifies to the equation for the evolution of Y_n. Further, the cost function is also expressed in terms of Y_n as $\ell(Y_n, u_n) = \frac{1}{2}Y_n^2 + \frac{\nu}{2}u_n^2$, and equation (4.3) $Y_{n+1} = Y_n + u_n$.

Using the reformulation of the control of the mean the problem therefore reduces to a problem appearing in the existing theory [106]. In particular, the MPC subproblem to determine the optimal control for the horizon N is solved explicitly for the previous dynamics. We computed for a horizon N the MPC control at time n and initial data Y_0 as $(u_N^{MPC})_n(Y_0) = v_1$, where

$$(v_j)_{j=1}^N := \arg\min \sum_{j=n}^{n+N} \ell(Y_j, u_j),\ Y_{j+1} = Y_j + u_j, Y_n = Y_0.$$

For a fixed time horizon $T = 100$, fixed initial datum Y_o and fixed N we then compute the value of the cost functional for

$$J_T^{u_N^{MPC}} = \sum_{n=0}^{T} \ell(Y_j, (u_N^{MPC})_n)$$

where $Y_{j+1} = Y_j + (u_N^{MPC})_n(Y_n)$. Further, we compute $J_{100}^{u_N^{MPC}}$ to obtain the optimal cost V_{100}^*.

According to Lemma 3.3.4 we obtain the behavior of the MPC cost $J_T^{u_N^{MPC}}$ in relation to the optimal cost V_{100}^* in Figure 4.2. As expected for larger MPC horizons we observe convergence towards the optimal cost. The performance bound α_N is negative for $N \leq 4$ and therefore the Theorem 4.2.5 can not be applied. In the results we choose $\nu = 10^2$. We observe that the bound on α_N is quite pessimistic and the distance of the estimated mismatch of the MPC controlled case to the optimal one is quite large for small horizons, i.e., of order 10^3 for the horizon $N = 5$.

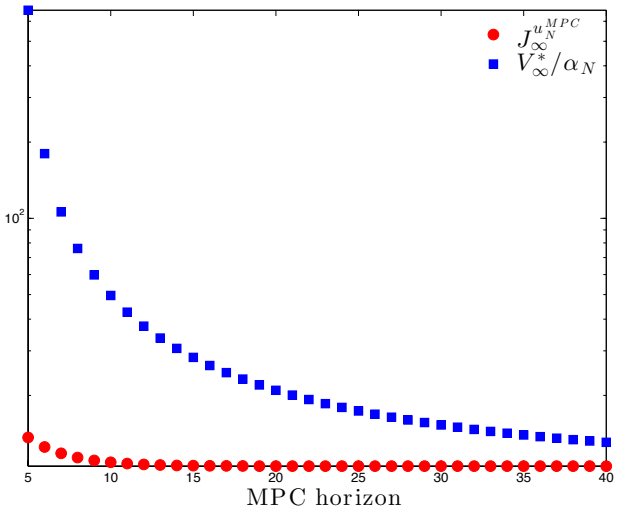

Figure 4.2: Value of the cost functional $J_T^{u_N^{MPC}}(X_0)$ for controls obtained using a MPC strategy with control horizon N (red) and presentation of the optimal costs $V_T^*(X_0)$ multiplied by $\frac{1}{\alpha_N}$ where α_N is computed as in [107, Theorem 5.4]. For $N \leq 4$ no estimate of the type (2.10) could be established.

We further investigate the behavior of the particle system (4.2) for controls with different MPC horizon. According to the behavior of the cost we expect that for increasing time horizon we are closer to the optimal cost. Defining

$$E_n := \int_{\mathbb{R}} x^2 f(x) dx.$$

we obtain from equation (4.2)

$$E_{n+1} = -E_n + 2Y_n^2 + u_n Y_n.$$

The running cost tries to minimizes a trade–off of the mean of the distribution and the control action. If the mean Y_n tends to zero, then we observe that the

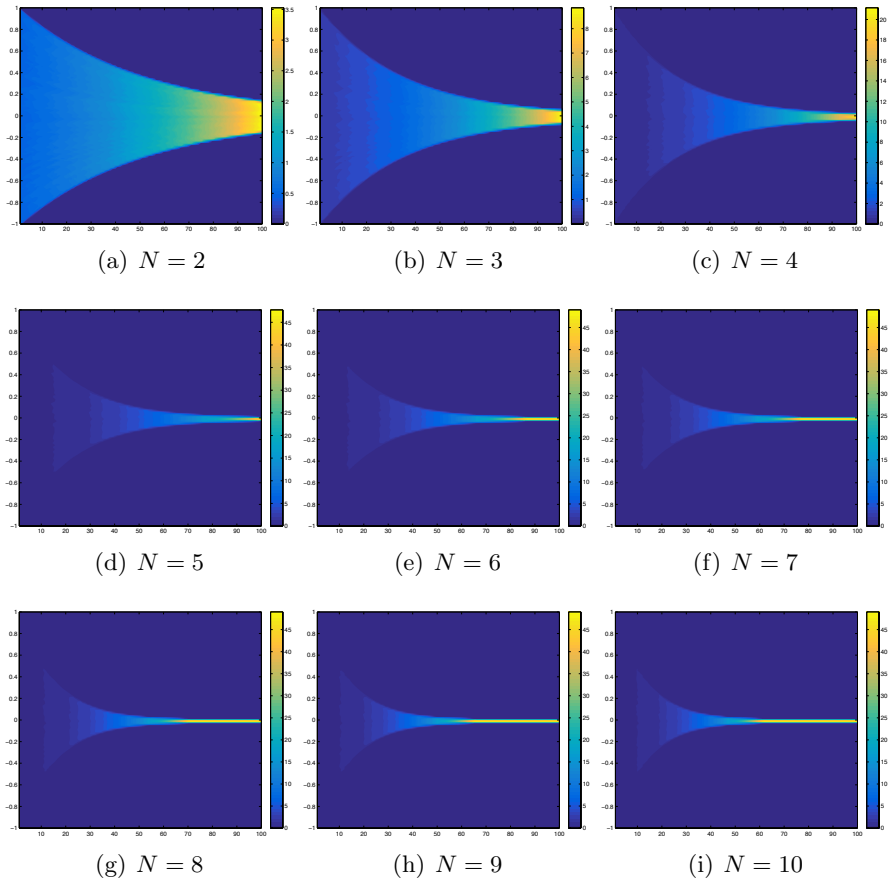

(a) $N = 2$ (b) $N = 3$ (c) $N = 4$

(d) $N = 5$ (e) $N = 6$ (f) $N = 7$

(g) $N = 8$ (h) $N = 9$ (i) $N = 10$

Figure 4.3: Experimental results for the optimization problem with varying optimization horizon N and regularization constant $\nu = 10^2$.

energy E_n tends to zero exponentially fast. Therefore, we expect with longer time horizon a mean Y_n closer to zero and small variance of the solution to the kinetic equation. We simulate using $M = 10^5$ discrete points randomly distributed on $\mathcal{X} = [-1, 1]$ as initial condition $f_{M,0}$ as in equation (4.1). The MPC control is computed according to the considerations above for $\nu = 10^2$ and $\nu = 10^3$ reported in Figure 4.3 and Figure 4.4. In both figures we show the computational results for the time evolution of the distribution f_n for $n = 0, \dots, 100$. As expected longer optimization horizons leads to a faster decay in the variance of the distribution f_n.

3.5 Conclusion

We have extended the estimates for the suboptimal MPC to the mean-field limit. The derived estimates yield performance bounds for general

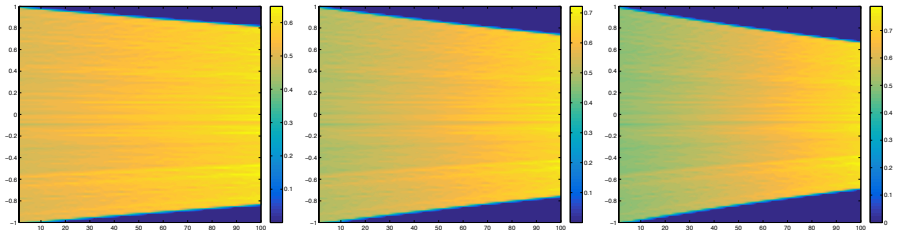

(a) $N = 2$ (b) $N = 3$ (c) $N = 4$

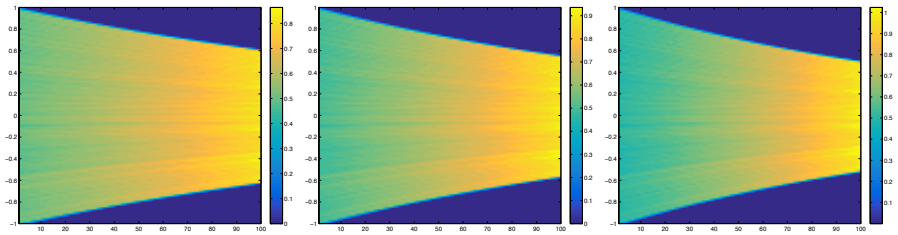

(d) $N = 5$ (e) $N = 6$ (f) $N = 7$

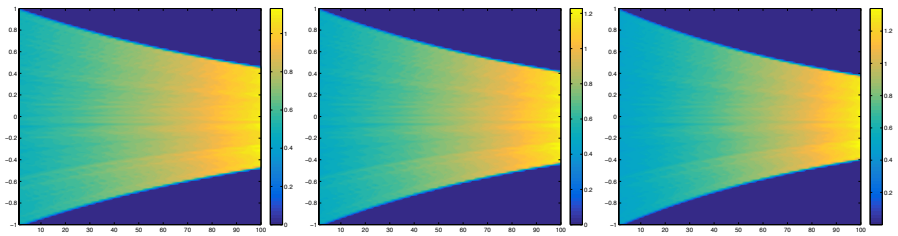

(g) $N = 8$ (h) $N = 9$ (i) $N = 10$

Figure 4.4: Experimental results for the optimization problem with varying optimization horizon N and regularization constant $\nu = 10^3$.

symmetric multi–agent dynamics. Except for the assumptions necessary to obtain the mean-field limit no additional requirements compared to the finite–dimensional theory are required. The results apply to common agent dynamics modeling for example swarming, alignment and economics. We exemplified the theoretical results as well as the estimates on a simple opinion formation model. The stability of the mean-field controller is still open and will be investigated in a forthcoming work. Further, the estimates on α_N are pessimistic due to its generality. It is expected that the bounds can be improved for specific problems as in the finite dimensional case.

Appendix Ch.3

We collect some results of [48] for convenience; see also [29, Theorem 4.1]. The Kantorowich–Rubenstein distance $\mathbf{d}_1(\mu,\nu)$ for measures $\mu,\nu\in\mathcal{P}(Q)$ is defined as

$$\mathbf{d}_1(\mu,\nu) := \sup\{\int \phi\, d(\mu-\nu); \phi : Q\to\mathbb{R}, \phi \text{ is 1 - Lipschitz }\}. \tag{5.1}$$

Theorem 3.5.1 (Theorem 2.1[48]). *Let Q^M be a compact subset of $\mathbb{R}^M$. Consider a sequence of functions $(u_M)_{M=1}^{\infty}$ with $u_M : Q^M\to\mathbb{R}$. Assume each $u_M(X)=u_M(x_1,\dots,x_M)$ is a symmetric function in all variables, i.e.,*

$$u_M(X) = u_M(x_{\sigma(1)},\dots,x_{\sigma(M)})$$

for any permutation σ on $\{1,\dots,M\}$. Let $\mathbf{d}_1$ be the Kantorowich–Rubenstein defined in (5.1) and let ω be a modulus of continuity independent of M. Assume that the sequence is uniformly bounded $\|u_M\|_{L^\infty(Q^M)}\le C$. Further assume that for all $X,Y\in Q^M$ and all M we have

$$|u_M(X)-u_M(Y)|\le\omega(\mathbf{d}_1(m_X^M,m_Y^M))$$

where $m_\xi^M\in\mathcal{P}(Q)$ is defined by $m_\xi^M(x)=\frac{1}{M}\sum_{i=1}^{M}\delta(x-\xi_i)$.

Then there exists a subsequence $(u_{M_k})_k$ of $(u_M)_M$ and a continuous map $U:\mathcal{P}(Q)\to\mathbb{R}$ such that

$$\lim_{k\to\infty}\sup_{X\in\mathbb{R}^M}|u_{M_k}(X)-U(m_X^{M_k})|=0. \tag{5.2}$$

Theorem 3.5.1 has been extended to the case of functions $g(x_i,X_{-i}) : \mathcal{X}^M\subset\mathbb{R}^M\to\mathbb{R}$ being symmetric only in X_{-i}. Here, $\mathcal{X}$ is a compact subset of $\mathbb{R}$. The corresponding result is given in [29, Section 4] and repeated here for convenience. For any permutation σ of the set $\{1,\dots,M\}\backslash\{i\}$ and all $x_i\in\mathbb{R}$ we have $g(x_i,X_{-i})=g(x_i,(x_{\sigma(j)})_{j\neq i})$. Moreover, there exists a modulus of continuity ω such that for all $x_i,y_i\in\mathbb{R}$ and all M we have

$$\|g(x_i,X_{-i})-g(y_i,Y_{-i})\|\le\omega(\|x_i-y_i\|)+\omega(\mathbf{d}_1(m_{X_{-i}}^{M-1},m_{Y_{-i}}^{M-1})).$$

Further assume that $\|g(X)\|_{L^\infty(\mathbb{R}^M)} \leq C$. Then, $g(x_i, X_{-i}) : \mathbb{R}^M \to \mathbb{R}$ can be extended to a function $G_M : \mathcal{X} \times \mathcal{P}(\mathcal{X}) \to \mathbb{R}$ by

$$G_M(x, \nu) = \inf_{X_{-i} \in \mathbb{R}^{M-1}} \{g(x, X_{-i}) + \omega(\mathbf{d}_1(m^{M-1}_{X_{-i}}, \nu))\}. \tag{5.3}$$

It can be shown as before that $(G_M)_M$ is a sequence of uniformly equi–continuous functions on $\mathcal{X} \times \mathcal{P}(\mathcal{X})$. Therefore, $(G_M)_M$ converges to a function $G : \mathcal{X} \times \mathcal{P}(\mathcal{X})$, see also [29, Theorem 4.1].

Part II

Structure preserving schemes and multivariate models

Chapter 4

Structure preserving schemes for nonlinear Fokker–Planck equations

4.1 Introduction

In this paper we construct and discuss a steady-state preserving method for a wide class of nonlinear Fokker-Planck equations of the form

$$\begin{cases} \partial_t f(w,t) = \nabla_w \cdot \Big[\mathcal{B}[f](w,t) f(w,t) + \nabla_w (D(w) f(w,t)) \Big], \\ f(w,0) = f_0(w), \end{cases} \tag{1.1}$$

where $t \geq 0$, $w \in \Omega \subseteq \mathbb{R}^d$, $d \geq 1$, $f(w,t) \geq 0$ is the unknown distribution function, $\mathcal{B}[\cdot]$ is a bounded operator which describes aggregation dynamics and $D(\cdot) \geq 0$ is a diffusion function.

A typical example is given by mean-field models of collective behavior where the nonlocal operator $\mathcal{B}[\cdot]$ has the form

$$\mathcal{B}[f](w,t) = S(w) + \int_{\mathbb{R}^d} P(w, w_*)(w - w_*) f(w_*, t) dw_*, \tag{1.2}$$

with $P : \mathbb{R}^{d \times d} \to \mathbb{R}^+$ and $S : \mathbb{R}^d \to \mathbb{R}^d$. With the choice (1.2) equation (1.1) describes typical features of the collective behavior in multiagent systems with nonlocal type interactions. These models of collective behavior has been extensively discussed in the last decades at the particle, kinetic and hydrodynamic level [10, 14, 23, 22, 50, 51, 52, 71, 141, 164]. In particular, many heterogeneous phenomena like swarming behaviors, human crowds motion and formation of wealth distributions are described by these type of PDEs under special assumptions. We refer to [142, 145], and the references therein, for a recent overview of such models.

In the following, we focus on the construction of numerical methods for such problems which are able to preserve the structural properties of the PDE, like non negativity of the solution, entropy dissipation and large time behavior. The methods here developed are second order accurate, they do not require any restriction on the mesh size and are capable to capture the asymptotic steady states with arbitrary accuracy. These properties are essential for a correct description of the underlying physical problem.

The derivation of the schemes follows the main lines of the seminal work of Chang–Cooper for the linear Fokker-Planck equation [41, 60, 137, 156]. However, in the nonlinear case, the exact stationary solution is unknown and a more advanced treatment is needed in order to find a good approximation to the problem. Similar approaches for nonlinear Fokker-Planck equations were previously derived in [40, 127]. Related methods for the case of nonlinear degenerate diffusions equations were proposed in [28, 58] and with nonlocal terms in [42, 50]. We refer also to [8] for the development of methods based on stochastic approximations and to [101] for a recent survey on schemes which preserve steady states of balance laws and related problems.

Although we derive the schemes in the case of Fokker-Planck equations, the methods can be easily applied to more general problems where the solution depends on additional parameters and the PDE is of Vlasov-Fokker-Planck type. In this case, preservation of the steady states is of fundamental importance in order to develop asymptotic-preserving methods [78].

The rest of the paper is organized as follows. In the next Section we first derive the Chang-Cooper type schemes in one-dimension with a particular attention to the steady state preserving properties. Extension to the multi-dimensional case are also considered. We then prove non negativity of solutions for explicit and semi-implicit schemes and entropy inequality for a class of one dimensional Fokker-Planck models. In Section 3 we introduce a modification of the schemes based on a more general entropy dissipation principle. We show that these entropic schemes preserve stationary solutions and derive sufficient conditions for non negativity of explicit and semi-implicit schemes. Several applications of the schemes are finally presented in Section 4 for various nonlinear Fokker-Planck problems describing collective behaviors in socio-economic and life sciences. Some conclusions are reported at the end of the manuscript.

4.2 Chang-Cooper type schemes

In the following we focus on the design of numerical schemes for (1.1) which we rewrite in divergence form as

$$\partial_t f(w,t) = \nabla_w \cdot [(\mathcal{B}[f](w,t) + \nabla_w D(w)) f(w,t) + D(w)\nabla_w f(w,t)]. \quad (2.1)$$

We can define the d-dimensional flux

$$\mathcal{F}[f](w,t) = (\mathcal{B}[f](w,t) + \nabla_w D(w))f(w,t) + D(w)\nabla_w f(w,t), \tag{2.2}$$

therefore (2.1) reads

$$\partial_t f(w,t) = \nabla_w \cdot \mathcal{F}(w,t). \tag{2.3}$$

4.2.1 Derivation of the schemes

In the one-dimensional case $d = 1$ equation (2.3) becomes

$$\partial_t f(w,t) = \partial_w \mathcal{F}[f](w,t), \quad w \in \mathcal{I} \subseteq \mathbb{R}, \tag{2.4}$$

where now

$$\mathcal{F}[f](w,t) = (\mathcal{B}[f](w,t) + D'(w))f(w,t) + D(w)\partial_w f(w,t) \tag{2.5}$$

using the compact notation $D'(w) = \partial_w D(w)$. Typically, when $\mathcal{I}$ is a finite size set the problem is complemented with no-flux boundary conditions at the extremal points. In the sequel we assume $D(w) \neq 0$ in the internal points of $\mathcal{I}$.

We introduce an uniform spatial grid $w_i \in \mathcal{I}$, such that $w_{i+1} - w_i = \Delta w$. We denote as usual $w_{i\pm1/2} = w_i \pm \Delta/2$ and define the cell average as follows

$$f_i(t) = \frac{1}{\Delta w}\int_{w_{i-1/2}}^{w_{i+1/2}} f(w,t)dw. \tag{2.6}$$

Integration of equation (2.4) yields

$$\frac{d}{dt}f_i(t) = \frac{\mathcal{F}_{i+1/2}[f](t) - \mathcal{F}_{i-1/2}[f](t)}{\Delta w}, \tag{2.7}$$

where for each $t \geq 0$ $\mathcal{F}_{i\pm1/2}[f](t)$ is the numerical flux function characterizing the discretization.

Let us set $\mathcal{C}[f](w,t) = \mathcal{B}[f](w,t) + D'(w)$ and adopt the notations $D_{i+1/2} = D(w_{i+1/2})$, $D'_{i+1/2} = D'(w_{i+1/2})$. We will consider a general flux function which is combination of the grid points $i+1$ and i

$$\mathcal{F}_{i+1/2}[f] = \tilde{\mathcal{C}}_{i+1/2}\tilde{f}_{i+1/2} + D_{i+1/2}\frac{f_{i+1} - f_i}{\Delta w}, \tag{2.8}$$

where

$$\tilde{f}_{i+1/2} = (1 - \delta_{i+1/2})f_{i+1} + \delta_{i+1/2}f_i. \tag{2.9}$$

For example, the standard approach based on central difference is obtained by considering for all i the quantities

$$\delta_{i+1/2} = 1/2, \qquad \tilde{\mathcal{C}}_{i+1/2} = \tilde{\mathcal{C}}[f](w_{i+1/2}, t).$$

It is well-known, however, that such a discretization method is subject to restrictive conditions over the mesh size Δw in order to keep non negativity of the solution.

Here, we aim at deriving suitable expressions for $\delta_{i+1/2}$ and $\tilde{\mathcal{C}}_{i+1/2}$ in such a way that the method yields nonnegative solutions, without restriction on Δw, and preserves the steady state of the system with arbitrary order of accuracy.

First, observe that at the steady state the numerical flux should vanish. From (2.8) we get

$$\frac{f_{i+1}}{f_i} = \frac{-\delta_{i+1/2}\tilde{\mathcal{C}}_{i+1/2} + \dfrac{D_{i+1/2}}{\Delta w}}{(1-\delta_{i+1/2})\tilde{\mathcal{C}}_{i+1/2} + \dfrac{D_{i+1/2}}{\Delta w}}. \tag{2.10}$$

Similarly, if we consider the analytical flux imposing $\mathcal{F}[f](w,t) \equiv 0$, we have

$$D(w)\partial_w f(w,t) = -(\mathcal{B}[f](w,t) + D'(w))f(w,t), \tag{2.11}$$

which is in general not solvable, except in some special cases due to the nonlinearity on the right hand side. We may overcome this difficulty in the quasi steady-state approximation integrating equation (2.11) on the cell $[w_i, w_{i+1}]$

$$\int_{w_i}^{w_{i+1}} \frac{1}{f(w,t)}\partial_w f(w,t)dw = -\int_{w_i}^{w_{i+1}} \frac{1}{D(w)}(\mathcal{B}[f](w,t)+D'(w))dw, \tag{2.12}$$

which gives

$$\frac{f(w_{i+1},t)}{f(w_i,t)} = \exp\left\{-\int_{w_i}^{w_{i+1}} \frac{1}{D(w)}(\mathcal{B}[f](w,t) + D'(w))dw\right\}. \tag{2.13}$$

Now, by equating the ratio f_{i+1}/f_i and $f(w_{i+1},t)/f(w_i,t)$ of the numerical and exact flux, and setting

$$\tilde{\mathcal{C}}_{i+1/2} = \frac{D_{i+1/2}}{\Delta w}\int_{w_i}^{w_{i+1}} \frac{\mathcal{B}[f](w,t) + D'(w)}{D(w)}dw \tag{2.14}$$

we recover

$$\delta_{i+1/2} = \frac{1}{\lambda_{i+1/2}} + \frac{1}{1-\exp(\lambda_{i+1/2})}, \tag{2.15}$$

where

$$\lambda_{i+1/2} = \int_{w_i}^{w_{i+1}} \frac{\mathcal{B}[f](w,t) + D'(w)}{D(w)}dw = \frac{\Delta w\,\tilde{\mathcal{C}}_{i+1/2}}{D_{i+1/2}}. \tag{2.16}$$

The numerical flux function (2.8)-(2.9) with $\tilde{\mathcal{C}}_{i+1/2}$ and $\delta_{i+1/2}$ defined by (2.14) and (2.15)-(2.16) vanishes when the corresponding flux (4.10) is equal to zero over the cell $[w_i, w_{i+1}]$. Moreover the nonlinear weight functions

$\delta_{i+1/2}$ defined by (2.15)-(2.16) are such that $\delta_{i+1/2} \in (0,1)$. The latter result follows from the simple inequality $\exp(x) \geq 1 + x$. We refer to this type of schemes as structure preserving Chang-Cooper (SP-CC) type schemes.

By discretizing (2.16) through the midpoint rule

$$\int_{w_i}^{w_{i+1}} \frac{\mathcal{B}[f](w,t) + D'(w)}{D(w)} dw = \frac{\Delta w(\mathcal{B}_{i+1/2} + D'_{i+1/2})}{D_{i+1/2}} + O(\Delta w^3), \quad (2.17)$$

we obtain the second order method defined by

$$\lambda^{\text{mid}}_{i+1/2} = \frac{\Delta w(\mathcal{B}_{i+1/2} + D'_{i+1/2})}{D_{i+1/2}} \quad (2.18)$$

and

$$\delta^{\text{mid}}_{i+1/2} = \frac{D_{i+1/2}}{\Delta w(\mathcal{B}_{i+1/2} + D'_{i+1/2})} + \frac{1}{1 - \exp(\lambda^{\text{mid}}_{i+1/2})}. \quad (2.19)$$

Higher order accuracy of the steady state solution can be obtained using suitable higher order quadrature formulas for the integral (2.14). We refer to Section 4.4 for examples and more details. For linear problems of the form $\mathcal{B}[f](w,t) = \mathcal{B}(w)$ with constant diffusion $D' = 0$, the above scheme (2.18)-(2.19) is referred to as the Chang-Cooper method [60, 137].

Remark 3.

- *If we consider the limit case $D_{i+1/2} \to 0$ in (2.18)-(2.19) we obtain the weights*

$$\delta_{i+1/2} = \begin{cases} 0, & \mathcal{B}_{i+1/2} > 0, \\ 1, & \mathcal{B}_{i+1/2} < 0 \end{cases}$$

  and the scheme reduces to a first order upwind scheme for the corresponding aggregation equation.

- *For linear problems of the form $\mathcal{B}[f](w,t) = \mathcal{B}(w)$ the exact stationary state $f^\infty(w)$ can be directly computed from the solution of*

$$D(w)\partial_w f^\infty(w) = -(\mathcal{B}(w) + D'(w))f^\infty(w), \quad (2.20)$$

  together with the boundary conditions. Explicit examples of stationary states will be reported in Section 4.4.

  Using the knowledge of the stationary state we have

$$\frac{f^\infty_{i+1}}{f^\infty_i} = \exp\left\{-\int_{w_i}^{w_{i+1}} \frac{1}{D(w)}(\mathcal{B}(w) + D'(w))dw\right\} = \exp\left(-\lambda^\infty_{i+1/2}\right), \quad (2.21)$$

  therefore

$$\lambda^\infty_{i+1/2} = \log\left(\frac{f^\infty_i}{f^\infty_{i+1}}\right) \quad (2.22)$$

Table 2.1: Different choices of the weights in (2.9)

Scheme	$\delta_{i+1/2}$	$\lambda_{i+1/2}$
Central difference	$1/2$	0
SP-CC	$\dfrac{1}{\lambda_{i+1/2}} + \dfrac{1}{1-\exp(\lambda_{i+1/2})}$	$\displaystyle\int_{w_i}^{w_{i+1}} \frac{\mathcal{B}[f](w,t) + D'(w)}{D(w)} dw$
SP-CC$_2$ (midpoint)	$\dfrac{1}{\lambda_{i+1/2}} + \dfrac{1}{1-\exp(\lambda_{i+1/2})}$	$\dfrac{\Delta w(\mathcal{B}_{i+1/2} + D'_{i+1/2})}{D_{i+1/2}}$
SP-CC$_E$ (exact)	$\dfrac{1}{\log(f_i^\infty) - \log(f_{i+1}^\infty)} + \dfrac{f_{i+1}^\infty}{f_{i+1}^\infty - f_i^\infty}$	$\log\left(\dfrac{f_i^\infty}{f_{i+1}^\infty}\right)$

and

$$\delta_{i+1/2}^\infty = \frac{1}{\log(f_i^\infty) - \log(f_{i+1}^\infty)} + \frac{f_{i+1}^\infty}{f_{i+1}^\infty - f_i^\infty}. \tag{2.23}$$

In this case, the numerical scheme preserves the steady state exactly. Finally, in Table 2.1 we summarize the different expressions of the weight functions.

4.2.2 The multi-dimensional case

In order to extend the previous approach to multi-dimensional situations we consider here the case of two dimensional problems $d = 2$. We introduce a uniform mesh $(w_i, v_j) \in \Omega \subseteq \mathbb{R}^2$, with $\Delta w = w_{i+1} - w_i$ and $\Delta v = v_{j+1} - v_j$. We denote by C_{ij} the cell $[w_{i-1/2}, w_{i+1/2}] \times [v_{j-1/2}, v_{j+1/2}]$, with $w_{i+1/2} = w_i + \Delta w/2$ and $v_{j+1/2} = v_j + \Delta v/2$. Let $f_{ij}(t)$ be the cell average defined as

$$f_{i,j} = \frac{1}{\Delta w \Delta v} \int \int_{C_{ij}} f(w, v, t) dw dv. \tag{2.24}$$

Integration of the nonlinear Fokker-Planck equation (2.3) yields

$$\frac{d}{dt} f_{i,j} = \frac{\mathcal{F}_{i+1/2,j}[f] - \mathcal{F}_{i-1/2,j}[f]}{\Delta w} + \frac{\mathcal{F}_{i,j+1/2}[f] - \mathcal{F}_{i,j-1/2}[f]}{\Delta v}, \tag{2.25}$$

being $\mathcal{F}_{i\pm1/2,j}[f]$, $\mathcal{F}_{i,j\pm1/2}[f]$ flux functions characterizing the numerical discretization. The quasi-stationary approximations over the cell $[w_i, w_{i+1}] \times$

$[v_i, v_{i+1}]$ of the two dimensional problem now read

$$\begin{aligned}\int_{w_i}^{w_{i+1}} \frac{1}{f(w,v_j,t)}\partial_w f(w,v_j,t)dw &= -\int_{w_i}^{w_{i+1}} \frac{\mathcal{B}[f](w,v_j,t)+\partial_w D(w,v_j)}{D(w,v_j)}dw,\\ \int_{v_j}^{v_{j+1}} \frac{1}{f(w_i,v,t)}\partial_v f(w_i,v,t)dv &= -\int_{v_j}^{v_{j+1}} \frac{\mathcal{B}[f](w_i,v,t)+\partial_v D(w_i,v)}{D(w_i,v)}dv.\end{aligned} \tag{2.26}$$

Therefore, setting

$$\begin{aligned}\tilde{\mathcal{C}}_{i+1/2,j} &= \frac{D_{i+1/2,j}}{\Delta w}\int_{w_i}^{w_{i+1}} \frac{\mathcal{B}[f](w,v_j,t)+\partial_w D(w,v_j)}{D(w,v_j)}dw\\ \tilde{\mathcal{C}}_{i,j+1/2} &= \frac{D_{i,j+1/2}}{\Delta v}\int_{v_j}^{v_{j+1}} \frac{\mathcal{B}[f](w_i,v,t)+\partial_v D(w_i,v)}{D(w_i,v)}dv\end{aligned} \tag{2.27}$$

and by considering the natural generalization of the one-dimensional numerical flux

$$\begin{aligned}\mathcal{F}_{i+1/2,j}[f] &= \tilde{\mathcal{C}}_{i+1/2,j}\tilde{f}_{i+1/2,j} + D_{i+1/2,j}\frac{f_{i+1,j}-f_{i,j}}{\Delta w}\\ \tilde{f}_{i+1/2,j} &= (1-\delta_{i+1/2,j})f_{i+1,j} + \delta_{i+1/2,j}f_{i,j}\\ \mathcal{F}_{i,j+1/2}[f] &= \tilde{\mathcal{C}}_{i,j+1/2}\tilde{f}_{i,j+1/2} + D_{i,j+1/2}\frac{f_{i,j+1}-f_{i,j}}{\Delta v}\\ \tilde{f}_{i,j+1/2} &= (1-\delta_{i,j+1/2})f_{i,j+1} + \delta_{i,j+1/2}f_{i,j},\end{aligned} \tag{2.28}$$

we define $\delta_{i+1/2,j}$ and $\delta_{i,j+1/2}$ in such a way that we preserve the steady state solution for each dimension. The CC type structure preserving methods are then given by

$$\begin{aligned}\delta_{i+1/2,j} &= \frac{1}{\lambda_{i+1/2,j}} + \frac{1}{1-\exp(\lambda_{i+1/2,j})},\\ \lambda_{i+1/2,j} &= \frac{\Delta w\tilde{\mathcal{C}}_{i+1/2,j}}{D_{i+1/2,j}}\end{aligned} \tag{2.29}$$

and

$$\begin{aligned}\delta_{i,j+1/2} &= \frac{1}{\lambda_{i,j+1/2}} + \frac{1}{1-\exp(\lambda_{i,j+1/2})},\\ \lambda_{i,j+1/2} &= \frac{\Delta v\tilde{\mathcal{C}}_{i,j+1/2}}{D_{i,j+1/2}}.\end{aligned} \tag{2.30}$$

The cases of higher dimension $d \geq 3$ may be derived in a similar way.

4.2.3 Main properties

In order to study the structural properties of the numerical schemes, like conservations, non negativity and entropy property, we restrict to the one-dimensional case. To start with we consider the following simple result.

Lemma 4.2.1. *Let us consider the scheme (2.7)-(2.8) for $i = 0, \dots, N$ with no flux boundary conditions $\mathcal{F}_{N+1/2} = \mathcal{F}_{-1/2} = 0$. We have*

$$\sum_{i=0}^{N} \frac{d}{dt} f_i(t) = 0, \quad \forall\, t > 0. \tag{2.31}$$

Proof. From equation (2.34) we have

$$\sum_{i=0}^{N} \frac{df_i}{dt} = \frac{1}{\Delta w} \sum_{i=0}^{N} (\mathcal{F}_{i+1/2} - \mathcal{F}_{i-1/2}). \tag{2.32}$$

Now since

$$\sum_{i=0}^{N} (\mathcal{F}_{i+1/2} - \mathcal{F}_{i-1/2}) = \mathcal{F}_{N+1/2} - \mathcal{F}_{-1/2}, \tag{2.33}$$

by imposing no flux boundary conditions we conclude. □

Positivity preservation

Concerning non negativity, first we prove a result for the explicit scheme. We introduce a time discretization $t^n = n\Delta t$ with $\Delta t > 0$ and $n = 0, \dots, T$ and consider the simple forward Euler method

$$f_i^{n+1} = f_i^n + \Delta t \frac{\mathcal{F}_{i+1/2}^n - \mathcal{F}_{i-1/2}^n}{\Delta w}. \tag{2.34}$$

Proposition 4.2.2. *Under the time step restriction*

$$\Delta t \le \frac{\Delta w^2}{2(M\Delta w + D)}, \quad M = \max_i |\tilde{\mathcal{C}}_{i+1/2}^n|, \tag{2.35}$$

the explicit scheme (2.34) with flux defined by (2.15)-(2.16) preserves non-negativity, i.e $f_i^{n+1} \ge 0$ if $f_i^n \ge 0$, $i = 0, \dots, N$.

Proof. The scheme reads

$$\begin{aligned} f_i^{n+1} = f_i^n + \frac{\Delta t}{\Delta w} \Bigg[& \left((1 - \delta_{i+1/2}^n) \tilde{\mathcal{C}}_{i+1/2}^n + \frac{D_{i+1/2}}{\Delta w} \right) f_{i+1}^n \\ & + \left(\tilde{\mathcal{C}}_{i+1/2}^n \delta_{i+1/2}^n - \tilde{\mathcal{C}}_{i-1/2}^n (1 - \delta_{i-1/2}^n) - \frac{1}{\Delta w} (D_{i+1/2} + D_{i-1/2}) \right) f_i^n \\ & - \left(\tilde{\mathcal{C}}_{i-1/2}^n \delta_{i-1/2}^n - \frac{D_{i-1/2}}{\Delta w} \right) f_{i-1}^n \Bigg]. \end{aligned} \tag{2.36}$$

From (2.36) the coefficients of f_{i+1}^n and f_{i-1}^n should satisfy

$$(1-\delta_{i+1/2})\tilde{\mathcal{C}}_{i+1/2}^n + \frac{D_{i+1/2}}{\Delta w} \geq 0, \qquad -\delta_{i-1/2}\tilde{\mathcal{C}}_{i-1/2}^n + \frac{D_{i-1/2}}{\Delta w} \geq 0, \quad (2.37)$$

or equivalently

$$\lambda_{i+1/2}\left(1 - \frac{1}{1-\exp\lambda_{i+1/2}}\right) \geq 0, \qquad \frac{\lambda_{i-1/2}}{\exp\lambda_{i-1/2}-1} \geq 0, \quad (2.38)$$

which holds true thanks to the properties of the exponential function. In order to ensure the non negativity of the scheme the time step should satisfy the restriction $\Delta t \leq \Delta w/\nu$, with

$$\nu = \max_{0\leq i\leq N}\left\{\tilde{\mathcal{C}}_{i+1/2}^n\delta_{i+1/2}^n - \tilde{\mathcal{C}}_{i-1/2}^n(1-\delta_{i-1/2}^n) - \frac{D_{i+1/2}+D_{i-1/2}}{\Delta w}\right\}. \quad (2.39)$$

Being M defined in (2.35), and $0 \leq \delta_{i\pm1/2} \leq 1$, we obtain the prescribed bound. □

Remark 4. *Higher order SSP methods* [102] *are obtained by considering a convex combination of forward Euler methods. Therefore, the non negativity result can be extended to general SSP methods.*

In practical applications, it is desirable to avoid the parabolic restriction $\Delta t = O(\Delta w^2)$ of explicit schemes. Unfortunately, fully implicit methods originate a nonlinear system of equations due to the nonlinearity of $\mathcal{B}[f]$ and the dependence of the weights $\delta_{i\pm1/2}$ from the solution. However, we can prove that nonnegativity of the solution holds true also for the semi-implicit case

$$f_i^{n+1} = f_i^n + \Delta t\frac{\hat{\mathcal{F}}_{i+1/2}^{n+1} - \hat{\mathcal{F}}_{i-1/2}^{n+1}}{\Delta w}, \quad (2.40)$$

where

$$\hat{\mathcal{F}}_{i+1/2}^{n+1} = \tilde{\mathcal{C}}_{i+1/2}^n\left[(1-\delta_{i+1/2}^n)f_{i+1}^{n+1} + \delta_{i+1/2}^n f_i^{n+1}\right] + D_{i+1/2}\frac{f_{i+1}^{n+1} - f_i^{n+1}}{\Delta w}. \quad (2.41)$$

We have

Proposition 4.2.3. *Under the time step restriction*

$$\Delta t < \frac{\Delta w}{2M}, \qquad M = \max_i|\tilde{\mathcal{C}}_{i+1/2}^n| \quad (2.42)$$

the semi-implicit scheme (2.40) preserves nonnegativity, i.e $f_i^{n+1} \geq 0$ *if* $f_i^n \geq 0$, $i = 0,\dots,N$.

Proof. Equation (2.40) corresponds to

$$
\begin{aligned}
&f_i^{n+1}\left\{1-\frac{\Delta t}{\Delta w}\left[\tilde{\mathcal{C}}_{i+1/2}^n\delta_{i+1/2}^n-\tilde{\mathcal{C}}_{i-1/2}^n(1-\delta_{i-1/2}^n)-\frac{1}{\Delta w}(D_{i+1/2}+D_{i-1/2})\right]\right\}\\
&+f_{i+1}^{n+1}\left\{-\frac{\Delta t}{\Delta w}\left[(1-\delta_{i+1/2}^n)\tilde{\mathcal{C}}_{i+1/2}^n+\frac{D_{i+1/2}}{\Delta w}\right]\right\}\\
&+f_{i-1}^{n+1}\left\{-\frac{\Delta t}{\Delta w}\left[-\tilde{\mathcal{C}}_{i-1/2}^n\delta_{i-1/2}^n+\frac{D_{i-1/2}}{\Delta w}\right]\right\}=f_i^n
\end{aligned}
\tag{2.43}
$$

thanks to the definition of the flux function introduced in (2.8)-(2.9). Using the indentity $\lambda_{i+1/2}^n=\Delta w\tilde{\mathcal{C}}_{i+1/2}^n/D_{i+1/2}$ we obtain

$$
\begin{aligned}
&f_i^{n+1}\left\{1+\frac{\Delta t}{\Delta w^2}\left[D_{i+1/2}\frac{\lambda_{i+1/2}^n}{\exp(\lambda_{i+1/2}^n)-1}+D_{i-1/2}\frac{\lambda_{i-1/2}^n}{\exp(\lambda_{i-1/2}^n)-1}\exp(\lambda_{i-1/2}^n)\right]\right\}\\
&+f_{i+1}^{n+1}\left\{-\frac{\Delta t}{\Delta w^2}D_{i+1/2}\frac{\lambda_{i+1/2}^n}{\exp(\lambda_{i+1/2}^n)-1}\exp(\lambda_{i+1/2}^n)\right\}\\
&+f_{i-1}^{n}\left\{-\frac{\Delta t}{\Delta w^2}D_{i-1/2}\frac{\lambda_{i-1/2}^n}{\exp(\lambda_{i-1/2}^n)-1}\right\}=f_i^n.
\end{aligned}
\tag{2.44}
$$

Let us denote $\alpha_{i+1/2}^n=\dfrac{\lambda_{i+1/2}^n}{\exp(\lambda_{i+1/2}^n)-1}\geq 0$ and

$$
\begin{aligned}
R_i^n&=1+\frac{\Delta t}{\Delta w^2}\left[D_{i+1/2}\alpha_{i+1/2}^n+D_{i-1/2}\alpha_{i-1/2}^n\exp(\lambda_{i-1/2}^n)\right]\\
Q_i^n&=-\frac{\Delta t}{\Delta w^2}D_{i+1/2}\alpha_{i+1/2}^n\exp(\lambda_{i+1/2}^n)\\
P_i^n&=-\frac{\Delta t}{\Delta w^2}D_{i-1/2}\alpha_{i-1/2}^n,
\end{aligned}
\tag{2.45}
$$

we can write

$$
R_i^n f_i^{n+1}-Q_i^n f_{i+1}^{n+1}-P_i^n f_{i-1}^{n+1}=f_i^n. \tag{2.46}
$$

If we introduce the matrix

$$
(\mathcal{A}[f^n])_{ij}=\begin{cases}R_i^n, & j=i\\ -Q_i^n, & j=i+1,1\leq i\leq N\\ -P_i^n, & j=i-1,0\leq i\leq N-1,\end{cases} \tag{2.47}
$$

with $R_i^n>0$, $Q_i^n\geq 0$, $P_i^n\geq 0$ defined in (2.45) the semi-implicit scheme may be expressed in matrix form as follows

$$
\mathcal{A}[\mathbf{f}^n]\mathbf{f}^{n+1}=\mathbf{f}^n, \tag{2.48}
$$

with $\mathbf{f}^n = (f_0^n, \dots, f_N^n)$. Since $\mathbf{f}^n \geq 0$, in order to prove that $\mathbf{f}^{n+1} \geq 0$ it is sufficient to show $\mathcal{A}[f^n]^{-1} \geq 0$. Now, $\mathcal{A}[\cdot]$ is a tridiagonal matrix with positive diagonal elements and if $\mathcal{A}$ is strictly diagonally dominant we can conclude that $\mathcal{A}^{-1} \geq 0$.

The matrix $\mathcal{A}$ is strictly diagonally dominant if and only if

$$|R_i^n| > |Q_i^n| + |P_i^n|, \qquad i = 0, 1 \dots, N, \tag{2.49}$$

condition which holds true if

$$\begin{aligned} 1 &> \frac{\Delta t}{\Delta w^2}\left[D_{i+1/2}\alpha_{i+1/2}^n\left(\exp(\lambda_{i+1/2}^n) - 1\right) - D_{i-1/2}\alpha_{i-1/2}^n\left(\exp(\lambda_{i-1/2}^n) - 1\right)\right] \\ &= \frac{\Delta t}{\Delta w^2}\left[D_{i+1/2}\lambda_{i+1/2}^n - D_{i-1/2}\lambda_{i-1/2}^n\right] = \frac{\Delta t}{\Delta w}\left[\tilde{\mathcal{C}}_{i+1/2}^n - \tilde{\mathcal{C}}_{i-1/2}^n\right]. \end{aligned} \tag{2.50}$$

□

Remark 5.

- *Higher order semi-implicit approximations can be constructed following* [36]*. Note, however, that the determination of nonnegative semi-implicit schemes with optimal stability regions is an open problem which goes beyond te purpose of the present manuscript.*

- *A similar argument permits to prove nonnegativity of the scheme with the fully implicit fluxes*

$$\mathcal{F}_{i+1/2}^{n+1} = \tilde{\mathcal{C}}_{i+1/2}^{n+1}\left[(1 - \delta_{i+1/2}^{n+1})f_{i+1}^{n+1} + \delta_{i+1/2}f_i^{n+1}\right] + D_{i+1/2}\frac{f_{i+1}^{n+1} - f_i^{n+1}}{\Delta w}, \tag{2.51}$$

with

$$\Delta t < \frac{\Delta w}{2M}, \quad M = \max_{0 \leq i \leq N} |\tilde{\mathcal{C}}_{i+1/2}^{n+1}|. \tag{2.52}$$

Similarly, we obtain the nonlinear system

$$\mathcal{A}[\mathbf{f}^{n+1}]\mathbf{f}^{n+1} = \mathbf{f}^n, \tag{2.53}$$

where the matrix $\mathcal{A}[\mathbf{f}^{n+1}]$ has the same structure (2.47) with the entries evaluated at time $n+1$. The above system can be solved iteratively at each time step

$$\begin{aligned} \mathbf{f}_0^{n+1} &= \mathbf{f}^n, \\ \mathbf{f}_{k+1}^{n+1} &= \mathcal{A}^{-1}[\mathbf{f}_k^{n+1}]\mathbf{f}^n, \qquad k = 0, 1, \dots \end{aligned} \tag{2.54}$$

where now each iteration step is explicit and can be made non negative under a stability restriction analogous to (2.42). Therefore, if $\mathbf{f}_k^{n+1} \to \mathbf{f}^{n+1}$ as $k \to +\infty$ we can infer the nonnegativity of the scheme under the condition (2.52), being $\mathcal{A}[\mathbf{f}^{n+1}] \geq 0$ strictly diagonally dominant and then $\mathcal{A}[\mathbf{f}^{n+1}]^{-1} \geq 0$.

Entropy property

In order to discuss the entropy property we consider the prototype equation

$$\partial_t f(w,t) = \partial_w \left[(w-u) f(w,t) + \partial_w (D(w) f(w,t)) \right], \qquad w \in I = [-1,1], \tag{2.55}$$

with $-1 < u < 1$ a given constant and boundary conditions

$$\partial_w (D(w) f(w,t)) + (w-u) f(w,t) = 0, \qquad w = \pm 1. \tag{2.56}$$

If the stationary state f^∞ exists equation (2.55) may be written in the *Landau form* as

$$\partial_t f(w,t) = \partial_w \left[D(w) f(w,t) \partial_w \log \left(\frac{f(w,t)}{f^\infty(w)} \right) \right], \tag{2.57}$$

or in the *non logarithmic Landau form* as

$$\partial_t f(w,t) = \partial_w \left[D(w) f^\infty(w) \partial_w \left(\frac{f(w,t)}{f^\infty(w)} \right) \right]. \tag{2.58}$$

We define the relative entropy for all positive functions $f(w,t), g(w,t)$ as follows

$$\mathcal{H}(f,g) = \int_I f(w,t) \log \left(\frac{f(w,t)}{g(w,t)} \right), \tag{2.59}$$

we have [92]

$$\frac{d}{dt} \mathcal{H}(f, f^\infty) = -\mathcal{I}_D(f, f^\infty), \tag{2.60}$$

where the dissipation functional $\mathcal{I}_D(\cdot,\cdot)$ is defined as

$$\begin{aligned} \mathcal{I}_D(f, f^\infty) &= \int_{\mathcal{I}} D(w) f(w,t) \left(\partial_w \log \left(\frac{f(w,t)}{f^\infty(w)} \right) \right)^2 dw, \\ &= \int_{\mathcal{I}} D(w) f^\infty(w,t) \partial_w \log \left(\frac{f(w,t)}{f^\infty(w)} \right) \partial_w \left(\frac{f}{f^\infty} \right) dw. \end{aligned} \tag{2.61}$$

Of course we might consider other entropies like the L^2 entropy which is defined as

$$\begin{aligned} L^2(f, f^\infty) &= \int_I \frac{(f(w,t) - f^\infty(w))^2}{f^\infty(w)} dw, \\ \frac{d}{dt} L_2(f, f^\infty) &= -J_D(f, f^\infty), \end{aligned} \tag{2.62}$$

with

$$J_D(f, f^\infty) = 2 \int_{\mathcal{I}} D(w) f^\infty \left(\partial_w \left(\frac{f(w,t)}{f^\infty(w)} \right)^2 \right), \tag{2.63}$$

see [92] for further examples.

Lemma 4.2.4. *In the case $\mathcal{B}[f](w,t) = \mathcal{B}(w)$ the numerical flux function (2.8)-(2.9) with $\tilde{\mathcal{C}}_{i+1/2}$ and $\delta_{i+1/2}$ given by (2.14)-(2.15) can be written in the form (2.58) and reads*

$$\mathcal{F}^n_{i+1/2} = \frac{D_{i+1/2}}{\Delta w} \hat{f}^\infty_{i+1/2} \left(\frac{f^n_{i+1}}{f^\infty_{i+1}} - \frac{f^n_i}{f^\infty_i} \right), \tag{2.64}$$

with

$$\hat{f}^\infty_{i+1/2} = \frac{f^\infty_{i+1} f^\infty_i}{f^\infty_{i+1} - f^\infty_i} \log \left(\frac{f^\infty_{i+1}}{f^\infty_i} \right). \tag{2.65}$$

Proof. In the hypothesis $\mathcal{B}[f](w,t) = \mathcal{B}(w)$ the definition of $\lambda_{i+1/2}$ does not depends on time, i.e. $\lambda_{i+1/2} = \lambda^\infty_{i+1/2}$ and if a steady state exists we may write

$$\log f^\infty_i - \log f^\infty_{i+1} = \lambda_{i+1/2}. \tag{2.66}$$

Furthermore, the flux function $\mathcal{F}^n_{i+1/2}$ assumes the following form

$$\begin{aligned} \mathcal{F}^n_{i+1/2} &= \frac{D_{i+1/2}}{\Delta w} \left[\lambda_{i+1/2} \tilde{f}^n_{i+1/2} + (f^n_{i+1} - f^n_i) \right] \\ &= \frac{D_{i+1/2}}{\Delta w} \left[\lambda_{i+1/2} (f^n_{i+1} + \delta_{i+1/2} (f^n_i - f^n_{i+1})) + (f^n_{i+1} - f^n_i) \right], \end{aligned} \tag{2.67}$$

where

$$\delta_{i+1/2} = \frac{1}{\log f^\infty_i - \log f^\infty_{i+1}} + \frac{f^\infty_{i+1}}{f^\infty_{i+1} - f^\infty_i}. \tag{2.68}$$

Hence we have

$$\begin{aligned} \mathcal{F}^n_{i+1/2} &= \frac{D_{i+1/2}}{\Delta w} \left[\log \left(\frac{f^\infty_i}{f^\infty_{i+1}} \right) \left(f^n_{i+1} + \frac{f^n_i - f^n_{i+1}}{\log f^\infty_i - \log f^\infty_{i+1}} + \frac{f^\infty_{i+1}}{f^\infty_{i+1} - f^\infty_i} (f^n_i - f^n_{i+1}) \right) \right], \\ &= \frac{D_{i+1/2}}{\Delta w} \left[\log \left(\frac{f^\infty_i}{f^\infty_{i+1}} \right) \left(\frac{f^n_i - f^n_{i+1}}{\log f^\infty_i - \log f^\infty_{i+1}} + \frac{f^\infty_{i+1} f^\infty_i}{f^\infty_{i+1} - f^\infty_i} \left(\frac{f^n_i}{f^\infty_i} - \frac{f^n_{i+1}}{f^\infty_{i+1}} \right) \right) \right] \end{aligned} \tag{2.69}$$

which gives (2.64). □

Theorem 4.2.5. *Let us consider $\mathcal{B}[f](w,t) = w - u$ as in equation (2.55). The numerical flux (2.8)-(2.9) with $\tilde{\mathcal{C}}_{i+1/2}$ and $\delta_{i+1/2}$ given by (2.14)-(2.15) satisfies the discrete entropy dissipation*

$$\frac{d}{dt} \mathcal{H}_\Delta(f, f^\infty) = -\mathcal{I}_\Delta(f, f^\infty), \tag{2.70}$$

where

$$\mathcal{H}_{\Delta w}(f, f^\infty) = \Delta w \sum_{i=0}^{N} f_i \log \left(\frac{f_i}{f^\infty_i} \right) \tag{2.71}$$

and I_Δ is the positive discrete dissipation function

$$\mathcal{I}_\Delta(f, f^\infty) = \sum_{i=0}^{N} \left[\log\left(\frac{f_{i+1}}{f^\infty_{i+1}}\right) - \log\left(\frac{f_i}{f^\infty_i}\right)\right] \cdot \left(\frac{f_{i+1}}{f^\infty_{i+1}} - \frac{f_i}{f^\infty_i}\right) \hat{f}^\infty_{i+1/2} D_{i+1/2} \geq 0. \tag{2.72}$$

Proof. From the definition of relative entropy we have

$$\begin{aligned} \frac{d}{dt}\mathcal{H}(f, f^\infty) &= \Delta w \sum_{i=0}^{N} \frac{df_i}{dt}\left(\log\left(\frac{f_i}{f^\infty_i}\right) + 1\right) \\ &= \Delta w \sum_{i=0}^{N} \left(\log\left(\frac{f_i}{f^\infty_i}\right) + 1\right)(\mathcal{F}_{i+1/2} - \mathcal{F}_{i-1/2}), \end{aligned} \tag{2.73}$$

and after summation by parts we get

$$\frac{d}{dt}\mathcal{H}(f, f^\infty) = -\Delta w \sum_{i=0}^{N} \left[\log\left(\frac{f_{i+1}}{f^\infty_{i+1}}\right) - \log\left(\frac{f_i}{f^\infty_i}\right)\right] \mathcal{F}_{i+1/2}. \tag{2.74}$$

Thanks to the identity of Lemma 4.2.4 we may conclude since the function $(x - y)\log(x/y)$ is non-negative for all $x, y \geq 0$. □

4.3 Entropic average type schemes

In this section we introduce a second class of structure preserving numerical scheme based on the entropy dissipation principle. To this aim, let us consider the general class of nonlinear Fokker-Planck equation with gradient flow structure [22, 50, 54]

$$\partial_t f(w,t) = \nabla_w \cdot [f(w,t)\nabla_w \xi(w,t)], \qquad w \in \Omega \subseteq \mathbb{R}^d, \tag{3.1}$$

and no-flux boundary conditions. In the case of equation (1.1) with constant diffusion D we have

$$\nabla_w \xi(w,t) = \mathcal{B}[f](w,t) + D\nabla_w \log f(w,t). \tag{3.2}$$

We focus on the following prototype of function $\xi(w,t)$, $w \in \mathbb{R}^d$

$$\xi = (U * f)(w,t) + D \log f(w,t), \tag{3.3}$$

which in our case corresponds to

$$\mathcal{B}[f](w,t) = \nabla_w (U * f)(w,t), \tag{3.4}$$

with $U(w)$ an interaction potential.

The corresponding free energy is given by

$$\mathcal{E}(t) = \frac{1}{2}\int_{\mathbb{R}^d}(U * f)(w,t)f(w,t)dw + D\int_{\mathbb{R}^d}\log f(w,t)f(w,t)dw. \tag{3.5}$$

We have

$$\frac{d}{dt}\mathcal{E}(t) = \int_{\mathbb{R}^d}\partial_t f(w,t)dw + \int_{\mathbb{R}^d}((U * f)(w,t) + D\log f(w,t))\partial_t f(w,t)dw. \tag{3.6}$$

Hence from (3.1) and (3.3) and upon integration by parts we obtain the dissipation of the free energy $\mathcal{E}(t)$ along solutions

$$\frac{d}{dt}\mathcal{E}(t) = -\int_{\mathbb{R}^d}|\nabla_w\xi|^2 f(w,t)dw = -\mathcal{I}(t), \tag{3.7}$$

where $\mathcal{I}(\cdot)$ is the entropy dissipation function.

4.3.1 Derivation of the schemes

Let us consider the discrete version of the entropy of the system given by

$$\mathcal{E}_\Delta(t) = \Delta w\sum_{j=0}^{N}\left[\frac{1}{2}\Delta w\sum_{i=0}^{N}U_{j-i}f_i f_j + Df_j\log f_j\right] \tag{3.8}$$

Therefore, we have

$$\begin{aligned}\frac{d}{dt}\mathcal{E}_\Delta &= \Delta w\sum_{j=0}^{N}\left[\Delta w\sum_{i=0}^{N}U_{j-i}f_i\frac{df_j}{dt} + D\left(\log f_j + 1\right)\frac{df_j}{dt}\right]\\ &= \Delta w\sum_{j=0}^{N}\left[\Delta w\sum_{i=0}^{N}U_{j-i}f_i + D\log f_j + 1\right]\frac{df_j}{dt}.\end{aligned} \tag{3.9}$$

Now using the general discrete conservative formulation

$$\frac{df_j}{dt} = \frac{\mathcal{F}_{j+1/2} - \mathcal{F}_{j-1/2}}{\Delta w},$$

and the fact that $\xi_j = U * f_j + D\log f_j$ we get

$$\frac{d}{dt}\mathcal{E}_\Delta = \sum_{j=0}^{N}(\xi_j + 1)(\mathcal{F}_{j+1/2} - \mathcal{F}_{j-1/2}). \tag{3.10}$$

Furthermore, after summation by parts we can write the last term as follows

$$\frac{d}{dt}\mathcal{E}_\Delta = -\sum_{j=0}^{N}(\xi_{j+1} - \xi_j)\mathcal{F}_{j+1/2}. \tag{3.11}$$

Now, integrating (3.2) in the one-dimensional case we obtain

$$\xi_{j+1} - \xi_j = \Delta w\, \tilde{\mathcal{B}}_{j+1/2} + D \log\left(\frac{f_{j+1}}{f_j}\right). \tag{3.12}$$

Let us now consider a general scheme in the form (2.7), which in our case can be rewritten as

$$\mathcal{F}_{i+1/2} = \left(\tilde{\mathcal{B}}_{j+1/2} + \frac{D}{\Delta w}\log\left(\frac{f_{j+1}}{f_j}\right) K_{j+1/2}\right) \tilde{f}_{j+1/2} \tag{3.13}$$

with

$$K_{j+1/2} = \frac{1}{\tilde{f}_{j+1/2}} \frac{f_{j+1} - f_j}{(\log f_{j+1} - \log f_j)}, \qquad f_{j+1} \neq f_j. \tag{3.14}$$

Therefore, we have

$$\begin{aligned} \frac{d}{dt}\mathcal{E}_\Delta = -\Delta w \sum_{j=0}^{N} &\left(\tilde{\mathcal{B}}_{j+1/2} + \frac{D}{\Delta w}\log\left(\frac{f_{j+1}}{f_j}\right)\right) \\ &\left(\tilde{\mathcal{B}}_{j+1/2} + \frac{D}{\Delta w}\log\left(\frac{f_{j+1}}{f_j}\right) K_{j+1/2}\right) \tilde{f}_{j+1/2}. \end{aligned} \tag{3.15}$$

Thus we cannot prove that the discrete entropy functional (3.8) is dissipated by the Chang-Cooper type scheme developed in the previous sections, unless $K_{j+1/2} \equiv 1$. This latter requirement is satisfied if we consider the new entropic flux function

$$\tilde{f}^E_{i+1/2} = \begin{cases} \dfrac{f_{i+1} - f_i}{\log f_{i+1} - \log f_i} & f_{i+1} \neq f_i, \\ f_{i+1} & f_{i+1} = f_i. \end{cases} \tag{3.16}$$

We will refer to the above approximation of the solution at the grid point $i + 1/2$ as *entropic average* of the grid points i and $i + 1$. In the general case of the flux function (4.10) with non constant diffusion the resulting numerical flux reads

$$\mathcal{F}^E_{i+1/2} = D_{i+1/2}\left(\frac{\tilde{\mathcal{C}}_{i+1/2}}{D_{i+1/2}} + \frac{\log f_{i+1} - \log f_i}{\Delta w}\right) \tilde{f}^E_{i+1/2}. \tag{3.17}$$

Finally, concerning the stationary state, we obtain immediately imposing the numerical flux equal to zero

$$\frac{\tilde{\mathcal{C}}_{i+1/2}}{D_{i+1/2}} + \frac{\log f_{i+1} - \log f_i}{\Delta w} = 0,$$

and therefore we get

$$\frac{f_{i+1}}{f_i} = \exp\left(-\frac{\Delta w\, \tilde{\mathcal{C}}_{i+1/2}}{D_{i+1/2}}\right). \tag{3.18}$$

By equating the above ratio with the quasi-stationary approximation (2.13) we get the same expression for $\tilde{\mathcal{C}}_{i+1/2}$ as in (2.14)

$$\tilde{\mathcal{C}}_{i+1/2} = \frac{D_{i+1/2}}{\Delta w} \int_{w_i}^{w_{i+1}} \frac{\mathcal{B}[f](w,t) + D'(w)}{D(w)} dw. \tag{3.19}$$

4.3.2 Main properties

A fundamental result concerning the entropic average (3.16) is the following Lemma.

Lemma 4.3.1. *The entropy average defined in (3.16) may be written as a convex combination with nonlinear weights*

$$\tilde{f}^E_{i+1/2} = \delta^E_{i+1/2} f_i + (1 - \delta^E_{i+1/2}) f_{i+1}, \tag{3.20}$$

where

$$\delta^E_{i+1/2} = \frac{f_{i+1}}{f_{i+1} - f_i} + \frac{1}{\log f_i - \log f_{i+1}} \in (0,1). \tag{3.21}$$

Proof. From (3.21) we have

$$\begin{aligned} \tilde{f}^E_{i+1/2} &= f_{i+1} + \delta^E_{i+1/2}(f_i - f_{i+1}) \\ &= f_{i+1} - f_{i+1} + \frac{f_i - f_{i+1}}{\log f_i - \log f_{i+1}} \\ &= \frac{f_{i+1} - f_i}{\log f_{i+1} - \log f_i}, \end{aligned} \tag{3.22}$$

that is (3.17). It is a easy computation to verify that $\delta^E_{i+1/2}$ lies in the interval $(0,1)$. □

Remark 6. *As a consequence the Chang-Cooper type average (2.9) and the entropic average (3.16) define the same quantity at the steady state when $f_i = f_i^\infty$. In fact, the Chang-Cooper type weights (2.23) are the same as (3.21).*

We can summarize our findings of Section 4.3.1 as follows.

Theorem 4.3.2. *The numerical flux (3.17)-(3.16) for a constant diffusion D satisfies the discrete entropy dissipation*

$$\frac{d}{dt}\mathcal{E}_\Delta = -\mathcal{I}_\Delta(t), \tag{3.23}$$

where $\mathcal{E}_\Delta$ is given by (3.8) and I_Δ is the discrete entropy dissipation function

$$\mathcal{I}_\Delta = \Delta w \sum_{j=0}^{N} (\xi_{j+1} - \xi_j)^2 \tilde{f}^E_{i+1/2} \geq 0, \tag{3.24}$$

with $\xi_{j+1} - \xi_j$ defined as in (3.12).

Remark 7. *On the contrary to the Chang-Cooper average the restrictions for the non negativity property of the solution are stronger. In fact, by the same arguments we used in the previous section, non negativity of the explicit scheme requires*

$$(1-\delta^E_{i+1/2})\tilde{\mathcal{C}}^n_{i+1/2}+\frac{D_{i+1/2}}{\Delta w}\geq 0, \qquad -\delta^E_{i-1/2}\tilde{\mathcal{C}}^n_{i-1/2}+\frac{D_{i-1/2}}{\Delta w}\geq 0. \tag{3.25}$$

However, the weights do not possess any special structure that permits to avoid a constraint of the mesh size Δw which now must satisfy

$$\Delta w \leq \min_i \left\{ \frac{D_{i+1/2}}{|\tilde{\mathcal{C}}^n_{i+1/2}|}, \frac{D_{i-1/2}}{|\tilde{\mathcal{C}}^n_{i-1/2}|} \right\}. \tag{3.26}$$

Therefore, similar to central differences, we have a restriction on the mesh size which becomes prohibitive for small values of the diffusion function $D(w)$. It is easy to verify that the same condition is necessary also for the non negativity of semi-implicit approximations.

Next we consider the case of linear flux $\mathcal{B}[f](w,t)=B(w)$. The following Lemma holds true.

Lemma 4.3.3. *In the case $\mathcal{B}[f](w,t)=B(w)$ the numerical flux (3.17)-(3.16) corresponds to the form (2.57) and reads*

$$\tilde{\mathcal{F}}^E_{i+1/2}=\frac{D_{i+1/2}}{\Delta w}\tilde{f}^E_{i+1/2}\left(\log\left(\frac{f_{i+1}}{f^\infty_{i+1}}\right)-\log\left(\frac{f_i}{f^\infty_i}\right)\right). \tag{3.27}$$

Proof. If a stationary $f^\infty(w)$ state exists it nullify the flux and we have

$$\tilde{\mathcal{C}}_{i+1/2}=-\frac{D_{i+1/2}}{\Delta w}\left(\log f^\infty_{i+1}-\log f^\infty_i\right). \tag{3.28}$$

From the definition of the entropic flux (3.17) we obtain

$$\begin{aligned}\tilde{\mathcal{F}}^E_{i+1/2}=&\tilde{\mathcal{C}}_{i+1/2}\tilde{f}^E_{i+1/2}+\frac{D_{i+1/2}}{\Delta w}\log\frac{f_{i+1}}{f_i}\tilde{f}^E_{i+1/2}\\ =&\frac{D_{i+1/2}}{\Delta w}\tilde{f}^E_{i+1/2}\left[(\log f_{i+1}-\log f_i)-(\log f^\infty_{i+1}-\log f^\infty_i)\right],\end{aligned} \tag{3.29}$$

from which we conclude. □

We can now state the following entropy dissipation results for problem (2.55) in the nonlogarithmic Landau form (2.58).

Theorem 4.3.4. *Let us consider $\mathcal{B}[f](w,t)=w-u$ as in equation (2.55). The numerical flux (3.17)-(3.16) with $\tilde{\mathcal{C}}_{i+1/2}$ given by (2.14) satisfies the discrete entropy dissipation*

$$\frac{d}{dt}\mathcal{H}_\Delta(f,f^\infty)=-\mathcal{I}^E_\Delta(f,f^\infty), \tag{3.30}$$

where $\mathcal{H}_{\Delta w}(f, f^\infty)$ *is given by* (2.71) *and* I^E_Δ *is the positive discrete dissipation function*

$$\mathcal{I}^E_\Delta(f, f^\infty) = \sum_{i=0}^{N} \left[\log\left(\frac{f_{i+1}}{f^\infty_{i+1}}\right) - \log\left(\frac{f_i}{f^\infty_i}\right)\right]^2 D_{i+1/2}\tilde{f}^E_{i+1/2} \geq 0. \tag{3.31}$$

Proof.

$$\frac{d}{dt}\mathcal{H}(f, f^\infty) = -\Delta w \sum_{i=0}^{N} \left[\log\left(\frac{f_{i+1}}{f^\infty_{i+1}}\right) - \log\left(\frac{f_i}{f^\infty_i}\right)\right] \mathcal{F}^E_{i+1/2} \tag{3.32}$$

and being

$$\mathcal{F}^E_{i+1/2} = \frac{D_{i+1/2}}{\Delta w}\left[\log\left(\frac{f_{i+1}}{f^\infty_{i+1}}\right) - \log\left(\frac{f_i}{f^\infty_i}\right)\right] \tilde{f}^E_{i+1/2}$$

we have

$$\frac{d}{dt}\mathcal{H}(f, f^\infty) = -\sum_{i=0}^{N} \left[\log\left(\frac{f_{i+1}}{f^\infty_{i+1}}\right) - \log\left(\frac{f_i}{f^\infty_i}\right)\right]^2 D_{i+1/2}\tilde{f}^E_{i+1/2}. \tag{3.33}$$

□

4.4 Applications

In this section we present several numerical examples of Fokker-Planck equations solved with the structure-preserving schemes here introduced. An essential aspect for the accurate description of the steady state is the approximation of the integral defining the quasi-stationary solution

$$\lambda_{i+1/2} = \int_{w_i}^{w_{i+1}} \frac{\mathcal{B}[f](w,t) + D'(w)}{D(w)} dw. \tag{4.1}$$

Except for simple linear cases, a suitable quadrature formula is required. In the following numerical examples we consider open Newton-Cotes formulas up to order 6 and Gauss-Legendre quadrature.

4.4.1 Example 1: Opinion dynamics in bounded domains

Let us consider the evolution of a distribution function described by (1.1), with $w \in I$, where $I = [-1, 1]$, and

$$\mathcal{B}[f](w,t) = \int_I P(w, w_*)(w - w_*) f(w_*, t) dw_*, \qquad D(w) = \frac{\sigma^2}{2}(1 - w^2)^2. \tag{4.2}$$

The model describes the evolution of the distribution functions of agents having opinion w at time t (see [145, 164] for more details).

In the simplified case $P \equiv 1$ the corresponding stationary distribution reads

$$f_\infty(w) = \frac{C}{(1-w^2)^2}\left(\frac{1+w}{1-w}\right)^{u/(2\sigma^2)} \exp\Big\{-\frac{(1-uw)}{\sigma^2(1-w^2)}\Big\}, \tag{4.3}$$

with $\sigma \in \mathbb{R}$ a given parameter, $C > 0$ is a normalization constant and $u = \int_I w f(w,t)dw$,.

We consider as initial distribution

$$f(w,0) = \beta\left[\exp\left(-c(w+1/2)^2\right) + \exp\left(-c(w-1/2)^2\right)\right], \qquad c = 30, \tag{4.4}$$

with $\beta > 0$ a normalization constant. Since diffusion vanishes at the boundaries we present results for the Chang-Cooper type numerical schemes SP–CC only.

In Figure 4.1 we compute the relative L^1 error of the numerical solution with respect to the exact (4.3) stationary state using $N = 80$ points for the SP–CC scheme with various quadrature rules. We will adopt the notation SP–CC$_k$, $k = 2, 4, 6, G$ when (4.1) is approximated with second, fourth, sixth order Newton–Cotes quadrature or Gaussian quadrature respectively. It is possible to observe how the different integration methods capture the steady state with different accuracy. In particular with the Gaussian quadrature, performed with $M = 6$ quadrature points, we essentially reach the machine precision. In the same figure we illustrate how SP–CC scheme dissipates the relative entropy (2.71) in the case of two coarse grids with $N = 10$ and $N = 20$ points.

In Table 4.2 we estimate the overall order of convergence of the SP–CC scheme for several integration methods. Here we used $N = 20, 40, 80$, with reference solutions computed with $N = 640$ points. The time integration has been performed with an explicit RK4 method and the time step chosen in such a way that the CFL condition for the positivity of the scheme is satisfied, i.e. $\Delta t = O(\Delta w^2)$. As expected the method is second order accurate in the transient regimes and, as it capture the steady state, assumes the order of the quadrature method.

In the general case $P(w, w_*) \neq 1$ and it is not possible to give an analytical formulation of the steady state solution $f^\infty(w,t)$. In Figure 4.2 we represent a typical evolution of an aggregation model in the bounded confidence case [145]

$$P(w, w_*) = \chi(|w - w_*| \leq \Delta), \tag{4.5}$$

where $\chi(\cdot)$ is the indicator function, for $\Delta = 0.4$, $\Delta = 0.8$. Here, the evolution has been computed through a SP–CC with Gauss quadrature, the integral $\mathcal{B}[f](w,t)$ has been evaluated through a trapezoidal method.

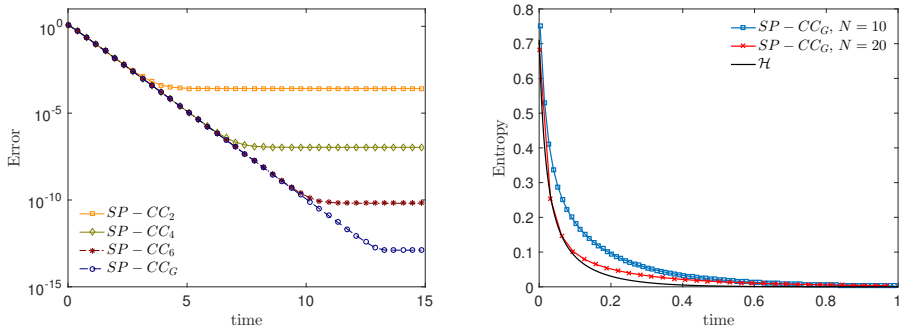

Figure 4.1: **Example 1**. Left: evolution of the relative L^1 error with respect to the stationary solution (4.3) for the SP–CC scheme with different quadrature methods. Solution for the initial data (4.4) over the time interval $[0, 10]$, $\sigma^2/2 = 0.1$, $N = 80$, $\Delta t = \Delta w^2/16\sigma^2$. Right: dissipation of the numerical entropy for SP–CC scheme with Gaussian quadrature for two coarse grids with $N = 10$ and $N = 20$ points.

	$SP-CC_k$			
Time	2	4	6	G
1	1.9470	1.9773	1.9762	1.9762
5	1.9700	3.2323	2.3724	2.3522
10	1.9695	3.9156	6.8517	7.3252

Table 4.2: **Example 1**. Estimation of the order of convergence toward the reference stationary state for explicit SP–CC, $N = 20, 40, 80$, reference solution computed with $N = 640$, $\sigma^2/2 = 0.1$, $\Delta t = \Delta w^2/16\sigma^2$.

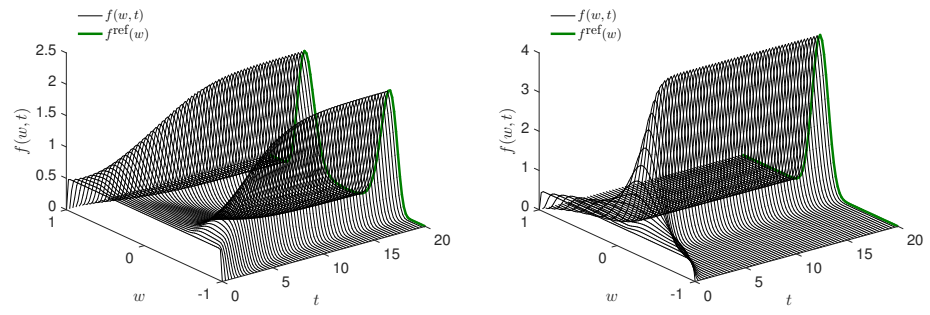

(a) (b)

Figure 4.2: **Example 1**. Opinion model in the bounded confidence case with **(a)** $\Delta = 0.4$, **(b)** $\Delta = 0.8$. In both cases we considered $\Delta w = 0.05$, $\sigma^2/2 = 0.01$, $\Delta t = \Delta w^2/16\sigma^2$. The reference solution (green) has been computed with a discretization of the computational domain of $N = 640$ gridpoints.

4.4.2 Example 2: Wealth evolution in unbounded domains

Let us consider equation (1.1) with $w \in \mathbb{R}^+$ and

$$\mathcal{B}[f](w,t) = \int_{\mathbb{R}^+} a(w,w_*)(w-w_*)f(w_*,t)dw_*, \qquad D(w) = \frac{\sigma^2}{2}w^2. \quad (4.6)$$

With the above choice, the Fokker-Planck equation describes the evolution of the wealth distribution w at time t in a large set of interacting economic agents (see [142, 145] for details).

In the case of constant interaction $a(w,w_*) \equiv 1$ the steady state of the equation is analytically computable

$$f^\infty(w) = \frac{(\mu-1)^\mu}{\Gamma(\mu)w^{1+\mu}} \exp\left\{-\frac{\mu-1}{w}\right\}, \quad (4.7)$$

where $\mu = 1 + 2/\sigma^2$ is the so-called Pareto exponent. In the numerical test we consider the initial distribution

$$f(w,0) = \beta\left[\exp\left(-c(w-u)^2\right)\right], \qquad c = 20, \quad (4.8)$$

with $\beta > 0$ a normalization constant.

Again, due to degeneracy of the diffusion on the left boundary we report results only for SP–CC schemes. In Figure 4.3 we present the solution with $u = 2$ in the domain $[0, L]$, $L = 10$. In both figures $a(\cdot,\cdot) = 1$ whereas the diffusion constant assumes different values. We report the evolution of the solution and the relative L^1 error with respect to the stationary state using $N = 201$ points for the semi–implicit SP–CC scheme (SISP–CC). We observe how the introduced methods describe the stationary state with different levels of accuracy. Note that, at the right boundary we must introduce an artificial boundary condition in order to truncate the computational domain. In our numerical results we impose the quasi stationary condition (2.13) in order to evaluate $f_{N+1}(t)$, that is

$$\frac{f_{N+1}(t)}{f_N(t)} = \exp\left\{-\int_{w_N}^{w_{N+1}} \frac{\mathcal{B}[f]+D(w)}{D(w)}dw\right\}. \quad (4.9)$$

In Table 4.3 we estimate the overall order of convergence of the SISP–CC scheme for several integration methods with $N = 51, 101, 201$ for the domain $[0, L]$, $L = 10$, with reference solutions computed with $N = 1601$ gridpoints. The time step is chosen in such a way that the CFL condition for the positivity of the scheme is satisfied, i.e. $\Delta t = O(\Delta w)$. We can observe that for short times the order of accuracy is limited by the semi–implicit method, which is first order accurate, whereas as we approach to the stationary solution the order depends on the quadrature formula used.

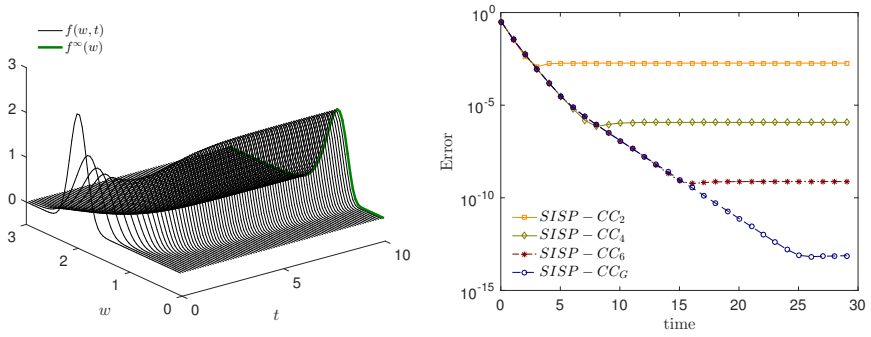

Figure 4.3: **Example 2**. Left: evolution of the density $f(w,t)$ for (4.6) with $P(\cdot,\cdot) = 1$, $u = 2$, $\sigma^2/2 = 0.1$, $L = 10$. In green we report the analytical steady state solution (4.7). Right: evolution of the relative L^1 error for the different quadratures methods for the semi–implicit SP–CC scheme in the case $a(\cdot,\cdot) = 1$, $\sigma^2/2 = 0.1$ and $\Delta w = 0.05$

	$SP - CC_k$			
Time	2	4	6	G
1	1.3047	1.5010	1.5021	1.5021
10	1.9893	4.0634	2.8122	2.8682
20	1.9894	3.9842	6.0784	10.0422

Table 4.3: **Example 2**. Estimation of the order of convergence toward the reference stationary state for the semi–implicit SP-CC scheme, $N = 51, 101, 201$, reference solution computed with $N = 1601$, $\sigma^2/2 = 0.1$.

4.4.3 Example 3: 2D model of swarming

Let us consider a self-propelled swarming model of Cucker-Smale type [22] with diffusion. In this model the evolving distribution $f(x, w, t)$ represents the density of individuals (birds, fishes, ...) in position $x \in \mathbb{R}^d$ having velocity $w \in \mathbb{R}^d$ at time $t > 0$. We have the following dynamic

$$\begin{aligned}\partial_t f(x,w,t) + w\nabla_x f(x,w,t) =& \nabla_w \cdot \Big[\alpha w(|w|^2-1)f(x,w,t) \\ &+ (w-u_f)f(x,w,t) + D\nabla_w f(x,w,t)\Big],\end{aligned} \tag{4.10}$$

with

$$u_f(x,t) = \frac{\int_{\mathbb{R}^{2d}} K(x,y) w f(y,w,t) dw dy}{\int_{\mathbb{R}^{2d}} K(x,y) f(y,w,t) dw dy}, \tag{4.11}$$

and $K(w, y) > 0$ a localization kernel, $\alpha > 0$ a self-propulsion term and $D > 0$ a constant noise intensity.

The space homogeneous version of the model (4.10) may be formulated in terms of the nonlinear Fokker–Planck equation (1.1) with

$$\begin{aligned}\mathcal{B}[f](w,t) &= \alpha w(|w|^2-1) + \int_{\mathbb{R}^2} P(w,w_*)(w-w_*)f(w_*,t)dw_*, \\ D(w) &= D,\end{aligned} \tag{4.12}$$

with α a positive constant and $P(w, w_*) \equiv 1$. The above equation can be written as a gradient flow. In fact, if we define

$$\xi(w,t) = \Phi(w) + (U * f)(w,t) + D\log f(w,t), \tag{4.13}$$

with $U(w)$ a Coloumb potential and $\Phi(w)$ a confining potential given by

$$\Phi(w) = \alpha\left(\frac{|w|^4}{4} - \frac{|w|^2}{2}\right), \tag{4.14}$$

the equation reads

$$\partial_t f(w,t) = \nabla_w \cdot \left(f(w,t)\nabla_w \xi(w,t)\right), \qquad w \in \mathbb{R}^2. \tag{4.15}$$

A free energy functional which dissipates along solutions is defined by

$$\mathcal{E}(t) = \int_{\mathbb{R}^2} \left(\alpha\frac{|w|^4}{4} + (1-\alpha)\frac{|w|^2}{2}\right) f(w,t)dw - \frac{1}{2}|u_f|^2 + D\int_{\mathbb{R}^2} f(w,t)\log f(w,t)dw, \tag{4.16}$$

with

$$u_f(t) = \frac{\int_{\mathbb{R}^2} w f(w,t)dw}{\int_{\mathbb{R}^2} f(w,t)dw}. \tag{4.17}$$

$\alpha = 0$	$SP - CC_k$				$SP - EA_k$			
Time	2	4	6	G	2	4	6	G
1	2.1387	2.1387	2.1387	2.1387	2.4142	2.4142	2.4142	2.4142
5	6.9430	6.9430	6.9430	6.9430	10.0712	10.0712	10.0712	10.0712
10	20.0127	20.0127	20.0127	20.0127	23.9838	23.9838	23.9838	23.9838
$\alpha = 1$	$SP - CC_k$				$SP - EA_k$			
Time	2	4	6	G	2	4	6	G
1	2.5310	2.5310	2.5310	2.5310	2.2614	2.2892	2.2892	2.2892
5	2.0498	7.6659	7.6659	7.6659	2.0635	10.9818	10.9818	10.9818
10	2.0503	18.7697	18.7697	18.7697	2.0613	14.8321	14.8321	14.8321

Table 4.4: **Example 3**. Estimation of the order of convergence for the one-dimensional swarming model for the explicit SP–CC and SP–EA over the domain $[-L, L]$ with $L = 5$, $N = 21, 41, 81$, $D = 0.4$, $\Delta t = \Delta w^2/L^2$.

Stationary solutions should satisfy the identity $\nabla_w \xi = 0$ and have the form

$$f^\infty(w) = C \exp\left\{ -\frac{1}{D}\left[\alpha\frac{|w|^4}{4} + (1-\alpha)\frac{|w|^2}{2} - \bar{u}\cdot w\right]\right\}, \tag{4.18}$$

with $C > 0$ a normalization constant and $\bar{u} = u_f$. It is possible to prove the following result (see [22] for more details).

Theorem 4.4.1. *Let us consider equation (4.10) in the space-homogeneous case, i.e. (1.1) with $\mathcal{B}[f](w,t)$ and diffusion as in (4.12), exhibits a phase transition in the following sense*

i) For small enough diffusion coefficient $D > 0$ there is a function $u = u(D)$ with $\lim_{D\to 0} u(D) = 1$, such that $f^\infty(w)$ with $u = (u(D), 0, \ldots, 0)$ is a stationary solution of the original problem.

ii) For large enough diffusion coefficients $D > 0$ the only stationary solution is the symmetric distribution given by (4.18) with $u_f \equiv 0$.

Since diffusion is constant, we compute the solution both using SP–CC type schemes and the entropic average schemes SP–EA. We use the same subscript notation concerning the quadrature formula adopted. In Table 4.4 we estimate the order of convergence of the SP–CC and SP–EA schemes in the 1D case for several integration methods. We can observe how each method reach spectral accuracy in the case $\alpha = 0$, i.e. when (4.12) is smooth and has an exponential decay of the tails.

In Figure 4.4 we show that, as expected, on a coarse grid the SP–EA method becomes unstable for vanishing diffusions, whereas the SP–CC scheme remains stable and reduces to first order upwinding. In this case the solution

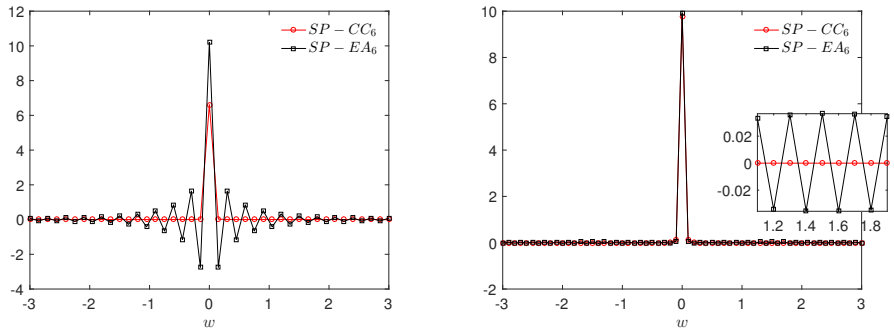

Figure 4.4: **Example 3**. Stationary solution for the one-dimensional swarming model with $\alpha = 1$ and $D = 0.001$, $N = 41$ (left) and $N = 61$ (right). As expected the SP–EA scheme produces instabilities for a vanishing diffusion. The SP–CC scheme remains stable and first order accurate.

becomes close to a Dirac delta in the velocity space. Finally, in Figure 4.5 we present the resulting 2D nonlinear Fokker–Planck equation for swarming with $\mathcal{B}[f](w,t)$ and $D(w)$ in (4.12), for several values of the diffusion coefficient and fixed self-propulsion $\alpha = 2$. The semi-implicit numerical scheme has been used, with a 6th order open Newton–Cotes quadrature method. It is possible to observe the threshold phenomenon occurring for an increasing diffusion prescribed by Theorem 4.4.1. The results obtained with the two different schemes are essentially equivalent in this case.

4.5 Conclusion

The construction of structure–preserving schemes for nonlinear Fokker–Planck equations has been studied. Two different types of schemes have been constructed. The first type represents a natural extension of the so–called Chang–Cooper scheme to the nonlinear case. The second type of schemes represents a modification with better entropy dissipation properties. Both methods are second order accurate and capable to preserve the stationary state with arbitrary accuracy. However, non negativity restrictions are more severe for the second type of schemes. Even if the analysis is performed in the one-dimensional case, extensions to multidimensional situations are also considered. Several applications to linear and nonlinear Fokker-Planck equations arising in socio-economic sciences are presented and show the generality of the present approach. Extensions of the schemes to include nonlinear diffusion terms and higher order schemes in the limiting of vanishing diffusion are actually under study and will be presented elsewhere.

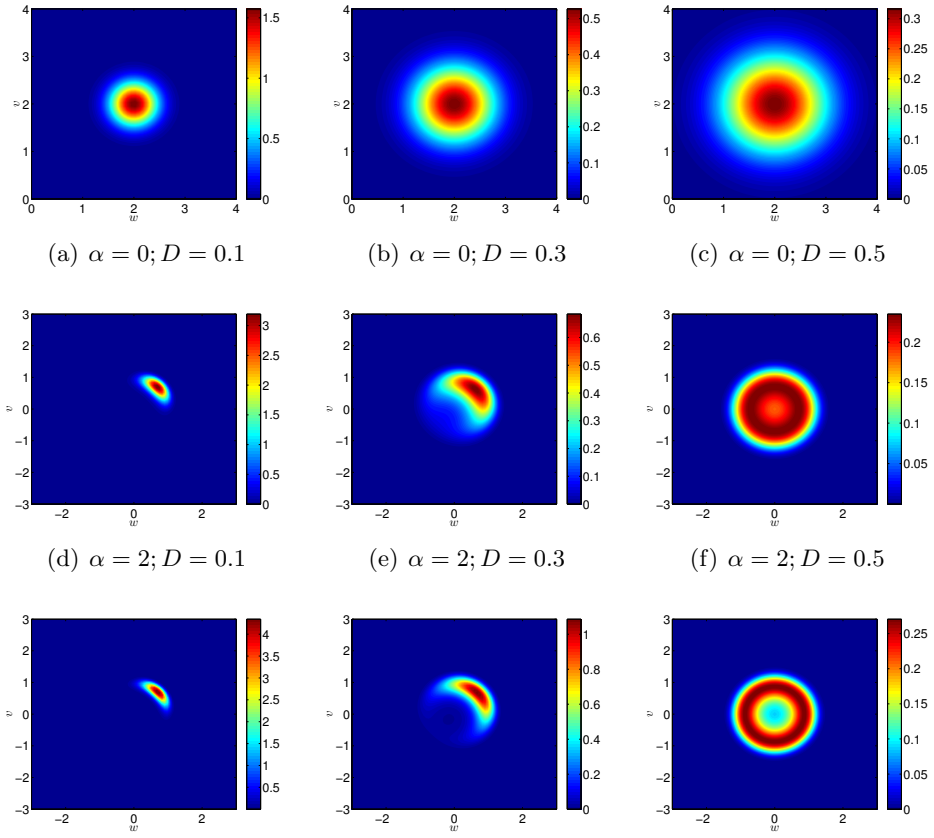

(a) $\alpha = 0; D = 0.1$ (b) $\alpha = 0; D = 0.3$ (c) $\alpha = 0; D = 0.5$

(d) $\alpha = 2; D = 0.1$ (e) $\alpha = 2; D = 0.3$ (f) $\alpha = 2; D = 0.5$

(g) $\alpha = 4; D = 0.1$ (h) $\alpha = 4; D = 0.3$ (i) $\alpha = 4; D = 0.5$

Figure 4.5: **Example 3**. Stationary state of the two-dimensional swarming model for several values of the diffusion coefficient $D > 0$ and fixed self-propulsion $\alpha = 0, 2, 4$. In the case $\alpha > 0$ for increasing values of D the mean of the stationary distribution approaches to $[0, 0]$. We considered a discretization $(w, v) \in [-L, L] \times [-L, L]$, $L = 3$, $\Delta w = \Delta v = 0.05$ and $\Delta t = dw/L$. The initial distribution is a bivariate normal distribution centered in $(2, 2)$ and diagonal covariance matrix with $\sigma_w^2 = \sigma_v^2 = 0.5$.

Chapter 5

Opinion dynamics over complex networks

5.1 Introduction

In recent years, the importance of large scale social networks has grown enormously and their study has raised lots of attentions, with the aim to understand how their structure and connections may influence the spread of opinions and ideas through human networks [1, 12, 17, 72, 80, 150, 153]. A major research topic is how to model the information exchange and, in particular, to understand and analyze the effects of interpersonal influence on processes such as opinion formation and creation and removal of new connections. The latter aspect is closely related to the construction of graph models for complex networks and has emerged as one of the most active research fields [3, 15, 20, 143, 159]. The empirical studies of technological and communication networks has been actively investigated thanks to a huge amount of data coming from the online platforms. From the theoretical point of view it is an unprecedented laboratory for testing the collective behavior of large populations of agents [21, 171]. The need to handle with millions, and often billions, of vertices implied a considerable shift of interest to large-scale statistical properties of graphs.

In this context kinetic theory may play a major role in designing effective models to characterize the statistical features of the opinion dynamics over such large collection of data. In particular, it can be used to analyze the so called *stylized facts* of the dynamics, like the asymptotic degree distribution of the connections in the network and the large time opinion behavior. To this aim, in this paper, we extend the kinetic model of opinion formation introduced in [164] to the case where each agent possesses a certain number of connections in the network. These connections evolve accordingly to a preferential attachment dynamics for the removal and creation of new connections. In this sense, the model here proposed falls in the general class

of kinetic models for socio-economic problems where the dynamics of the model is influenced by additional characteristics of the agents, like personal conviction, leadership and knowledge [11, 39, 82, 84, 145, 146, 147].

In principle, the modeling here proposed is not limited to a particular kind of opinion dynamics and one can adapt other models developed in the literature [37, 82, 162] to evolve over networks by following the ideas presented in this paper. We mention here that recently opinion models have been considered in the context of optimal control in [6, 11, 12]. In a recent note [12] we faced the solution of an optimal control problem for a model of opinion dynamics described by a system of ordinary differential equations over an evolving network. More precisely we considered a network with a fixed number of vertices and edges which modifies its configuration of connections in time through a preferential attachment rewiring process.

A further contribution of the present manuscript is the development of numerical methods which are capable to describe correctly the large time behavior of the system. In particular we will focus on finite-difference schemes for the mean-field description of the opinion model over the network inspired by the well-known Chang–Cooper method [41, 40, 60, 127]. We remark that, at variance with the standard Chang–Cooper method, the Fokker-Planck model considered here is nonlinear. Similar schemes for nonlinear Fokker-Planck equations have been previously introduced in [40, 127].

The rest of the chapter is organized as follows. In Section 2 we introduce the kinetic model and describe the evolution of the network of connections. The main properties of the network and the evolution of some macroscopic quantities, like the mean and the variance of the opinion over the network, are discussed. Next in Section 3 we derive a Fokker-Planck model for the opinion dynamics under the classical quasi-invariant scaling. This permits to compute asymptotic stationary solutions of the opinion over the graph in some simplified situations. Section 4 is devoted to the construction of numerical methods for the above problems. Monte Carlo methods for the Boltzmann model and finite difference schemes for the Fokker-Planck model which are capable to describe correctly the steady states of the system are introduced. Finally in Section 5 several numerical examples illustrate our findings and show the behavior of the model. In separate Appendices we report proofs related to the main properties of the network and to the positivity preservation property of the finite difference scheme.

5.2 The kinetic model

In this section we introduce a general mathematical model based on a kinetic description for the study of the opinion formation on a large evolving network.

5.2.1 Opinion dynamics

Let us consider a large system of agents interacting through a given network. We associate to each agent an opinion w, which varies continuously in a closed subset whose bounds denote two extreme and opposite opinions, and its number of connections c, as a discrete variable varying between 0 and the maximum number of connections allowed by the network. Note that this maximum number typically is a fixed value which is several orders of magnitude smaller then the size the network.

We are interested in the evolution of the density function

$$f = f(w, c, t), \qquad f : I \times \mathcal{C} \times \mathbb{R}^+ \to \mathbb{R}^+ \tag{2.1}$$

where $w \in I, I = [-1, 1]$ is the opinion variable, $c \in \mathcal{C} = \{0, 1, 2, \dots, c_{\max}\}$ is a discrete variable describing the number of connections and $t \in \mathbb{R}^+$ denotes as usual the time variable. For each time $t \geq 0$ we can compute the following marginal density

$$\rho(c, t) = \int_I f(w, c, t) dw, \tag{2.2}$$

which defines the evolution of the number of connections of the agents or equivalently the degree distribution of the network. In the sequel we assume that the total number of agents is conserved, namely

$$\sum_{c=0}^{c_{\max}} \rho(c, t) = 1. \tag{2.3}$$

The overall opinion distribution is defined likewise as the following marginal density function

$$g(w, t) = \sum_{c=0}^{c_{\max}} f(w, c, t). \tag{2.4}$$

We express the evolution of the opinions by a binary interaction rule. From a microscopic point of view we suppose that the agents modify their opinion through binary interactions which depend on opinions and number of connections. If two agents with opinion and number of connections (w, c) and (w_*, c_*) meet, their post-interaction opinions are given by

$$\begin{cases} w' &= w - \eta P(w, w_*; c, c_*)(w - w_*) + \xi D(w, c), \\ w'_* &= w_* - \eta P(w_*, w; c_*, c)(w_* - w) + \xi_* D(w_*, c_*), \end{cases} \tag{2.5}$$

where $w, w_* \in I = [-1, 1]$ denote the pre-interaction opinions and w', w'_* the opinions after the exchange of information between the two agents. Note that, in the present setting the compromise function $P(\cdot, \cdot; \cdot, \cdot)$ depends both on the opinions and on the number of connections of each agent. In (2.7) the nonnegative parameter η influences the compromise rate while

ξ, ξ_* are centered random variables with the same distribution Θ with finite variance ς^2 and taking values on a Borel set $\mathcal{B} \subset \mathbb{R}$. The function $D(\cdot,\cdot) \geq 0$ describes the local relevance of the diffusion for a given opinion and number of connections. We will consider by now a general interaction potential such that $0 \leq P(w, w_*, c, c_*) \leq 1$.

In absence of diffusion, $\xi, \xi_* \equiv 0$, from (2.7) we have

$$|w' - w'_*| = |1 - \eta(P(w, w_*; c, c_*) + P(w_*, w; c_*, c))||w - w_*|, \tag{2.6}$$

then the post-exchange distances between agents are still in the reference interval $[-1, 1]$ if we consider $\eta \in (0, 1)$. In agreement with [6, 11, 82, 164] we can state the following result which derives the conditions on the noise term to ensure that the post-interaction opinions do not leave the reference interval.

Proposition 5.2.1. *If we assume that* $0 < P(w, w_*; c, c_*) \leq 1$ *and*

$$|\xi| < d, \qquad |\xi_*| < d,$$

where

$$d = \min_{(w,c)\in I\times\mathcal{C}} \left\{ \frac{(1-w)}{D(w,c)}, D(w,c) \neq 0 \right\},$$

then the binary interaction rule (2.7) *preserves the bounds being the post interaction opinions* w, w_* *contained in* $I = [-1, 1]$.

The evolution in time of the density function $f(w, c, t)$ is described by the following integro-differential equation of Boltzmann-type

$$\frac{d}{dt} f(w, c, t) + \mathbb{N}[f(w, c, t)] = Q(f, f)(w, c, t), \tag{2.7}$$

where $\mathbb{N}[\cdot]$ is an operator related to the evolution of the connections in the network and $Q(\cdot,\cdot)$ is the binary interaction operator defined as follows

$$Q(f, f) = \sum_{c_*=0}^{c_{\max}} \int_{\mathcal{B}^2\times I} \left({}'B \frac{1}{J} f({}'w, c) f({}'w_*, c_*) - B f(w, c) f(w_*, c_*) \right) dw_* d\xi d\xi_*, \tag{2.8}$$

where $({}'w, {}'w_*)$ are the pre-interaction opinions generated by the couple (w, w_*) after the interaction. The term J denotes the Jacobian of the transformation $(w, w_*) \to (w', w'_*)$ and the kernels ${}'B, B$ define the binary interaction. Here and in the rest of the section, for notation simplicity, the explicit dependence from the time variable is omitted.

We will consider interaction kernels of the following form

$$B_{(w,w_*)\to(w',w'_*)} = \lambda \Theta(\xi)\Theta(\xi_*)\chi(|w'| \leq 1)\chi(|w'_*| \leq 1), \tag{2.9}$$

where $\lambda > 0$ is a constant relaxation rate representing the interaction frequency.

In order to write the collision operator $Q(\cdot,\cdot)$ in weak form we consider a test function $\psi(w)$ to get

$$\begin{aligned}&\int_I Q(f,f)(w,c)\psi(w)dw = \\ &\quad \lambda \sum_{c_*=0}^{c_{\max}} \left\langle \int_{I^2} \left(\psi(w') - \psi(w)\right) f(w_*,c_*) f(w,c) dw dw_* \right\rangle,\end{aligned} \tag{2.10}$$

where the brackets $< \cdot >$ denotes the expectation with respect to the random variables ξ, ξ_*. Equation (2.7) may be written in weak form as follows

$$\begin{aligned}&\frac{d}{dt}\int_I f(w,c,t)\psi(w)dw + \int_I \mathbb{N}[f(w,c,t)]\psi(w)dw = \\ &\quad \lambda \sum_{c_*=0}^{c_{\max}} \left\langle \int_{I^2} \left(\psi(w') - \psi(w)\right) f(w_*,c_*,t) f(w,c,t) dw dw_* \right\rangle.\end{aligned} \tag{2.11}$$

An alternative form, obtained by symmetry is the following

$$\begin{aligned}&\frac{d}{dt}\int_I f(w,c,t)\psi(w)dw + \int_I \mathbb{N}[f(w,c,t)]\psi(w)dw = \\ &\quad \frac{\lambda}{2} \sum_{c_*=0}^{c_{\max}} \left\langle \int_{I^2} \left(\psi(w') + \psi(w'_*) - \psi(w) - \psi(w_*)\right) \right. \\ &\quad \left. f(w_*,c_*,t) f(w,c,t) dw dw_* \right\rangle.\end{aligned} \tag{2.12}$$

5.2.2 Evolution of the network

We introduced in the previous paragraphs the operator $\mathbb{N}[\cdot]$, characterizing the evolution of the agents in the discrete space of connections. This, of course, corresponds to the evolution of the underlying network of connections between the agents. Here we will specify the details of the model considered in the present paper, inspired by [175].

The operator $\mathbb{N}[\cdot]$ is defined through a combination of preferential attachment and uniform processes describing the evolution of the connections of the agents by removal and adding links in the network. These processes are strictly related to the generation of stationary scale-free distributions [20].

More precisely, for each $c = 1, \dots, c_{\max} - 1$ we define

$$\begin{aligned}&\mathbb{N}[f(w,c,t)] = \\ &\quad -\frac{2V_r(f;w)}{\gamma+\beta}\left[(c+1+\beta)f(w,c+1,t) - (c+\beta)f(w,c,t)\right] \\ &\quad -\frac{2V_a(f;w)}{\gamma+\alpha}\left[(c-1+\alpha)f(w,c-1,t) - (c+\alpha)f(w,c,t)\right],\end{aligned} \tag{2.13}$$

where $\gamma = \gamma(t)$ is the mean density of connectivity defined as

$$\gamma(t) = \sum_{c=0}^{c_{\max}} c\rho(c,t), \tag{2.14}$$

$\alpha, \beta > 0$ are attraction coefficients, and $V_r(f;w) \geq 0$, $V_a(f;w) \geq 0$ are characteristic rates of the removal and adding steps, respectively. The first term in (2.13) describes the net gain of $f(w,c,t)$ due to the removal of connections between agents whereas the second term represents the net gain due to the process of addition of connections. The factor 2 has been kept in evidence since connections are removed and created pairwise.

At the boundary we have the following equations

$$\begin{aligned}
\mathbb{N}[f(w,0,t)] =& -\frac{2V_r(f;w)}{\gamma+\beta}(\beta+1)f(w,1,t) \\
&+\frac{2V_a(f;w)}{\gamma+\alpha}\alpha f(w,0,t), \\
\mathbb{N}[f(w,c_{\max},t)] =& \frac{2V_r(f;w)}{\gamma+\beta}(c_{\max}+\beta)f(w,c_{\max},t) \\
&-\frac{2V_a(f;w)}{\gamma+\alpha}(c_{\max}-1+\alpha)f(w,c_{\max}-1,t),
\end{aligned} \tag{2.15}$$

which are derived from (2.13) taking into account the fact that, in the dynamics of the network, connections cannot be removed from agents with 0 connections and cannot be added to agents with $c_{\max}$ connections.

Remark 8. *If one defines the characteristic rates as*

$$V_r(f;w) = U_r\frac{\gamma+\beta}{\gamma_f+\beta g(w,t)}, \quad V_a(f;w) = U_a\frac{\gamma+\alpha}{\gamma_f+\alpha g(w,t)}, \tag{2.16}$$

where

$$\gamma_f(w,t) = \sum_{c=0}^{c_{max}} cf(w,c,t), \tag{2.17}$$

and U_a, U_r are constants, the dynamics in (2.13) corresponds to a combination of a preferential attachment process ($\alpha, \beta \approx 0$) and a uniform process ($\alpha, \beta \gg 1$) for each agent with opinion w, with respect to the probability density of connections $f(w,c,t)/g(w,t)$.

The evolution of the network of connections can be recovered taking $\psi(w) = 1$ in the master equation (2.11). From equation (2.2) we have

$$\frac{d}{dt}\rho(c,t) + \int_I \mathbb{N}[f(w,c,t)]\,dw = 0. \tag{2.18}$$

From the above definition of the network operator $\mathbb{N}[\cdot]$ it follows that

$$\frac{d}{dt}\sum_{c=0}^{c_{\max}}\rho(c,t)=0. \tag{2.19}$$

Then, for the collisional operator defined in (2.10) and the choice of $\mathbb{N}[\cdot]$ in (2.13), the total number of agents is conserved.

Let us take into account the evolution of the mean density of connectivity γ defined in (2.14). We can prove that, for each $t \geq 0$

$$\begin{aligned}\frac{d}{dt}\gamma(t) =& -2\int_I V_r(f;w)\frac{\gamma_f+\beta g(w,t)}{\gamma+\beta}dw\\ &+2\int_I V_a(f;w)\frac{\gamma_f+\alpha g(w,t)}{\gamma+\alpha}dw\\ &+\frac{2\beta}{\gamma+\beta}\int_I V_r(f;w)f(w,0,t)\,dw\\ &-\frac{2(c_{\max}+\alpha)}{\gamma+\alpha}\int_I V_a(f;w)f(w,c_{\max},t)\,dw.\end{aligned} \tag{2.20}$$

Therefore, γ is not conserved in general. Asymptotically, conservation is recovered in the case $\beta = 0$, if the characteristic rates are given by (2.16) with $U_a = U_r$ or are constants with $V_a = V_r$, and for a sufficiently fast decay of the density function $f(w, c_{\max}, t)$.

In Appendix 5.6-5.6 we report the explicit computations of the conservation of the total number of connections (2.19) and of the evolution of the mean density of connectivity (2.20).

In the particular case where V_a and V_r are constants independent of f and w, then the operator $\mathbb{N}[\cdot]$ is linear and will be denoted by $\mathcal{L}[\cdot]$. In this case, the evolution of the network of connections is independent from the opinion and we get the closed form

$$\frac{d}{dt}\rho(c,t)+\mathcal{L}[\rho(c,t)]=0, \tag{2.21}$$

where

$$\begin{aligned}\mathcal{L}[\rho(c,t)] =& -\frac{2V_r}{\gamma+\beta}\left[(c+1+\beta)\rho(c+1,t)-(c+\beta)\rho(c,t)\right]\\ &-\frac{2V_a}{\gamma+\alpha}\left[(c-1+\alpha)\rho(c-1,t)-(c+\alpha)\rho(c,t)\right],\end{aligned} \tag{2.22}$$

and at the boundary

$$\begin{aligned}\mathcal{L}[\rho(0,t)] =& -\frac{2V_r}{\gamma+\beta}(\beta+1)\rho(1,t)+\frac{2V_a}{\gamma+\alpha}\alpha\rho(0,t),\\ \mathcal{L}[\rho(c_{\max},t)] =& \frac{2V_r}{\gamma+\beta}(c_{\max}+\beta)\rho(c_{\max},t)\\ &-\frac{2V_a}{\gamma+\alpha}(c_{\max}-1+\alpha)\rho(c_{\max}-1,t).\end{aligned} \tag{2.23}$$

Note that the dynamics described by (2.22) corresponds again to a combination of preferential attachment processes ($\alpha, \beta \approx 0$) and uniform processes ($\alpha, \beta \gg 1$) with respect to the probability density of connections $\rho(c,t)$.

Concerning the large time behavior of the network of connections, in the linear case with $V_r = V_a$, $\beta = 0$ and now denoting by γ the asymptotic value of the density of connectivity, it is possible to prove the following result.

Proposition 5.2.2. *For each $c \in \mathcal{C}$ the stationary solution to (2.21) or equivalently*

$$(c+1)\rho_\infty(c+1) = \frac{1}{\gamma+\alpha}\left[(c(2\gamma+\alpha)+\gamma\alpha)\rho_\infty(c) - \gamma(c-1+\alpha)\rho_\infty(c-1)\right] \tag{2.24}$$

is given by

$$\rho_\infty(c) = \left(\frac{\gamma}{\gamma+\alpha}\right)^c \frac{1}{c!}\alpha(\alpha+1)\cdots(\alpha+c-1)\rho_\infty(0) \tag{2.25}$$

where

$$\rho_\infty(0) = \left(\frac{\alpha}{\alpha+\gamma}\right)^\alpha. \tag{2.26}$$

Detailed computations are given in Appendix 5.6.

Further approximations are possible in the cases $\alpha \gg 1$ and $\alpha \approx 0$. For big values of α the preferential attachment process, described by the master equation (2.22), is destroyed and the network approaches to a random network, whose degree distribution is the Poisson distribution [21]. In fact, in the limit $\alpha \to +\infty$ we have $(\alpha+\gamma)^c \approx \alpha(\alpha+1)\cdots(\alpha+c-1)$ and

$$\rho_\infty(c) = \lim_{\alpha\to+\infty}\left(1+\frac{\gamma}{\alpha}\right)^{-\alpha}\gamma^c = \frac{e^{-c}}{c!}\gamma^c.$$

In the second case, for $\gamma \geq 1$ and small values of α, the distribution can be correctly approximated with a truncated power-law with unitary exponent

$$\rho_\infty(c) = \left(\frac{\alpha}{\gamma}\right)^\alpha \frac{\alpha}{c}.$$

5.2.3 Evolution of the moments

In order to study the evolution of the mean opinion, defined as

$$m_w(c,t) = \int_I w f(w,c,t)dw,$$

we consider $\psi(w) = w$ in (2.12)

$$\begin{aligned}\frac{d}{dt}\int_I w f(w,c,t)dw + \int_I w\mathbb{N}\left[f(w,c,t)\right]dw = \\ \frac{\lambda}{2}\sum_{c_*=0}^{c_{\max}}\left\langle\int_{I^2}\left(w'+w'_*-w-w_*\right)f(w_*,c_*,t)f(w,c,t)dwdw_*\right\rangle.\end{aligned} \tag{2.27}$$

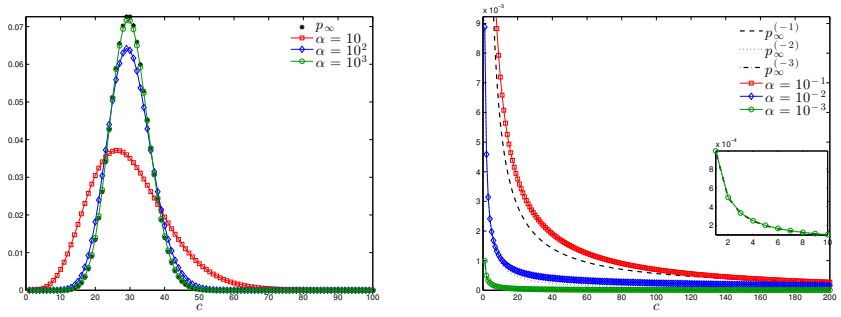

Figure 2.1: Stationary states of (2.21) with relaxation coefficients $V_r = V_a = 1$, mean density of connectivity $\gamma = 30$, $c_{\max} = 1500$ and several values of the attraction parameters α, and having fixed $\beta = 0$. Left: convergence toward the Poisson distribution for big values of α. Right: convergence toward a power-law distribution in the limit $\alpha \to 0$, we indicated with $p_\infty^{(-k)}, k = 1, 2, 3$ the $\alpha-$dependent stationary solutions for $\alpha = 10^{-1}, 10^{-2}, 10^{-3}$, respectively.

We obtain

$$\frac{d}{dt} m_w(c,t) + \int_I w \mathbb{N}\left[f(w,c,t)\right] dw = \frac{\eta\lambda}{2} \sum_{c_*=0}^{c_{\max}} \int_{I^2} (w - w_*) \left[P(w_*, w; c_*, c) - P(w, w_*; c, c_*)\right] f(w_*, c_*, t) f(w, c, t) dw_* dw.$$

Of course, if the compromise function $P(\cdot,\cdot;\cdot,\cdot)$ is symmetric with respect to the pairs (w, w_*) and (c, c_*) the overall opinion on the network is conserved

$$\frac{d}{dt} \sum_{c=0}^{c_{\max}} m_w(c,t) = 0.$$

In addition, if the operator $\mathbb{N}[\cdot]$ is linear, the evolution of the mean opinion obeys the same closed differential equation of the network of connections

$$\frac{d}{dt} m_w(c,t) + \mathcal{L}[m_w(c,t)] = 0. \tag{2.28}$$

Therefore, all the conclusions of the previous section hold also for the mean opinion on the network.

More generally we will consider compromise functions $P(\cdot,\cdot;\cdot,\cdot)$ with the following form

$$P(w, w_*; c, c_*) = H(w, w_*) K(c, c_*), \tag{2.29}$$

where $0 \leq H(\cdot,\cdot) \leq 1$ represents the positive compromise propensity and $0 \leq K(\cdot,\cdot) \leq 1$ a function taking into account the influence of number

connections in the opinion exchange process. Note that, in this case, even if we consider a symmetric compromise function H and a linear network operator we have

$$\begin{aligned}&\frac{d}{dt}m_w(c,t) + \mathcal{L}[m_w(c,t)] = \\ &\quad\frac{\eta\lambda}{2}\sum_{c_*=0}^{c_{\max}} B(t,c,c_*)\left[K(c_*,c) - K(c,c_*)\right] \\ &\qquad\qquad\int_{I^2} H(w_*,w)(w-w_*)f(w_*,c_*,t)f(w,c,t)dw_*dw,\end{aligned} \tag{2.30}$$

and the evolution of the mean opinion cannot be expressed in closed form due to the influence of the different connections that the agents possess. This is a fundamental difference compared to classical kinetic models of opinion [164].

In the case of the second moment of the opinion $\phi(w) = w^2$, if we assume a symmetric function P, by denoting

$$E_w(c,t) = \int_I w^2 f(w,c,t)dw$$

we get

$$\begin{aligned}&\frac{d}{dt}E_w(c,t) + \int_I w^2\mathbb{N}[f(w,c,t)]\,dw = \\ &\quad\eta\lambda\sum_{c_*=0}^{c_{\max}}\int_{I^2} P(w_*,w;c_*,c)^2(w-w_*)^2 f(w_*,c_*,t)f(w,c,t)dw_*dw \\ &\quad+\lambda\varsigma^2\int_I D^2(c,w)f(w,c,t)dw,\end{aligned} \tag{2.31}$$

which, in the case of a linear operator $\mathcal{L}[\cdot]$ with $P = 1$ and in absence of noise $D = 0$, simplifies to

$$\begin{aligned}&\frac{d}{dt}E_w(c,t) + \mathcal{L}[E_w(c,t)] = \\ &\quad\eta\lambda\left(E_w(c,t) + \rho(c,t)\sum_{c_*=0}^{c_{\max}} E_w(c_*,t) - 2m_w(c,t)\sum_{c_*=0}^{c_{\max}} m_w(c_*,t)\right).\end{aligned} \tag{2.32}$$

Equation (2.32) together with (2.21) and (2.28) form a closed system for the evaluation of the second order moment of the opinion.

5.3 Fokker-Planck modeling

In general it is difficult to obtain analytic results on the large time behavior of the opinion for the kinetic equation introduced in the previous section. A

step toward the simplification of the analysis is the derivation of asymptotic states of the Boltzmann-type equation derived from a simplified Fokker-Planck-type models [145]. Here we recall briefly the approach usually referred to as the quasi-invariant opinion limit [11, 39, 164].

5.3.1 Derivation of the model

The idea is to rescale the interaction frequency λ, the interaction propensity η and the diffusion variance ς^2 at the same time, in order to maintain asymptotically the memory of the microscopic interactions. Let us introduce the scaling parameter $\varepsilon > 0$ and consider the scaling

$$\eta = \varepsilon, \qquad \lambda = \frac{1}{\varepsilon}, \qquad \varsigma^2 = \varepsilon\sigma^2. \tag{3.1}$$

The above scaling corresponds to the case where the interaction kernel concentrates on binary interactions producing very small changes in the agents' opinion but, at the same time, the number of interactions becomes very large. From a modeling point of view we require that the scaling (3.1) preserves the macroscopic properties of the kinetic system in the limit $\varepsilon \to 0$, i.e. the evolution of the mean and the variance of opinion derived in Section 5.2.3.

The scaled equation (2.11) reads

$$\begin{aligned} &\frac{d}{dt}\int_I f(w,c,t)\psi(w)dw + \int_I \mathbb{N}\left[f(w,c,t)\right]\psi(w)\,dw = \\ &\qquad \frac{1}{\varepsilon}\sum_{c_*=0}^{c_{\max}} \left\langle \int_{I^2} (\psi(w') - \psi(w)) f(w_*,c_*,t) f(w,c,t) dw dw_* \right\rangle, \end{aligned} \tag{3.2}$$

with scaled binary interactions given by

$$w' - w = \varepsilon P(w, w_*; c, c_*)(w_* - w) + \xi_\varepsilon D(w) + O(\varepsilon^2), \tag{3.3}$$

where ξ_ϵ is a centered random variable with variance $\varepsilon\sigma^2$. Since as $\varepsilon \to 0$ we have $w' \to w$ we can consider the Taylor expansion of ψ around w to get

$$\psi(w') - \psi(w) = (w' - w)\psi'(w) + \frac{1}{2}(w' - w)^2\psi''(\bar{w}), \tag{3.4}$$

where for some $\theta \in [0,1]$

$$\bar{w} = \theta w + (1-\theta)w,$$

and from (3.2) we obtain

$$\begin{aligned} \frac{1}{\varepsilon}\sum_{c_*=0}^{c_{\max}} \Bigg\langle \int_{I^2} &(w' - w)\psi'(w) + \frac{1}{2}(w' - w)^2\psi''(w) \\ &f(w_*,c_*,t) f(w,c,t) dw dw_* \Bigg\rangle + R(\varepsilon), \end{aligned} \tag{3.5}$$

where $R(\varepsilon)$ indicates the remainder, given by

$$R(\varepsilon) = \frac{1}{2\varepsilon} \sum_{c_*=0}^{c_{\max}} \left\langle \int_{I^2} (w' - w)^2 (\psi''(\bar{w}) - \psi''(w)) f(w_*, c_*, t) f(w, c, t) dw dw_* \right\rangle. \tag{3.6}$$

Therefore, the scaled binary interaction term reads

$$\sum_{c_*=0}^{c_{\max}} \int_{I^2} \left[P(w, w_*; c, c_*)(w_* - w)\psi'(w) + \frac{\sigma^2}{2} D(w, c)^2 \psi''(w) \right] f(w_*, c_*, t) f(w, c, t) dw dw_* + R(\varepsilon) + O(\varepsilon). \tag{3.7}$$

By similar arguments of [164] it can be rigorously shown that $R(\varepsilon)$ in (3.6) decays to zero in the limit $\varepsilon \to 0$. Thus, as $\varepsilon \to 0$ we recover

$$\frac{d}{dt} \int_I f(w, c, t)\psi(w) dw + \int_I \mathbb{N}[f(w, c, t)]\psi(w) dw = \sum_{c_*=0}^{c_{\max}} \left[\int_{I^2} P(w, w_*; c, c_*)(w_* - w)\psi'(w) f(w_*, c_*, t) f(w, c, t) dw_* dw + \frac{\sigma^2}{2} \int_I D(w, c)^2 \psi''(w) f(w, c, t) dw \right]. \tag{3.8}$$

Integrating backward by parts equation (3.8) we obtain the following Fokker-Planck differential equation for the evolution of the opinions' distribution on the evolving network

$$\frac{\partial}{\partial t} f(w, c, t) + \mathbb{N}[f(w, c, t)] = \frac{\partial}{\partial w} \mathcal{P}[f] f(w, c, t) + \frac{\sigma^2}{2} \frac{\partial^2}{\partial w^2} (D(w, c)^2 f(w, c, t)) \tag{3.9}$$

where

$$\mathcal{P}[f](w, c, t) = \sum_{c_*=0}^{c_{\max}} \int_I P(w, w_*; c, c_*)(w_* - w) f(w_*, c_*, t) dw_*. \tag{3.10}$$

5.3.2 Stationary solutions

In this section we will show how in some cases it is possible to compute explicitly the steady state solution of the Fokker-Planck system (4.9). We restrict to linear operators $\mathcal{L}[\cdot]$ and asymptotic solutions of the form

$$f_\infty(w, c) = g_\infty(w)\rho_\infty(c), \tag{3.11}$$

where $\rho_\infty(c)$ is the steady state distribution of the connections (see Proposition 5.2.2) and

$$\int_I f_\infty(w,c)dw = \rho_\infty(c), \qquad \sum_{c=0}^{c_{\max}} f_\infty(w,c) = g_\infty(w). \tag{3.12}$$

From the definition of the linear operator $\mathcal{L}[\cdot]$ we have $\mathcal{L}[\rho_\infty(c)] = 0$, so stationary solutions of type (3.11) satisfy the following equation

$$\frac{\partial}{\partial w}\mathcal{P}[f_\infty]f_\infty(w,c) + \frac{\sigma^2}{2}\frac{\partial^2}{\partial w^2}(D(w,c)^2 f_\infty(w,c)) = 0. \tag{3.13}$$

Under some simplifications we can analytically solve equation (3.13), as shown in [11, 164]. If we assume (2.29), i.e. $P(w,w_*;c,c_*) = H(w,w_*)K(c,c_*)$, the operator $\mathcal{P}[f_\infty]$ can be written as follows

$$\begin{aligned}\mathcal{P}[f_\infty](w,c) &= \left(\sum_{c_*=0}^{c_{\max}} K(c,c_*)\rho_\infty(c_*)\right)\left(\int_I H(w,w_*)(w_*-w)g_\infty(w_*)dw_*\right)\\ &=: \mathcal{K}[\rho_\infty](c)\mathcal{H}[g_\infty](w),\end{aligned} \tag{3.14}$$

and if we further assume that $K(c,c_*) = \bar{K}(c_*)$ is independent from c, and $H(w,w_*) = \bar{H}(w)$ independent from w_*, we have

$$\mathcal{K}[\rho_\infty] = \sum_{c_*=0}^{c_{\max}} \bar{K}(c_*)\rho_\infty(c_*) =: \kappa, \quad \mathcal{H}[g_\infty] = \bar{H}(w)\left(w - \bar{m}_w\right),$$

where $\bar{m}_w = \sum_{c=0}^{c_{\max}} m_w(c,t)$.

Finally, if we consider $D(w,c) = D(w)$, equation (3.13) reads

$$\left(\kappa\frac{\partial}{\partial w}\bar{H}(w)\left(w-\bar{m}_w\right)g_\infty(w) + \frac{\sigma^2}{2}\frac{\partial^2}{\partial w^2}D(w)^2 g_\infty(w)\right)\rho_\infty(c) = 0. \tag{3.15}$$

Therefore, on the support of $\rho_\infty(c)$, stationary solutions can be derived from the following equation

$$\kappa\bar{H}(w)\left(w-\bar{m}_w\right)g_\infty(w) + \frac{\sigma^2}{2}\frac{\partial}{\partial w}D(w)^2 g_\infty(w) = 0, \tag{3.16}$$

which corresponds to the solution of the ordinary differential equation

$$\frac{dg_\infty}{dw} = 2\left(\frac{\kappa}{\sigma^2}\frac{\bar{H}(w-\bar{m}_w)}{D^2} - \frac{D'}{D}\right)g_\infty. \tag{3.17}$$

Thus, we obtain

$$g_\infty(w) = \frac{C_0}{D(w)^2}\exp\left\{\frac{2\kappa}{\sigma^2}\int^w \frac{\bar{H}(v)}{D(v)^2}(\bar{m}_w - v)\,dv\right\}, \tag{3.18}$$

where the constant C_0 is chosen such that the total mass of g_∞ is equal to one. Some explicit examples are given below.

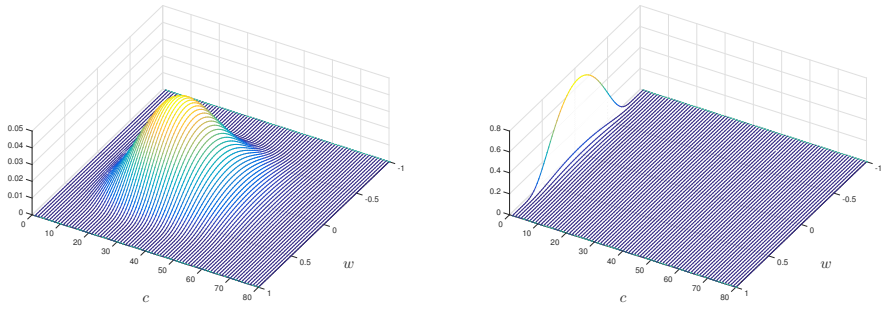

Figure 3.2: Stationary solutions of type $f_\infty(w,c) = g_\infty(w)p_\infty(c)$, where $g_\infty(w)$ is given by (3.19) with $\kappa = 1$, $m_w = 0$, $\sigma^2 = 0.05$ and $p_\infty(c)$ defined by (2.25), with $V_r = V_a = 1$, $\gamma = 30$ and $\alpha = 10$ on the left and $\alpha = 0.1$ on the right.

1. In the case $H \equiv 1$ and $D(w) = 1 - w^2$, the steady state solution is given by

$$g_\infty(w) = C_0(1+w)^{-2+\bar{m}_w\kappa/\sigma^2}(1-w)^{-2-m_w\kappa/\sigma^2}\exp\left\{-\frac{\kappa(1-\bar{m}_w w)}{\sigma^2(1-w^2)}\right\}. \tag{3.19}$$

2. For $H(w,w_*) = 1 - w^2$ and $D(w) = 1 - w^2$, the steady state solution is given by

$$g_\infty(w) = C_0(1-w)^{-2+(1-\bar{m}_w)\kappa/\sigma^2}(1+w)^{-2+(1+\bar{m}_w)\kappa/\sigma^2}. \tag{3.20}$$

In Figure 3.2 as an example we report the stationary solution $f_\infty(w,c) = g_\infty(w)\rho_\infty(c)$, where $g_\infty(w)$ is given by (3.19) and $p_\infty(c)$ defined by (2.25) for various α.

5.4 Numerical methods

In this section we consider the development of numerical methods for the kinetic models studied in the previous sections. First we consider direct simulation Monte Carlo methods for the Boltzmann model (2.8) introduced in Section 5.2. Here the major difficulty is to consider a probabilistic interpretation of the dynamics induced by the network operator $\mathbb{N}[\cdot]$, whereas the opinion interaction follows the standard binary sampling approach (see [145] for details). Next we consider the derivation of numerical schemes for the Fokker-Planck model (4.9), derived in Section 6.4. In particular we will focus on the construction of finite-difference methods which are capable to describe correctly the large time behavior of the model. To this aim we will consider a nonlinear version of the Chang–Cooper type discretization which has the nice feature of preserving the steady states and the non-negativity of the numerical solution [60, 127].

5.4.1 Direct simulation Monte Carlo

One of the most common approaches to solve Boltzmann-type equations is based Monte Carlo methods. Let us consider the initial value problem given by equation (2.7) with initial condition $f(w, c, t = 0) = f_0(w, c)$, the solution at time $t^n = n \cdot \Delta t^n, n \geq 1$ is obtained as a composition of the solutions of the following problems: we first integrate the network term for all $c \in \mathcal{C}$ along the time interval $[t^n, t^{n+1/2}]$

$$\begin{cases} \dfrac{d}{dt}\tilde{f}(w, c, t) + \mathbb{N}[\tilde{f}(w, c, t)] = 0, \\ \tilde{f}(w, c, 0) = f_0(w, c) \end{cases} \tag{4.1}$$

then we solve over $[t^{n+1/2}, t^{n+1}]$ the interaction step

$$\begin{cases} \dfrac{d}{dt}f(w, c, t) = Q(f, f)(w, c, t), \\ f(w, c, 0) = \tilde{f}(w, c, t^{n+1/2}). \end{cases} \tag{4.2}$$

The described process may be iterated in order to obtain the numerical solution of the initial equation at each time step. At variance with standard Monte Carlo methods for opinion dynamics, see for example [145], here we face the additional difficulty of the network evolution. In the sequel we describe the details of the Monte Carlo method for the network evolution in the simplified case $\mathbb{N}[\cdot] = \mathcal{L}[\cdot]$.

Let $f^n = f(w, c, t^n)$ the empirical density function for the density of agents at time t^n with opinion $w \in [-1, 1]$ and connections $c \in \mathcal{C}$. For a any given opinion w the solution of the transport step is given for each $c > 0$ and $c < c_{\max}$ by

$$\begin{aligned} f^{n+1}(w, c) = &\left(1 - \Delta t\frac{V_r(c+\beta)}{\gamma^n + \beta} - \Delta t\frac{V_a(c+\alpha)}{\gamma^n + \alpha}\right) f^n(w, c) \\ &+ \Delta t\frac{V_r(c+\beta)}{\gamma^n + \beta} f^n(w, c-1) + \Delta t\frac{V_a(c+\alpha)}{\gamma^n + \alpha} f^n(w, c+1), \end{aligned} \tag{4.3}$$

with boundary conditions

$$\begin{aligned} f^n(w, 0) &= \left(1 - \Delta t\frac{V_a(c+\alpha)}{\gamma^n + \alpha}\right) f^n(w, 0) + \Delta t\frac{V_a(c+\alpha)}{\gamma^n + \alpha} f^n(w, 1), \\ f^n(w, c_{\max}) &= \left(1 - \Delta t\frac{V_r(c+\beta)}{\gamma^n + \beta}\right) f^n(w, c_{\max}) + \Delta t\frac{V_r(c_{\max}+\beta)}{\gamma^n + \beta} f^n(w, c_{\max} - 1), \end{aligned} \tag{4.4}$$

and temporal discretization such that

$$\Delta t \leq \min\left\{\frac{\gamma^n + \beta}{V_r(c_{\max} + \beta)}, \frac{\gamma^n + \alpha}{V_a(c_{\max} + \alpha)}\right\}. \tag{4.5}$$

An algorithm to simulate the above equation reads as follows

Algorithm 5.4.1.

1. *Sample* (w_i^0, c_i^0)*, with* $i = 1, \dots, N_s$*, from the distribution* $f^0(w, c)$*.*
2. **for** $n = 0$ **to** $n_{tot} - 1$
   (a) *Compute* $\gamma^n = \frac{1}{N_s} \sum_{j=1}^{N_s} c_j^n$*;*
   (b) *fix* Δt *such that condition (4.5) is satisfied.*
   (c) **for** $k = 1$ **to** N_s
      i. *compute the following probabilities rates*

$$p_k^{(a)} = \frac{\Delta t V_a(c_k^n + \alpha)}{\gamma^n + \alpha}, \qquad p_k^{(r)} = \frac{\Delta t V_r(c_k^n + \beta)}{\gamma^n + \beta},$$

      ii. *set* $c_k^* = c_k^n$*.*
      iii. **if** $0 \le c_k^* \le c_{max} - 1$*,*
      with probability $p_k^{(a)}$ *add a connection:* $c_k^* = c_k^* + 1$*;*
      iv. **if** $1 \le c_k^* \le c_{max}$*,*
      with probability $p_k^{(r)}$ *remove a connection:* $c_k^* = c_k^* - 1$*;*
   end for
   (d) *set* $c_i^{n+1} = c_i^*$*, for all* $i = 1, \dots, N_s$*.*

end for

The collision step may be solved through a binary interaction algorithm [8, 145], where the basic idea is to solve the binary exchange of information described by (2.7), under the quasi-invariant opinion scaling (3.1).

The time-discrete scheme reads

$$f^{n+1}(w, c) = \left(1 - \frac{\Delta t}{\varepsilon}\right) f^n(w, c) + \frac{\Delta t}{\varepsilon} Q_\varepsilon^+(f^n, f^n)(w, c), \tag{4.6}$$

where we have made explicit the dependence of $Q(f, f)$ on the frequency of interactions $1/\varepsilon$ and with $Q_\varepsilon^+(f^n, f^n)$ we denoted the gain part, namely it accounts the density of opinions gained at position w after the binary interaction (2.7). The collisional step (4.6) is a convex combinations of probability density under the time step constrain $\Delta t \le \varepsilon$, which has to be coupled with (4.5). For further details on the algorithm we refer to [8, 145].

In Figure 4.3 we show the two stationary states, already presented in Figure 3.2, computed through the Monte Carlo procedure just described, where we use $N_s = 2 \times 10^4$ samples to reconstruct the density and scaling parameter $\varepsilon = 0.01$ and $\Delta t = \varepsilon$.

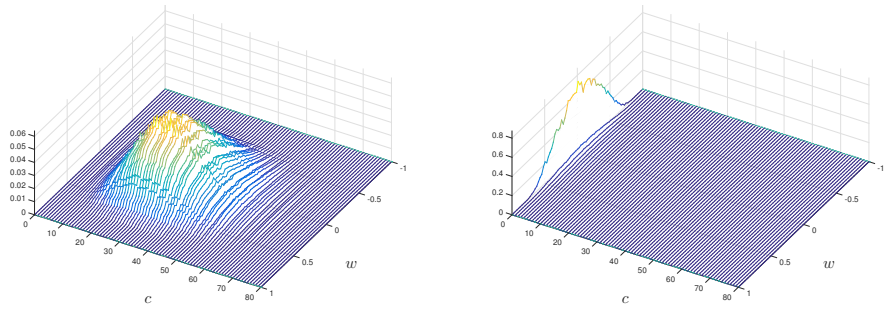

Figure 4.3: Stationary solutions captured via Monte Carlo simulations, with $N_s = 2 \times 10^4$ samples. Parameters of the model are chosen as follows $\sigma^2 = 0.05$, $V_r = V_a = 1$, $\beta = 0$, $\alpha = 10$ on the right hand side and $\alpha = 0.1$ on the left hand side.

5.4.2 Chang–Cooper type numerical schemes

We consider the Fokker-Planck system (4.9) that we will rewrite in the form

$$\frac{\partial}{\partial t} f(w,c,t) + \mathbb{N}\left[f(w,c,t)\right] = \frac{\partial}{\partial w}\mathcal{F}[f] \tag{4.7}$$

where

$$\mathcal{F}[f] = \left(\mathcal{P}[f] + \sigma^2 D'(w,c)D(w,c)\right) f(w,c,t) + \frac{\sigma^2}{2} D(w,c)^2 \frac{\partial}{\partial w} f(w,c,t), \tag{4.8}$$

and $\mathcal{P}[f]$ is given by (3.10).

The above equation is complemented with the initial data $f(w,c,0) = f_0(w,c)$ and considered in the domain $(w,c) \in I \times \mathcal{C}$ with zero flux boundary condition on w. Note that in the variable c the equation is in discrete form and therefore the discretization we will consider acts only on the continuous opinion variable $w \in I$.

Let us introduce a uniform grid $w_i = -1 + i\Delta w$, $i = 0, \dots, N$ with $\Delta w = 2/N$, we denote by $w_{i\pm 1/2} = w_i \pm \Delta w/2$ and define

$$f_i(c,t) = \frac{1}{\Delta w} \int_{w_{i-1/2}}^{w_{i+1/2}} f(w,c,t)\, dw.$$

Integrating equation (4.7) yields

$$\frac{\partial}{\partial t} f_i(c,t) + \mathbb{N}\left[f_i(c,t)\right] = \frac{\mathcal{F}_{i+1/2}[f] - \mathcal{F}_{i-1/2}[f]}{\Delta w}, \tag{4.9}$$

where $\mathcal{F}_i[f]$ is the flux function characterizing the numerical discretization.

We assume a flux function as a combination of upwind and centered discretization as in the classical Chang–Cooper flux

$$\mathcal{F}_{i+1/2}[f] = \left((1-\delta_{i+1/2})(\mathcal{P}[f_{i+1/2}] + \sigma^2 D'_{i+1/2} D_{i+1/2}) + \frac{\sigma^2}{2\Delta w} D^2_{i+1/2}\right) f_{i+1} + \left(\delta_{i+1/2}(\mathcal{P}[f_{i+1/2}] + \sigma^2 D'_{i+1/2} D_{i+1/2}) - \frac{\sigma^2}{2\Delta w} D^2_{i+1/2}\right) f_i, \tag{4.10}$$

where $D_{i+1/2} = D(w_{i+1/2}, c)$ and $D'_{i+1/2} = D'(w_{i+1/2}, c)$.

The weights $\delta_{i+1/2}$ have to be chosen in such a way that a steady state solution is preserved. Moreover, as it is shown in Appendix 5.6, this choice permits also to preserve nonnegativity of the numerical density.

Preservation of the steady states corresponds to assume that the numerical flux vanishes when f is at the steady state f^∞. Imposing the numerical flux equal to zero, from (4.10) we get

$$\frac{f_{i+1}}{f_i} = \frac{-\delta_{i+1/2}(\mathcal{P}[f_{i+1/2}] + \sigma^2 D'_{i+1/2} D_{i+1/2}) + \frac{\sigma^2}{2\Delta w} D^2_{i+1/2}}{(1-\delta_{i+1/2})(\mathcal{P}[f_{i+1/2}] + \sigma^2 D'_{i+1/2} D_{i+1/2}) + \frac{\sigma^2}{2\Delta w} D^2_{i+1/2}}. \tag{4.11}$$

Solving with respect to $\delta_{i+1/2}$ yields

$$\delta_{i+1/2} = \frac{\sigma^2 D^2_{i+1/2}}{2\Delta w(\mathcal{P}[f_{i+1/2}] + \sigma^2 D'_{i+1/2} D_{i+1/2})} + \frac{1}{1 - f_i/f_{i+1}}. \tag{4.12}$$

On the other hand the same computation directly on the flux (4.8) gives the differential equation

$$\frac{\sigma^2 D(w,c)^2}{2} \frac{\partial}{\partial w} f(w,c,t) = -\left(\mathcal{P}[f] + \sigma^2 D'(w,c) D(w,c)\right) f(w,c,t), \tag{4.13}$$

which in general cannot be solved, except is some special cases as discussed in the previous section, due to the nonlinear term on the right hand side. A possible way to overcome this difficulty is to consider a quasi steady-state approximation as follows. We first integrate the previous equation in the cell $[w_i, w_{i+1}]$ to get

$$\int_{w_i}^{w_{i+1}} \left(\frac{1}{f}\frac{\partial}{\partial w} f\right)(w,c,t)\, dw = -\frac{2}{\sigma^2} \int_{w_i}^{w_{i+1}} \frac{1}{D(w,c)^2} \left(\mathcal{P}[f] + \sigma^2 D'(w,c) D(w,c)\right)\, dw,$$

and then

$$\frac{f_{i+1}}{f_i} = \exp\left(-\frac{2}{\sigma^2} \int_{w_i}^{w_{i+1}} \frac{1}{D(w,c)^2} \left(\mathcal{P}[f] + \sigma^2 D'(w,c) D(w,c)\right)\, dw\right). \tag{4.14}$$

Next we can approximate the integral on the right hand side with a suitable quadrature formula. Because of singularities at the boundaries $w = \pm 1$ of the integrand function we can resort on open formula of Newton-Cotes type. For example, using the simple midpoint rule a second order approximation is obtained

$$\frac{f_{i+1}}{f_i} \approx \exp\left(-\frac{2\Delta w}{\sigma^2}\frac{1}{D^2_{i+1/2}}\left(\mathcal{P}[f_{i+1/2}] + \sigma^2 D'_{i+1/2} D_{i+1/2}\right)\right). \tag{4.15}$$

Now by equating (4.15) and (4.11) we recover the following expression of the weight functions

$$\delta_{i+1/2} = \frac{1}{\lambda_{i+1/2}} + \frac{1}{1 - \exp(\lambda_{i+1/2})}, \tag{4.16}$$

where

$$\lambda_{i+1/2} = \frac{2\Delta w}{\sigma^2}\frac{1}{D^2_{i+1/2}}\left(\mathcal{P}[f_{i+1/2}] + \sigma^2 D'_{i+1/2} D_{i+1/2}\right). \tag{4.17}$$

Note that here, at variance with the standard Chang–Cooper scheme [60], the weights depend on the solution itself as in [127]. Thus, we have a nonlinear scheme which preserves the steady state with second order accuracy. In particular, by construction, the weight in (4.16) are nonnegative functions with values in $[0, 1]$.

Higher order accuracy of the steady state can be recovered using a more general numerical flux given by

$$\begin{aligned}\mathcal{F}_{i+1/2}[f] = &\\ &\frac{D^2_{i+1/2}}{\Delta w}\left((1-\delta_{i+1/2})\int_{w_i}^{w_{i+1}} \frac{\mathcal{P}[f] + \sigma^2 D'(w,c)D(w,c)}{D(w,c)^2}\, dw + \frac{\sigma^2}{2}\right) f_{i+1}\\ &+ \frac{D^2_{i+1/2}}{\Delta w}\left(\delta_{i+1/2}\int_{w_i}^{w_{i+1}} \frac{\mathcal{P}[f] + \sigma^2 D'(w,c)D(w,c)}{D(w,c)^2}\, dw - \frac{\sigma^2}{2}\right) f_i,\end{aligned} \tag{4.18}$$

and taking

$$\lambda_{i+1/2} = \frac{2}{\sigma^2}\int_{w_i}^{w_{i+1}} \frac{1}{D(w,c)^2}\left(\mathcal{P}[f] + \sigma^2 D'(w,c)D(w,c)\right) dw. \tag{4.19}$$

It is easy to verify that, independently of the quadrature method used to evaluate the integrals in (4.18)-(4.19) the weights always satisfy (4.16). In this way, thanks to (4.14), higher order approximations of the integrals in (4.18)-(4.19) lead to higher order evaluations of the steady state solution.

5.5 Numerical Results

In this section we perform several numerical test to validate our modeling and numerical setting. We focus on the case $\alpha < 1$, since it represents the most relevant case in complex networks [3, 175]. For this case in fact we proved in Section 5.2.2 the emergence of truncated power law distributions for the network's connectivity. Except for the first test case, where we analyze the numerical convergence of the Boltzmann model in the quasi-invariant limit, in all the other tests the opinion dynamics evolves according to (4.9). Thus, in Test 2,3,4 the evolution is performed via the implicit-explicit scheme (6.14) described in the appendix with the numerical flux (4.10) based on the midpoint approximation (4.15) and using $N = 80$ grid points in w. We used $\Delta w = 2/N$ and a time step satisfying the stability condition (6.22) in the Appendix. The choice of parameters for the different tests is summarized in Table 4.1, the compromise and local diffusion functions, $P(c, c_*; w, w_*)$ and $D(w, c)$, and additional parameters will be introduced in every single test.

5.5.1 Test 1

We first consider the simple test case where the opinion evolves independently of the network and we validate the Chang–Cooper type scheme (6.14) with the flux (4.18) comparing its convergence with respect to the DSMC method.

We simulate the dynamics with the linear compromise function $P(w, w_*; c, c_*) = 1$, and $D(w, c) = 1 - w^2$, thus we can use the results (3.19), to compare the solutions obtained through the numerical scheme with the analytical one. The other parameters of the model are reported in Table 4.1 and we define the following initial data

$$g_0(w) = \frac{1}{2\sqrt{2\pi\sigma_F^2}}(\exp\{-(w+1/2)^2/(2\sigma_F^2)\} + \exp\{-(w-1/2)^2/(2\sigma_F^2)\}). \tag{5.1}$$

Test	σ^2	σ_F^2	σ_L^2	$c_{\max}$	V_r	V_a	γ_0	α	β
#1	5×10^{-2}	6×10^{-2}	–	250	1	1	30	1×10^{-1}	0
#2	5×10^{-2}	6×10^{-2}	–	250	–	–	30	1×10^{-1}	0
#3	5×10^{-3}	4×10^{-2}	2.5×10^{-2}	250	1	1	30	1×10^{-4}	0
#4	1×10^{-3}	–	–	250	1	1	30	1×10^{-1}	0

Table 4.1: Parameters in the various test cases

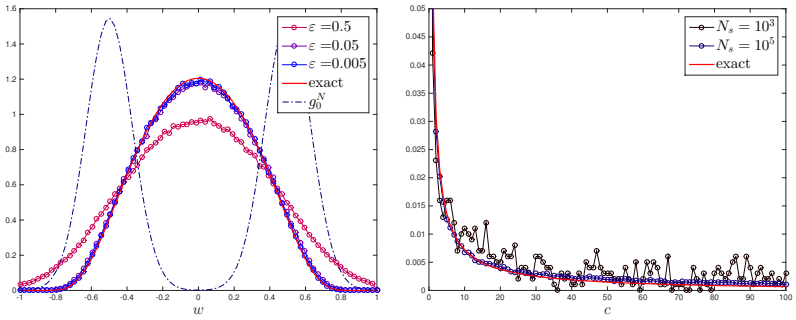

Figure 5.4: Test 1. One-dimensional setting: on the left, convergence of (4.6) to the stationary solution (3.19), of the Fokker-Planck equation, for decreasing values of the parameter ε, g_0^N represents the initial distribution. On the right, convergence of the Monte-Carlo (4.3) to the reference solution (2.24) for increasing values of the the number of samples N_s.

In Figure 5.4, on the left hand-side, we report the qualitative convergence of the Monte-Carlo methods for the Boltzmann dynamics, see [8, 146] for further details on the Binary Interaction algorithms, where we consider $N_s = 10^5$ samples to reconstruct the opinion's density $g(w,t)$ on a grid of $N = 80$ points. The figure shows that for decreasing values of the scaling parameter $\varepsilon = \{0.5, 0.05, 0.005\}$, we have the convergence to the reference solutions (3.19) of the Fokker-Planck equation. On the right we report the convergence to the stationary solution of the connectivity distribution (2.24) for $\alpha = 0.1$ and $V = 1$ and with $c_{\max} = 250$. In this case we show two different qualitative behaviors for an increasing number of samples $N_s = \{10^3, 10^5\}$ and for sufficient large times.

In Figure 5.5, on the left-hand side we report the qualitative solution of the Chang–Cooper type scheme integrated with the explicit Euler method, on the right-hand side we depict the decay of the L_1 relative error to the reference solution (3.19) i.e.

$$\frac{\|g^N - g_\infty\|_1}{\|g_\infty\|_1}, \tag{5.2}$$

with g^N representing the approximated solution of the numerical scheme. We test the convergence of the scheme for different quadrature rules, and additionally we compared them with the error of the Monte-Carlo simulation. The plot on the right-hand side shows how the Change Cooper type scheme is able to reach high order of accuracy, for high order quadrature rules in (4.18)-(4.19). For the discretization we consider the following parameters: $N = 80$, $\Delta w = 2/N$ and $\Delta t = (\Delta w)^2/(4\sigma^2)$ with a final time $T = 10$. The DSMC method (Binary Interaction algorithm) is performed with $\varepsilon = 0.0005$ and with $N_s = 10^5$ samples.

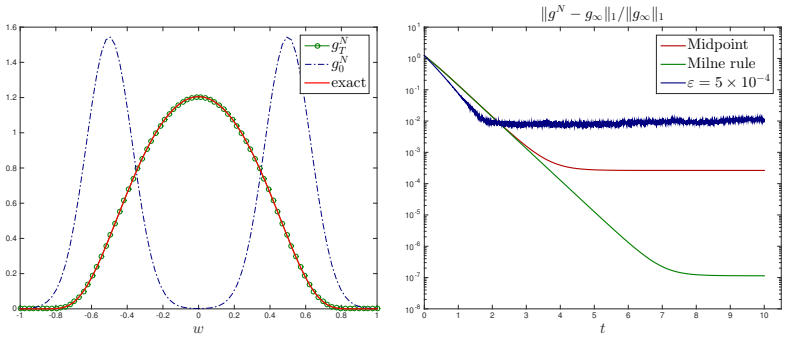

Figure 5.5: Test 1. One-dimensional setting: on the left, the solution of the Chang–Cooper type scheme with the flux (4.18) is indicated with g_T^N and compared with the stationary solution (3.19), also the initial data g_0^N (5.1) is reported. On the right we report the decay of the L^1 relative error (5.2) for different choices of the quadrature rule, mid–point rule (4.15) and Milne's rule (respectively of 2^{nd} and 4^{th} order).

5.5.2 Test 2

Next we consider a second validation test in the full case where the opinion and the evolution of the network are coupled, again with a constant compromise function $P(w, w_*; c, c_*) = 1$ and local diffusion function $D(w, c) = 1-w^2$. In this case we are still able to characterize the analytical solution of the model as the product of the two stationary solution for the opinion variable and the connectivity, i.e. $f_\infty(w, c) = \rho_\infty(c)g_\infty(w)$. We consider the initial data

$$f_0(w, c) = \frac{2}{3}p_0(c)g_0^+(w) + \frac{1}{3}p_0(c - c_0)g_0^-(w), \tag{5.3}$$

where

$$p_0(c) = k_0 \max\{c(c - 2\gamma_0), 0\}, \qquad g_0^\pm(c) = \frac{1}{\sqrt{2\pi\sigma_F^2}}(\exp\{-(w \pm 1/2)^2/(2\sigma_F^2)\}. \tag{5.4}$$

and with coefficient $c_0 = 20$ and $k_0 = 3/(20\gamma_0^3)$. The parameters are defined in Table 4.1 except for the characteristic rates, which will be defined in two different ways in the following. We want to study the decay of the L^1 relative error with respect to the time, as depicted in Figure 5.5.

In the first case we consider constant characteristic rates, i.e. $V = V_a = V_r$, showing that for increasing values of V the convergence of the numerical scheme is faster. This is not surprising, since for larger values of V the dynamics of the connectivity distribution relaxes faster towards the stationary state.

We report in Figure 5.6 the evolution of the density $f(w, c, t)$ in the time frame $[0, T]$ with $T = 20$, where on the plane (z, c) the distribution of the

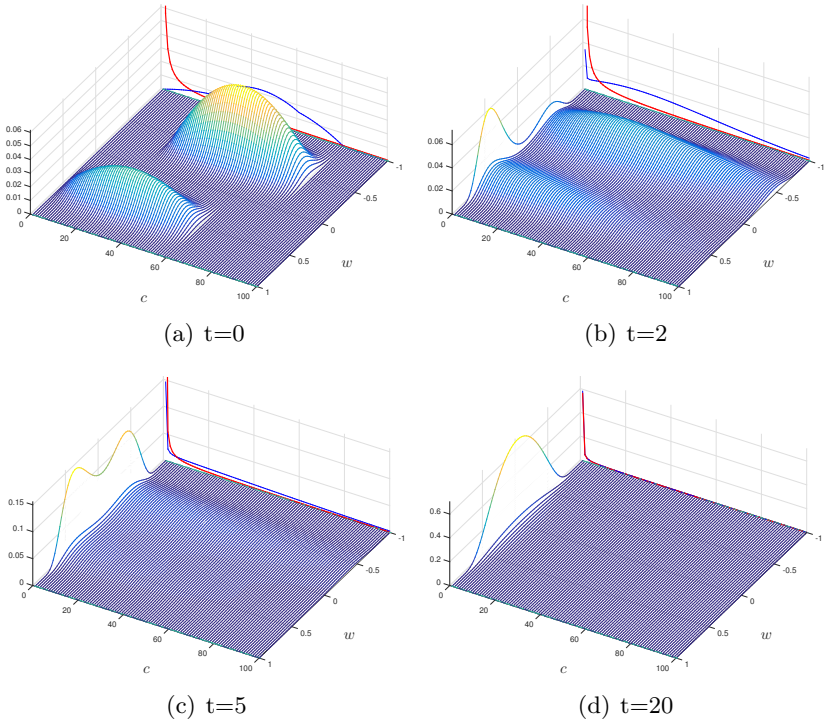

(a) t=0 (b) t=2

(c) t=5 (d) t=20

Figure 5.6: Test 2. From left to right and from the top to the bottom: evolution of the density $f(w, c, t)$ at different time steps. The plot (a) represents the initial data $f_0(w, c)$ (5.3) and plot (d) the stationary solution. On the plane (z, c) we depict with a blu line the marginal distribution $p(c, t)$ of the solution at time t, with red line we represent the reference marginal distribution of the stationary solution.

connections $\rho(c, t)$ is represented in order to better enlighten the convergence to the power-law like distribution.

In a second test we performed the same simulation but with characteristic rates defined as in Remark 8, thus

$$V_r(f; w) = U_r \frac{\gamma + \beta}{\gamma_f + \beta g(w, t)}, \quad V_a(f; w) = U_a \frac{\gamma + \alpha}{\gamma_f + \alpha g(w, t)} \tag{5.5}$$

with $U = U_a = U_r$, $\beta = 0$ and $\gamma_f(t) = \sum_{c=0}^{c_{\max}} c f(w, c, t)$. Simulations shows that in this case the same stationary solution are obtained.

We report in Figure 5.7 the decay of the errors for different values of the characteristic rates, in the two different cases $V = \{10^3, 10^4, 10^5\}$ for the constant rate and $U = \{10^3, 10^4, 10^5\}$ for the variable rates. In both cases we observe a faster convergence to the stationary solution for increasing values of the characteristic rates. Observe that, the same order of accuracy of the mid–point rule in Figure 5.5 is recovered, on the other hand, small

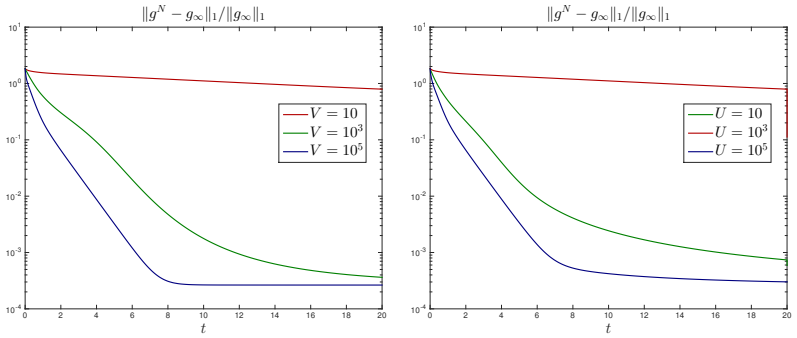

Figure 5.7: Test 2. Decay of the L^1 relative error with respect to the stationary solution (3.19). On the left, fixed characteristic rates $V = \{10^3, 10^4, 10^5\}$, on the right, variable characteristic rates defined as in (5.5) with $U = \{10^3, 10^4, 10^5\}$. In both cases for increasing values of the characteristic rate V and U the stationary state is reached faster.

differences in the decay are observed between the two cases. In Figure 5.8, we enlighten the different evolution of the transient solution at time $t = 1$, of the simulation in Figure 6. On the left we depict the solution with constant characteristic rates, on the right with variable characteristic rates, which shows that lower density in the opinion leads to faster spread on the connections.

5.5.3 Test 3

In this test we analyze the influence of the connections over the opinion dynamics by considering a compromise function of the type

$$P(w, w_*; c, c_*) = H(w, w_*)K(c, c_*),$$

where $H(w, w_*) = 1 - w^2$ and $K(\cdot, \cdot)$, which models the influence of the connectivity on the opinion evolution, is defined as follows

$$K(c, c_*) = \left(\frac{c}{c_{\max}}\right)^{-a} \left(\frac{c_*}{c_{\max}}\right)^{b}, \tag{5.6}$$

for $a, b > 0$. This type of kernel assigns higher relevance into the opinion dynamics to higher connectivity and low influence to low connectivity. The diffusivity is weighted by $D(w, c) = 1 - w^2$.

We perform a first computation with initial data

$$f_0(w, c) = C_0 \begin{cases} \rho_\infty(c) \exp\{-(w + \frac{1}{2})^2)/(2\sigma_F^2)\}, & \text{if } 0 \le c \le 20, \\ \rho_\infty(c) \exp\{-(w - \frac{3}{4})^2/(2\sigma_L^2)\}, & \text{if } 60 \le c \le 80, \\ 0, & \text{otherwise,} \end{cases} \tag{5.7}$$

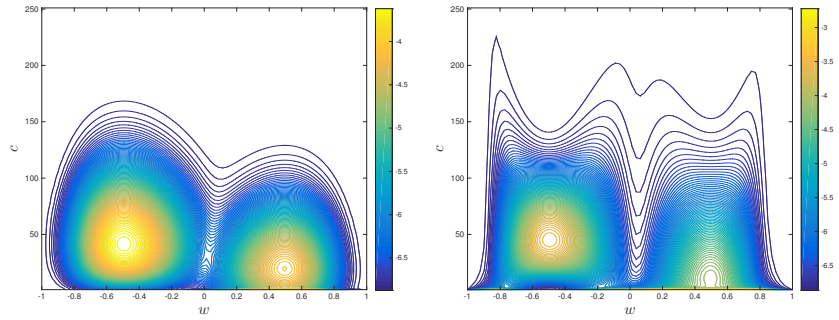

Figure 5.8: Test 2. Evolution at time $t = 1$ of the initial data $f_0(w, c)$ (5.3) as isoline plot. On the left in the case of constant characteristic rate on the right variable characteristic rates defined as in (5.5). The right plot shows that for lower opinion's density the evolution along the connection is faster and slower where the opinions are more concentrated.

where the choice of parameters is reported in the third line of Table 4.1 and $a = b = 3$ for the interaction function $K(\cdot, \cdot)$ (5.6). The evolution is performed through the Chang–Cooper type scheme with $\Delta w = 2/N$ and $N = 80$. We study the evolution of the system in the time interval $[0, T]$ with $T = 2.5$.

In Figure 5.9 we report the result of the simulation. The initial configuration is is split in two parts, the majority concentrated around opinion $\bar{w}_F = -1/2$ and only a small portion concentrated around $\bar{w}_L = 3/4$. From the upper-right and bottom-left figures we observe that, because of the anisotropy induced by $K(c, c_*)$, the density with a low level of connectivity is immediately influenced by the small concentration of density around w_L with a large level of connectivity; the bottom-right plot shows the final configuration.

In Figure 5.10 we depict, on the left-hand side, the initial and final marginal density of the opinion, respectively $g(w, 0)$ and $g(w, T)$, showing the change of the total opinion. On the right, we enlighten the change of opinion plotting the evolution of the average opinion.

5.5.4 Test 4

In the last test case, we consider a connection dependent Hegselmann-Krause model [113], known also as bounded confidence model, where agents interact only with agents whose opinion lays within a certain range of confidence. Thus, we define the following compromise function

$$P(w, w_*; c, c_*) = \chi_{\{|w-w_*| \leq \Delta(c)\}}(w_*), \tag{5.8}$$

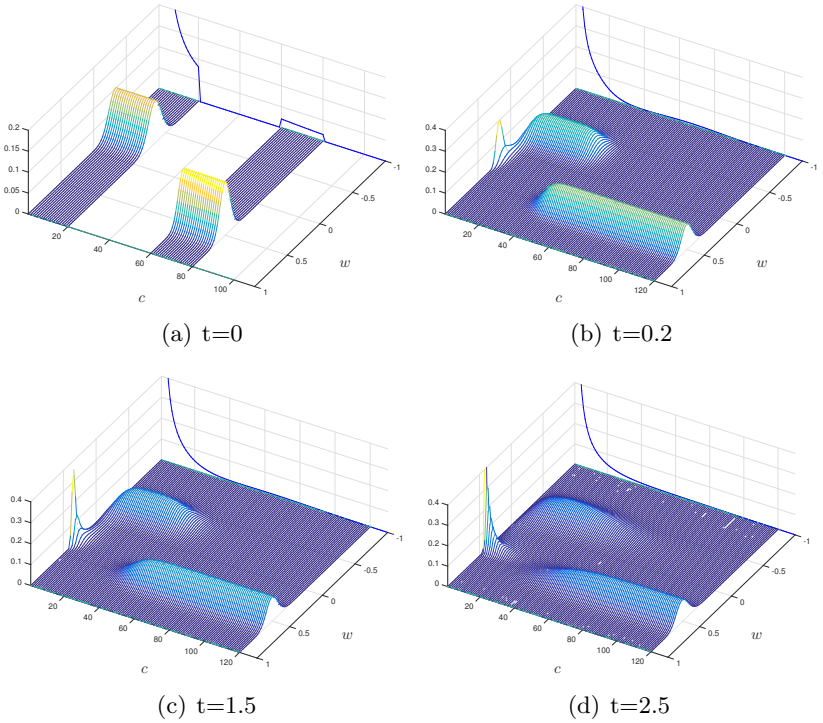

(a) t=0 (b) t=0.2

(c) t=1.5 (d) t=2.5

Figure 5.9: Test 3. From left to right and from the first row to the second row, evolution of the initial data (5.7) in time frame $[0, T]$ with $T = 2$. The evolution shows how a small portion of density with high connectivity can bias the majority of the population towards their position. (Note: The density is scaled according to the marginal distribution $\rho(c, t)$ in order to better show its evolution, the actual marginal density $\rho(c, t)$ is depicted in the background, scaled by a factor 10).

where $\Delta(c)$ is the connection dependent confidence level. We define the initial data

$$f_0(w, c) = \frac{1}{2}\rho_\infty(c), \tag{5.9}$$

therefore the opinion is uniformly distributed on the interval $I = [-1, 1]$ and it decreases along $c \in [0, c_{\max}]$ following $\rho_\infty(c)$, as in (2.24), with parameters defined in Table 4.1 and $D(w, c) = 1 - w^2$. The evolution is performed through the Chang–Cooper type scheme with $\Delta w = 2/N$, with $N = 80$. We consider the evolution of the system in the time interval $[0, T]$, with $T = 100$.

We study first a confidence level independent from the number of connections, therefore we set $\Delta(c) = \Delta = 0.25$. In Figure 5.11 the evolution of the initial data (5.9) shows the classical behavior of Hegselmann-Krause model, where opinions' clusters emerge.

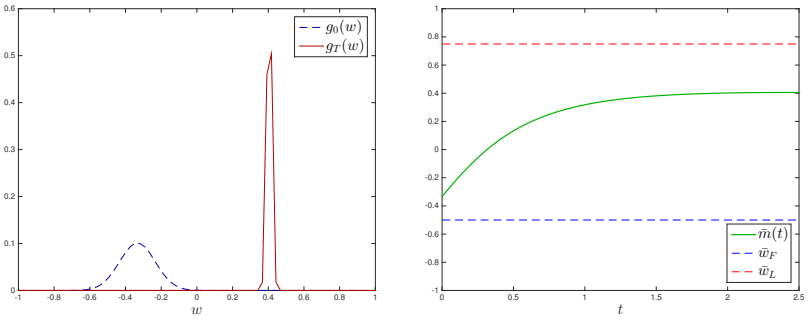

Figure 5.10: Test 3. On the left-hand side final and initial state of the marginal distribution $g(w,t)$ of the opinion, the green line represents the evolution of the average opinion $\bar{m}(t)$, the red and blue dashed lines represent respectively the opinions $\bar{w}_L = 0.75$ and $\bar{w}_F = -0.5$, which are the two leading opinions of the initial data (5.7).

Next, we perform a second computation where the confidence bound depends on the number of connections as follows

$$\Delta(c) = d_0 \frac{c}{c_{\max}}. \tag{5.10}$$

This choice reflects a behavior where agents with higher number of connections are prone to larger level of confidence. We report in Figure 5.12 the evolution of (5.9), where $\Delta(c)$ creates an heterogeneous emergence of clusters with respect to the connectivity level: for higher level of connectivity consensus is reached, since the bounded confidence level is larger, instead for lower levels of connectivity multiple clusters appears, up to the limiting case $c = 0$, where the opinions are not influenced by the consensus dynamics.

5.6 Conclusions

The construction of kinetic models and numerical methods for the spreading of opinions over time dependent large scale networks has been considered. First we have introduced a Boltzmann model for the opinion interactions based on a preferential attachment process for the creation of new connections between agents. If the preferential attachment is independent from the agents' opinion the large time behavior of the network can be described analytically and originates both Poisson type distributions as well as truncated power laws. Next, we derived the corresponding mean-field approximation which permits to have a deeper understanding of the asymptotic behavior of the opinion dynamics and to compute analytically stationary states in simplified situations. Robust numerical methods, based on stochastic as well as deterministic techniques have been introduced and their property discussed. The results, for various test cases, show that the present approach

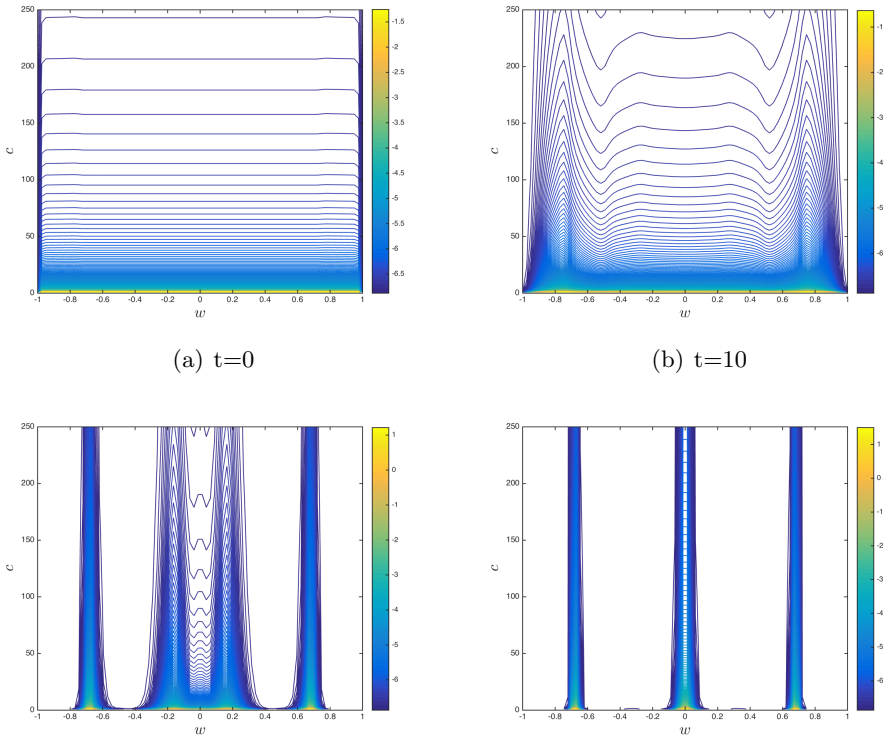

(a) t=0 (b) t=10

(c) t=50 (d) t=100

Figure 5.11: Test 4. Evolution of the Fokker-Planck model (4.9) where the interaction are described by (5.8) with $\Delta = 0.25$, in the time frame $[0, T]$ with $T = 100$. The evolution shows the emergence of three main opinion clusters, which are not affected by the connectivity variable. (Note: In order to better show its evolution, we represent the solution as $\log(f(w, c, t) + \epsilon)$, with $\epsilon = 0.001$.)

is capable to reproduce realistic opinion/network distributions including the emergence of opinion clusters. In principle, the model here introduced admits various extensions. First, one may consider the case where the number of agents in the network is not conserved, as it happens in a real social network. Moreover, control problems with the aim to force consensus over the network may be introduced. These subjects are actually under study and the results will be presented elsewhere.

Appendix Ch.5: Properties of the network

In this section we report explicit computations concerning the properties of the network operator $\mathbb{N}[\cdot]$.

Conservation of the total number of agents

First we show that

$$\sum_{c=0}^{c_{\max}} \mathbb{N}[f(w,c,t)]\,dw = 0. \tag{6.1}$$

From (2.13) we have

$$\begin{aligned}
\sum_{c=1}^{c_{\max}-1} \mathbb{N}[f(w,c,t)] =& -\frac{2V_r(f;w)}{\gamma+\beta}\sum_{c=1}^{c_{\max}-1}\left[(c+1+\beta)f(w,c+1,t)-(c+\beta)f(w,c,t)\right]\\
&-\frac{2V_a(f;w)}{\gamma+\alpha}\sum_{c=1}^{c_{\max}-1}\left[(c-1+\alpha)f(w,c-1,t)-(c+\alpha)f(w,c,t)\right]\\
=&-\frac{2V_r(f;w)}{\gamma+\beta}\left[(c_{\max}+\beta)f(w,c_{\max},t)-(\beta+1)f(w,1,t)\right]\\
&+\frac{2V_a(f;w)}{\gamma+\alpha}\left[(c_{\max}-1+\alpha)f(w,c_{\max}-1,t)-\alpha f(w,0,t)\right].
\end{aligned}$$

Using the boundary conditions (2.15) we have the desired property. As a consequence we obtain the conservation of the total number of agents

$$\frac{d}{dt}\sum_{c=0}^{c_{\max}}\rho(c,t) = -\int_I \sum_{c=0}^{c_{\max}} \mathbb{N}[f(w,c,t)]\,dw = 0. \tag{6.2}$$

Mean density of connectivity

Next we consider the evolution of the mean density of connectivity $\gamma(t)$. We prove that

$$\begin{aligned}
\sum_{c=0}^{c_{\max}} c\mathbb{N}[f(w,c,t)] =& 2V_r(f;w)\frac{\gamma_f+\beta g(w,t)}{\gamma+\beta} - 2V_a(f;w)\frac{\gamma_f+\alpha g(w,t)}{\gamma+\alpha}\\
&-\frac{2V_r(f;w)}{\gamma+\beta}\beta f(w,0,t)+\frac{2V_a(f;w)}{\gamma+\alpha}(c_{\max}+\alpha)f(w,c_{\max},t).
\end{aligned} \tag{6.3}$$

In fact, thanks to (2.13), in the internal points we have

$$\begin{aligned}
-\sum_{c=1}^{c_{\max}-1} c\mathbb{N}[f(w,c,t)] =& \frac{2V_r(f;w)}{\gamma+\beta}\sum_{c=1}^{c_{\max}-1} c\left[(c+1+\beta)f(w,c+1,t)\right.\\
&\left.-(c+\beta)f(w,c,t)\right]\\
&+\frac{2V_a(f;w)}{\gamma+\alpha}\sum_{c=1}^{c_{\max}-1} c\left[(c-1+\alpha)f(w,c-1,t)\right.\\
&\left.-(c+\alpha)f(w,c,t)\right].
\end{aligned} \tag{6.4}$$

We observe that the first sum in (6.4) is equal to

$$\begin{aligned}
&\frac{2V_r(f;w)}{\gamma+\beta}\sum_{c=1}^{c_{\max}-1}[c(c+1)f(w,c+1,t)-c^2f(w,c,t)]\\
&\qquad+\frac{2V_r(f;w)}{\gamma+\beta}\beta\sum_{c=1}^{c_{\max}-1}[cf(w,c+1,t)-cf(w,c,t)],\\
&=\frac{2V_r(f;w)}{\gamma+\beta}\left[c_{\max}(c_{\max}+\beta)f(w,c_{\max},t)-(\gamma_f+\beta g(w,t))+\beta f(w,0,t)\right].
\end{aligned}\tag{6.5}$$

Similarly the second sum in (6.4) is equal to

$$\begin{aligned}
&\frac{2V_a(f;w)}{\gamma+\alpha}\sum_{c=1}^{c_{\max}-1}[c(c-1)f(w,c-1,t)-c^2f(w,c,t)]\\
&\qquad+\frac{2V_a(f;w)}{\gamma+\alpha}\alpha\sum_{c=1}^{c_{\max}-1}[cf(w,c-1,t)-cf(w,c,t)],\\
&=\frac{2V_a(f;w)}{\gamma+\alpha}\left[\gamma_f(w,t)-c_{\max}(c_{\max}-1)f(w,c_{\max}-1,t)-c_{\max}f(w,c_{\max},t)\right]\\
&\qquad+\frac{2V_a(f;w)}{\gamma+\alpha}\alpha\left[g(w,t)-c_{\max}f(w,c_{\max}-1,t)-f(w,c_{\max},t)\right].
\end{aligned}\tag{6.6}$$

Using the boundary condition for $c=c_{\max}$ (since the one at $c=0$ does not play any role here) we have

$$\begin{aligned}
-c_{\max}\mathbb{N}[f(w,c_{\max},t)]=&-c_{\max}\frac{2V_r(f;w)}{\gamma+\beta}(c_{\max}+\beta)f(w,c_{\max},t)\\
&+c_{\max}\frac{2V_a(f;w)}{\gamma+\alpha}(c_{\max}-1+\alpha)f(w,c_{\max}-1,t),
\end{aligned}\tag{6.7}$$

which together with the above computations yields (6.3).

As a consequence we have

$$\begin{aligned}
\frac{d}{dt}\gamma(t)=&-2\int_I V_r(f;w)\frac{\gamma_f+\beta g(w,t)}{\gamma+\beta}dw+2\int_I V_a(f;w)\frac{\gamma_f+\alpha g(w,t)}{\gamma+\alpha}dw\\
&+\frac{2\beta}{\gamma+\beta}\int_I V_r(f;w)f(w,0,t)\,dw-\frac{2(c_{\max}+\alpha)}{\gamma+\alpha}\int_I V_a(f;w)f(w,c_{\max},t)\,dw
\end{aligned}\tag{6.8}$$

Asymptotic behavior

In the following we compute the explicit stationary solution $\rho_\infty(c)$ for the evolution of $\rho(c,t)$ in the linear case with $V_a = V_r$, $\beta = 0$ and assuming

$$\sum_{c=0}^{c_{\max}} \rho_\infty(c) = 1, \qquad \sum_{c=0}^{c_{\max}} c\rho_\infty(c) = \gamma_\infty.$$

Note that in the sequel, for notation simplicity, we denote by $\gamma = \gamma_\infty$ the asymptotic stationary value reached by the mean density of connectivity.

Proposition 5.6.1. *For each $c \in \mathcal{C}$ the stationary solution to (2.21) or equivalently*

$$(c+1)\rho_\infty(c+1) = \frac{1}{\gamma+\alpha}\left[(c(2\gamma+\alpha)+\gamma\alpha)\rho_\infty(c) - \gamma(c-1+\alpha)\rho_\infty(c-1)\right] \tag{6.9}$$

is given by

$$\rho_\infty(c) = \left(\frac{\gamma}{\gamma+\alpha}\right)^c \frac{1}{c!}\alpha(\alpha+1)\cdots(\alpha+c-1)\rho_\infty(0) \tag{6.10}$$

where

$$\rho_\infty(0) = \left(\frac{\alpha}{\alpha+\gamma}\right)^\alpha. \tag{6.11}$$

Proof. Let us show (6.10) by induction. First, from the boundary condition (2.23) at $c = 0$ we immediately have

$$\rho_\infty(1) = \left(\frac{\gamma}{\gamma+\alpha}\right)\alpha\rho_\infty(0). \tag{6.12}$$

Now let us assume that (6.10) holds true for c, we want to prove that

$$\rho_\infty(c+1) = \left(\frac{\gamma}{\gamma+\alpha}\right)^{c+1} \frac{1}{(c+1)!}\alpha(\alpha+1)\cdots(\alpha+c)\rho_\infty(0). \tag{6.13}$$

From (6.9) we have

$$\begin{aligned}
(c+1)\rho_\infty(c+1) =& \frac{1}{\gamma+\alpha}\left[(c(2\gamma+\alpha)+\gamma\alpha)\left(\frac{\gamma}{\gamma+\alpha}\right)^c \frac{1}{c!}\alpha(\alpha+1)\cdots(\alpha+c-1)\rho_\infty(0)\right.\\
&\left.-\gamma(c-1+\alpha)\left(\frac{\gamma}{\gamma+\alpha}\right)^{c-1}\frac{1}{(c-1)!}\alpha\cdots(\alpha+c-2)\rho_\infty(0)\right]\\
=& \left(\frac{\gamma}{\gamma+\alpha}\right)^c \frac{1}{(c-1)!}\alpha\cdots(\alpha+c-1)\left[\frac{c(2\gamma+\alpha)+\gamma\alpha}{c(\gamma+\alpha)} - 1\right]\rho_\infty(0)\\
=& \left(\frac{\gamma}{\gamma+\alpha}\right)^{c+1}\frac{1}{c!}\alpha\cdots(\alpha+c-1)(\alpha+c)\rho_\infty(0).
\end{aligned}$$

By direct inspection one verifies that also the boundary condition (2.23) at $c = c_{\max}$ is verified. □

Appendix Ch. 5: Properties of the implicit-explicit scheme

Let us consider the following implicit-explicit discretization of (4.9)

$$\frac{f_i^{n+1} - f_i^n}{\Delta t} + \mathbb{N}[f_i^{n+1}] = \frac{\mathcal{F}_{i+1/2}^n - \mathcal{F}_{i-1/2}^n}{\Delta w}, \tag{6.14}$$

where $f_i^n = f_i^n(c)$, endowed with a positive initial condition $f_i^0(c) = f_i(c,0)$. The main motivation for the time discretization above is related to the severe stability constraints of an explicit scheme applied to the network operator which would require the time step to be $O(1/c_{\max})$ where $c_{\max} \gg 1$.

Positivity

In order to study the nonnegativity property of scheme (6.14) it is convenient to rewrite it as a sequence of two steps

$$\begin{aligned} f_i^{n+1/2} &= f_i^n + \Delta t \frac{\mathcal{F}_{i+1/2}^n - \mathcal{F}_{i-1/2}^n}{\Delta w} \\ f_i^{n+1} &= f_i^{n+1/2} - \Delta t \mathbb{N}[f_i^{n+1}]. \end{aligned} \tag{6.15}$$

The first step involves the Chang–Cooper type scheme and reads

$$\begin{aligned} f_i^{n+1/2} = f_i^n + \frac{\Delta t}{\Delta w}\Bigg[&\Big((1-\delta_{i+1/2})B_{i+1/2}^n + \frac{1}{\Delta w}C_{i+1/2}\Big) f_{i+1}^n \\ &- \Big((1-\delta_{i-1/2})B_{i-1/2}^n - \delta_{i+1/2}B_{i+1/2}^n\Big) f_i^n - \frac{1}{\Delta w}\Big(C_{i+1/2} + C_{i-1/2}\Big) f_i^n \\ &- \Big(\delta_{i-1/2}B_{i-1/2}^n - \frac{1}{\Delta w}C_{i-1/2}\Big) f_{i-1}^n \Bigg], \end{aligned} \tag{6.16}$$

where $B_{i+1/2}^n, C_{i+1/2}$ are given by

$$\begin{aligned} B_{i+1/2}^n(c) &= \frac{D_{i+1/2}^2}{\Delta w}\int_{w_i}^{w_{i+1}} \frac{1}{D(w,c)^2}(\mathcal{P}[f](w,c,t^n) + \sigma^2 D'(w,c)D(w,c))dw, \\ C_{i+1/2} &= \frac{\sigma^2}{2}D_{i+1/2}^2 \geq 0. \end{aligned} \tag{6.17}$$

From the definition of the weight functions $\delta_{i+1/2}$ in (4.16), the coefficients of f_{i+1}^n, f_{i-1}^n, satisfy

$$\begin{aligned} (1-\delta_{i+1/2})B_{i+1/2}^n + \frac{1}{\Delta w}C_{i+1/2} \geq 0, \\ -\delta_{i-1/2}B_{i-1/2}^n + \frac{1}{\Delta w}C_{i-1/2} \geq 0. \end{aligned} \tag{6.18}$$

In fact, setting $x = B^n_{i+1/2}\Delta w/C_{i+1/2}$, $y = B^n_{i-1/2}\Delta w/C_{i-1/2}$ the two inequalities are equivalent to show that $\forall\, x, y \in \mathbb{R}$

$$x\left(1 - \frac{1}{1-e^x}\right) \geq 0, \qquad \frac{y}{e^y - 1} \geq 0, \tag{6.19}$$

which follow from the properties of the exponential function.

Then, in order to ensure the nonnegativity of the scheme the time step must satisfy the restriction

$$\Delta t \leq \frac{\Delta w}{\nu^n}, \tag{6.20}$$

where

$$\nu^n = \max_i \left\{(1-\delta_{i-1/2})B^n_{i-1/2} - \delta_{i+1/2}B^n_{i+1/2} + \frac{1}{\Delta w}C_{i+1/2} + \frac{1}{\Delta w}C_{i-1/2}\right\}. \tag{6.21}$$

Now, since the functions $D(w,c), P(w,w_*;c,c_*)$ are bounded for all $w \in I, c \in \mathcal{C}$ we have that

$$|B^n_{i+1/2}| \leq 2 + \sigma^2 M, \qquad C_{i+1/2} \leq \sigma^2/2$$

where $M = \max_i |D'_{i+1/2}|$, and the condition (6.20) simplifies to

$$\Delta t \leq \frac{1}{2}\frac{\Delta w}{\left(2 + \sigma^2 M + \frac{\sigma^2}{2\Delta w}\right)}. \tag{6.22}$$

Therefore, we have shown

Proposition 5.6.2. *Under the time step restriction (6.22) the first step in (6.15) preserves nonnegativity, namely* $f_i^{n+1/2}(c) \geq 0$ *if* $f_i^n(c) \geq 0$, $i = 1, \ldots, N$, $c \in \mathcal{C}$.

Typically when σ^2 is large this will originate a parabolic stability condition that requires $\Delta t = O(\Delta w^2)$. This can be avoided taking the diffusive part implicitly, however, since we were mostly interested in the case of small values of σ^2 we will not pursue this direction here.

Next, we consider the second step

$$f_i^{n+1}(c) = f_i^{n+1/2}(c) - \Delta t \mathbb{N}[f_i^{n+1}(c)]. \tag{6.23}$$

Note that in general the fully implicit evaluation of $\mathbb{N}[\cdot]$ would require the use of a suitable iterative solver due to the nonlinearity in f_i^{n+1}. We therefore will consider a semi-implicit linearized version of the operator.

The scheme can be written as

$$\begin{aligned}&\left[1 + d^{n+1/2}(c) + a^{n+1/2}(c) + b^{n+1/2}(c)\right] f_i^{n+1}(c)\\ &- a^{n+1/2}(c) f_i^{n+1}(c+1) - b^{n+1/2}(c) f_i^{n+1}(c-1) = f_i^{n+1/2}(c),\end{aligned} \tag{6.24}$$

where

$$\begin{aligned}
&a^{n+1/2}(c) = \Delta t v_r^{n+1/2}(c+1+\beta), && c = 0,\dots,c_{\max}-1\\
&b^{n+1/2}(c) = \Delta t v_a^{n+1/2}(c-1+\alpha), && c = 1,\dots,c_{\max}\\
&d^{n+1/2}(c) = -\Delta t v_r^{n+1/2} + \Delta t v_a^{n+1/2}, && c = 1,\dots,c_{\max}-1\\
&a^{n+1/2}(c_{\max}) = 0, \qquad b^{n+1/2}(0) = 0,\\
&d^{n+1/2}(0) = b^{n+1/2}(1) - a^{n+1/2}(0),\\
&d^{n+1/2}(c_{\max}) = -b^{n+1/2}(c_{\max}) + a^{n+1/2}(c_{\max}-1),
\end{aligned} \tag{6.25}$$

and we have set $v_r^{n+1/2} = 2V_r^{n+1/2}/(\gamma^{n+1/2}+\beta)$ and $v_a^{n+1/2} = 2V_a^{n+1/2}/(\gamma^{n+1/2}+\alpha)$. Since alle quantities $a^{n+1/2}(\cdot)$, $b^{n+1/2}(\cdot)$ defined in (6.25) are nonnegative, equations (6.24)-(6.25) define a diagonally dominant matrix of size $(c_{\max}+1)\times(c_{\max}+1)$ if

$$\begin{aligned}
&\Delta t \le \frac{1}{v_r^{n+1/2} - v_a^{n+1/2}}, && \frac{v_r^{n+1/2}}{v_a^{n+1/2}} > 1,\\
&\Delta t \le \frac{1}{v_r^{n+1/2}(1+\beta) - v_a^{n+1/2}\alpha}, && \frac{v_r^{n+1/2}}{v_a^{n+1/2}} > \frac{\alpha}{(1+\beta)},\\
&\Delta t \le \frac{1}{v_a^{n+1/2}(c_{\max}-1+\alpha) - v_r^{n+1/2}(c_{\max}+\beta)}, && \frac{v_a^{n+1/2}}{v_r^{n+1/2}} > \frac{(c_{\max}+\beta)}{(c_{\max}-1+\alpha)}.
\end{aligned} \tag{6.26}$$

Note that when the above conditions on $v_r^{n+1/2}$ and $v_a^{n+1/2}$ are not satisfied, no time step restriction occurs. These conditions are not restrictive since in practice $\gamma^{n+1/2} \gg 1$ and so $v_a^{n+1/2} \ll 1$ and $v_r^{n+1/2} \ll 1$. Thus, we have

Proposition 5.6.3. *Under the time step restriction (6.26) the second step in (6.15) preserves nonnegativity, namely $f_i^{n+1}(c) \ge 0$ if $f_i^{n+1/2}(c) \ge 0$, $i = 1,\dots,N$, $c \in \mathcal{C}$.*

Remark 9. *In particular, in the case where the rates are defined by (2.16) since*

$$g_i^{n+1} = \sum_{c=0}^{c_{max}} f_i^{n+1}(c) = \sum_{c=0}^{c_{max}} f_i^{n+1/2}(c) = g_i^{n+1/2},$$

the previous arguments applies to the fully implicit evaluation of $V_a^{n+1} = V_a(f_i^{n+1}; w_i)$ and $V_r^{n+1} = V_r(f_i^{n+1}; w_i)$.

Conservations and stability

Let us consider the conservation properties of the scheme with respect to the variable w. Let us observe that from scheme (6.14) we get

$$\sum_{i=0}^{N} f_i^{n+1}(c) = \sum_{i=0}^{N} f_i^n(c) - \Delta t \sum_{i=0}^{N} \mathbb{N}[f_i^{n+1}] + \frac{\Delta t}{\Delta w} \sum_{i=0}^{N} \left(\mathcal{F}_{i+1/2}^n - \mathcal{F}_{i-1/2}^n \right). \tag{6.27}$$

Now since

$$\begin{aligned} \sum_{i=0}^{N} \left(\mathcal{F}_{i+1/2}^n - \mathcal{F}_{i-1/2}^n \right) &= \sum_{i=0}^{N-1} \mathcal{F}_{i+1/2}^n - \sum_{i=1}^{N} \mathcal{F}_{i-1/2}^n + \mathcal{F}_{N+1/2}^n - \mathcal{F}_{-1/2}^n \\ &= \mathcal{F}_{N+1/2}^n - \mathcal{F}_{-1/2}^n, \end{aligned}$$

by imposing no-flux boundary conditions, i.e.

$$\mathcal{F}_{N+1/2}^n = 0, \qquad \mathcal{F}_{-1/2}^n = 0, \tag{6.28}$$

we obtain that for all $n \geq 0$ the following conservation equation for the density of connections is satisfied

$$\rho^{n+1}(c) = \rho^n(c) - \Delta t \sum_{i=0}^{N} \mathbb{N}[f_i^{n+1}]. \tag{6.29}$$

Summing over c in the above equation yields the conservation of the total number of agents

$$\sum_{c=0}^{c_{\max}} \rho^{n+1}(c) = \sum_{c=0}^{c_{\max}} \rho^n(c). \tag{6.30}$$

From this identity we have

Proposition 5.6.4. *Under the time step restrictions (6.22) and (6.26), the numerical scheme defined by (6.14) is stable in the discrete L_1-norm.*

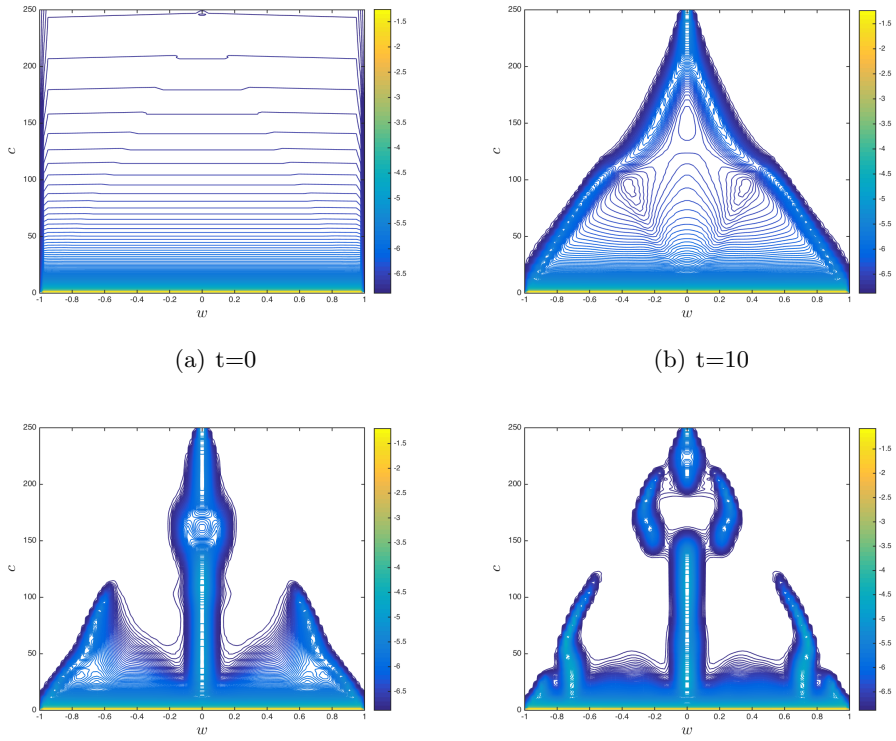

(a) t=0 (b) t=10

(c) t=50 (d) t=100

Figure 5.12: Test 4. Evolution of the solution of the Fokker-Planck model (4.9), where the interaction are described by (5.8) with $\Delta(c) = d_0 c/c_{\max}$ and $d_0 = 1.01$, in the time frame $[0, T]$ with $T = 100$. The choice of $\Delta(c)$ reflects in the heterogeneous emergence of clusters with respect to the connectivity level: for higher level of connectivity consensus is reached, instead for lower levels of connectivity multiple opinion clusters are present. (Note: In order to better show its evolution, we represent the solution as $\log(f(w, c, t) + \epsilon)$, with $\epsilon = 0.001$.)

Chapter 6

Kinetic models for collective decision-making

6.1 Introduction

The fallibility of human judgement is evident in our everyday life, especially regarding our self-evaluation ability. Several tests have been designed in cognitive psychology and clinical research in order to find an experimental evidence for this phenomenon, see [85, 86, 111, 112] and the references therein, showing that subjects are in general overconfident about the correctness of their belief. This lack in *metacognition*, i.e. the self-assessment of our own knowledge skills, goes hand in hand with the grade of competence of each subject.

The correlation between *competence* and *metacognitive skills* is somehow double and might be summarized in the following sentence: "the same knowledge that underlies the ability to produce correct judgement is also the knowledge that underlies the ability to recognize correct judgement" [124]. Here the authors found a systematic bias of the most incompetent agents on their metacognition than the most experts; behavior which is usually known as *Dunning-Kruger effect*. In other words, incompetence not only bring people to poor choices but also disable to recognize that these are wrong or improvable. Further, the overconfidence of the novices emerges together with the under-confidence of highly competent individuals which tend to negatively estimate their skills.

This coupled deviation from an objective self-evaluation of personal abilities has been recently investigated in [131], where authors asked how people deal with individual differences in competence, in the context of a collective perceptual decision-making task, developing a metric for estimating how participants weight their partner's opinion relative to their own. Empirical experiments, replicated across three slightly different countries as Denmark, Iran, and China, show how participants assigned nearly equal weights to

each other's opinions regardless of the real differences in their competence. This *equality bias*, whereby people behave as if they are as good or as bad as their partner, is particularly costly for a group when a competence gap separates its members.

Drawing inspiration from these recent results, we propose a multi-agent model which takes into account the influence of competence during the formation of a collective decision [39, 146]. After the seminal models for wealth/opinion exchange for a multi-agent system introduced in [59, 157, 164] some recent works considered additional parameters to quantify the personal knowledge or conviction [39, 81, 82, 146] or constrained versions of these models [6, 11, 117]. For example, individuals with high conviction are resistant to change opinion, and can play the role of leaders [11, 82]. In [125] there exists a threshold conviction beyond of which one of the two choices provided to the individuals prevails, spontaneously breaking the existing symmetry of the initial set-up.

More precisely, we introduce a binary exchange mechanism for opinion and competence deriving a kinetic equation of Boltzmann-type [6, 11, 39, 84, 145, 146, 164]. The binary collision terms for competence and opinion describe different processes:

- the competence evolution depends on a social background in which individuals grow and on the possibility for less competent agents to learn from the more competent ones;
- the opinion dynamics depend by a competence based compromise process which includes an equality bias effect and change of opinion through self-thinking;
- agents are driven toward an a-priori correct choice in dependence on their competence grade;

In order to derive a nonlinear equation of Boltzmann-type for the joint evolution of competence and opinion in the limit of a large number of interacting agents, we resort to the principles of classical kinetic theory (we refer to the recent monograph [145] for an introduction to the subject). Furthermore, to simplify the study of the asymptotic behavior of the model, we obtain a Fokker-Planck approximation of the dynamic in the so-called quasi-invariant scaling.

The rest of the chapter is organized as follows, in Section 6.2 we introduce the binary interaction model for competence and opinion. We discuss the competence-based interactions between agents formulating a definition of collective optimal decision which is coherent with the experimental setting of [131]. Then the equality bias function is introduced acting as a modification of the effective competence into perceived competence. In Section 6.3 we derive the Boltzmann-type model and study the evolution of the moments

under some specific assumptions. The Fokker-Planck approximation is then obtained in Section 6.4, and we derive the stationary marginal density of the competence variable. Finally in Section 6.5 we present several numerical experiments which show that the model is capable to describe correctly the decision-making process based on agents' competence and to include the equality bias effects. The latter, as expected, drive the system towards suboptimal decisions.

6.2 Modelling opinion and competence

In this section we discuss the modelling of opinion dynamics through binary exchanges, the analogous of dyadic interaction in the reference experimental literature [131, 18]. The mathematical approach follows several recent works on alignment processes in socio-economical dynamics [39, 146, 164, 82, 145, 84, 87, 139, 138].

6.2.1 Evolution of competence

It is evident that one of the main factors playing a role is the social background in which an individual grows and lives, then it is natural to assume that competence is, in part, inherited from the environment. Moreover, we clearly have the possibility to improve specific competences during interactions with more competent agents.

Similarly to the works [39, 146, 145] we describe the evolution of the competence of an individual in terms of a scalar variable $x \in X$, where $X \subset \mathbb{R}^+$. Let $z \in \mathbb{R}^+$ be the degree of competence achieved from the background in each interaction; in what follows we will always suppose that $C(z)$ is a distribution with bounded mean

$$\int_{\mathbb{R}^+} C(z)dz = 1, \qquad \int_{\mathbb{R}^+} zC(z)dz = m_B. \tag{2.1}$$

We define the new amount of competence after a binary interaction between two agents with competence x and x_* as follows

$$\begin{cases} x' &= (1-\lambda(x))x + \lambda_C(x)x_* + \lambda_B(x)z + \kappa x \\ x'_* &= (1-\lambda(x_*))x_* + \lambda_C(x_*)x + \lambda_B(x_*)z + \kappa x_*, \end{cases} \tag{2.2}$$

where $\lambda(\cdot), \lambda_C(\cdot)$ and $\lambda_B(\cdot)$ quantify the amounts of competence lost by individual by the natural process of forgetfullness [146], the competence gained thanks to the interaction with other agents and the expertise gained from the background respectively. Moreover, κ is a zero-mean random variable with finite second order moment σ^2_κ, taking into account the possible unpredictable changes of the competence process. A possible choice for $\lambda_C(x)$ is $\lambda_C(x) = \lambda_C\chi(x \geq \bar{x})$, where $\chi(\cdot)$ is the indicator function and $\bar{x} \in X$ a

minimum level of competence required to the agents for increasing their own skills by interactions.

With the dynamics (2.2) we introduced a general process in which agents respectively loose and gain competence interacting with the other agents and with the background. It is reasonable then to assume that both the processes of gain and loss, which are weighted by the coefficients λ, λ_C and λ_B, are bounded by zero. Thus if $\lambda \in [\lambda_-, \lambda_+]$, with $\lambda_- > 0$ and $\lambda_+ < 1$, and $\lambda_C(x), \lambda_B(x) \in [0, 1]$ the random part may be chosen to satisfy $\kappa \geq -1 + \lambda_+$. For example, κ may be uniformly distributed in $[-1 + \lambda_+, 1 - \lambda_+]$.

Let $g(x, t)$ be the density function of individuals with competence $x \in X$ at time $t \geq 0$. Resorting to the standard Boltzmann-type setting, we refer to [145] for an extensive treatment, it is possible to describe in weak form the evolution of such density function as follows

$$\frac{d}{dt}\int_X \psi(x)g(x,t)dx = \left\langle \int_{\mathbb{R}^+\times X} (\psi(x') - \psi(x))g(x,t)C(z)dxdz \right\rangle, \tag{2.3}$$

where x' is the post-interaction competence given in (2.2), the brackets $< \cdot >$ indicate the expectation with respect to the random variable κ and $\psi(\cdot)$ is a test function. By imposing $\psi(x) = x$ we obtain an equation for the evolution of the mean-competence $m_x(t)$

$$\begin{aligned}\frac{d}{dt}m_x(t) = \frac{1}{2}\Bigg(\int_{X^2} (\lambda_C(x) - \lambda(x))(x + x_*)g(x,t)g(x_*,t)dxdx_* + \\ \int_{\mathbb{R}^+\times X} \lambda_B(x) z g(x,t)C(z)dxdz\Bigg),\end{aligned} \tag{2.4}$$

which, for $\lambda_C(x) = \lambda_C, \lambda_B(x) = \lambda_B, \lambda(x) = \lambda$, yields

$$\frac{d}{dt}m_x(t) = -(\lambda - \lambda_C)m_x(t) + \lambda_B m_B, \tag{2.5}$$

whose solution is given by

$$m_x(t) = m_x(0)e^{-(\lambda-\lambda_C)t} + \frac{\lambda_B m_B}{\lambda - \lambda_C}(1 - e^{-(\lambda-\lambda_C)t}). \tag{2.6}$$

Therefore if $\lambda > \lambda_C$ we obtain the asymptotic exponential convergence of the mean competence m_x toward $\lambda_B m_B/(\lambda - \lambda_C)$. Note that, if we assume $\lambda = \lambda_B + \lambda_C$ we have that the average competence of the system tends to the mean competence induced by the variable $z \in \mathbb{R}^+$. Finally we remark that, compared to previous models where the notion of knowledge/convinction has been introduced [39, 146], here we have a fully binary dynamics which includes also the possibility to increase the agents' competence as a result of the interaction with the other agents.

6.2.2 The dynamics of competence based decisions

Let us now consider a system of binary interacting agents, each of them endowed with two quantities (w, x), representing their opinions concerning a certain decision and the competence respectively. Let $I = [-1, 1]$ be the set of possible opinions for each interaction where the two extremal points ± 1 represent two alternative decisions.

Two agents identified by the couples (x, w) and (x_*, w_*) modify their opinions after interaction according to the following rules

$$\begin{cases} w' = w - \alpha_S S(x)(w - w_d) - \alpha_P P(x, x_*; w, w_*)(w - w_*) + \eta D(x, w) \\ w'_* = w_* - \alpha_S S(x_*)(w_* - w_d) - \alpha_P P(x_*, x; w_*, w)(w_* - w) + \eta_* D(x_*, w_*), \end{cases} \tag{2.7}$$

where $w, w_* \in I$ denote the pre-interaction opinions and w', w'_* the opinions after the exchange of information between the two agents. The positive function $S(\cdot)$ drives the agent toward the correct choice $w_d \in \{-1, 1\}$ with a rate dependent on its competence level, representing an individual decision making strength. For example, a possible choice for the function $S(\cdot)$ is $S(x) = \text{const.} > 0$ if $x > \bar{x}$ and $S(x) = 0$ elsewhere. In this case the agent needs to achieve a competence threshold $\bar{x}$ in order to perceive the correct choice. Observe that in (2.7) we introduced an interaction function $P(\cdot, \cdot; \cdot, \cdot)$ depending both on the competence and on the opinion of the pair of agents. The nonnegative parameters α_S, α_P characterize the drift toward the target opinion $w_d \in I$ and the interaction rate, respectively. The random variables η, η_* are centered and with the same distribution Θ with finite variance σ^2. The function $D(\cdot, \cdot) \geq 0$ represents the local relevance of the diffusion for a given opinion and competence, whereas the evolutions of the competences x, x_* are given by (2.2).

In absence of diffusion $\eta, \eta_* = 0$ and for a constant drift $S(\cdot) = S \leq 1$ we have

$$|w' - w'_*| \leq |1 - \alpha_S S - \alpha_P (P(x, x_*; w, w_*) + P(x_*, x; w_*, w))||w - w_*|.$$

Then the post-exchange decisions are still in the reference interval $[-1, 1]$ if we assume $0 \leq P(\cdot, \cdot; \cdot, \cdot) \leq 1$ and $\alpha_S + 2\alpha_P \leq 2$. We can prove the following result which identifies the condition on the noise term in order to ensure that the post-interaction opinions do not leave the reference interval.

Proposition 6.2.1. *We assume* $0 < P(x, x_*; w, w_*) \leq 1$, $S(\cdot) = S \leq 1$ *and*

$$|\eta| < (1 - \alpha_P + \alpha_S)d, \qquad |\eta_*| < (1 - \alpha_P + \alpha_S)d, \qquad \alpha_P \leq 1,$$

where

$$d = \min_{(x,w) \in X \times I} \left\{ \frac{(1 - w)}{D(x, w)}, D(x, w) \neq 0 \right\}.$$

Then the binary interaction rule (2.7) *preserves the bounds being* $w', w'_* \in [-1, 1]$.

Proof. The proof is analogous to those in [82, 6, 11], therefore we omit the details. □

The introduction of a drift term follows from the set-up of the two-alternative forced choice tasks (TAFC) addressed in [30, 152]. The (TAFC) task is a classic behavioral experiment: at each trial agents are called to recognize a noisy visual stimulus choosing between two alternatives. The individual decision-making involves in its mathematical description a drift term representing the fact that an increasing experience/competence drives the agent towards the correct decision.

The compromise function $0 \leq P(\cdot,\cdot;\cdot,\cdot) \leq 1$ depends on both the particles' opinion and competence. As an example, a possible structure for the interaction function is given by the following

$$P(w, w_*; x, x_*) = Q(w, w_*)R(x, x_*), \tag{2.8}$$

where $0 \leq Q(\cdot,\cdot) \leq 1$ represents the positive compromise propensity and $0 \leq R(\cdot,\cdot) \leq 1$ is a function taking into account the competence of two interacting agents.

Empirical experiments have been done in order to measure the impact of competence on collective decision-making tasks [124, 131, 18]. In general, the participants are organized in dyads which are called to make a decision about a visual stimulus. Among others two opposite models taking into account the influence of the competence, or *sensitivity* in the psychology literature, might be considered. The first proposes that nothing except the opinions is communicated between individuals, in case of disagreement we randomly select an opinion which coincides with the decision of the studied dyad. We will refer to this model as coin-flip model (CF). The second model takes strongly into account the competence of individuals: the decisions are communicated and in case of disagreement the opinion of the most competent prevails and then coincides with the decision of the dyad. This second model is called maximum competence model (MC).

The aforementioned models can be described in our mathematical setting by considering a compromise propensity $Q(w, w_*) = 1$. Therefore the CF model may be described by considering a Bernoulli process $\mathcal{B}(p)$, with typical parameter $p = 1/2$. In other words, in the CF case, the competence does not play any role in the decision process. We will consider an averaged version of this model (aCF), which corresponds to $R_{aCF}(\cdot,\cdot) = 1/2$. The MC model, in our setting, is obtained by the Heaviside-type function

$$R_{MC}(x, x_*) = \begin{cases} 1 & x < x_* \\ 1/2 & x = x_* \\ 0 & x > x_*. \end{cases} \tag{2.9}$$

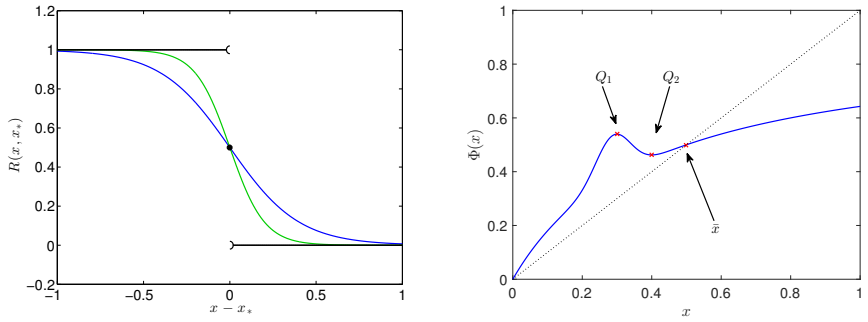

Figure 2.1: Left: Heaviside-type competence-based interaction function $R_{MC}(x, x_*)$ and two examples of its continuous version defined in (2.10) obtained with $c = 5$ and $c = 10$. Right: equality bias function $\Phi(x)$ of (2.13), the choice of coefficients a_1, a_2, a_3, a_4 has been done such that $x_{Q_1} = 0.3, x_{Q_2} = 0.4$ and $\bar{x} = 0.5$.

In terms of the competence gap $x - x_*$ we can approximate the discontinuous function (2.9) of the MC model with a smoothed continuous version (cMC)

$$R_{cMC}(x, x_*) = \frac{1}{1 + e^{c(x - x_*)}}, \tag{2.10}$$

with $c \gg 1$. We depict in Figure 2.1, left plot, the behavior of the function $R(\cdot, \cdot)$ for different choices of the constant $c > 0$. We can observe how in the half-plane $x > x_*$ the most competent agent is scarcely influenced by the less skilled one, while in the half-plane $x < x_*$ the situation is inverted and we see how an agent with less competence is influenced by the more competent one.

6.2.3 Dynamics of decisions under equality bias

On the basis of the decision process built in section 6.2.2, we modify the microscopic model (2.7)–(2.8) in order to mathematically describe the phenomenon called *equality bias* in collective decision–making communities. Our set-up is inspired by some recent works of the experimental psychology literature [131, 18] and the references therein. Their findings are consistent with the well-known cognitive bias called Dunning-Kruger effect regarding a misjudgment of personal competence of unskilled people, which overestimate their own ability. At the same time the most skilled individuals tends to underestimate their competence, implicitly believing that their knowledge is accessible to everyone [124].

Let us consider an agents with competence $x \in X$. We introduce the equality bias function

$$\begin{aligned} \Phi : X &\mapsto X \\ x &\to \Phi(x) \end{aligned} \tag{2.11}$$

which measures the agent's perceived level of competence. The choice of the equality bias function $\Phi(\cdot)$ is related to the subjective self-confidence in making decisions and experimental results show it is strictly dependent on the degree of competence of the interacting agents.

Following the mathematical setting introduced in Section 6.2.2 we modify the function $P(\cdot,\cdot;\cdot,\cdot)$ as

$$P(\Phi(x),\Phi(x_*);w,w_*). \tag{2.12}$$

In particular in the case (2.8) the competence based interaction function modifies in $R(\Phi(x),\Phi(x_*))$ whose shape depends now on the perceived competence. Therefore the equality bias emerges as a result of the binary interactions of a multi-agent system with lack of metacognition. In agreement with the experimental measurements of [124], and in order to exemplify the action of the equality bias function, we depict in Figure 2.1 the function

$$\Phi(x) = x\left(\frac{a_1}{x+a_2} + a_3\exp\left\{-h(x-a_4)^2\right\}\right), \tag{2.13}$$

with coefficients $a_1, a_2, a_3, a_4 > 0$. In the presented equality bias function we fixed the value $x_d \in X$, that measures the average competence of a population: the agents with competence $x > x_d$ may be identified with the most competent part of the system. Moreover, as experimentally suggested, it exists a local maximum Q_1 in $x = x_{Q_1}$ for the overestimation of the competence of unskilled agents, together with the local minimum Q_2 in $x = x_{Q_2}$. The asymptotic perceived competence depends on a_1, whose speed is weighted by a_2. Therefore we choose the coefficients a_2, a_3, a_4 in such a way that $\Phi(x_d) = x_d$ and for $x = x_{Q_1}, x = x_{Q_2}$ we find a local maximum and minimum respectively. The coefficient $h > 0$ is a scaling parameter. In the rest of the paper we will refer to the dynamics of decisions under the action of the equality bias with (EB).

6.3 A Boltzmann model for opinion and competence

In this section we derive a kinetic model for opinion and competence reflecting the behavior introduced in the binary interaction model for opinion and competence in (2.2)–(2.7).

Let $f = f(x,w,t)$ be the density of individuals with competence $x \in X \subset \mathbb{R}^+$ and opinion $w \in I = [-1,1]$ at time $t \geq 0$. We derive the kinetic description for the evolution of the density function $f = f(x,w,t)$ through classic methods of kinetic theory [145]. Let $g(x,t)$ be the marginal density of the competence variable $x \in X$

$$g(x,t) = \int_I f(x,w,t)dw, \tag{3.1}$$

and $\int_X g(x,t) = 1$ for each $t \geq 0$.

The evolution in time of the introduced density function is then given by the integro-differential equation of the Boltzmann-type

$$\frac{\partial}{\partial t} f(x,w,t) = Q(f,f)(x,w,t), \tag{3.2}$$

where $f(x,v,0) = f_0(x,w)$ and $Q(\cdot,\cdot)$ is defined as follows

$$Q(f,f)(x,w,t) = \int_{\mathbb{R}^+}\int_{\mathcal{B}^2}\int_{X\times I} C(z)\Big({}'B\frac{1}{J}f({}'x,{}'w,t)f({}'x_*,{}'w_*,t) - Bf(x,w,t)f(x_*,w_*,t)\Big)dw_*dx_*d\eta d\eta_* dz, \tag{3.3}$$

indicating with $({}'w,{}'w_*)$ the pre-interaction opinions given by (w,w_*) after the interaction and $({}'x,{}'x_*)$ the pre-interaction competences. The term $J = J(x,w;x_*,w_*)$ denotes as usual the Jacobian of the transformations $(w,w_*) \to (w',w'_*)$, $(x,x_*) \to (x',x'_*)$ via (2.2) and (2.7). The kernels ${}'B, B$ characterize the binary interaction and in the following will be considered of the form

$$B^{(x,x_*)\to(x',x'_*)}_{(w,w_*)\to(w',w'_*)} = \beta\Theta(\eta)\Theta(\eta_*)\chi(|w'|\leq 1)\chi(|w'_*|\leq 1)\chi(x'\in X)\chi(x'_*\in X), \tag{3.4}$$

where $\beta > 0$ is a scaling constant.

The presence of the Jacobian in the definition of the binary operator (1.3) may be avoided by considering its weak formulation. Let us consider a test function $\psi(x,w)$, we get

$$\begin{aligned}
&\int_{X\times I} Q(f,f)(x,w,t)\psi(x,w)dwdx \\
&\quad = \beta\Big\langle \int_{\mathbb{R}^+}\int_{X^2\times I^2} (\psi(x',w') - \psi(x,w)) \\
&\qquad f(x,w,t)f(x_*,w_*,t)C(z)dwdw_*dxdx_*dz\Big\rangle \\
&\quad = \frac{\beta}{2}\Big\langle \int_{\mathbb{R}^+}\int_{X^2\times I^2} (\psi(x',w') + \psi(x'_*,w'_*) - \psi(x,w) - \psi(x_*,w_*)) \\
&\qquad f(x,w,t)f(x_*,w_*,t)C(z)dwdw_*dxdx_*dz\Big\rangle,
\end{aligned} \tag{3.5}$$

where the brackets $<\cdot>$ denotes the expectation with respect to the random variables η, η_*. The weak formulation of the initial value problem (3.2) for

the initial density $f_0(x,w)$ is given for each $t \geq 0$ by

$$\begin{aligned}\frac{\partial}{\partial t}\int_{X\times I}\psi(x,w)f(x,w,t)dwdx \\ = \frac{\beta}{2}\Big\langle \int_{\mathbb{R}^+}\int_{X^2\times I^2}(\psi(x',w')+\psi(x'_*,w'_*)-\psi(x,w)-\psi(x_*,w_*)) \\ f(x,w,t)f(x_*,w_*,t)C(z)dwdw_*dxdx_*dz\Big\rangle.\end{aligned} \tag{3.6}$$

From the weak formulation in (3.6) we can derive the evolution of the macroscopic quantities like the moments for the opinion which may be obtained choosing as a test function $\psi(x,w) = \psi(w) = 1, w, w^2$.

6.3.1 Collective decision and variance

It is straightforward to observe that setting $\psi = 1$ we obtain the conservation of the total number of agents. The mean opinion of the overall agents is defined as

$$U(t) = \int_{X\times I} wf(x,w,t)dwdx, \tag{3.7}$$

which represents the *collective decision* of the system at time t, see [47, 93, 95]. The evolution of the collective decision is derived as marginal quantity from equation (3.6) for $\psi(x,w) = w$

$$\begin{aligned}\frac{\partial}{\partial t}\int_{X\times I} wf(x,w,t)dwdx = \alpha_S\beta\int_{X\times I}S(x)(w_d-w)f(x,w,t)dwdx \\ + \frac{\alpha_P\beta}{2}\int_{X^2\times I^2}(P(x,x_*;w,w_*)-P(x_*,x;w_*,w))(w-w_*) \\ f(x,w,t)f(x_*,w_*,t)dwdw_*dxdx_*.\end{aligned} \tag{3.8}$$

If the interaction function $P(\cdot,\cdot;\cdot,\cdot)$ is a symmetric function and $S(x) = s \in [0,1]$, equation (3.8) reduces to

$$\frac{d}{dt}U(t) = \alpha_S\beta s\,(w_d - U(t))\,, \tag{3.9}$$

whose solution at each $t \geq 0$ is $U(t) = w_d + (U_0 - w_d)\exp\{-\alpha_S\beta st\}$, with $U_0 = U(0)$ the initial collective decision. Therefore, in the limit $t \to +\infty$, the asymptotic collective decision converges exponentially toward $w_d \in \{-1,1\}$, i.e. $U_\infty = w_d$.

In the case of the aCF model $P \equiv 1/2$ and $S(\cdot) \equiv 0$, the mean opinion of the overall system is then conserved, which implies $U(t) = U_0$ for all $t \geq 0$. Further if we consider a MC model, with interactions between agents based

only on the competence variable and for $S \equiv 0$, from (3.8) we have

$$\begin{aligned}
&\frac{d}{dt}\int_{X\times I} wf(x,w,t)dxdw = \\
&\alpha_P\beta\int_{X^2\times I^2} R_{MC}(x,x_*)(w_*-w)f(x,w,t)f(x_*,w_*,t)dwdw_*dxdx_* \\
&-\frac{\alpha_P\beta}{2}\int_{X^2\times I^2}(w_*-w)f(x,w,t)f(x_*,w_*,t)dwdw_*dxdx_*,
\end{aligned} \tag{3.10}$$

being $R_{MC}(x,x_*) - R_{MC}(x_*,x) = 2R_{MC}(x,x_*) - 1$ with $R_{MC} \equiv 0$ in the half space $x > x_*$, which leads to

$$\begin{aligned}
\frac{d}{dt}\int_X u(x,t)dx =&\alpha_P\beta\int_X\left[\frac{U^+(x,t)-U^-(x,t)}{2}\right]\rho(x,t)dx \\
&+\alpha_P\beta\int_X\left[\frac{\rho^-(x,t)-\rho^+(x,t)}{2}\right]u(x,t)dx
\end{aligned} \tag{3.11}$$

where $u(x,t) = \int_I wf(x,w,t)dw$ is the mean opinion relative to the competence level $x \in X$ and

$$\begin{aligned}
U^+(x,t) &= \int_{x<x_*}\int_I w_*f(x_*,w_*,t)dw_*dx_*; \\
\rho^+(x,t) &= \int_{x<x_*}\int_I f(x_*,w_*,t)dw_*dx_*.
\end{aligned} \tag{3.12}$$

In particular $U^+(x,t)$ and $\rho^+(x,t)$ indicate the average opinion and the density of agents with competence greater than $x \in X$ respectively. We define also $U^-(x,t) = U(t) - U^+(x,t)$ and $\rho^-(x,t) = 1 - \rho^+(x,t)$ for each $x \in X$ and $t \geq 0$. Therefore, the variations of the mean opinion of agents with fixed competence $u(x,t)$ follow the choice of the most competent agents.

The second order moment for the opinion of the overall system is defined as

$$E(t) = \int_{X\times I} w^2 f(x,w,t)dwdx \tag{3.13}$$

and its evolution may be obtained from (3.6) with $\psi(x,w) = w^2$

$$\begin{aligned}
\frac{d}{dt}E(t) &= \alpha_S^2\beta \int_{X\times I} S^2(x)(w-w_d)^2 f(x,w,t)dwdx \\
&+ \frac{\alpha_P^2\beta}{2}\int_{X^2\times I^2}[P^2(x,x_*;w,w_*) + P^2(x_*,x;w_*,w)](w-w_*)^2 \\
&\qquad f(x,w,t)f(x_*,w_*,t)dwdw_*dxdx_* \\
&- \alpha_P\beta\int_{X^2\times I^2}(w-w_*)[wP(x,x_*;w,w_*) - w_*P(x_*,x;w_*,w)] \\
&\qquad f(x,w,t)f(x_*,w_*,t)dwdw_*dxdx_* \\
&- 2\alpha_S\beta\int_{X\times I} S(x)w(w-w_d)f(x,w,,t)dwdx \\
&+ \alpha_S\alpha_P\beta\int_{X^2\times I^2}(w-w_*)[S(x)P(x,x_*;w,w_*)(w-w_d) - S(x_*) \\
&\qquad P(x_*,x;w_*,w)(w_*-w_d)]f(x,w,t)f(x_*,w_*,t)dwdw_*dxdx_* \\
&+ \alpha_P\beta\sigma^2\int_{X\times I} D^2(x,w)f(x,w,t)dwdx.
\end{aligned} \tag{3.14}$$

In the simplified situation $P(x,x_*;w,w_*) = p \in [0,1]$, $S(x) = s \in [0,1]$, $\alpha_S = \alpha_P = \alpha$ and in absence of diffusion, the equation (3.14) assumes the following form

$$\begin{aligned}
\frac{d}{dt}E(t) &= \alpha^2\beta s^2\int_{X\times I}(w-w_d)^2 f(x,w,t)dwdx \\
&- 2\alpha\beta s\int_{X\times I}(w^2 - ww_d)f(x,w,t)dwdx \\
&+ \alpha\beta p(\alpha p - 1 + \alpha s)\int_{X^2\times I^2}(w-w_*)^2 f(x,w,t)f(x_*,w_*,t)dw_*dx_*dwdx.
\end{aligned} \tag{3.15}$$

Since under the same conditions $U(t)$ is solution of equation (3.9) and therefore converges for large time toward the correct choice w_d, we obtain that $E(t)$ converges exponentially to w_d^2 if

$$\alpha \le \min\Big\{1, \frac{2(s+p)}{(s+p)^2+p^2}\Big\}, \tag{3.16}$$

that is

$$\int_{X\times I}(w-w_d)^2 f(x,w,t)dwdx = E(t) - w_d^2, \tag{3.17}$$

under the above assumptions, converges toward zero in the limit $t \to +\infty$. We showed that the steady state solution of the interacting system is the Dirac delta $\delta(w-w_d)$ centered in the decision $w_d \in \{-1,1\}$.

6.4 Fokker-Planck approximation

In order to obtain analytic results on the large-time behavior from Boltzmann-type models, a classical mathematical tool is given by the derivation of approximated Fokker-Planck models through scaling techniques [6, 11, 14, 39, 91, 145, 146]. In what follows we apply this approach, also known as quasi-invariant limit [145, 164], to the model derived in the latter section.

We introduce a scaling parameter $\epsilon > 0$ and the following scaled quantities

$$\lambda \to \epsilon\lambda, \qquad \lambda_B \to \epsilon\lambda_B, \qquad \lambda_C \to \epsilon\lambda_C, \qquad \sigma_\kappa \to \sqrt{\epsilon}\sigma_\kappa, \tag{4.1}$$

where we assumed $\lambda_B(x) = \lambda_B > 0, \lambda_C(x) = \lambda_C > 0$ and $\lambda(x) = \lambda > 0$. This corresponds to the situation where each interaction produces a small variation of the competence. The same strategy may be applied to the binary opinion model taking the interaction frequency $\beta = 1/\varepsilon$ and rescaling the interaction propensity α and the diffusion variance σ^2 as follows

$$\alpha_S \to \epsilon\alpha_S, \qquad \alpha_P \to \epsilon\alpha_P, \qquad \sigma \to \sqrt{\epsilon}\sigma. \tag{4.2}$$

The scaled equation (3.6) reads

$$\begin{aligned} \frac{\partial}{\partial t}\int_{X\times I}\psi(x,w)f(x,w,t)dwdx = \\ \frac{1}{\epsilon}\Big\langle \int_{\mathbb{R}^+}\int_{X^2\times I^2}(\psi(x',w')-\psi(x,w)) \\ f(x,w,t)f(x_*,w_*,t)C(z)dwdw_*dxdx_*dz\Big\rangle. \end{aligned} \tag{4.3}$$

Under the assumptions on the random variables involved in the binary exchanges κ, η, η_* we define the following mean quantities

$$\begin{aligned} < x'-x > &= -\lambda x + \lambda_C x_* + \lambda_B z =: G(x,x_*,z), \\ < w'-w > &= -\alpha_S S(x)(w-w_d) - \alpha_P P(x,x_*;w,w_*)(w-w_*) \\ &=: H_S(x,w) + H_P(x,x_*;w,w_*), \\ < (x'-x)^2 > &= G^2(x,x_*,z) + \sigma_\kappa^2 x^2, \\ < (w'-w)^2 > &= (H_S(x,w) + H_P(x,x_*;w,w_*))^2 + \sigma^2 D^2(x,w), \\ < (x'-x)(w'-w) > &= G(x,x_*,z)\left(H_S(x,w) + H_P(x,x_*;w,w_*)\right). \end{aligned}$$

Then, we have

$$
\begin{aligned}
&< \psi(x', w') - \psi(x, w) >= \\
&G(x, x_*, z)\frac{\partial \psi}{\partial x}(x, w) + (H_S(x, w) + H_P(x, x_*; w, w_*))\frac{\partial \psi}{\partial w}(x, w) \\
&+ \frac{1}{2}\Bigg[(G^2(x, x_*, z) + \sigma_\kappa^2 x^2)\frac{\partial^2 \psi}{\partial x^2}(x, w) + ((H_S(x, w) + H_P(x, x_*; w, w_*))^2 \\
&+ \sigma^2 D^2(x, w)\frac{\partial^2 \psi}{\partial w^2}(x, w)) + G(x, x_*, z)(H_S(x, w) + H_P(x, x_*; w, w_*))\frac{\partial^2 \psi}{\partial x \partial w}(x, w)\Bigg] \\
&+ r(x, x_*; w, w_*),
\end{aligned}
\tag{4.4}
$$

where $r(x, x_*; w, w_*)$ denotes the higher order terms of the Taylor expansion. From the quasi-invariant scalings introduced in (4.1)-(4.2) by rescaling

$$
\begin{aligned}
&G(x, x_*, z) \to \epsilon G(x, x_*, z), \\
&H_S(x, w) \to \epsilon H_S(x, w), \\
&H_P(x, x_*; w, w_*) \to \epsilon H_P(x, x_*; w, w_*),
\end{aligned}
\tag{4.5}
$$

equation (4.3) takes the form

$$
\begin{aligned}
&\frac{\partial}{\partial t}\int_{X\times I} \psi(x, w) f(x, w, t) dw dx = \int_{\mathbb{R}^+}\int_{X^2\times I^2} \Bigg[G(x, x_*, z)\frac{\partial \psi}{\partial x}(x, w) \\
&+ H_S(x, w)\frac{\partial \psi}{\partial w}(x, w) + H_P(x, x_*; w, w_*)\frac{\partial \psi}{\partial w}(x, w) + \frac{\sigma_\kappa^2}{2}x^2\frac{\partial \psi}{\partial x^2}(x, w) \\
&+ \frac{\sigma^2}{2}D^2(x, w)\frac{\partial^2 \psi}{\partial w^2}(x, w)\Bigg] f(x, w, t) f(x_*, w_*, t) C(z) dw dw_* dx dx_* dz \\
&+ r(\epsilon) + O(\epsilon),
\end{aligned}
\tag{4.6}
$$

with

$$
\begin{aligned}
r(\epsilon) = \frac{1}{2\epsilon}\int_{\mathbb{R}^+}\int_{X^2\times I^2} \Bigg[&\epsilon^2\Big(G^2(x, x_*, z)\frac{\partial^2 \psi}{\partial x^2}(x, w) \\
&+ (H_S(x, w) + H_P(x, x_*; w, w_*))^2\frac{\partial^2 \psi}{\partial w^2}(x, w) \\
&+ G(x, x_*, z)(H_S(x, w) + H_P(x, x_*; w, w_*))\frac{\partial^2 \psi}{\partial x \partial w}(x, w)\Big) \\
&+ R(x, x_*; w, w_*)\Bigg] f(x, w, t) f(x_*, w_*, t) C(z) dw dw_* dx dx_* dz.
\end{aligned}
\tag{4.7}
$$

By similar arguments to [146, 164] it can be shown that the term $r(\epsilon)$ defined

in (4.7) decays to zero in the limit $\epsilon \to 0$. Finally for $\epsilon \to 0$ we obtain

$$\begin{aligned}\frac{\partial}{\partial t}\int_{X\times I}\psi(x,w)f(x,w,t)dwdx = \int_{\mathbb{R}^+}\int_{X^2\times I^2}\Bigg[G(x,x_*,z)\frac{\partial\psi}{\partial x}(x,w)\\ + H_S(x,w)\frac{\partial\psi}{\partial w}(x,w) + H_P(x,x_*;w,w_*)\frac{\partial\psi}{\partial w}(x,w)\Bigg]\\ f(x,w,t)f(x_*,w_*,t)C(z)dwdw_*dxdx_*dz\\ + \frac{\sigma_\kappa^2}{2}\int_{X^2\times I^2}x^2\frac{\partial\psi}{\partial x^2}(x,w)f(x,w,t)dwdx\\ + \frac{\sigma^2}{2}\int_{X^2\times I^2}D^2(x,w)\frac{\partial^2\psi}{\partial w^2}(x,w)f(x,w,t)dwdx.\end{aligned} \tag{4.8}$$

Integrating back by parts equation (4.8) we have the following nonlinear Fokker-Planck equation

$$\begin{aligned}\frac{\partial}{\partial t}f(x,w,t) = \frac{\partial}{\partial x}\mathcal{G}[f](x,t)f(x,w,t)\\ + \frac{\partial}{\partial w}\mathcal{H}[f]f(x,w,t) + \frac{\partial}{\partial w}\mathcal{K}[f]f(x,w,t)\\ + \frac{\sigma_\kappa^2}{2}\frac{\partial^2}{\partial x^2}(x^2f(x,w,t)) + \frac{\sigma^2}{2}\frac{\partial^2}{\partial w^2}(D^2(x,w)f(x,w,t)),\end{aligned} \tag{4.9}$$

where

$$\begin{aligned}\mathcal{G}[f](x,t) &= \int_{\mathbb{R}^+}\int_{X\times I}G(x,x_*,z)f(x_*,w_*,t)C(z)dw_*dx_*dz\\ &= \lambda x - \lambda_C m_x - \lambda_B m_B,\end{aligned} \tag{4.10}$$

being $m_x(t) = \int_{X\times I} xf(x,w,t)dwdx$, and where the functionals $\mathcal{H}[f], \mathcal{K}[f]$ are defined as follows

$$\begin{aligned}\mathcal{H}[f](x,w,t) &= \int_{X\times I}H_P(x,x_*;w,w_*)f(x_*,w_*,t)dw_*dx_*\\ \mathcal{K}[f](w_d) &= \int_{X\times I}H_S(x,w)f(x,w,t)dwdx.\end{aligned} \tag{4.11}$$

The Fokker-Planck equation (4.9) has been derived from (4.8) provided the boundary terms produced by integration vanish [145]. In particular, we

obtain the following conditions

$$\begin{aligned}
&\mathcal{G}[f](x,t) - \frac{\sigma_\kappa^2}{2}(x^2 f(x,w,t))\Big|_0^{+\infty} = 0,\\
&x^2 f(x,w,t)\Big|_0^{+\infty} = 0,\\
&(\mathcal{H}[f] + \mathcal{K}[f])f(x,w,t) - \frac{\sigma^2}{2}\frac{\partial}{\partial w}(D^2(x,w)f(x,w,t))\Big|_{-1}^{1} = 0,\\
&D^2(x,w)f(x,w,t)\Big|_{-1}^{1} = 0.
\end{aligned} \tag{4.12}$$

6.4.1 Stationary states for the marginal density

By direct integration of the Fokker-Planck equation (4.9) with respect to the variable w we obtain

$$\begin{aligned}
\frac{\partial}{\partial t}\int_I f(x,w,t)dw = &\\
&\frac{\partial}{\partial x}\int_I \mathcal{G}[f]f(x,t)f(x,w,t)dw + \mathcal{H}[f]f(x,w,t)\Big|_{-1}^{1}\\
&+ \mathcal{K}[f]f(x,w,t)\Big|_{-1}^{1} + \frac{\sigma_\kappa^2}{2}\frac{\partial^2}{\partial x^2}\Big(x^2\int_I f(x,w,t)dw\Big)\\
&+ \frac{\sigma^2}{2}\frac{\partial}{\partial w}D^2(x,w)f(x,w,t)\Big|_{-1}^{1}.
\end{aligned} \tag{4.13}$$

From the boundary conditions (4.12) equation (4.13) simplifies to

$$\frac{\partial}{\partial t}g(x,t) = \frac{\partial}{\partial x}(\lambda x - \lambda_C m_x - \lambda_B m_B)g(x,t) + \frac{\sigma_\kappa^2}{2}\frac{\partial^2}{\partial x^2}(x^2 g(x,t)), \tag{4.14}$$

being $g(x,t)$ the marginal density of the competence variable defined in (3.1). Furthermore, in Section 6.2.1 we showed that for large time $m_x \to \dfrac{\lambda_B m_B}{\lambda - \lambda_C}$ and it is therefore possible to give the analytic formulation of the stationary solution of (4.13). The solution of

$$\frac{\partial}{\partial x}\left(-\lambda x + \frac{\lambda\lambda_B}{\lambda - \lambda_C}m_B\right)g^\infty(x) = \frac{\sigma_\kappa^2}{2}\frac{\partial^2}{\partial x^2}(x^2 g^\infty(x)) \tag{4.15}$$

is given by

$$g^\infty(x) = \frac{c_{\lambda,\lambda_B,\lambda_C,\sigma_\kappa^2}}{x^{2+2\lambda/\sigma_\kappa^2}}\exp\Big\{-\frac{2}{\sigma_\kappa^2 x}\cdot\frac{\lambda\lambda_B m_B}{\lambda - \lambda_C})\Big\}, \tag{4.16}$$

where $c_{\lambda,\lambda_B,\lambda_C,\sigma_\kappa^2}$ is a constant chosen such that the total mass of g^∞ is equal to one.

Unlike the usual method for determining the stationary density developed in [39, 146], here the asymptotic competence has been derived from the complete Fokker-Planck equation (4.9) after the integration of the opinion variable, and under specific boundary conditions.

6.5 Numerics

In this section we propose several numerical tests for the Boltzmann-type model introduced in the previous paragraphs which show the emergence of suboptimal collective decisions under the hypothesis of equality bias compared to aCF and cMC models. All the results presented have been obtained through direct simulation Monte Carlo methods for the Boltzmann equation (see [145, 144]).

The Fokker-Planck regime is obtained via the quasi-invariant scaling (4.1)–(4.2) with $\epsilon = 0.01$. The local diffusion function has been considered in the case

$$D(x, w) = 1 - w^2 \tag{5.1}$$

which multiplies in the binary collision model (2.7) for the opinion, a uniform random variable with scaled variance σ^2. The choice (5.1) implies that the diffusion does not act on the agents with more extremal opinions. In the competence dynamics we considered $\lambda(x) = \lambda$, $\lambda_C(x) = \lambda_C$ and $\lambda_B(x) = \lambda_B$ and a uniform random variable κ with finite scaled variance σ_κ^2. The variable z is a uniform random variable in the interval $[0, 1]$.

6.5.1 Test 1: collective decision under equality bias

In this test we compute the collective decisions emerging from the Boltzmann-type model (3.2) with interaction function (2.8) and $Q(w, w_*) = 1$ and $R(x, x_*)$ defined in the reference cases aCF-cMC and EB. The binary interaction terms defined in (2.2)–(2.7) have been considered for a choice of constants coherent with the bounds described in Section 6.2. In this test we considered a vanishing drift term $S(x) = 0$, for each $x \in X$.

We compare the emerging collective decisions in the aCF and cMC cases considering the action of the equality bias function described in equation (2.13). In this test we take into account the compromise behavior of two strongly polarized populations with equal sizes (case A) and with different sizes (case B). In both cases the group of competent agents is characterized at $t = 0$ by opinions in the interval $w \in [-1, -0.75]$, whereas the second population, composed by the less competent agents, expresses opinions $w \in [0.75, 1]$. In the case of populations with different size we considered an initial distribution such that the number of competent agents is five time larger then the number of the incompetent ones. In Figure 5.2 we exemplified the initial configurations for the two tests: Test 1A and Test 1B. We chose the

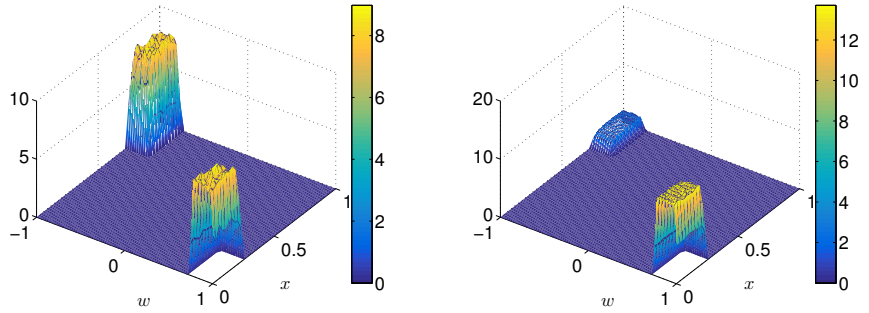

Figure 5.2: Left: **Test 1A**, initial configuration of the multi-agent system with an equal size of competent and incompetent agents. Right: **Test 1B**, initial configuration of the multi-agent system with a different size of competent and incompetent agents, in particular the number of competent agents is five times smaller than the size of the incompetent agents.

parameters $\lambda_C = \lambda_B = 10^{-2}, \lambda = \lambda_C + \lambda_B$ and $\sigma_\kappa^2 = 10^{-2}$ for the evolution of the competence variable.

In Figure 5.4 we show the kinetic and particle solutions of the Test 1A for a system of interacting agents in the aCF-cMC and EB1-EB2 models, where the case of equality bias has been considered for two examples of equality bias functions $\Phi_1(x)$ and $\Phi_2(x)$ of the type introduced in Section 6.2.3, see equation (2.13), and whose behaviors are reported in Figure 5.3. Further in Figure 5.3 we compare the stationary distribution for the competence variable emerging form the Monte Carlo method and its analytic formulation obtained in Section 6.4.1. In particular, in Figure 5.4 we can observe how the emerging collective decisions of the EB1 and EB2 cases are significantly shifted from the decision emerging in a model cMC.

In Figure 5.5 we show the stationary distributions of the opinion variable in the four models of interactions both the Test 1A (left) and Test 1B (right). We observe how the EB1-EB2 models in general defines a decision which is suboptimal with respect to the competence based model cMC. Further in presence of a strong overestimation of the opinions of the less skilled agents, like in the EB2 model, we see how the emerging decision may perform worse than an aCF model. In the case of the Test 1B we see how for asymmetric populations the emerging decision may be deviated toward the positions of the less competent agents, even in the cMC case. The same behavior is highlighted in Figure 5.6 where we find the evolution of the mean opinion of the multi-agent systems which leads to the formation of the collective decisions.

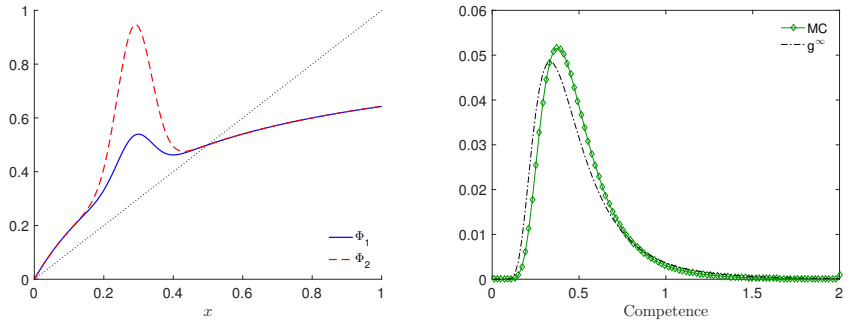

Figure 5.3: **Test 1**. Left: two examples of equality bias functions $\Phi(x)$ if the form introduced in (2.13) and passing through $\bar{x} = 0.5$ with $a_1 = 0.9$ and scaling parameter $h = 10^2$. In the rest of the paper we will refer to them as $\Phi_1(x)$ and $\Phi_2(x)$. Right: convergence of the Monte Carlo method toward the analytic steady state for $\epsilon = 0.01$.

6.5.2 Test 2: competence driven optimal decision

We consider here the action of the term driving the system to the correct decision introduced in the opinion dynamics (2.7). In the described dynamics we included a competence-dependent force with a rate given by $S(\cdot)$ representing an increasing evidence in supporting the a-priori right choice $w_d \in \{-1, 1\}$. In particular, let us consider

$$S(x) = \begin{cases} \min\{1, x\} & x \geq x_d \\ 0 & x \leq x_d \end{cases} \tag{5.2}$$

and $\lambda_C = \lambda_C \chi(x \geq x_d)$. In the proposed set-up we intended to mimic the fact that extremely low skilled people ($x \leq x_d$), in addition to make wrong choices, have not the ability to realize the inaccuracy of their decision, a phenomenon which follows from the Dunning-Kruger effect. In Figure 5.7 we report the evolution of the multi-agent system with the same initial configuration as in Test 1B. The forcing term is characterized by (5.2) with $x_d = 0.3$, which drives the opinions of sufficiently competent agents toward $w_d = -1$. Here the equality bias functions $\Phi_1(x)$ and $\Phi_2(x)$, represented in Figure 5.2, influence the speed of convergence of the opinions toward w_d. We compare in Figure 5.8 the convergences toward w_d for the models aCF-cMC and EB1-EB2. We consider the parameters $\lambda_C = \lambda_B = 10^{-2}, \lambda = \lambda_C + \lambda_B$ and $\sigma_\kappa^2 = 10^{-2}$ for the evolution of the competence variable.

6.5.3 Test 3: bounded confidence case

In the last test case we consider bounded confidence interactions [6, 14, 35]. Often we notice how more well-educated, more capable and more competent

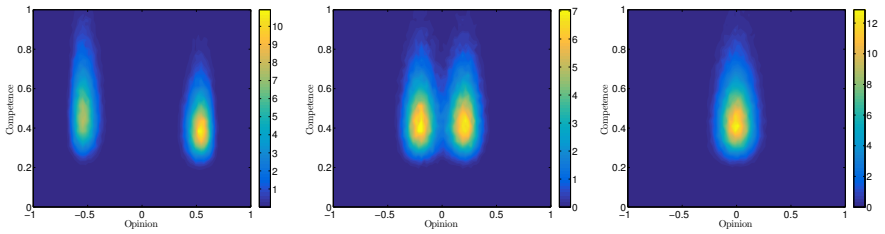

(a) aCF t=1 (b) aCF t=3 (c) aCF t=10

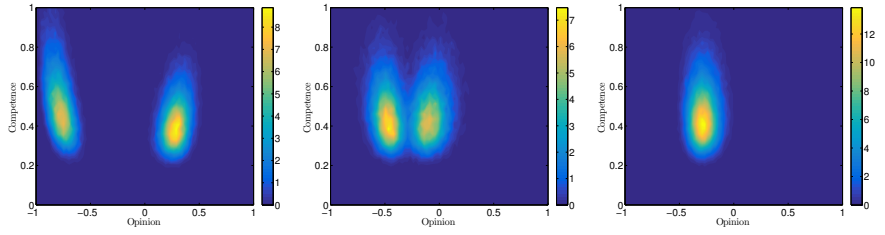

(d) cMC t=1 (e) cMC t=3 (f) cMC t=10

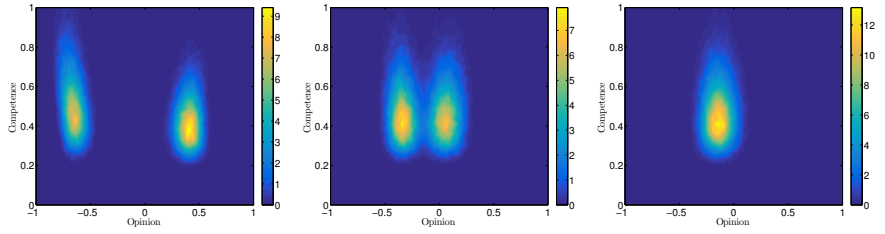

(g) EB1 t=1 (h) EB1 t=3 (i) EB1 t=10

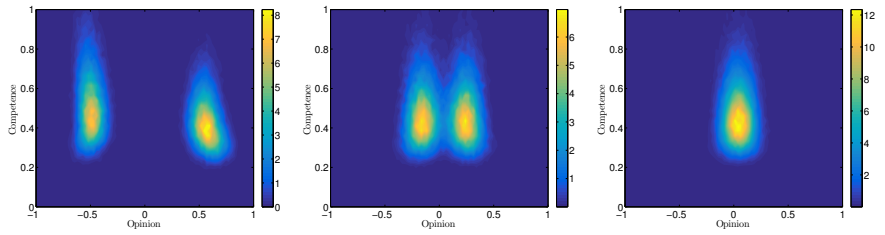

(j) EB2 t=1 (k) EB2 t=3 (l) EB2 t=10

Figure 5.4: **Test 1A**: kinetic solution at different time steps in the aCF-cMC and EB1-EB2 model cases, respectively form the first row. The choice of constants in this test is: $c = 10$, $\lambda_B = \lambda_C = 10^{-2}$, $\sigma_\kappa^2 = 10^{-2}$ and $\lambda = \lambda_B + \lambda_C$. The mean competence of the multi-agent system is $\bar{x} = 0.5$. We see how the equality bias, through the equality bias functions $\Phi_1(x)$ and $\Phi_2(x)$ presented in Figure 5.3, influences the opinion dynamics, driving the collective decision toward suboptimal states with respect to the cMC model.

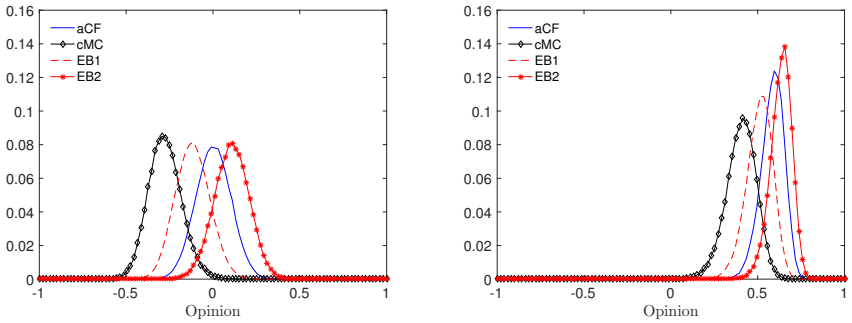

Figure 5.5: Asymptotic distributions of the opinion variable for the models aCF-cMC-EB1-EB2 Left: **Test 1A**, case of initial configuration with equal size of competent and incompetent agents. Right: **Test1B**, case of asymmetric populations as in Figure 5.2. The choice of constants is $c = 10$, $\lambda_B = \lambda_C = 10^{-2}$, $\sigma_\kappa^2 = 10^{-2}$ and $\lambda = \lambda_B + \lambda_C$, the equality bias functions are sketched in Figure 5.3.

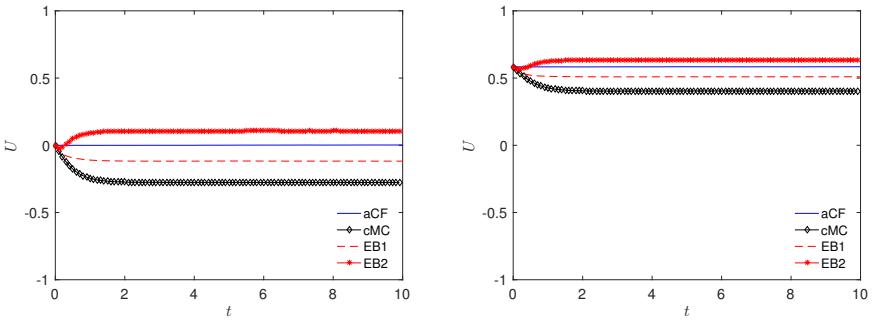

Figure 5.6: Collective decisions of the multi-agent system for the reference models aCF-cMC-EB1-EB2 with the choice of parameters $c = 10$, $\lambda_B = \lambda_C = 10^{-2}$, $\sigma_\kappa^2 = 10^{-2}$ and $\lambda = \lambda_B + \lambda_C$. Left: **Test 1A**. Right: **Test1B**.

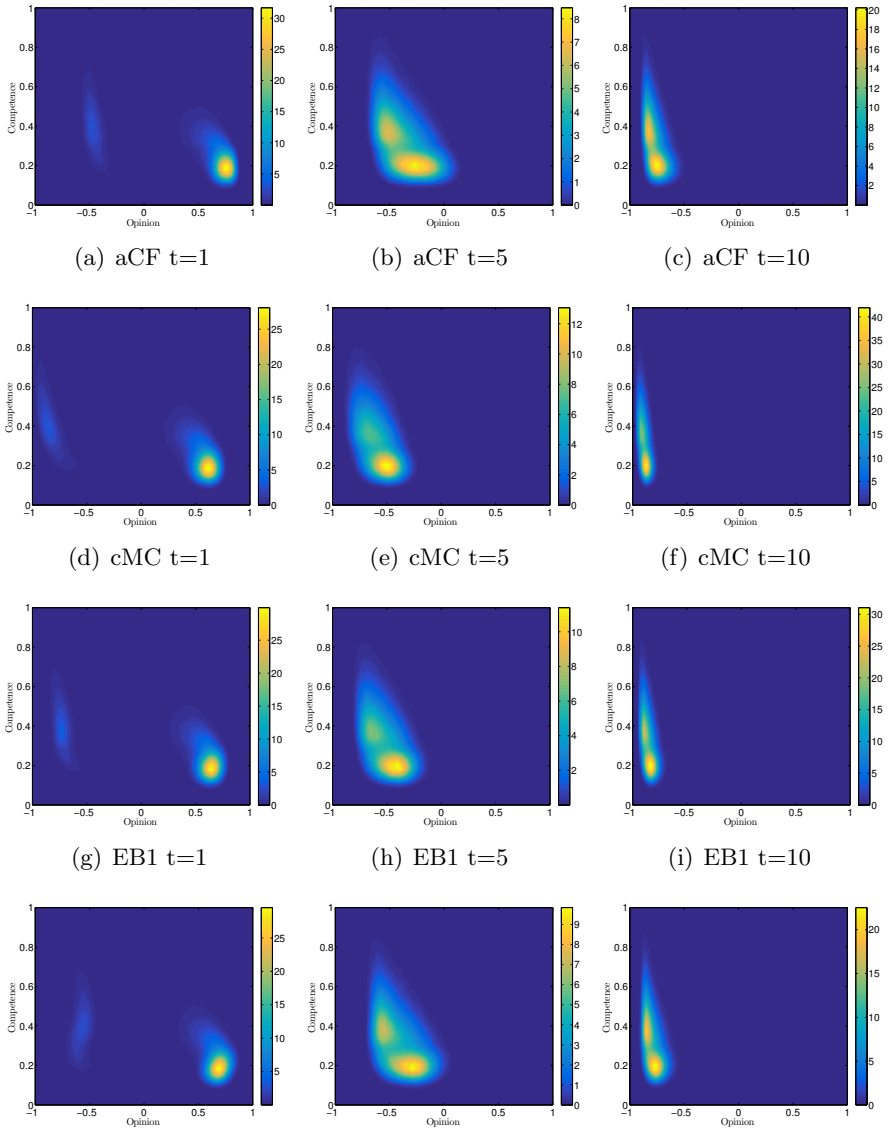

(a) aCF t=1 (b) aCF t=5 (c) aCF t=10

(d) cMC t=1 (e) cMC t=5 (f) cMC t=10

(g) EB1 t=1 (h) EB1 t=5 (i) EB1 t=10

(j) EB2 t=1 (k) EB2 t=5 (l) EB2 t=10

Figure 5.7: **Test 2**. Kinetic solution for the opinion dynamics with forcing term with rate (5.2) at different time steps. The evolution of the competence variable is given by $\lambda_B = 10^{-2}$, $\lambda_C(x) = \lambda_C \chi(x \geq x_d)$ where $\lambda_C = 10^{-2}$ and $x_d = 0.3$, $\lambda = \lambda_B + \lambda_C$, and $\sigma_\kappa^2 = 10^{-2}$. We present the behavior of the reference models aCF-cMC and EB1-EB2 under the action of the equality bias functions $\Phi_1(x), \Phi_2(x)$ for three time steps.

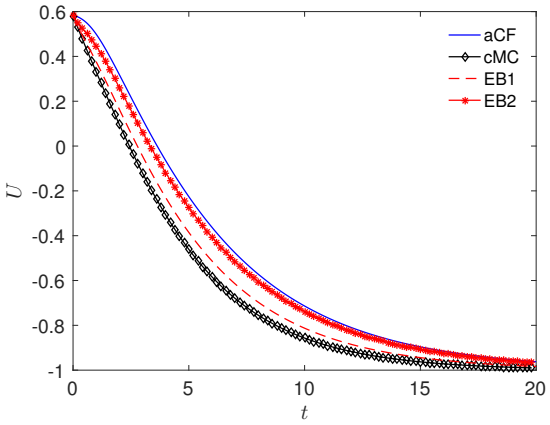

Figure 5.8: **Test 2**. Convergence of the mean decision in the reference models aCF-cMC and EB1-EB2 under the action of the forcing term with rate (5.2) and $x_d = 0.3$. The equality bias function $\Phi_1(x)$, which has been sketched in Figure 5.2, slows down the convergence speed of the collective decision toward $w_d = -1$.

people are also those best disposed to dialogue. Then competence is generally associated to the predisposition to listen other people. The higher this quality, greater is the ability to value other opinions. Vice versa, a person unwilling to listen and dialogue is usually marked by a lower level of the described trait. Therefore, it is natural to consider a bounded confidence model where the threshold on the exchanges of opinions depends on the degree of competence.

In particular, we consider a compromise function $P(x, x_*; w, w_*)$ with the following form

$$P(x, x_*; w, w_*) = \chi(|w - w_*| \leq \gamma\Delta(x, x_*)), \tag{5.3}$$

where $\Delta(x, x_*)$ is a competence-dependent function that ranges in the closed interval $[0, 1]$ taking into account the maximum distance under which the interactions are allowed, and $\gamma > 0$ is a constant value. A possible choice of for the function $\Delta(\cdot, \cdot)$ is

$$\Delta(x, x_*) = R_{cMC}(x, x_*), \tag{5.4}$$

where the function $R(\cdot)$ has been defined in (2.10). We observe how for the choice $\gamma = 2$ and $\Delta(x, x_*) = R_{MC}$ the bounded confidence interaction function reproduces the behavior of a maximum competence model.

In the biased case the bounded confidence model becomes

$$P(x, x_*; w, w_*) = \chi(|w - w_*| \leq \gamma\Delta(\Phi(x), \Phi(x_*))). \tag{5.5}$$

We perform the numerical test in the case of absence of driving force, i.e. $S(\cdot) = 0$. In Figure 5.9 we report the initial configuration of the multi-agent system for the test and the asymptotic density function of the opinion

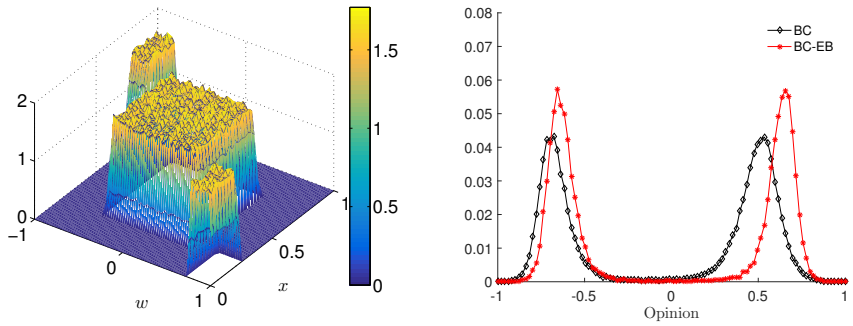

Figure 5.9: **Test 3**. Left: initial configuration of the multi-agent system, we considered the case with three population. Right: asymptotic marginal density for the opinion variable, we observe how the bounded confidence interaction function introduced in (5.3), $\gamma = 1/2$, splits the system in two populations for which the equality bias emerges separately as an action of the equality bias function $\Phi_2(x)$.

variable taking into account the bounded confidence interaction function (5.3) and its biased version (5.5). We chose the parameters $\lambda_C = \lambda_B = 10^{-3}$, $\lambda = \lambda_B + \lambda_C$ and $\sigma_\kappa = 10^{-4}$ for the evolution of the competence variable, the function $\Delta(x - x_*)$ is (5.4) with $c = 10^2$ and $\gamma = 1/2$.

In Figure 5.10 it is possible to observe how the evolution of opinion and competence deeply changes under the effect of an equality bias function. In particular we considered the equality bias function $\Phi_2(x), x \in X$ with the choice of parameter introduced in Figure 5.2. In Figure 5.9 (right plot) we report the asymptotic marginal density for the opinion variable. The system evolves towards two clusters, characterizing two subpopulations with different decisions driven by the most competent agents. Finally, it is possible to observe how the equality bias drives the system toward a suboptimal collective decision for both populations where the influence of less competent agents become more relevant.

6.6 Conclusion

We introduced kinetic models of multi-agent systems describing the decision-making process. The models are obtained in the limit of a large number of agents and weight the opinion of each agent through its competence. The binary interaction dynamics involve both the agents' opinion and competence, so that less competent agents can learn during interactions from the more competent ones. This lead to an optimal decision process where the results is a direct consequence of the agents' competence. The introduction of an equality bias in the model is obtained by considering a suitable function with a shape analogous to the one experimentally found in [124]. Numer-

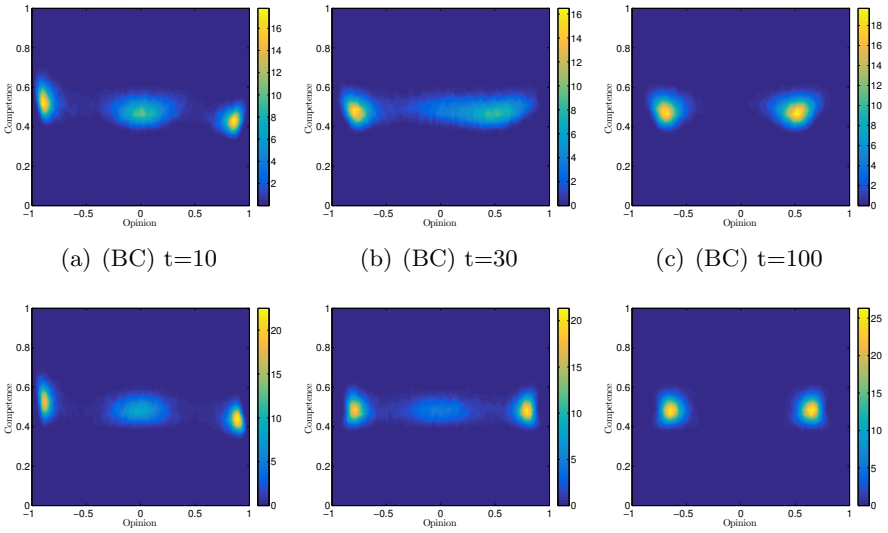

(a) (BC) t=10 (b) (BC) t=30 (c) (BC) t=100

(d) (BC-EB) t=10 (e) (BC-EB) t=30 (f) (BC-EB) t=100

Figure 5.10: **Test 3**. Evolution of the multi-agent-system in the bounded confidence case (BC), in the first row, and under the action of the equality bias function $\Phi_2(x)$ (BC-EB), in the second row. The evolution of the competence variable is given by $\lambda_C = \lambda_B = 10^{-3}$, $\lambda = \lambda_B + \lambda_C$ and $\sigma_\kappa = 10^{-4}$

ical results show that the presence of an equality bias leads the group to suboptimal decisions and in some cases to the emergence of the opinion of the less competent agents in the group. Finally, we point out that using the approach in [6, 117, 11] the present modeling may also address the influence of external forces (like the Press and the Media in general) affecting adversely the individual competence.

Part III

Uncertainty quantification

Chapter 7

Uncertainty quantification in control problems for flocking models

7.1 Introduction

The aggregate motion of a multi-agent system is frequently seen in the real world. Common examples are represented by schools of fish, swarms of bees and herds of sheep, each of them natural phenomena with important applications in many fields such as biology, engineering and economy [145]. As a consequence, the significance of new mathematical models, for understanding and predicting these complex dynamics, is widely recognized. Several heuristic rules of flocking have been introduced as alignment, separation and cohesion [154, 167]. Nowadays these mathematical problems, and their constrained versions, are deeply studied both from the microscopic viewpoint [4, 52, 138, 179] as well as their kinetic and mean-field approximations [6, 11, 71, 73, 76, 139]. We refer to [145] for a recent introduction on the subject.

In an applicative framework a fundamental step for the study of such models is represented by the introduction of stochastic parameters reflecting the uncertainty due to wide range of phenomena, such as the weathers influence during an experiment, temperature variations, or even human errors. Therefore quantifying the influence of uncertainties on the main dynamics is of paramount importance to build more realistic models and to give better predictions of their behavior. In the modeling of self-organized system, different ways to include random sources have been studied and analyzed, see for example [2, 108, 160, 167, 178]. In this paper we focus on the case where the uncertainty acts directly in the parameter characterizing the interaction dynamics between the agents.

We present a numerical approach having roots in the numerical techniques

for Uncertainty Quantification (UQ) and Model Predictive Control (MPC). Among the most popular methods for UQ, the generalized polynomial chaos (gPC) has recently received deepest attentions [176]. Jointly with Stochastic Galerkin (SG) this class of numerical methods are usually applied in physical and engineering problems, for which fast convergence is needed. Applications of gPC-Galerkin schemes to flocking dynamics, and their controlled versions, is almost unexplored in the actual state of art.

We give numerical evidence of threshold effects in the alignment dynamics due to the random parameters. In particular the presence of a negative tail in the distribution of the random inputs lead to the divergence of the expected values for the system velocities. The use of a selective model predictive control permits to steer the system towards the desired state even in such unstable regimes.

The rest of the chapter is organized as follows. In Section 8.2 we introduce briefly a Cucker-Smale dynamics with interaction function depending on stochastic parameters and analyze the system behavior in the case of uniform interactions. The gPC approach is then summarized in Section 7.3. Subsequently, in Section 7.4 we consider the gPC scheme in a constrained setting and derive a selective model predictive approximation of the system. Next, in Section 7.5 we report several numerical experiments which illustrate the different features of the numerical method. Extensions of the present approach are finally discussed in Section 7.6.

7.2 Cucker-Smale dynamics with random inputs

We introduce a Cucker-Smale type [71] differential system depending on a random variable $\theta \in \Omega \subseteq \mathbb{R}$ with a given distribution $f(\theta)$. Let $(x_i, v_i) \in \mathbb{R}^{2d}, d \geq 1$, evolving as follows

$$\begin{cases} \dot{x}_i(\theta, t) = v_i(\theta, t) \\ \dot{v}_i(\theta, t) = \dfrac{K(\theta, t)}{N} \displaystyle\sum_{j=1}^{N} H(x_i, x_j)(v_j(\theta, t) - v_i(\theta, t)) \end{cases} \tag{2.1}$$

where K is a time dependent random function characterizing the uncertainty in the interaction rates and $H(\cdot, \cdot)$ is a symmetric function describing the dependence of the alignment dynamics from the agents positions. In the following we will always suppose location–based interaction to be deterministic, in particular $H(x_i, x_j) := H(\int_\Omega x_i f(\theta) d\theta, \int_\Omega x_j f(\theta) d\theta)$. For simplicity of notation we will maintain $H(x_i, x_j)$. A classical choice of space dependent interaction function is related to the distance between two agents

$$H(x, y) = \frac{1}{(\zeta^2 + |x - y|^2)^\gamma}, \tag{2.2}$$

where $\gamma \geq 0$ and $\zeta > 0$ are given parameters. Mathematical results concerning the system behavior in the deterministic case ($K \equiv 1$) can be found in [71]. In particular unconditional alignment emerges for $\gamma < 1/2$. Let us observe that, even for the model with random inputs (2.1), the mean velocity of the system is conserved in time

$$\mathcal{V}(\theta, t) = \frac{1}{N} \sum_{i=1}^{N} v_i(\theta, t), \qquad \frac{d}{dt}\mathcal{V}(\theta, t) = 0, \tag{2.3}$$

since the symmetry of H implies

$$\sum_{i,j=1}^{N} H(x_i, x_j) v_j(\theta, t) = \sum_{i,j=1}^{N} H(x_i, x_j) v_i(\theta, t).$$

Therefore for each $t \geq 0$ we have $\mathcal{V}(\theta, t) = \mathcal{V}(\theta, 0)$.

7.2.1 The uniform interaction case

To better understand the leading dynamics let us consider the simpler uniform interaction case when $H \equiv 1$, leading to the following equation for the velocities

$$\dot{v}_i(\theta, t) = \frac{K(\theta, t)}{N} \sum_{j=1}^{N} (v_j(\theta, t) - v_i(\theta, t)) = K(\theta, t)(\mathcal{V}(\theta, 0) - v_i(\theta, t)). \tag{2.4}$$

The differential equation (2.4) admits an exact solution depending on the random input θ. More precisely if the initial velocities are deterministically known we have that

$$v_i(\theta, t) = \mathcal{V} + (v_i(0) - \mathcal{V}) \exp\left\{ - \int_0^t K(\theta, s) ds \right\}, \tag{2.5}$$

where $\mathcal{V} = \mathcal{V}(0)$ is the mean velocity of the system. In what follows we analyze the evolution of (2.5) for different choices of $K(\theta, t)$ and of the distribution of the random variable θ.

Example 1

Let us consider a random scattering rate written in terms of the following decomposition

$$K(\theta, t) = k(\theta) h(t) \tag{2.6}$$

where $h(t)$ is a nonnegative function depending on $t \in \mathbb{R}^+$. The expected velocity of the i-th agent is defined by

$$\bar{v}_i(t) = \mathbb{E}_\theta[v_i(\theta, t)] = \int_\Omega v_i(\theta, t) f(\theta) d\theta \tag{2.7}$$

then each agent evolves its expected velocity according to

$$\bar{v}_i(t) = \int_\Omega \left[\mathcal{V} + (v_i(0) - \mathcal{V}) \exp\left\{ -k(\theta) \int_0^t h(s)ds \right\} \right] f(\theta)d\theta. \tag{2.8}$$

For example, let us chose $k(\theta) = \theta$, where the random variable is normally distributed, i.e. $\theta \sim \mathcal{N}(\mu, \sigma^2)$. Then, for each $i = 1, \dots, N$, we need to evaluate the following integral

$$\mathcal{V} + \frac{v_i(0) - \mathcal{V}}{\sqrt{2\pi\sigma^2}} \int_{\mathbb{R}} \exp\left\{ -\theta \int_0^t h(s)ds \right\} \exp\left\{ -\frac{(\theta - \mu)^2}{2\sigma^2} \right\} d\theta. \tag{2.9}$$

The explicit form is easily found through standard techniques and yields

$$\bar{v}_i(t) = \mathcal{V} + (v_i(0) - \mathcal{V}) \exp\left\{ -\mu \int_0^t h(s)ds + \frac{\sigma^2}{2} \left(\int_0^t h(s)ds \right)^2 \right\}. \tag{2.10}$$

From (2.10) we observe a threshold effect in the asymptotic convergence of the mean velocity of each agent toward $\mathcal{V}$. It is immediately seen that if

$$\int_0^t h(s)ds > \frac{2\mu}{\sigma^2} \tag{2.11}$$

it follows that, for $t \to +\infty$, the expected velocity $\bar{v}_i$ diverges. In particular, if $h(s) \equiv 1$ we have that the solution starts to diverge as soon as $t > \mu/\sigma^2$. Note that, this threshold effect is essentially due to the negative tail of the normal distribution. In fact, if we now consider a random variable taking only nonnegative values, for example exponentially distributed $\theta \sim \text{Exp}(\lambda)$ for some positive parameter $\lambda > 0$, from equation (2.8) we obtain

$$\bar{v}_i(t) = \mathcal{V} + (v_i(0) - \mathcal{V}) \int_0^{+\infty} e^{-\theta t} \lambda e^{-\lambda\theta} d\theta, \tag{2.12}$$

which corresponds to

$$\bar{v}_i(t) = \mathcal{V} + (v_i(0) - \mathcal{V}) \frac{\lambda}{t + \lambda}, \tag{2.13}$$

and therefore $\bar{v}_i(t) \to \mathcal{V}$ as $t \to \infty$. Then independently from the choice of the rate $\lambda > 0$ we obtain for each agent convergences toward the average initial velocity of the system. Finally, in case of a uniform random variable $\theta \sim U([a, b])$ we obtain

$$\bar{v}_i(t) = \mathcal{V} + (v_i(0) - \mathcal{V}) \int_a^b \frac{1}{b - a} e^{-\theta t} d\theta \tag{2.14}$$

that is

$$\bar{v}_i(t) = \mathcal{V} + \frac{v_i(0) - \mathcal{V}}{b - a} \left(\frac{e^{-at}}{t} - \frac{e^{-bt}}{t} \right), \tag{2.15}$$

which implies the divergence of the system in time as soon as $a \in \mathbb{R}$ assumes negative values.

Example 2

Next we consider a random scattering rate with time-dependent distribution function, that is

$$K(\theta, t) = \theta(t) \tag{2.16}$$

with $\theta(t) \sim f(\theta, t)$. As an example we investigate the case of a normally distributed random parameter with given mean and time dependent variance, $\theta \sim \mathcal{N}(\mu, \sigma^2(t))$. It is straightforward to rewrite θ as a translation of a standard normal-distributed variable $\tilde{\theta}$, that is

$$\theta = \mu + \sigma(t)\tilde{\theta}, \tag{2.17}$$

where $\tilde{\theta} \sim \mathcal{N}(0, 1)$. The expected velocities read

$$\bar{v}_i(t) = \mathcal{V} + \frac{(v_i(0) - \mathcal{V})}{\sqrt{2\pi}} \int_{\mathbb{R}} \exp\left\{-\mu t - \tilde{\theta} \int_0^t \sigma(s)ds\right\} \exp\left\{-\frac{\tilde{\theta}^2}{2}\right\} d\tilde{\theta}, \tag{2.18}$$

which correspond to

$$\bar{v}_i(t) = \mathcal{V} + (v_i(0) - \mathcal{V}) \exp\left\{-\mu t + \frac{1}{2}\left(\int_0^t \sigma(s)ds\right)^2\right\}. \tag{2.19}$$

Similarly to the case of a time independent normal variable a threshold effect occurs for large times, i.e. the following condition on the variance of the distribution

$$\left(\int_0^t \sigma(s)ds\right)^2 > 2\mu t \tag{2.20}$$

implies the divergence of the system (2.4). As a consequence instability can be avoided by assuming a variance decreasing sufficiently fast in time. The simplest choice is represented by $\sigma(t) = 1/t^\alpha$ for some $\alpha \in [1/2, 1)$. The condition (2.20) becomes

$$\left(\frac{t^{1-\alpha}}{1-\alpha}\right)^2 > 2\mu t. \tag{2.21}$$

For example, if $\alpha = 1/2$ the previous condition implies that the system diverges for each $\mu < 2$.

7.3 A gPC based numerical approach

In this section we approximate the Cucker-Smale model with random inputs using a generalized polynomial chaos approach. For the sake of clarity we first recall some basic facts concerning gPC approximations.

7.3.1 Preliminaries on gPC approximations

Let $(\Omega, \mathcal{F}, P)$ be a probability space, that is a ordered triple with Ω any set, $\mathcal{F}$ a $\sigma-$algebra and $P : \mathcal{F} \to [0,1]$ a probability measure on $\mathcal{F}$, where we define a random variable

$$\theta : (\Omega, \mathcal{F}) \to (\mathbb{R}, \mathcal{B}_{\mathbb{R}}),$$

with $\mathcal{B}_{\mathbb{R}}$ the Borel set of $\mathbb{R}$. Moreover let us consider $S \subset \mathbb{R}^d, d \geq 1$ and $[0,T] \subset \mathbb{R}$ certain spatial and temporal subsets. For the sake of simplicity we focus on real valued functions depending on a single random input

$$g(x,\theta,t) : S \times \Omega \times T \to \mathbb{R}^d, \qquad g \in L^2(\Omega, \mathcal{F}, P). \tag{3.1}$$

In any case it is possible to extend the set-up of the problem to a $p-$dimensional vector of random variables $\theta = (\theta_1, \dots, \theta_p)$, see [97]. Let us consider now the linear space of polynomials of θ of degree up to M, namely $\mathbb{P}_M(\theta)$. From classical results in approximation theory it is possible to represent the distribution of random functions with orthogonal polynomials $\{\Phi_k(\theta)\}_{k=0}^M$, i.e. an orthogonal basis of $L^2(\Omega, \mathcal{F}, P)$

$$\mathbb{E}_\theta[\Phi_h(\theta)\Phi_k(\theta)] = \mathbb{E}_\theta[\Phi_h(\theta)^2]\delta_{hk}$$

with δ_{hk} the Kronecker delta function. Assuming that the probability law $P(\theta^{-1}(B)), \forall B \in \mathcal{B}_{\mathbb{R}}$, involved in the definition of the introduced function $g(x,\theta,t)$ has finite second order moment, then the complete polynomial chaos expansion of g is given by

$$g(x,\theta,t) = \sum_{m \in \mathbb{N}} \hat{g}_m(x,t)\Phi_m(\theta). \tag{3.2}$$

According to the Cameron-Martin theorem and to the Askey-scheme, results that pave a connection between random variables and orthogonal polynomials [45, 176, 177], we chose a set of polynomials which constitutes the optimal basis with respect to the distribution of the introduced random variable in agreement with Table 3.1.

Let us consider now a general formulation for a randomly perturbed problem

$$\mathcal{D}(x,t,\theta;g) = f(x,t,\theta) \tag{3.3}$$

where we indicated with $\mathcal{D}$ a differential operator. In general the randomness introduced in the problem by θ acts as a perturbation of $\mathcal{D}$, of the function g or occurs as uncertainty of the initial conditions. In this work we focus on the first two aspects assuming that initial positions and velocities are deterministically known.

Table 3.1: The different gPC choices for the polynomial expansions.

Probability law of θ	Expansion polynomials	Support
Gaussian	Hermite	$(-\infty, +\infty)$
Uniform	Legendre	$[a, b]$
Beta	Jacobi	$[a, b]$
Gamma	Laguerre	$[0, +\infty)$
Poisson	Charlier	$\mathbb{N}$

The generalized polynomial chaos method approximate the solution $g(x, \theta, t)$ of (3.3) with its Mth order polynomial chaos expansion and considers the Galerkin projections of the introduced differential problem, that is

$$\mathbb{E}_\theta \left[\mathcal{D}(x, t, \theta; g) \cdot \Phi_h(\theta)\right] = \mathbb{E}_\theta \left[f(x, \theta, t) \cdot \Phi_h(\theta)\right], \qquad h = 0, 1, \dots, M. \quad (3.4)$$

Due to the Galerkin orthogonality between the linear space $\mathbb{P}_M$ and the error produced in the representation of $g(x, \theta, t)$ with a truncated series, from (3.4) we obtain a set of $M + 1$ purely deterministic equations for the expansion coefficients $\hat{g}_m(x, t)$. These subproblems can be solved through classical discretization techniques. From the numerical point of view through a gPC-type method it is possible to achieve an exponential order of convergence to the exact solution of the problem, unlike Monte Carlo techniques for which the order is $O(1/\sqrt{M})$ where M is the number of samples.

7.3.2 Approximation gPC of the alignment model

We apply the described gPC decomposition to the solution of the non-homogeneous differential equation $v_i(\theta, t)$ in (2.5) and to the stochastic scattering rate $K(\theta, t)$, i.e.

$$v_i^M(\theta, t) = \sum_{m=0}^{M} \hat{v}_{i,m}(t)\Phi_m(\theta), \qquad K^M(\theta, t) = \sum_{l=0}^{M} \hat{K}_l(t)\Phi_l(\theta) \quad (3.5)$$

where

$$\hat{v}_{i,m}(t) = \mathbb{E}_\theta \left[v_i(\theta, t)\Phi_m(\theta)\right] \qquad \hat{K}_l(t) = \mathbb{E}_\theta \left[K(\theta, t)\Phi_l(\theta)\right]. \quad (3.6)$$

We obtain the following polynomial chaos expansion

$$\frac{d}{dt}\sum_{m=0}^{M} \hat{v}_{i,m}\Phi_m(\theta) = \frac{1}{N}\sum_{j=1}^{N} H(x_i, x_j) \sum_{l,m=0}^{M} \hat{K}_l(t)(\hat{v}_{j,m} - \hat{v}_{i,m})\Phi_l(\theta)\Phi_m(\theta).$$

Multiplying the above expression by an orthogonal element of the basis $\Phi_h(\theta)$ and integrating with respect to the distribution of θ

$$\mathbb{E}_\theta\left[\sum_{m=0}^{M}\frac{d}{dt}\hat{v}_{i,m}\Phi_m(\theta)\Phi_h(\theta)\right] = \mathbb{E}_\theta\left[\frac{1}{N}\sum_{j=1}^{N}H(x_i,x_j)\sum_{l,m=0}^{M}\hat{K}_l(t)(\hat{v}_{j,m}-\hat{v}_{i,m})\Phi_l(\theta)\Phi_m(\theta)\Phi_h(\theta)\right]$$

we find an explicit system of ODEs

$$\begin{aligned}\frac{d}{dt}\hat{v}_{i,h}(t) =& \frac{1}{\|\Phi_h\|^2 N}\sum_{j=1}^{N}H(x_i,x_j)\sum_{m=0}^{M}(\hat{v}_{j,m}-\hat{v}_{i,m})\sum_{l=0}^{M}\hat{K}_l(t)e_{lmh}\\ =& \frac{1}{N}\sum_{j=1}^{N}H(x_i,x_j)\sum_{m=0}^{M}(\hat{v}_{j,m}-\hat{v}_{i,m})\hat{K}_{mh}(t),\end{aligned} \tag{3.7}$$

where $e_{lmh} = \mathbb{E}_\theta[\Phi_l(\theta)\Phi_m(\theta)\Phi_h(\theta)]$ and

$$\hat{K}_{mh}(t) = \frac{1}{\|\Phi_h\|^2}\sum_{l=0}^{M}\hat{K}_l(t)e_{lmh}.$$

We recall that the gPC numerical approach preserves the mean velocity of the alignment model (2.4). In fact, from (3.7) follows

$$\begin{aligned}\sum_{i=1}^{N}\frac{d}{dt}\hat{v}_{i,h}(t) =& \frac{1}{N}\sum_{j,i=1}^{N}H(x_i,x_j)\sum_{m=0}^{M}\hat{K}_{mh}(t)\hat{v}_{j,m}\\ &- \frac{1}{N}\sum_{j,i=1}^{N}H(x_i,x_j)\sum_{m=0}^{M}\hat{K}_{mh}(t)\hat{v}_{i,m} = 0,\end{aligned} \tag{3.8}$$

thanks to the symmetry of H. More generally it can be shown that if

$$\frac{1}{N}\sum_{i=1}^{N}v_i(\theta,t) = \mathcal{V},$$

where $\mathcal{V}$ is time-independent, then its gPC decomposition is also mean-preserving since

$$\begin{aligned}\frac{1}{N}\sum_{i=1}^{N}\sum_{m=0}^{M}\mathbb{E}_\theta\left[v_i(\theta,t)\Phi_m(\theta)\right]\Phi_m(\theta) &= \sum_{m=0}^{M}\mathbb{E}_\theta\left[\frac{1}{N}\sum_{i=1}^{N}v_i(\theta,t)\Phi_m(\theta)\right]\Phi_m(\theta)\\ &= \mathcal{V}\sum_{m=0}^{M}\mathbb{E}_\theta\left[1\cdot\Phi_m(\theta)\right]\Phi_m(\theta) = \mathcal{V}.\end{aligned}$$

Remark 10. *The gPC approximation (3.7) can be derived equivalently without expanding the kernel function $K(\theta, t)$. In this way one obtains*

$$\frac{d}{dt}\hat{v}_{i,h}(t) = \frac{1}{N}\sum_{j=1}^{N} H(x_i, x_j)\sum_{m=0}^{M}(\hat{v}_{j,m} - \hat{v}_{i,m})\widehat{K}_{mh} \tag{3.9}$$

where now

$$\widehat{K}_{mh}(t) = \frac{1}{\|\Phi_h\|^2}\mathbb{E}_\theta[K(\theta, t)\Phi_m\Phi_h].$$

Note that, since in general $N \gg M$, the overall computational cost is $O(MN^2)$.

7.4 Selective control of the gPC approximation

In order stabilize the gPC approximation of the Cucker-Smale type model (2.1) with random inputs, we introduce an additional term which acts as control of the approximated dynamics. More specifically we modify the approximation of the alignment model (2.1) by introducing a control term $\hat{u}_h$ to the hth component of its gPC approximation

$$\frac{d}{dt}\hat{v}_{i,h}(t) = \frac{1}{N}\sum_{j=1}^{N} H(x_i, x_j)\sum_{m=0}^{M}\hat{K}_{mh}(t)(\hat{v}_{j,m}(t) - \hat{v}_{i,m}(t)) + \hat{u}_h Q(\hat{v}_{i,h}). \tag{4.1}$$

The control $\hat{u}_h$ is a solution of

$$\hat{u}_h = \arg\min_{\hat{u}_h \in \mathcal{U}_b}\left[\frac{1}{2}\int_0^T \frac{1}{N}\sum_{i=1}^{N}(\hat{v}_{i,h}(t) - \hat{v}_{d,h})^2 dt + \frac{\nu}{2}\int_0^T \hat{u}_h(t)^2 dt\right], \tag{4.2}$$

where we assume to have, for each $h = 1, \dots, M$, a bounded control $\hat{u}_h$ having value in a admissible set $\mathcal{U}_b \subset \mathbb{R}^d$, for example in the one-dimensional case we consider $\hat{u}_h \in [u_{h,L}, u_{h,R}]$. Parameter $\nu > 0$ is a regularization term and $(\hat{v}_{d,0}, \hat{v}_{d,1}, \dots, \hat{v}_{d,M})$ are the desired values for the gPC coefficients. For example

$$\hat{v}_{d,h} = \mathbb{E}_\theta[v_d\Phi_h(\theta)] = v_d\mathbb{E}[\Phi_h(\theta)] = \begin{cases} v_d & h = 0 \\ 0 & h = 1, \dots, M, \end{cases} \tag{4.3}$$

where v_d is a desired velocity.

Moreover the controller action is weighted by a bounded function,

$$Q : \mathbb{R}^d \to \mathbb{R}^d.$$

Due to the dependence of the controller effect from the single agent velocity, we refer to this approach as selective control, see [71].

In order to tackle numerically the above problem, whose direct solution is prohibitively expansive for large numbers of individuals, we make use of model predictive control (MPC) techniques, also referred to as receding horizon strategy or instantaneous control [135]. These techniques has been used in [6, 7, 11] in the case of deterministic alignment systems.

7.4.1 Selective model predictive control

Let us split the time interval $[0, T]$ in $\tilde{N}$ time intervals of length Δt with $t^n = n\Delta t$ with $n = 0, \dots, \tilde{N} - 1$. The basic idea of the model predictive control approach, is to consider a piecewise constant control

$$\hat{u}_h(t) = \sum_{n=0}^{\tilde{N}-1} \hat{\bar{u}}_h^n \, \chi_{[t^n, t^{n+1}]}(t).$$

In this way is possible to determine the value of the control $\hat{u}_h^n \in \mathbb{R}^d$, solving for a state $\bar{\hat{v}}_{i,h}$ the (reduced) optimization problem

$$\begin{aligned}
&\frac{d}{dt}\hat{v}_{i,h}(t) = \frac{1}{N}\sum_{j=1}^{N} H(x_i, x_j) \sum_{m=0}^{M} \hat{K}_{mh}(t)(\hat{v}_{j,m}(t) - \hat{v}_{i,m}(t)) + \hat{u}_h Q(\hat{v}_{i,h}(t)) \\
&\hat{v}_{i,h}(t^n) = \bar{\hat{v}}_{i,h}, \\
&\hat{u}_h^n = \arg\min_{\hat{u}_h \in \mathcal{U}_b} \int_{t^n}^{t^{n+1}} \frac{1}{N}\sum_{i=1}^{N} \left(\frac{1}{2}(\hat{v}_{i,h}(t) - \hat{v}_{d,h})^2 + \frac{\nu}{2}\hat{u}_h(t)^2 \right) ds,
\end{aligned} \tag{4.4}$$

Given the control $\hat{u}_h^n$ on the time interval $[t^n, t^{n+1}]$, we let evolve $\hat{v}_{i,h}$ according to the dynamics

$$\frac{d}{dt}\hat{v}_{i,h} = \frac{1}{N}\sum_{j=1}^{N} H(x_i, x_j) \sum_{m=0}^{M} \hat{K}_{mh}(t)(\hat{v}_{j,m}(t) - \hat{v}_{i,m}(t)) + \hat{u}_h^n Q(\hat{v}_{i,h}^n(t)) \tag{4.5}$$

in order to obtain the new state $\bar{\hat{v}}_{i,h} = \hat{v}_{i,h}(t^{n+1})$. We again solve (4.4) to obtain $\hat{u}_h^{n+1}$ with the modified initial data and we repeat this procedure until we reach $\tilde{N}\Delta t = T$.

The reduced optimization problem implies a reduction of the complexity of the initial problem since it depends only on the single real–valued variable $\hat{u}_h^n$. On the other hand the price to pay is that in general the solution of the problem is suboptimal respect to the full one (4.1)-(4.2).

The quadratic cost and a suitable discretization of (4.5) allow an explicit representation of $\hat{u}_h^n$ in terms of $\bar{\hat{v}}_{i,h}$ and $\hat{v}_{i,h}^{n+1}$, as a feedback controlled system

as follows

$$\begin{aligned}
\hat{v}_{i,h}^{n+1} &= \hat{v}_{i,h}^{n} + \frac{\Delta t}{N}\sum_{j=1}^{N} H_{ij}^{n}\sum_{m=0}^{M}\hat{K}_{mh}^{n}(\hat{v}_{j,m}^{n} - \hat{v}_{i,m}^{n}) + \Delta t\hat{u}_{h}^{n}Q_{i,h}^{n},\\
\hat{v}_{i,h}^{n} &= \bar{\hat{v}}_{i,h},\\
\hat{u}_{h}^{n} &= -\frac{\Delta t}{\nu N}\sum_{i=1}^{N}(\hat{v}_{i,h}^{n+1} - \hat{v}_{d,h})Q_{i,h}^{n},
\end{aligned} \tag{4.6}$$

where $H_{ij}^{n} \equiv H(x_i^n, x_j^n)$ and $Q_{i,h}^{n} \equiv Q(\hat{v}_{i,h}^{n})$. Note that since the feedback control $\hat{u}_h^n$ in (4.6) depends on the velocities at time $n+1$, the constrained interaction at time n is implicitly defined. The feedback controlled system in the discretized form results

$$\begin{aligned}
\hat{v}_{i,h}^{n+1} &= \hat{v}_{i,h}^{n} + \frac{\Delta t}{N}\sum_{j=1}^{N} H_{ij}^{n}\sum_{m=0}^{M}\hat{K}_{mh}^{n}(\hat{v}_{j,m}^{n} - \hat{v}_{i,m}^{n}) - \frac{\Delta t^2}{\nu N}\sum_{j=1}^{N}(\hat{v}_{j,h}^{n+1} - \hat{v}_{d,h})Q_{j,h}^{n}Q_{i,h}^{n},\\
\hat{v}_{i,h}^{n} &= \bar{\hat{v}}_{i,h}.
\end{aligned}$$

Again the action of the control is substituted by an implicit term representing the relaxation toward the desired component of the velocity $\hat{v}_{d,h}$, and it can be inverted in a fully explicit system.

Considering the scaling for the regularization parameter $\nu = \kappa\Delta t$, the previous scheme is a consistent discretization of the following continuos system

$$\begin{aligned}
\frac{d}{dt}\hat{v}_{i,h}(t) =& \frac{1}{N}\sum_{j=1}^{N} H(x_i, x_j)\sum_{m=0}^{M}\hat{K}_{mh}(t)(\hat{v}_{j,m}(t) - \hat{v}_{i,m}(t))\\
&+ \frac{1}{\kappa N}\sum_{j=1}^{N}(\hat{v}_{d,h} - \hat{v}_{j,h}(t))Q(\hat{v}_{j,h}(t))Q(\hat{v}_{i,h}(t)).
\end{aligned} \tag{4.7}$$

Now the control is explicitly embedded in the dynamics of the hth component of the gPC approximation as a feedback term, and the parameter $\kappa > 0$ determines its strength.

7.4.2 Choice of the selective control

For the specific choice of weight function $Q(\cdot) \equiv 1$ we refer in general to non selective control. Note that in this case the action of the control is not strong enough to control the velocity of each agent, indeed in this case we are able only to control the mean velocity of the system. In fact the control term is reduced to

$$\frac{1}{\kappa}(\hat{v}_{d,h} - \hat{\mathcal{V}}_h), \tag{4.8}$$

where $\hat{\mathcal{V}}_h$ is the $h-$th coefficient of the expansion of $\mathcal{V}$, that is

$$\hat{\mathcal{V}}_h = \frac{1}{N}\sum_{j=1}^{N} \hat{v}_{j,h}(t).$$

Then, only the projections of the mean velocity are steered toward the respective components of the target velocity, i.e. as soon as $\kappa \to 0$ it follows that $\hat{\mathcal{V}}_h = \hat{v}_{d,h}$. Therefore, the choice of the selective function $Q(\cdot)$ is of paramount importance to ensure the action of the control on the single agent.

In principle one can address directly the control problem on the original system (2.1) as

$$\begin{cases} \dot{x}_i(\theta,t) = v_i(\theta,t) \\ \dot{v}_i(\theta,t) = \dfrac{K(\theta,t)}{N}\displaystyle\sum_{j=1}^{N} H(x_i,x_j)(v_j(\theta,t) - v_i(\theta,t)) + uQ(v_i(\theta,t)), \end{cases} \tag{4.9}$$

where the control term u is solution of

$$u = \arg\min_{u\in\mathcal{U}_b}\left[\frac{1}{2}\int_0^T \frac{1}{N}\sum_{i=1}^{N}(v_i(\theta,t) - v_d)^2 dt + \frac{\nu}{2}\int_0^T u(t)^2 dt\right], \tag{4.10}$$

Here $v_d \in \mathbb{R}^d$ is a target velocity, $\nu > 0$ a regularization parameter and $\mathcal{U}_b$ the set of admissible control. Similarly to previous subsection, through the approach presented in [6, 7, 11], we can derive the time-continuos MPC formulation which explicitly embed the control term in the dynamics as follows

$$\begin{cases} \dot{x}_i(\theta,t) = & v_i(\theta,t) \\ \dot{v}_i(\theta,t) = & \dfrac{K(\theta,t)}{N}\displaystyle\sum_{j=1}^{N} H(x_i,x_j)(v_j(\theta,t) - v_i(\theta,t)) \\ & + \dfrac{1}{\kappa N}\displaystyle\sum_{j=1}^{N}(v_d - v_j(\theta,t))Q(v_j(t,\theta))Q(v_i(t,\theta)). \end{cases} \tag{4.11}$$

Now the gPC approximation of (4.11) can be obtained as in Section 7.3 and leads to the set of ODEs

$$\begin{aligned} \frac{d}{dt}\hat{v}_{i,h}(t) = & \frac{1}{N}\sum_{j=1}^{N} H(x_i,x_j)\sum_{m=0}^{M}\hat{K}_{mh}(t)(\hat{v}_{j,m}(t) - \hat{v}_{i,m}(t)) \\ & + \frac{1}{\kappa N}\sum_{j=1}^{N} R_h(v_i^M, v_j^M), \end{aligned} \tag{4.12}$$

where

$$R_h(v_i^M, v_j^M) = \frac{1}{\|\Phi_h\|^2}\mathbb{E}_\theta\left[(v_d - v_j^M)Q\left(v_i^M(\theta,t)\right)Q\left(v_j^M(\theta,t)\right)\Phi_h(\theta)\right]. \tag{4.13}$$

In general systems (4.12) and (4.7), without further assumptions on the selective function $Q(\cdot)$, are not equivalent. In addition to the non selective case, there exist at least one choice of selective control that makes the two approaches totally interchangeable. In fact, taking

$$Q(v_i) = \frac{v_d - v_i}{\sqrt{\frac{1}{N}\sum_{j=1}^N (v_d - v_j)^2}}, \tag{4.14}$$

and $Q(v_i) \equiv 0$ if $v_j = v_d$, $\forall j = 1, \dots, N$, we have that $Q(\cdot)$ is bounded and the control term in (4.12) takes the following form

$$\frac{1}{\kappa N}\sum_{j=1}^N R_h = \frac{1}{\kappa||\Phi_h||^2}\mathbb{E}_\theta\left[(v_d - v_i^M(\theta,t))\Phi_h(\theta)\right] = \frac{1}{\kappa}\left(\hat{v}_{d,h} - \hat{v}_{i,h}\right). \tag{4.15}$$

Similarly the control term in (4.7) reduces to

$$\frac{1}{\kappa N}\sum_{j=1}^N (\hat{v}_{d,h} - \hat{v}_{j,h}(t))Q(\hat{v}_{j,h}(t))Q(\hat{v}_{i,h}(t)) = \frac{1}{\kappa}\left(\hat{v}_{d,h} - \hat{v}_{i,h}\right), \tag{4.16}$$

and therefore system (4.12) coincides with (4.7). Note that as $\kappa \to 0$ both systems are driven towards the controlled state $\hat{v}_{i,h} = \hat{v}_{d,h}$ which implies a strong control over each single agent.

In Figure 4.1 we summarize the two equivalent approaches. In the case of non selective control and of selective function given by (4.14) the constrained gPC system can be obtained from our initial unconstrained model (2.1) through two different but equivalent methods. The first approximates the solution of the Cucker-Smale type model via the gPC projection and then introduces a control on the coefficients of the decomposition through a MPC approach in order to steer each component to $(\hat{v}_{d,0}, \hat{v}_{d,1}, \dots, \hat{v}_{d,M})$. Whereas the second method considers a constrained Cucker-Smale problem (4.9), introduces its continuous MPC approximation and then computes the gPC expansion of the resulting system of constrained differential equations.

Remark 11. *We remark that the choice of $Q(\cdot)$ stated in (4.14), for which the two approaches sketched in Figure 4.1 are identical, is equivalent to consider the constrained dynamics (4.9), modified as follows*

$$\begin{cases} \dot{x}_i(\theta,t) = v_i(\theta,t) \\ \dot{v}_i(\theta,t) = \dfrac{K(\theta,t)}{N}\displaystyle\sum_{j=1}^N H(x_i,x_j)(v_j(\theta,t) - v_i(\theta,t)) + u_i, \end{cases} \tag{4.17}$$

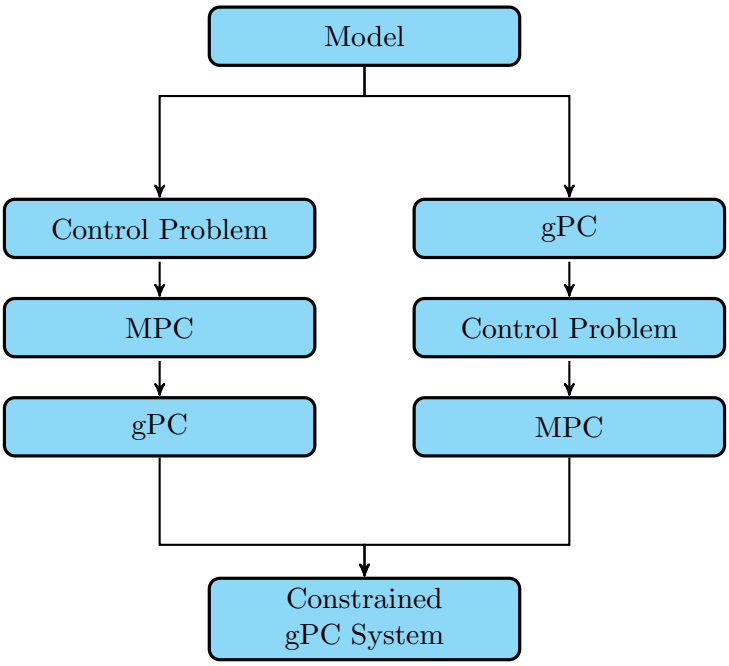

Figure 4.1: Sketch of the two numerical approaches to solve the control problem with uncertainty, combining MPC and gPC. In both cases, of non selective control, i.e. $Q(\cdot) \equiv 1$, and of selective control with $Q(\cdot)$ defined in (4.14) the two approaches are equivalent.

where the control term, u_i for each agent $i = 1, \dots, N$, is given by the minimization of the following functional

$$J(v_1, \dots, v_N; u_1, \dots, u_N) = \frac{1}{2} \int_0^T \frac{1}{N} \sum_{i=1}^{N} \left[(v_i(\theta, t) - v_d)^2 + \frac{\nu}{2} u_i(t)^2 \right] dt. \tag{4.18}$$

Since the functional is strictly convex, applying the (MPC) procedure on a single time interval for the discretized dynamics of (4.17)-(4.18), we obtain u_i in terms of feedback control

$$u_i = \frac{1}{\kappa}(v_d - v_i), \qquad i = 1, \dots, N. \tag{4.19}$$

Thus the same considerations on the equivalence of the approaches hold.

7.5 Numerical tests

We present some numerical experiments of the behavior of the flocking model in the case of a Hermite polynomial chaos expansion. This choice

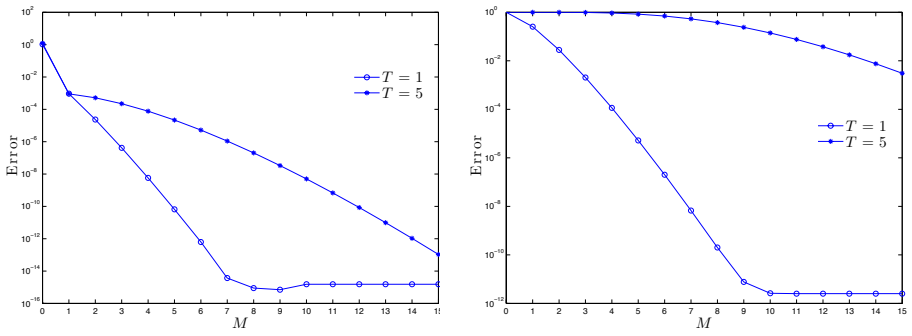

Figure 5.2: Error convergence for increasing number of polynomials in the gPC decomposition approximation. Left: convergence of the mean error at two fixed times $T = 1$ and $T = 5$. Right: convergence of the variance error. In both cases we considered a random time-independent scattering $K(\theta, t) = \theta$, where the random variable θ is normally distributed $N(2, 1/2)$. The system of ODEs is solved through a 4th order Runge-Kutta with $\Delta t = 10^{-5}$.

corresponds to the assumption of a normal distribution for the stochastic parameter in the Cucker-Smale type equation (2.1) and in its constrained behavior (4.7). Numerical results show that the introduced selective control with the weight function (4.14) is capable to drive the velocity to a desired state even in case of a dynamics dependent on a normally distributed random input, with fixed or time-dependent variance. In the uniform interaction case, since the effect of agents' positions do not influence the alignment we report only the results of the agents' velocities.

7.5.1 Unconstrained case

In Figures 5.2 and 5.3 we present numerical results for the convergence of the error using the gPC scheme described in equation (3.7) for $H \equiv 1$ and solved through a 4th order Runge-Kutta method. In particular Figure 5.2 shows the behavior of the error with respect to increasing terms of the gPC decomposition. Here we considered the average in time of the error for the mean and the variance at time $t > 0$ in the L^1 norm

$$E_{\bar{v}}(t) = \frac{1}{N}\sum_{i=1}^{N}\left|\frac{\bar{v}_i(t) - \bar{v}_i^M(t)}{\bar{v}_i(t)}\right| \qquad E_{\bar{\sigma}^2}(t) = \frac{1}{N}\sum_{i=1}^{N}\left|\frac{\bar{\sigma}_i^2(t) - \bar{\sigma}_i^{2,M}(t)}{\bar{\sigma}_i^2(t)}\right|, \tag{5.1}$$

where

$$\bar{\sigma}_i^2(t) = \mathbb{E}_\theta\left[\left(v_i(\theta, t) - \bar{v}_i(t)\right)^2\right] \tag{5.2}$$

with $v_i(\theta, t)$ and $\bar{v}_i(t)$ defined in (2.5) and (2.7). Observe that if the scattering rate $K(\theta, t)$ is of the from described in (2.6) with $h(\cdot) \equiv 1$ and $k(\theta) \sim \mathcal{N}(\mu, \sigma^2)$

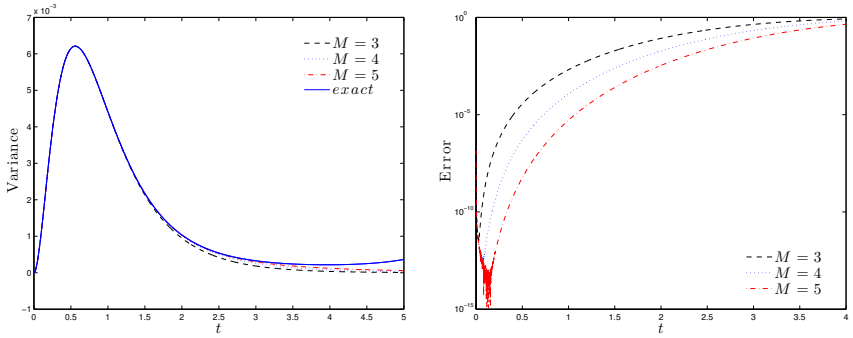

Figure 5.3: Evolution of the variance-error $E_{\bar{\sigma}^2}(t)$ defined in equation (5.1) for the gPC decomposition for the unconstrained model (2.4) with $K(\theta, t) = \theta \sim \mathcal{N}(2, 1/2)$ over the time interval $[0, T]$ with $T = 5$ and time step $\Delta t = 10^{-5}$.

than, in addition to the explicit evolution for the expected velocity as in (2.8), we can obtain the exact version for the evolution of the variance of the ith agent

$$\bar{\sigma}_i^2(t) = (v_i(0) - \mathcal{V})^2 \left(\exp\{-2\mu t + 2\sigma^2 t^2\} - \exp\{-2\mu t + \sigma^2 t^2\}\right). \tag{5.3}$$

In (5.1) we indicated with $\bar{\sigma}_i^{2,M}(t)$ the approximated variance

$$\bar{\sigma}_i^{2,M}(t) = \sum_{h=0}^{M} \hat{v}_{i,h}^2(t) \mathbb{E}_\theta[\Phi_h(\theta)^2] - \hat{v}_{i,0}^2(t). \tag{5.4}$$

It is easily seen how the error decays spectrally for increasing value of M, however the method is not capable to go above a certain accuracy and therefore for large M a threshold effect is observed. This can be explained by the large integration interval we have considered in the numerical computation, and by the well-known loss of accuracy of gPC for large times [97]. In the case of the error of the variance, Figure 5.3, the gPC approximation exhibits a slower convergence with respect to the convergence of the mean. Next in Figure 5.4 we see how for large times the solution of the differential equation (2.4) diverges and the numerical approximation is capable to describe accurately its behavior only through an increasing number of Hermite polynomials.

7.5.2 Constrained uniform interaction case

In Figure 5.5 we show different scenarios for the uniform interaction dynamics with constraints. In the first row we represents the solution for $N = 10$ agents, whose dynamics is described by equation (4.7) with $v_d = 1$, different values of κ originate different controls on the average of the system,

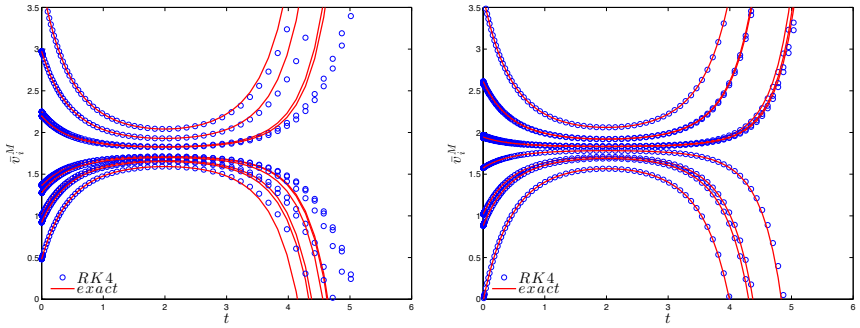

Figure 5.4: Left: 6th order Hermite gPC decomposition solved through a 4th order Runge-Kutta. Right: 10th order Hermite gPC decomposition solved through a 4th order Runge-Kutta. In both cases the final time considered is $T = 6$, with time step $\Delta t = 10^{-2}$.

which however do not prevent the system to diverge. In the second row we show the action of selective control (4.14). It is evident that, with this choice, we are able to control the system also in the case with higher variance.

Observe that the numerical results are coherent with the explicit solution of the controlled equation. Let us consider the time-independent scattering rate$K(\theta, t) = \theta \sim \mathcal{N}(\mu, \sigma^2)$, then from the equation

$$\frac{d}{dt} v_i(\theta, t) = \theta(\mathcal{V} - v_i(\theta, t)) + \frac{1}{\kappa}(v_d - v_i(\theta, t)) \tag{5.5}$$

we can compute the exact solution given $v_i(\theta, 0) = v_i(0)$

$$v_i(\theta, t) = \frac{\kappa\mathcal{V}\theta + v_d}{\kappa\theta + 1} + \left(v_i(0) - \frac{\kappa\mathcal{V}\theta + v_d}{\kappa\theta + 1} \right) \exp\left\{ - \left(\theta + \frac{1}{\kappa} \right) t \right\}. \tag{5.6}$$

The asymptotic behavior of the expected value of (5.6) can be studied similarly to what we did in Section 7.2.1. In other words in order to prevent the divergence of the leading term of the controlled expected exact solution we might study

$$\exp\left\{ - \left(\mu + \frac{1}{\kappa} \right) t + \frac{\sigma^2 t^2}{2} \right\}, \tag{5.7}$$

which diverge if

$$t > \frac{2}{\sigma^2} \left(\mu + \frac{1}{\kappa} \right). \tag{5.8}$$

Then for each fixed time we could select a regularization parameter $\kappa > 0$ so as to avoid the divergence of (5.6). Moreover we can observe that in the limit $\kappa \to 0$ the introduced selective control is capable to correctly drive the system (5.5) for each $t > 0$.

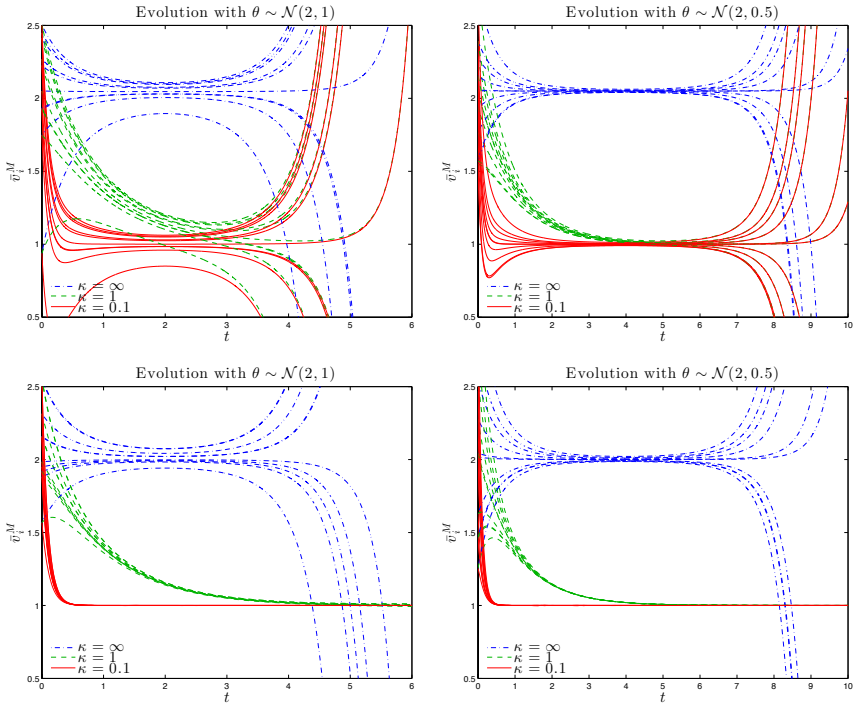

Figure 5.5: Evolution of the uniform interaction alignment model (4.7) with $N = 10$ agents, at $t = 0$ distributed around $\mathcal{V} = 2$ with unitary variance, depending on a normal random parameter. Left column: $\theta \sim \mathcal{N}(2, 1)$. Right column $\theta \sim \mathcal{N}(2, 0.5)$. The control term shows its ability to steer the system towards desired velocity $v_d = 1$, with different intensities $\kappa = 1$ and $\kappa = 0.1$, when $\kappa = \infty$ the control has no influence. First row shows the action of the control acting just on the average velocity, $Q \equiv 1$. Second row shows the action of selective control with $Q(\cdot)$ as in (4.14).

In Figure 5.6 we consider the system with random time-dependent scattering rate $\theta \sim \mathcal{N}(\mu, \sigma^2(t))$. The dynamics shows how, for the choice of time dependent variance described in Remark 7.2.1, that is $\sigma(t) = 1/t^\alpha$ with $\alpha = 1/2$, the convergence depends from the mean value of the random input. In particular numerical experiments highlight the threshold effect for $\mu = 2$ which we derived in Section 8.2. In the second figure we show that the action of the selective control (4.14), with desired velocity $v_d = \mathcal{V}$, is capable to stabilize the system and drive the velocities towards the desired state.

7.5.3 Constrained space dependent case

Next let us consider the full space non homogeneous constrained problem (2.1) with the interaction function defined in (2.2). In this case we assume

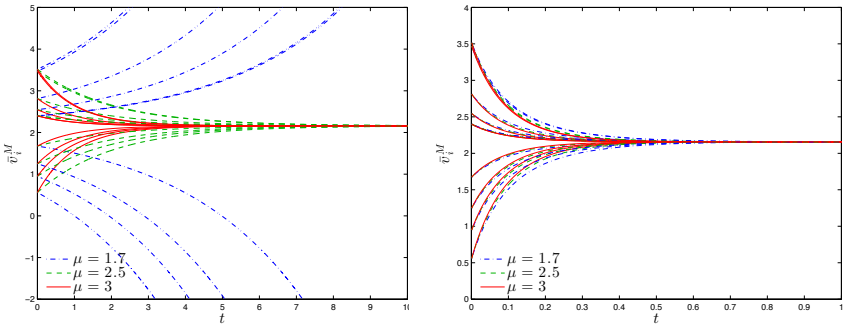

Figure 5.6: Solution of the uniform interaction case with time dependent random parameter θ distributed accordingly to a normal distribution $\mathcal{N}(\mu, \sigma^2(t))$, with a time-dependent standard deviation $\sigma(t) = 1/t^\alpha$, and $\alpha = 1/2$. Left: we see the threshold for different values of μ, i.e. for $\mu < 2$ the system diverges. Right: solution of the constrained model with $\kappa = 0.1$, observe that we are able to steer the system to the desired velocity $v_d = \mathcal{V}$, i.e. the initial mean velocity of the system, using the selective control described in (4.14).

that $K(\theta) = \theta$ with $\theta \sim \mathcal{N}(\mu, \sigma^2)$. In Figure 5.7 and 5.8 we consider a system of $N = 100$ agents with Gaussian initial position with zero mean and with variance 2 and Gaussian initial velocities clustered around ± 5 with variance $1/10$. The numerical results for (3.7) have been performed through a 10th order gPC expansion. The dynamics has been observed in the time interval $[0, 5]$ with $\Delta t = 10^{-2}$. In Figure 5.8 we see how the selective control is capable to drive the velocity of each agent to the desired state v_d. In fact in case of no control, see Figure 5.7, we have that the velocities of the system naturally diverges.

7.6 Conclusions

We proposed a general approach for the numerical approximation of flocking models with random inputs through gPC. The method is constructed in two steps. First the random Cucker-Smale system is solved by gPC. The presence of uncertainty in the interaction terms, which is a natural assumption in this kind of problems, leads to threshold effects in the asymptotic behavior of the system. Next a constrained gPC approximation is introduced and approximated though a selective model predictive control strategy. Relations under which the introduction of the gPC approximation and the model predictive control commute are also derived. The numerical examples illustrates that the assumption of positivity of the mean value of the random input is not sufficient for the alignment of the system but that a suitable

choice of the selective control is capable to stabilize the system towards the desired state. Extension of this technique to the case of a large number of interacting agents through mean-field and Boltzmann approximations are actually under study.

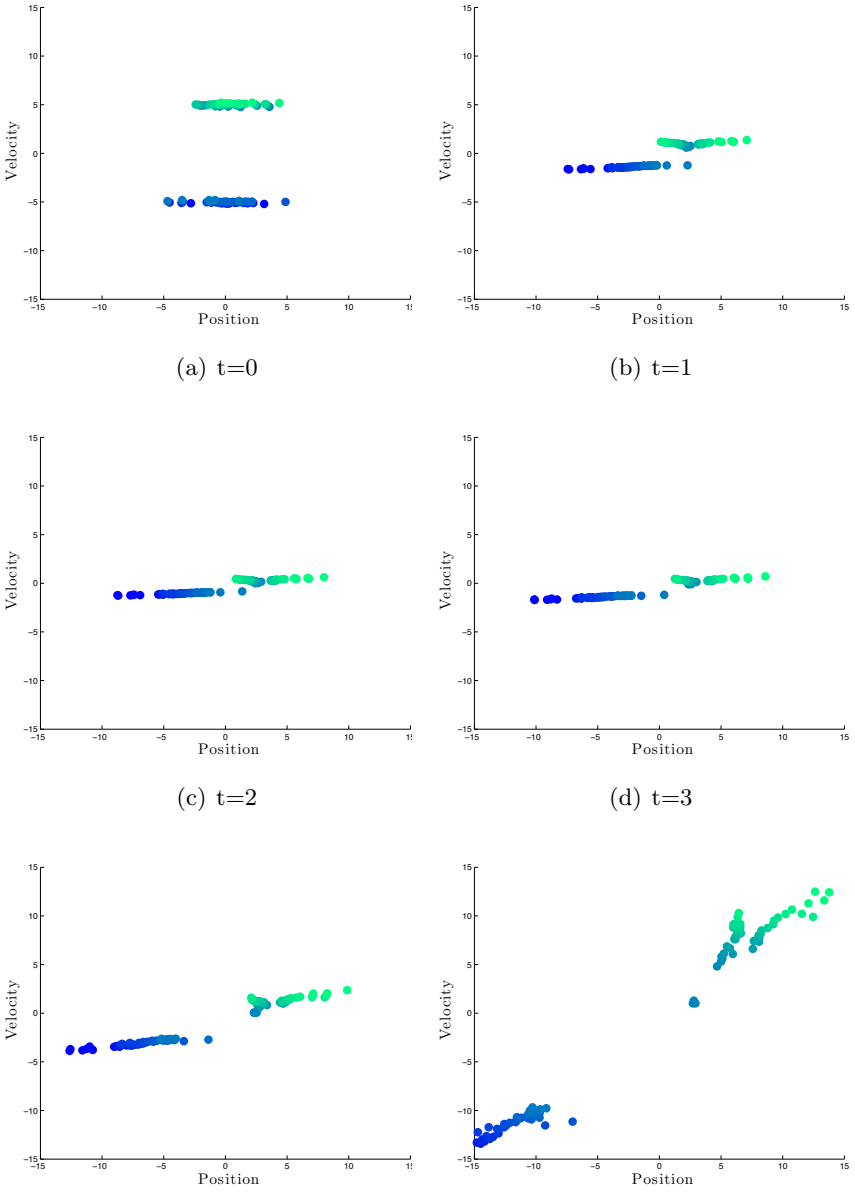

(a) t=0 (b) t=1

(c) t=2 (d) t=3

(e) t=4 (f) t=5

Figure 5.7: Numerical solution of (4.7), with $\gamma = 0.05 < 1/2$, $\zeta = 0.01$, through a 10th order gPC Hermite decomposition (3.7) with $\kappa = \infty$ with time step $\Delta t = 10^{-2}$. The random input is normally distributed $\theta \sim \mathcal{N}(2, 1)$.

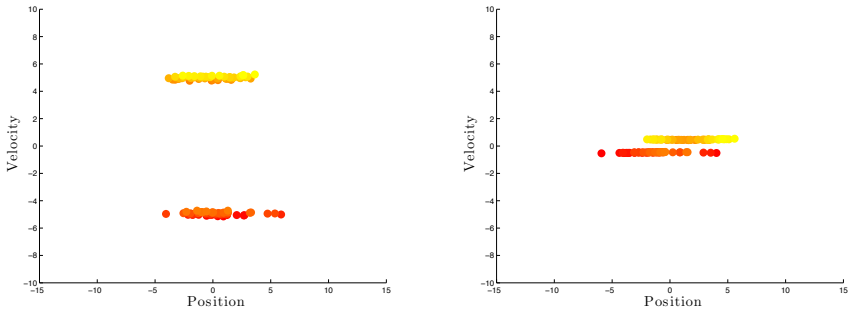

(a) t=0

(b) t=1

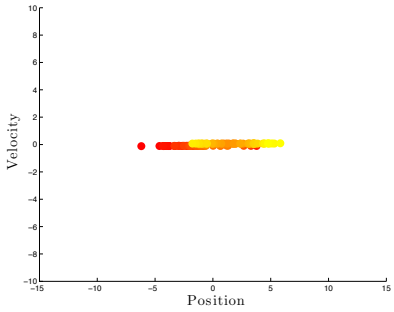

(c) t=2

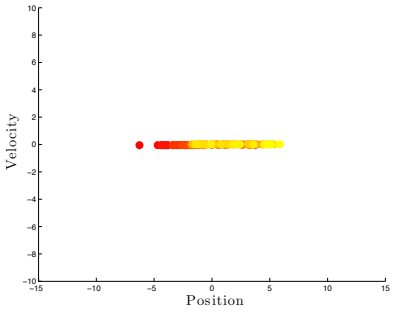

(d) t=3

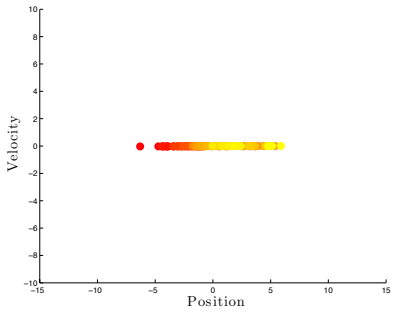

(e) t=4

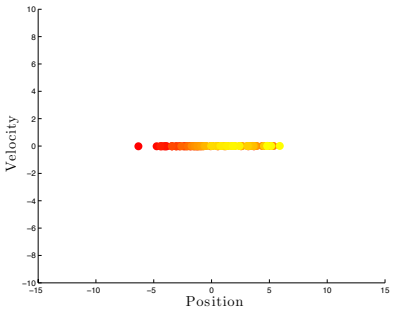

(f) t=5

Figure 5.8: Numerical solution of (4.7), with $\gamma = 0.05 < 1/2$, $\zeta = 0.01$, through a $6th$-order gPC Hermite decomposition for the selective control (3.7) with time step $\Delta t = 10^{-2}$. Here we considered a normally distributed random input $\theta \sim \mathcal{N}(2, 1)$, the desired velocity is $v_d = 0$ and the control parameter is $\kappa = 1$.

Chapter 8

Mean–field equations dependent on random inputs

8.1 Introduction

In the real world, the aggregate motion of a finite system of interacting agents may be affected by different kind of randomness, like perturbed boundary values, as well as unintelligible microscopic interactions. These strongly non-linear effects may strongly influence the agents' dynamics introducing threshold effects which potentially destroy an emerging pattern [13]. Thus, the introduction of uncertainty in mathematical modeling of these real world phenomena seems to be unavoidable for applications.

Among a rather extensive literature on alignment models for interacting systems, the Cucker-Smale model gained in the scientific research a special place thanks to its simplicity and mathematical elegance both. Without pretending to review the whole literature some references are [52, 53, 71, 139].

We will consider different ways to introduce random effects on the dynamics, in particular we concentrate to the case of uncertain initial value with a system of agents evolving through a deterministic model, as well as the case of stochastic interaction rules. These situations make the introduced models more realistic, miming the fact we can model these collective dynamics not by considering universal physical laws but making use of external data available from experiments. This is even more evident in many problems in socio-economic sciences where the interaction rules are based on observations and empirical evidence. Therefore, we can have at most statistical information of the modeling parameters. In order to fully understand simulation results and to produce effective predictions it is essential to incorporate uncertainty propagating in the dynamics from the beginning of the modeling.

In particular, in this chapter we focus on the construction of a novel numerical methods for the positivity preservation of statistical quantities of randomly perturbed equations of the collective behavior. The proposed

method conserves the property of fast convergence with respect to the random inputs.

8.2 Microscopic alignment dynamics with random inputs

In this section we introduce the main properties of an alignment model. First we discuss some results in the deterministic setting already presented in several works [52, 53], then we concentrates on the introduction of stochastic quantities.

8.2.1 Property of the deterministic Cucker–Smale model

In a deterministic setting we are interested in studying the dynamics of $N \in \mathbb{N}$ agents whose trajectories are given in the phase space by the Cuker-Smale second order system of differential equations. Hence, for each $i = 1, \dots, N$ we consider the following system fo ODEs

$$\begin{cases} \dot{x}_i(t) = v_i(t) \\ \dot{v}_i(t) = \dfrac{1}{N} \displaystyle\sum_{j=1}^{N} H(x_i, x_j)(v_j(t) - v_i(t)), \end{cases} \tag{2.1}$$

with initial locations and velocities $x_i(0) = x_{i,0}$, $v_i(0) = v_{i,0}$. In (2.1) we introduced the interaction function between the agents $i, j \in \{1, \dots, N\}$ indicated by $H(\cdot, \cdot)$ which depends on the agents' location. The classic space dependent interaction function acts on the space gaps between agents $|x_i - x_j|$, where the metric defined by $|\cdot|$ is Euclidean and whose expression is given by

$$H(x_i, x_j, \theta) = \frac{K}{(1 + |x_i, x_j|^2)^{\gamma}}. \tag{2.2}$$

We observe that being (2.2) a symmetric function, hence it is defined a symmetric adjacency matrix $\{a_{ij}\}$, $i, j = 1, \dots, N$

$$a_{ij} = \frac{H(x_i, x_j)}{N}. \tag{2.3}$$

A possible variant of the Cucker–Smale model has been described in [139] where the symmetry the introduced model is broken by considering an alignment based on the relative influence. Non-symmetric dynamics define more sophisticated models where the ith agent may interact with the jth agent but not vice versa, for example leader-follower models as well as limited perception models [9, 53, 66, 141]

In a deterministic setting, different regimes are described by the introduced model, depending on the choice of K, γ. In particular the following theorem holds

Theorem 8.2.1. *Assume that one of the following conditions holds*

i) $\gamma < 1/2$

ii) $\gamma \geq 1/2$ *and*

$$\left[\left(\frac{1}{2\gamma}\right)^{\frac{1}{2\gamma-1}} - \left(\frac{1}{2\gamma}\right)^{\frac{2\gamma}{2\gamma-1}}\right]\left(\frac{K^2}{8N^2\Lambda(v_0)}\right)^{\frac{1}{2\gamma-1}} > 2\Gamma(x_0) + 1, \quad (2.4)$$

where

$$\Gamma(x) = \frac{1}{2}\sum_{i\neq j}|x_i - x_j^2|, \qquad \Lambda(v) = \frac{1}{2}\sum_{i\neq j}|v_i - v_j|^2. \quad (2.5)$$

Then there exists a constant B_0 *such that* $\Gamma(x(t)) \leq B_0$ *for all* $t \in \mathbb{R}^+$ *while* $\Lambda(v(t))$ *converges toward zero as* $t \to +\infty$*, and the vectors* $x_i - x_j$ *tend to a limit vector* $\hat{x}_{ij}$*, for all* $i, j \leq N$*.*

We highlight that the result has been improved in the case $\gamma = 1/2$ for any initial data in [52]. Therefore in the case $\gamma \leq 1/2$ we will refer to unconditional alignment (or flocking) given that the velocities alignment does not depend on initial configuration of the system or on dimensionality. In this case all the agents of the population have the same velocity, they form a group with fixed mutual distances with a spatial profile which depends on the initial condition. If $\gamma > 1/2$ flocking may be expected under the condition of equation (2.4).

8.2.2 Cucker–Smale model dependent on random input

In what follows we will denote with $(\Omega, \mathcal{F}, P)$ the probability space where we define the random variable $\theta : (\Omega, \mathcal{F}) \to (\mathbb{R}, \mathcal{B}_{\mathbb{R}})$, where $\mathcal{F}$ a $\sigma-$algebra and $\mathcal{B}_{\mathbb{R}}$ the Borel set of $\mathbb{R}$. We will also assume that $\theta \in \Omega$ is endowed with known distribution function $g(\theta) \in \mathcal{P}(\Omega)$.

The CS may be affected by stochasticity in several way. In the following we enumerate possible stochastic dynamics depending on a single random input $\theta \in \Omega$:

a) Random perturbation of the initial data, i.e. for all $i = 1, \ldots, N$

$$x_i(\theta, 0) = x_i^0(\theta), \qquad v_i(\theta, 0) = v_i^0(\theta), \quad (2.6)$$

with known interaction function $H(x_i, x_j)$. Therefore the dynamics is written for all $i = 1, \dots, N$ as

$$\begin{cases} \dot{x}_i(\theta, t) = v_i(\theta, t), & x_i(\theta, 0) = x_i^0(\theta), v_i(\theta, 0) = v_i^0(\theta), \\ \dot{v}_i(\theta, t) = \dfrac{1}{N} \displaystyle\sum_{j=1}^{N} H(x_i(\theta, t), x_j(\theta))(v_j(\theta, t) - v_i(\theta, t)), \end{cases} \tag{2.7}$$

b) Random strength of interactions

$$H(x_i, x_j, \theta) = \frac{K(\theta)}{(1 + |x_i(\theta, t) - x_j(\theta, t)|^2)^\gamma}, \tag{2.8}$$

with $x_i(\theta, 0) = x_i^0$, $x_j(\theta, 0) = x_j^0$ and $\gamma > 0$ a given constants. A further simplification may be done by considering an interaction depending on the expected locations $\bar{x}_{i,j} = \mathbb{E}_\theta[x_{i,j}(\theta, t)]$. In this simplified situation we may rewrite the interaction function in (2.8) as

$$H(\bar{x}_i, \bar{x}_j, \theta) = K(\theta) H^{\text{det}}(\bar{x}_i, \bar{x}_j), \tag{2.9}$$

with

$$H^{\text{det}}(\bar{x}_i, \bar{x}_j) = H^{\text{det}}(|\bar{x}_i - \bar{x}_j|) := \frac{1}{(1 + |\bar{x}_i - \bar{x}_j|^2)^\gamma}. \tag{2.10}$$

c) Random alignment parameter

$$H(x_i, x_j, \theta) = \frac{K}{(1 + |x_i - x_j|^2)^{\gamma(\theta)}}, \tag{2.11}$$

with $K > 0$ is a constant, and the initial locations and velocities of the dynamics $x_i(\theta, 0) = x_i^0$ and $x_j(\theta, 0) = x_j^0$ are given. Again, a simplification may be done by considering an interaction depending on the expected locations $\bar{x}_{i,j} = \mathbb{E}_\theta[x_{i,j}(\theta, t)]$ in equation (2.11).

In the cases described by $(b) - (c)$ the Cucker–Smale model assumes the form

$$\begin{cases} \dot{x}_i(\theta, t) = v_i(\theta, t), & x_i(\theta, 0) = x_i^0, v_i(\theta, 0) = v_i^0, \\ \dot{v}_i(\theta, t) = \dfrac{1}{N} \displaystyle\sum_{j=1}^{N} H(x_i, x_j, \theta)(v_j(\theta, t) - v_i(\theta, t)), \end{cases} \tag{2.12}$$

where x_i^0, x_j^0 are given and the interaction function $H(x_i, x_j, \theta)$ is of the type described in (2.8) and (2.11). We can prove the following result

Lemma 8.2.2. *Let us consider the stochastic Cucker–Smale model* $(a) - (b) - (c)$*, then the mean velocity of the system is conserved in time*

$$\mathcal{V}(\theta, t) = \frac{1}{N} \sum_{i=1}^{N} v_i(\theta, t), \qquad \frac{d}{dt} \mathcal{V}(\theta, t) = 0. \tag{2.13}$$

Proof. We show the result in the setting of $(b)-(c)$. From (2.12) we have

$$\sum_{i=1}^{N}\sum_{j=1}^{N} H(x_i,x_j,\theta)v_j(\theta,t) = \sum_{i=1}^{N}\sum_{j=1}^{N} H(x_i,x_j,\theta)v_i(\theta,t), \tag{2.14}$$

and therefore $\mathcal{V}(\theta,t) = \mathcal{V}(\theta,0)$, for all $t \geq 0$. Similar considerations hold true in the case (a). □

In the non homogeneous case we can prove the following result for the evolution of the system of agents whose proof is reminiscent of well established results in the literature [52, 139].

Proposition 8.2.3. *Let $(\Omega,\mathcal{F},P)$ be a probability space and let us consider the evolution of the stochastic Cucker–Smale model in case of random strength as described in (2.8), i.e.*

$$\begin{cases} \dot{x}_i(\theta,t) = v_i(\theta,t), & i=1,\dots,N \\ \dot{v}_i(\theta,t) = \dfrac{1}{N}\sum_{j=1}^{N} \dfrac{K(\theta)}{(1+|x_i(\theta,t)-x_j(\theta,t)|^2)^{\gamma}}(v_j(\theta,t)-v_i(\theta,t)), \end{cases} \tag{2.15}$$

subject to deterministic initial conditions $x_i(\theta,0) = x_i^0$, $v_i(\theta,0) = v_i^0$ for all $i=1,\dots,N$. The support of the velocities exponentially collapse for large time for each $\theta \in \Omega$ provided $K(\theta) \geq 0$.

Proof. We considered deterministic initial conditions, therefore we can fix the positive radii $R_0^x > 0$ and $R_0^v > 0$ such that all the initial positions and velocities lie inside the discs $B(x,R_0^x)$ and $B(0,R_0^v)$ respectively. For each $\theta \in \Omega$ the solutions of the system are $C^1([0,\infty),\mathbb{R}^{2d})$, we define then for each $t \in [0,\infty)$

$$R^v(\theta,t) := \max_{i=1,\dots,N} |v_i(\theta,t)|. \tag{2.16}$$

Fix $\theta \in \Omega$, over each time interval (t_k,t_{k+1}) we can chose the index i such that $R^v(\theta,t) = |v_i(\theta,t)|$ for all $t \in (t_k,t_{k+1})$. Therefore, form an explicit calculation we have

$$\begin{aligned} \frac{d}{dt}R^v(\theta,t)^2 = &-\frac{2}{N}\sum_{j\neq i}[(v_i(\theta,t)-v_j(\theta,t))v_i(\theta,t)] \\ &\cdot \frac{K(\theta)}{(1+(|x_i(\theta,t)-x_j(\theta,t)|^2)^{\gamma}}. \end{aligned} \tag{2.17}$$

Being $(v_i(\theta,t)-v_j(\theta,t))v_i(\theta,t) \geq 0$, thanks to the choice of the index i, and $H(x_i,x_j,\theta) \geq 0$, we have that $R^v(\theta,t)$ is non-increasing and then for all $\theta \in \Omega$ and all $t \geq 0$ $R^v(\theta,t) \leq R_0^v$.

From the evolution of the position variable we have for all $\theta \in \Omega$ and $t \geq 0$

$$|x_i(\theta,t) - x_i^0| \leq 2R_0^v + R_0^v t, \tag{2.18}$$

thus

$$H(x_i(\theta,t),x_j(\theta,t),\theta) \geq \frac{K(\theta)}{(1+4R_0^2(1+t^2))^\gamma}, \tag{2.19}$$

with $R_0 = \min(R_0^x, R_0^v)$. Now, from (2.17) we have

$$\begin{aligned} \frac{d}{dt}R^v(\theta,t)^2 &\leq -\frac{2K(\theta)}{N(1+4R_0(1+t^2))^\gamma}\sum_{j\neq i}(v_i(\theta,t)-v_j(\theta,t))v_i(\theta,t) \\ &= -\frac{2K(\theta)}{(1+4R_0(1+t^2))^\gamma}R^v(\theta,t)^2. \end{aligned} \tag{2.20}$$

From the Gronwall's lemma we have for each $\theta \in \Omega$ and all $t \geq 0$

$$R^v(\theta,t) \leq R_0^v \exp\left(-\frac{1}{2}\int_0^f f(s)ds\right), \tag{2.21}$$

then, being

$$\lim_{t\to+\infty} t^{2\gamma} f(t) = \left(\frac{1}{R_0^2}\right)^\gamma, \tag{2.22}$$

we have that the function $f(t)$ is not integrable asymptotically for $\gamma \geq 1/2$ and

$$\lim_{t\to+\infty}\int_0^t f(s)ds = +\infty, \tag{2.23}$$

from which we conclude. □

Following a similar argument of [52] it is also possible in the hypotheses of Proposition 8.2.3 to prove that there exists $R_1^x > 0$ such that for all $\theta \in \Omega$ and $t \geq 0$

$$|x_i(\theta,t) - x_i^0| \leq R_1^x, \qquad i = 1,\dots,N. \tag{2.24}$$

This implies that $x_i(\theta,t) \in B(x,\bar{R}^x)$ with $\bar{R}^x = R_1^x + R_0^x$.

Remark 12. *In the simplified situation*

$$H(x_i,x_j,\theta) = K(\theta)H^{det}(\bar{x}_i,\bar{x}_j)$$

what has been proved in Proposition 8.2.3 still holds true, in fact

$$|x_i(\theta,t) - x_j(\theta,t)| \leq 2R_0^x + 2R_0^v \tag{2.25}$$

and we have

$$\left|\int_\Omega (x_i(\theta,t) - x_i(\theta,t))g(\theta)d\theta\right| = |\bar{x}_i - \bar{x}_j| \leq 2R_0^x + 2R_0^v. \tag{2.26}$$

Therefore for all $t \geq 0$, $\theta \in \Omega$ and $i,j = 1,\dots,N$

$$H^{det}(|\bar{x}_i - \bar{x}_j|) \geq \frac{1}{(1+4R_0^2(1+t^2))^\gamma}. \tag{2.27}$$

Let us consider the evolution of the system (2.12) with interaction function described in the case (c) with deterministic initial conditions

$$H(\bar{x}_i, \bar{x}_j\theta) = \frac{K}{(1+|\bar{x}_i - \bar{x}_j|^2)^{\gamma(\theta)}}. \tag{2.28}$$

We study the behavior of the system of agents in a neighborhood of the deterministic value $\gamma_0 \leq 1/2$ for which unconditional alignment does emerge. In other words we linearize the function $H(\cdot,\cdot,\cdot)$ as follows

$$H(\bar{x}_i, \bar{x}_j, \theta) = H(\bar{x}_i, \bar{x}_j, \gamma_0) + \frac{\partial H}{\partial \gamma}(\bar{x}_i, \bar{x}_j, \tilde{\gamma})(\gamma(\theta) - \gamma_0), \tag{2.29}$$

with

$$\tilde{\gamma} = \lambda\gamma_0 + (1-\lambda)\gamma(\theta), \qquad \lambda \in [0,1]. \tag{2.30}$$

Then (2.29) corresponds to

$$\begin{aligned} H(\bar{x}_i, \bar{x}_j, \theta) =& H(\bar{x}_i, \bar{x}_j|, \gamma_0) \\ &- \frac{K\log(1+|\bar{x}_i - \bar{x}_j|^2)}{(1+|\bar{x}_i - \bar{x}_j|^2)^{\tilde{\gamma}}}(\gamma(\theta) - \gamma_0) + \mathcal{O}(\gamma^2), \end{aligned} \tag{2.31}$$

Therefore, in a neightbourhood of γ_0 the function $H(\cdot,\cdot,\cdot)$ may be approximated as follows

$$\begin{aligned} H(\bar{x}_i, \bar{x}_j, \theta) \approx& H(\bar{x}_i, \bar{x}_j, \gamma_0) \\ &- \log(1+|\bar{x}_i - \bar{x}_j|^2) H(\bar{x}_i, \bar{x}_j, \gamma_0)(\gamma(\theta) - \gamma_0). \end{aligned} \tag{2.32}$$

Hence, in this case the dynamics (2.12) may be formulated as follows

$$\begin{cases} \dot{x}_i(\theta,t) = & v_i(\theta,t), \\ \dot{v}_i(\theta,t) = & \dfrac{1}{N}\displaystyle\sum_{j=1}^{N} H(\bar{x}_i, \bar{x}_j, \gamma_0)(v_j(\theta,t) - v_i(\theta,t)) \\ & -\dfrac{1}{N}\displaystyle\sum_{j=1}^{N} H(\bar{x}_i, \bar{x}_j, \gamma_0)\log(1+|\bar{x}_i - \bar{x}_j|^2) \\ & \qquad (\gamma(\theta) - \gamma_0)(v_j(\theta,t) - v_i(\theta,t)). \end{cases} \tag{2.33}$$

Proposition 8.2.4. *Let $(\Omega, \mathcal{F}, P)$ be a probability space and let us consider the evolution of (2.12) with interaction as in (2.28). In a neighborhood of $\gamma_0 \leq 1/2$, the asymptotic convergence of the velocities is therefore guaranteed if*

$$\gamma(\theta) < \gamma_0 + \frac{1}{\log(1+\bar{R}^x)}, \tag{2.34}$$

for all $\theta \in \Omega$, where $\bar{R}^x$ depends only on the initial particles' locations.

Proof. In a neighborhood of $\gamma_0 \leq 1/2$ the dynamics may be linearized as in (2.33), from which we obtain the condition

$$\gamma(\theta) < \gamma_0 + \frac{1}{\log(1 + |\bar{x}_i - \bar{x}_j|)}, \tag{2.35}$$

for all $i, j = 1, \dots, N$. Thanks to what we have shown we know that there exists $\bar{R}^x$ such that $|\bar{x}_i - \bar{x}_j| \leq \bar{R}^x$, $i \neq j$, for all $t \geq 0$ form which we have

$$\log(1 + |\bar{x}_i - \bar{x}_j|) \leq \log(1 + \bar{R}^x). \tag{2.36}$$

Thus the condition (2.35) assumes the following form

$$\gamma(\theta) < \gamma_0 + \frac{1}{\log(1 + \bar{R}^x)}, \tag{2.37}$$

for all $\theta \in \Omega$. □

Remark 13. *The evolution of the expected locations and velocities may be obtained from* (2.33) *by direct integration of the random variable, which gives*

$$\begin{cases} \bar{x}_i(t) &= \bar{v}_i(t), \\ \bar{v}_i(t) &= \dfrac{1}{N}\displaystyle\sum_{j=1}^{N} H(|\bar{x}_i - \bar{x}_j|, \gamma_0)(\bar{v}_j(\theta, t) - \bar{v}_i(\theta, t)) \\ & \quad -\dfrac{1}{N}\displaystyle\sum_{j=1}^{N} H(|\bar{x}_i - \bar{x}_j|, \gamma_0)\log(1 + |\bar{x}_i - \bar{x}_j|^2) \\ & \qquad \cdot \int_\Omega (\gamma(\theta) - \gamma_0)(v_j(\theta, t) - v_i(\theta, t))dw(\theta), \end{cases} \tag{2.38}$$

and the support of the expected velocities collapses if the condition (2.37) *is satisfied.*

8.3 Mean-field limit of stochastic models

In what follows we sketch a formal way to obtain the mean-field limit of the Cucker–Smale model dependent from a random quantity.

Let us consider first the case (a) in Section 8.2. Here the stochasticity affects the initial values of the problem whereas the coefficients of the interaction are supposed to be deterministic. In this case for each fixed $\theta \in \Omega$ we define the empirical distribution density associated to a solution of (2.7) as follows

$$f^N(x, v, \theta, t) = \frac{1}{N}\sum_{i=1}^{N} \delta(x - x_i(\theta, t))\delta(v - v_i(\theta, t)), \tag{3.1}$$

with δ the Dirac delta distribution. We observe how for each $t \geq 0$ and $\omega \in \Omega$ the empirical measure define a probability measure in $\mathcal{P}(\mathbb{R}^{2d})$. We assume that for each $t \geq 0$ and $\theta \in \Omega$ the particles $(x_i(\theta,t), v_i(\theta,t))_{i=1}^N \in \bar{S} \subset \mathbb{R}^{2d} \times \mathbb{R}^{2d}$ remain in a fixed compact domain. For the Cucker–Smale model the hypothesis is fulfilled by considering, for example, a compactly supported initial distribution $f(x,v,\theta,0)$. In such a way, thanks to the Prohorov's theorem we have that the sequence $f^N(x,v,\theta,t)$ is weakly-*-relatively-compact and there exists a subsequence $(f^{N_k}(x,v,\theta,t))_k$ and a function $f : \mathbb{R} \to \mathcal{P}(\mathbb{R}^{2d})$ such that

$$f^{N_k} \to_{k\to+\infty} f, \qquad \text{weak*-convergence in } \mathcal{P}(\mathbb{R}^{2d}), \tag{3.2}$$

pointwise in time and almost surely with respect to $\theta \in \Omega$. Therefore, in a similar fashion of [53] we may obtain the mean-field version of the Cucker–Smale model of flocking in the hypothesis (a) which corresponds to

$$\partial_t f(x,v,\theta,t) + v \cdot \nabla_x f(x,v,\theta,t) = \nabla_v \cdot [\mathcal{H}[f](x,v,\theta,t) f(x,v,\theta,t)], \tag{3.3}$$

where

$$\mathcal{H}[f](x,v,\theta,t) = \int_{\mathbb{R}^{2d}} \frac{K}{(1+|x-y|^2)^\beta}(v-w) f(y,w,\theta,t) dy dw, \tag{3.4}$$

and $f(x,v,\theta,0) = f^0(x,v,\theta)$.

We derive the mesoscopic level of description in the cases (b) and (c) making use of BBGKY hierarchy in statistical mechanics [63, 109]. Let us define the $N-$particle density function

$$f^{(N)} = f^{(N)}(x_1, v_1, \dots, x_N, v_N, \theta, t), \tag{3.5}$$

whose evolution, tanks to the mass conservation, is described in the terms of the Liouville equation

$$\partial_t f^{(N)} + \sum_{i=1}^N v_i \cdot \nabla_{x_i} f^{(N)} = -\frac{1}{N} \sum_{i=1}^N \nabla_{v_i} \cdot \left(\sum_{j=1}^N H(x_i, x_j, \theta)(v_j - v_i) f^{(N)} \right). \tag{3.6}$$

Further, we define the marginal distribution

$$f^{(1)}(x_1, v_1, \theta, t) = \int_{\mathbb{R}^{2d(N-1)}} f^{(N)}(x_1, v_1, x_{2,\dots,N}, v_{2,\dots,N}, \theta, t) dx_{2,\dots,N} dv_{2,\dots,N}, \tag{3.7}$$

where

$$(x_{2,\dots,N}, v_{2,\dots,N}) = (x_2, v_2, \dots, x_N, v_N). \tag{3.8}$$

By direct integration of (3.6) against $dx_{2,\dots,N}, dv_{2,\dots,N}$ the transport term corresponds to

$$\int_{\mathbb{R}^{2d(N-1)}} \sum_{i=1}^{N} v_i \nabla_{x_i} f^{(N)} dx_{2,\dots,N} dv_{2,\dots,N} = v_1 \nabla_{x_1} f^{(1)}(x_1, v_1, \theta, t). \tag{3.9}$$

For what it may concern the last term of (3.6), thanks to the interchangeability of the particles we have

$$\begin{aligned} &\frac{1}{N} \sum_{i=1}^{N} \int_{\mathbb{R}^{2d(N-1)}} \sum_{j=1}^{N} \nabla_{v_i} H(x_i, x_j, \theta)(v_j - v_i) f^{(N)} dx_{2,\dots,N} dv_{2,\dots,N} = \\ &\frac{1}{N} \int_{\mathbb{R}^{2d(N-1)}} \sum_{j=2}^{N} \nabla_{v_1} H(x_1, x_j, \theta)(v_j - v_1) f^{(N)} dx_{2,\dots,N} dv_{2,\dots,N}, \end{aligned} \tag{3.10}$$

By taking a closer look to this term we can observe how, thanks to the symmetry of the problem for all $2 \leq j, k \leq N$, $j \neq k$ we have

$$\begin{aligned} &\int_{\mathbb{R}^{2d(N-1)}} H(x_1, x_j, \theta)(v_j - v_1) f^{(N)} dx_{2,\dots,N} dv_{2,\dots,N} = \\ &\int_{\mathbb{R}^{2d(N-1)}} H(x_1, x_k, \theta)(v_k - v_1) f^{(N)} dx_{2,\dots,N} dv_{2,\dots,N}. \end{aligned} \tag{3.11}$$

Therefore (3.10) corresponds to

$$\frac{N-1}{N} \int_{\mathbb{R}^{2d(N-1)}} H(x_1, x_2, \theta)(v_2 - v_1) f^{(N)} dx_{2,\dots,N} dv_{2,\dots,N}. \tag{3.12}$$

Similarly to $f^{(1)}(x_1, v_1, \theta, t)$, let us define then the marginal density function $f^{(2)}(x_1, v_1, x_2, v_2, \theta, t)$ as

$$f^{(2)}(x_1, v_1, x_2, v_2, \theta, t) = \int_{\mathbb{R}^{2d(N-2)}} f^{(N)} dx_{3,\dots,N} dv_{3,\dots,N}. \tag{3.13}$$

We can then reformulate (3.12) as

$$\frac{N-1}{N} \nabla_{v_1} \int_{\mathbb{R}^{2d}} H(x_1, x_2, \theta)(v_2 - v_1) f^{(2)} dx_2 dv_2. \tag{3.14}$$

Finally, the integration of (3.6) against $dx_{2,\dots,N}, dv_{2,\dots,N}$ gives

$$\begin{aligned} &\partial_t f^{(1)}(x_1, v_1, \theta, t) + v_1 \cdot \nabla_{x_1} f^{(1)} = \\ &\qquad - \frac{N-1}{N} \int_{\mathbb{R}^{2d}} H(x_1, x_2, \theta, t)(v_2 - v_1) f^{(2)} dx_2 dv_2. \end{aligned} \tag{3.15}$$

Now, we define

$$\begin{aligned} f(x_1, v_1, \theta, t) &= \lim_{N \to +\infty} f^{(1)}(x_1, v_1, \theta, t), \\ \tilde{f}(x_1, v_1, x_2, v_2, \theta, t) &= \lim_{N \to +\infty} f^{(2)}(x_1, v_1, x_2, v_2, \theta, t), \end{aligned} \tag{3.16}$$

and we make the usual ansatz for the propagation of chaos

$$\tilde{f}(x_1, v_1, x_2, v_2, \theta, t) = f(x_1, v_1, \theta, t) f(x_2, v_2, \theta, t). \tag{3.17}$$

From (3.15) we have

$$\partial_t f(x, v, \theta, t) + v \cdot \nabla_x f(x, v, \theta, t) = \nabla_v \left[\mathcal{H}[f](x, v, \theta, t) f(x, v, \theta, t) \right], \tag{3.18}$$

where

$$\mathcal{H}[f](x, v, \theta, t) = \int_{\mathbb{R}^{2d}} H(x, y, \theta)(v - w) f(y, w, \theta, t) dw dy, \tag{3.19}$$

and the definition of $H(x, y, \theta)$ depends on special case introduced in Section 8.2.

We highlight how, for the simplified formulations for the N agent microscopic system obtained by considering for all $i, j = 1, \dots, N$ the interaction $H(\bar{x}_i, \bar{x}_j, \theta)$, we cannot consider standard techniques in order to derive the mean-field equation. The mean–field formulation which may be derived is unknown in the actual state of the art.

8.4 Numerics

In this section we make use of the Stochastic Galerkin (SG) numerical methods for differential problem focussing on the alignment model introduced in the latter section. In particular we will apply a numerical technique called generalized polynomial chaos (gPC) developed in recent years based on SG [13, 77, 97, 176, 177]. For this reason in the following we refer to these methods as gPC-SG.

Further, we propose a novel approach for the derived mean–field equations of the latter section of this chapter having roots in the mean–field Monte Carlo methods developed in [8, 9] where the particle dynamics is now computed through SG-gPC scheme.

8.4.1 gPC approximation

We consider a basis of the polynomial space $\mathbb{P}^M$ given by the set of M orthogonal polynomials $\{\Phi_k(\theta)\}_{k=0}^M$. We approximate the position and the velocity of the ith agent as follows

$$x_i(\theta, t) \approx x_i^M = \sum_{k=0}^{M} \hat{x}_{i,k}(t) \Phi_k(\theta), \qquad v_i(\theta, t) \approx v_i^M = \sum_{k=0}^{M} \hat{v}_{i,k} \Phi_k(\theta), \tag{4.1}$$

where

$$\hat{x}_{i,k} = \mathbb{E}_\theta[x_i(\theta, t)\Phi_k(\theta)], \qquad \hat{v}_{i,k} = \mathbb{E}_\theta[v_i(\theta, t)\Phi_k(\theta)]. \tag{4.2}$$

From (2.15) we obtain the following chaos expansion for (x_i^M, v_i^M)

$$\begin{cases} \dfrac{d}{dt}\displaystyle\sum_{k=0}^{M}\hat{x}_{i,k}(t)\Phi_k(\theta) = \sum_{k=0}^{M}\hat{v}_{i,k}(t)\Phi_k(\theta), \\ \dfrac{d}{dt}\displaystyle\sum_{k=0}^{M}\hat{v}_{i,k}(t)\Phi_k(\theta) = \frac{1}{N}\sum_{j=1}^{N}\sum_{r=0}^{M} H(x_i(\theta,t), x_j(\theta,t),\theta)(\hat{v}_{i,r}(t) - \hat{v}_{j,r})\Phi_r(\theta) \end{cases}$$

Upon multiplying (8.4.1) by the orthogonal polynomial $\Phi_h(\theta)$ for each $h = 0,\dots,M$ and integrating with respect to the random variable, thanks to the orthogonality, we obtain the following set of equations for each agent $i = 1,\dots,N$

$$\begin{cases} \dfrac{d}{dt}\hat{x}_{i,h}(t) &= \hat{v}_{i,h}(t), \\ \dfrac{d}{dt}\hat{v}_{i,h}(t) &= \dfrac{1}{N}\displaystyle\sum_{j=1}^{N}\sum_{r=0}^{M} e_{rh}^{ij}(\hat{v}_{j,r}(t) - \hat{v}_{i,r}(t)) \end{cases} \tag{4.3}$$

where

$$e_{rh}^{ij} = \frac{1}{\|\Phi_h(\theta)\|^2}\int_\Omega \frac{K(\theta)}{(1+|x_i^M - x_j^M|^2)^\gamma}\Phi_r(\theta)\Phi_h(\theta)dg(\theta), \tag{4.4}$$

define a time-dependent matrix $\mathcal{E} = \left[e_{rh}^{ij}\right]_{r,h=0,\dots,M}$

Remark 14. *Numerically we observe how equation (4.4) induces a high computational cost, forcing to estimate an integral for each time step. In the simplified situation $H(x_i, x_j, \theta) = K(\theta)H^{det}(\bar{x}_i, \bar{x}_j)$ the dynamics in (4.3) assumes the form*

$$\begin{cases} \dfrac{d}{dt}\hat{x}_{i,h}(t) &= \hat{v}_{i,h}(t), \\ \dfrac{d}{dt}\hat{v}_{i,h}(t) &= \dfrac{1}{N}\displaystyle\sum_{j=1}^{N} H^{det}(\bar{x}_i, \bar{x}_j)\sum_{r=0}^{M} e_{rh}(\hat{v}_{j,r}(t) - \hat{v}_{i,r}(t)), \end{cases} \tag{4.5}$$

with

$$e_{rh} = \frac{1}{\|\Phi_h\|^2}\int_\Omega K(\theta)\Phi_r(\theta)\Phi_h(\theta)dg(\theta). \tag{4.6}$$

From (4.6) the square matrix $\mathcal{E} = \{e_{rh}\}_{r,h=0,\dots,M}$ may be precomputed before the dynamics, dramatically decreasing the computational efforts.

8.4.2 MC–gPC methods for mean-field equations

In Section 8.3 we formally derived the mesoscopic description of a system of agents of the introduced stochastic alignment dynamics. In what follows

we propose a novel computational methods for mean–field equations capable to efficiently approximate statistical quantities of the system and to conserve their positivity.

We remark how the statistical quantities of the mean–field equations may be derived from their gPC decomposition (MF–gPC), in fact we may obtain with standard passages

$$\partial_t \hat{f}_h(x,v,t) + v \cdot \nabla_x \hat{f}_h(x,v,t) = \nabla_v \left[\sum_{r=0}^{M} \mathcal{H}_{rh}(x,v,t) \hat{f}_r(x,v,t) \right], \qquad (4.7)$$

with

$$\mathcal{H}_{rh} = \frac{1}{\|\Phi_h\|^2} \int_{\mathbb{R}^{2d}} \int_{\Omega} H(x,y,\theta)\Phi_h(\theta)\Phi_r(\theta) dg(\theta) d\theta (v-w) \hat{f}_r(y,w,t) dw dy$$

and $f^M(x,v,\theta,t) \approx \sum_{k=0}^{M} \hat{f}_k(x,v,t)\Phi_k(\theta)$. Similarly to classical spectral methods, the solution of (4.7) is not positive in each polynomial space and the necessary positivity of statistical quantities cannot be guaranteed. This fact represents a serious drawback for the description of transport phenomena in collective behavior. In fact, the main motivation of these models is to give real science approximation, further, at the actual state of the art, steady state solutions are often determined through energy inequalities [22, 50, 148], generating entropy schemes [148].

In order to overcome these difficulties, in what follows, we propose an effective numerical methods for the solution of mean–field equations of the collective behavior dependent on random parameters having roots in the mean-field Monte Carlo algorithm (MF–MC) proposed in [8, 9]. We will refer to the resulting numerical scheme as MC–gPC. In Figure 4.1 we represent through a scheme the approach to MF equations depending on a random input. In particular the right branch of the scheme introduce the MC-gPC algorithm which allow to preserve the positivity of macroscopic statistical quantities like mean and variance.

Recall that the main advantage of deriving numerical scheme at the mesoscopic level relies in its computational cost. In fact, in a purely particle setting nonlocal nonlinear mean-field equations are extremely expensive with an overall cost of $\mathcal{O}(M^2N^2)$. We can reduce this cost by using a Monte Carlo evaluation of the summation term as described in Algorithm 8.4.1. The overall cost of a MC-gPC is in fact $\mathcal{O}(M^2SN)$, where $S \leq N$.

Algorithm 8.4.1 (**MC-gPC for MF stochastic equations**).

1. *Consider N samples $(x_i(\theta,t), v_i(\theta,t))$ with $i = 1,\dots,N$ computed from the distribution $f(x,v,\theta,t)$, initial deterministic distribution $f_0(x,v)$, and $S \leq N$;*

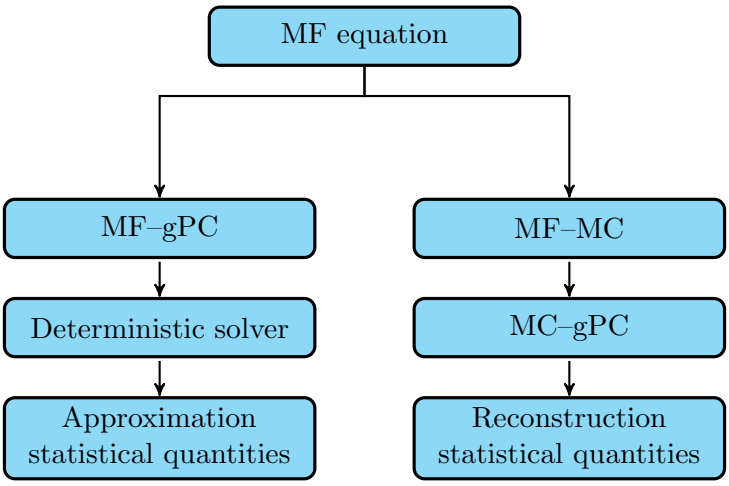

Figure 4.1: In this graph we sketch the two possible approach to numerical solution of MF equation depending on a random input. On the left, we first project through SG techniques the MF equation, a deterministic solver solves the coupled system of equations in order to post-process the statistical quantities of interest. On the right, we propose an alternative method relying on the MF–MC algorithm: the MF equation is formulated at the particle level, gPC–SG scheme determine the spectrally accurate evolution of the at the micro level we can reconstruct statistical informations like mean and variance.

2. *for* $n = 0$ *to* $T - 1$

   for $i = 1$ *to* N

   a) *sample* S *particles* $j_1, \dots, j_S$ *uniformly without repetition among all particles;*

   b) *perform gPC-SG up to order* $M \geq 0$ *over the set of* $S \leq N$ *particles: we need to compute the dynamics for* $(\hat{x}_{j_s,h}, \hat{v}_{j_s,h})$ *where* $s = 1, \dots, S$ *and* $h = 0, \dots, M$.

   c) *compute the velocity change*

$$\hat{v}_{i,h}^{n+1} = \hat{v}_{i,h} + \frac{\Delta t}{S} \sum_{s=1}^{S} \sum_{r=0}^{M} e_{rh}^{ij_s} (\hat{v}_{j_s,r} - \hat{v}_{i,r})$$

   end for

3. *Reconstruction* $\mathbb{E}_\theta[f(x, v, \theta, n\Delta t)]$.

end for

The overall cost of the introduced algorithm reduces to $\mathcal{O}(M^2SN)$, of course in the case $S = N$ we obtain the original cost for the explicit Euler for an N particle system. Observe that the introduced method is still spectrally accurate with respect to the random variable $\theta \in \Omega$.

8.4.3 Applications

In this section we present some numerical experiments for the behavior of alignment models dependent of a random input. We first show how a random alignment model of the Cucker–Smale type evolves both in the case of random strength of interaction and in the case of stochastic alignment parameter, namely the cases $(b) - (c)$ described in Section 8.2. Hence, we will the MCgPC numerical strategy for mean–field equations. In particular we will show how the method is spectrally accurate for the random quantities and preserves the positivity of the mean distribution.

Test 1: The particle case

In Figure 4.2 we present the evolution of a population of four flocks with centers in $(-1,1),(1,1),(1,-1),(-1,-1)$, radius $1/2$ and velocities given by the outbound normal unit vector. The interaction strength $K(\theta)$ is here supposed to be dependent on a random input $\theta \sim U([-1,1])$, in particular we considered $K(\theta) = (\theta+1)/10 \geq 0$.

We solved the approximating gPC system by considering an expansion of order $M = 10$ with Legendre polynomials. The time-integration has been performed through a RK4 method with fixed time step $\Delta t = 10^{-2}$. We can observe how, the velocities of each agent of the system are aligned for large times.

In Figure 4.3 we consider two concentric flocks with radial incoming velocities with unit modulus. Here the interaction is again of the type $H(x_i, x_j, \theta) = K(\theta)H^{\text{det}}(\bar{x}_i, \bar{x}_j)$ with $K(\theta) = (\theta + 2)$ and θ with normal distribution $\theta \sim N(0,1)$. We solved the approximating gPC system by considering an expansion of the order $M = 10$ with Hermite polynomials. The time-integration has been performed through a RK4 method with fixed time step $\Delta t = 10^{-2}$. The presence of negative tails in the distribution of θ forces the mean velocities of the system diverge in finite time. In this case a selective control mechanism capable to drive the velocities toward a desired state has been developed in the last chapter of the present thesis, see [13].

In Figure 4.4 we present the evolution the stochastic CS model of the type (c), i.e. the case of stochastic alignment parameter $\gamma(\theta)$. We considered here the evolution of the randomly perturbed system in a neighborhood of

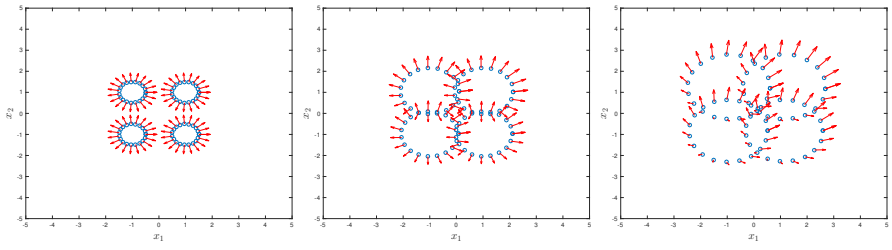

(a) $t = 0$ (b) $t = 0.5$ (c) $t = 1.5$

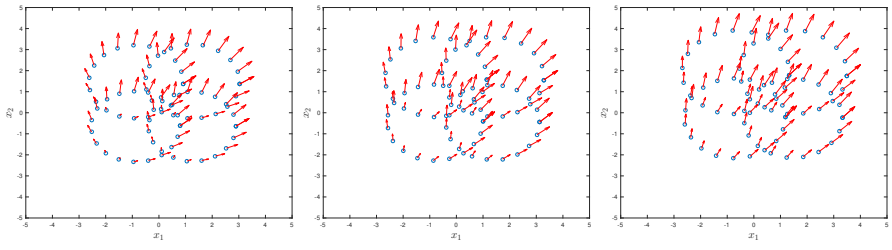

(d) $t = 2.5$ (e) $t = 3.5$ (f) $t = 4.5$

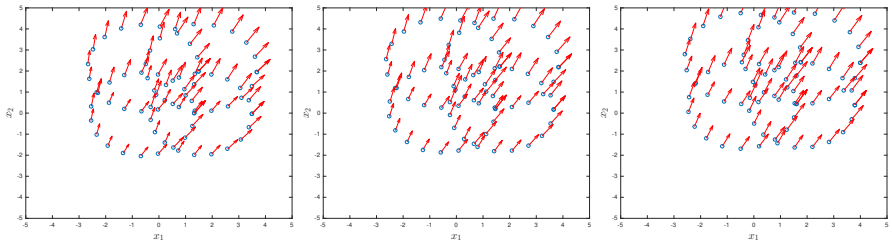

(g) $t = 5.5$ (h) $t = 6.5$ (i) $t = 7.5$

Figure 4.2: Evolution of the stochastic CS model with random strength $K(\theta) = (\theta + 1)/10$, where $\theta \sim U([-1, 1])$. The space-dependent interactions between agents are weighted by $H^{\text{det}}(\bar{x}_i, \bar{x}_j)$, where $\gamma = 0.1$. The model has been approximated by a 10th order gPC-SG coupled system, solved through RK4 with $\Delta t = 10^{-2}$.

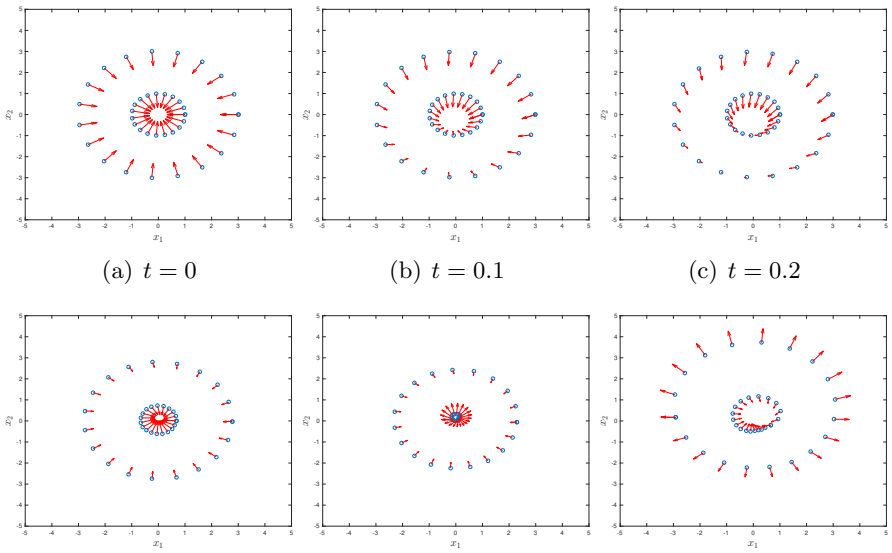

(a) $t = 0$ (b) $t = 0.1$ (c) $t = 0.2$

(d) $t = 0.8$ (e) $t = 0.9$ (f) $t = 1.0$

Figure 4.3: Evolution of the stochastic CS model with random strength $K(\theta) = \theta + 2$, where $\theta \sim N(0, 1)$. The space-dependent interactions between agents are weighted by $H^{\text{det}}(\bar{x}_i, \bar{x}_j)$, where $\gamma = 0.3$. The model has been approximated by a 10th order gPC-SG coupled system, solved through RK4 with $\Delta t = 10^{-2}$.

$\gamma_0 \leq 1/2$. In particular $\gamma(\theta)$ is of the form

$$\gamma(\theta) = \gamma_0 + \epsilon\theta, \qquad \theta \sim U([-1,1]).$$

Hence, the gPC-SG system of equations has been derived by considering Legendre polynomials up to order $M = 10$. We can observe how the system aligns its velocities.

Test 2: The mean–field case

We show in this section the effectivity of the MC–gPC method for large systems of agents. We consider first the uniform interaction case, i.e. $H(x, y, \theta) = K(\theta)$. In Figure 4.5 we compare the behavior of the estimated mean density $\mathbb{E}_\theta[f(x, v, \theta, t)]$ obtained through the MC–gPC algorithm with the one of a standard deterministic solver for the coupled gPC system of deterministic equations

$$\partial_t \hat{f}_h(v,t) = \frac{1}{\|\Phi_h\|^2} \nabla_v \left[\sum_{r=0}^{M} e_{rh} \hat{f}_r(v,t) \right], \tag{4.8}$$

In Figure 4.5 we compare the evolution of $\mathbb{E}_\theta[f(v, \theta, t)]$ computed through $MF - gPC$ and MC–gPC with initial density function $f_0(v)$ of the form

$$f_0(v) = \beta[\exp\{-c(v-2)^2\} + \exp\{-c(v+2)^2\}], \qquad c = 20$$

where β is a normalization constant. we study the convergence of the temperature of the second order moment of the system approximated by a MC–gPC method, with respect to the variable $\theta \sim U([-1, 1])$, $K(\theta) = 2 + \theta > 0$. For the computation we considered $N = 10^6$ particles computing the evolution over the time interval $[0, 1]$ with time step $\Delta t = 10^{-2}$, the MC–gPC method considered an increasing number of interacting particles $S = 10, 10^2, 10^4$.

In Figure 4.6 we report the evolution over $[0, 30]$ of a 2D mean–field non homogeneous Cucker–Smale over the domain $[-4, 4]$ with random interaction $H(x, y, \theta)$ model through MC–gPC. At the microscopic level in particular we considered $H(x_i, x_j, \theta) = H^{\text{det}}(\bar{x}_i, \bar{x}_j)K(\theta)$, $K(\theta) = \theta + 2$ with $\theta \sim U([-1, 1])$. The reconstruction step of the mean density for position and velocity has been done through a 100×100 grid both in space and velocity. We can observe how the velocities of the system are aligned in finite time.

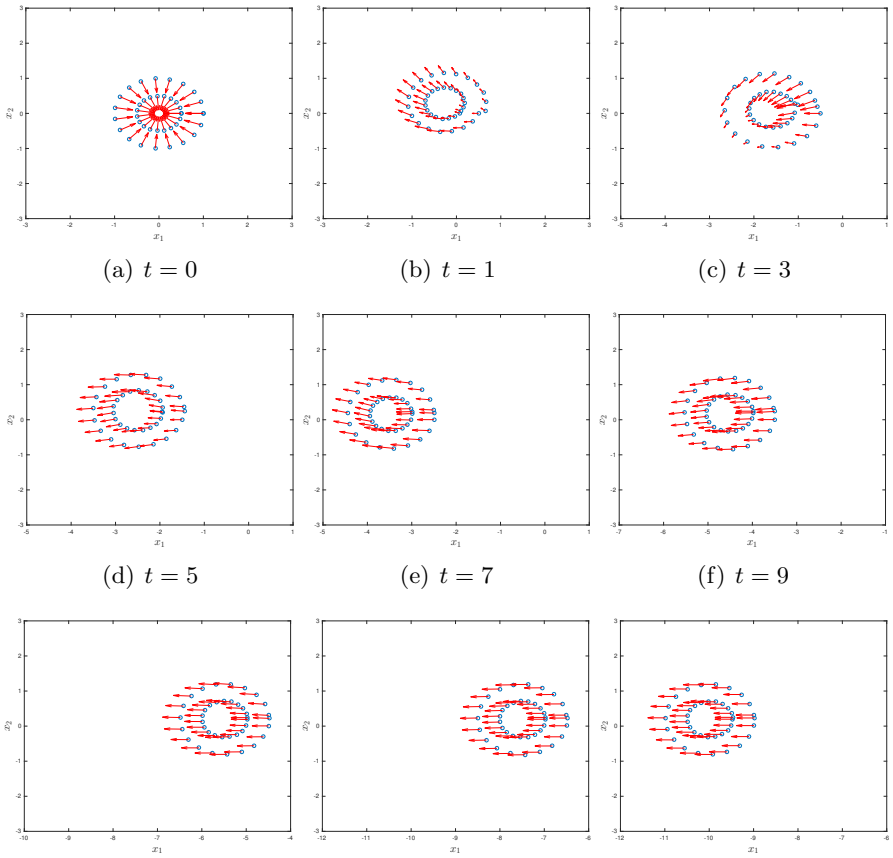

(a) $t = 0$ (b) $t = 1$ (c) $t = 3$

(d) $t = 5$ (e) $t = 7$ (f) $t = 9$

(g) $t = 11$ (h) $t = 15$ (i) $t = 20$

Figure 4.4: Evolution of the stochastic CS model with random exponent $\gamma(\theta)$, where $\gamma_0 = 1/2$, $\epsilon = 0.01$ and $\theta \sim U([-1, 1])$. The space-dependent interactions between agents are weighted by $H^{\text{det}}(\bar{x}_i, \bar{x}_j)$. The model has been approximated by a 10th order gPC-SG system, solved through RK4 with $\Delta t = 10^{-2}$.

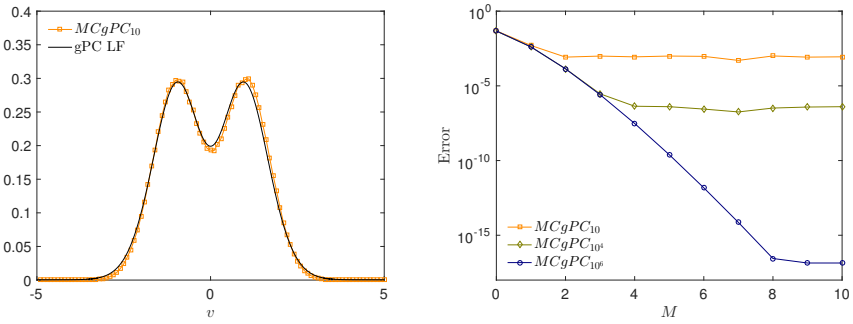

Figure 4.5: Left: we compare the MC–gPC method for the computation of the mean distribution of the homogeneous MF equation, $K(\theta) = \theta + 2$, $\theta \sim U([-1, 1])$, with a deterministic solver of the system of equations (4.8). The MF-gPC is solved through a Lax–Friedrichs scheme with $N = 2001$ gridpoints. Right: relative error for the second order moment for increasing dimension of the polynomial space $M = 0, \dots, 10$. The three curves correspond to MCgPC for an increasing number of interacting particles at each time step, namely $S = 10, 10^2, 10^6$

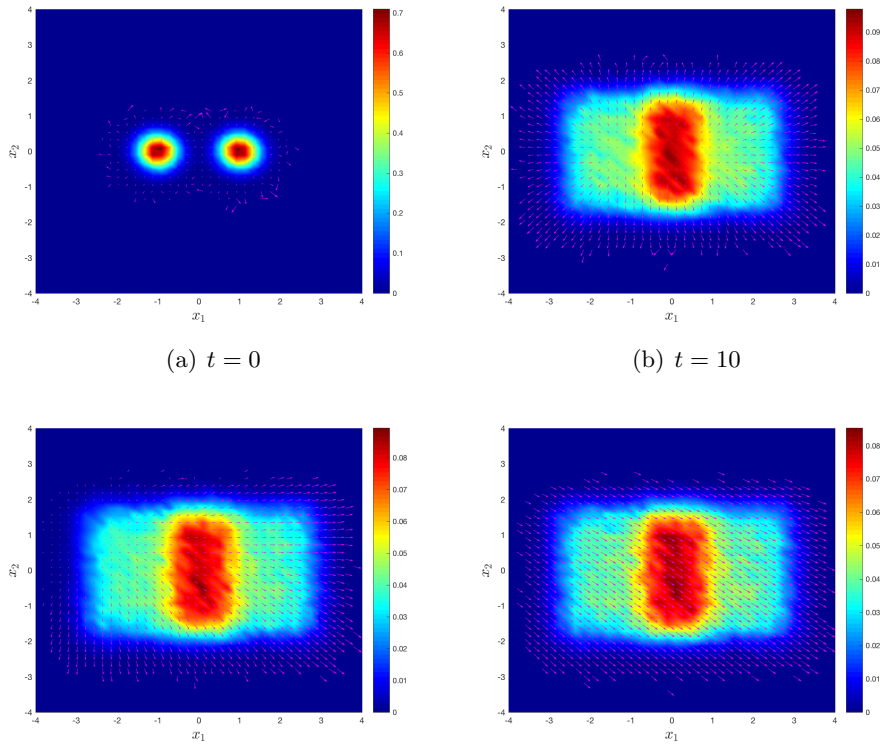

(a) $t = 0$ (b) $t = 10$

(c) $t = 20$ (d) $t = 30$

Figure 4.6: Evolution of the 2D Cucker–Smale type model at the mesoscopic level with $H(x_i, x_j, \theta) = H^{\text{det}}(\bar{x}_i, \bar{x}_j)K(\theta)$, $K(\theta) = \theta + 2$, $\theta \sim U([-1, 1])$. The MC–gPC algorithm has been implemented with $S = 10$ in the mean–field part and $M = 5$ for the gPC.

Appendix A

The Boltzmann equation

The equation that we are going to introduce has been developed by Ludwig Boltzmann in 1872 and it is based on the physical model of a perfect diluite gas of a large but fixed number of particles ($N > 10^{23}$), whose dynamics are regulated in terms of classical Newtonian mechanics. Each particle has its own position and velocity moving of linear motion before a collision with another particle. A fundamental assumption of this model is dictated by the nature of possible collisions, which are assumed to be binary. The collisions between two particles obey to physical conservation laws of momentum and energy. The Boltzmann equation may be derived by considering the Grad limit, see [57, 96, 99, 155] for rigorous computations. Without intending to review the whole literature, some introductory references on the argument are also [56, 169, 170]. In the following we will introduce the physical model proposed by Boltzmann and then we will give some analytic excerpts for the existence of solutions of the related Cauchy problem for the Boltzmann equation in the space homogeneous case.

A.1 Physical model

Let D be an open, limited and regular subset of $\mathbb{R}^3$. For each $t \geq 0$ let $f(x, v, t)$ be a function depending on $x \in D, v \in \mathbb{R}^3$. Therefore we define the Boltzmann equation as follows

$$\begin{cases} \dfrac{\partial f(x,v,t)}{\partial t} + v \cdot \nabla_x f(x,v,t) = Q(f,f) \\ f(x,v,0) = f_0(x,v). \end{cases} \tag{1.1}$$

The function $f : D \times \mathbb{R}^3 \times [0, +\infty) \to \mathbb{R}^+$ is a probability density function in the phase space, i.e. for each time $t \geq 0$ we have

$$\int_{D\times\mathbb{R}^3} f(x,v,t)dxdv = 1. \tag{1.2}$$

In (1.1) we introduced the so-called collision operator

$$Q(f,f)(x,v,t) = \int_{\mathbb{R}^3\times S^2} [f(x,v^*,t)f(x,w^*,t) - f(x,v,t)f(x,w,t)] \\ B\left(|v-w|, \frac{v-w}{|v-w|}\cdot\sigma\right) d\sigma dw, \tag{1.3}$$

where v^*, w^* are the post-collisional velocities given by the transformation

$$\begin{aligned} v^* &= v + [(w-v)\cdot\sigma]\cdot\sigma \\ w^* &= w + [(w-v)\cdot\sigma]\cdot\sigma \end{aligned} \tag{1.4}$$

and with $S^2 = \{\sigma \in \mathbb{R}^3 : |\sigma| = 1\}$ the unit sphere. In equation (1.3) the object $B(\cdot,\cdot)$ is known as collision kernel and the variation of the density function $f(\cdot,\cdot,\cdot)$ is uniquely determined by binary collision of the particles, induced by specific potential functions $\phi(\cdot)$. Let us restrict our analysis to the case where no external forces influence the dynamics, we further suppose that the center of mass of the system evolves linearly and that the center of mass coincides with the origin of the axes. We consider potentials depending on the inter-particle distance $\rho = \sqrt{x^2+y^2}$ which define a purely repulsive force, i.e. we have

$$\phi(\rho) = -\frac{c}{\rho^{s-1}}, \qquad s \in \mathbb{R}, s > 2. \tag{1.5}$$

Through classic mechanics techniques we can define an explicit form for the collision kernel [98, 126]. In the case (1.5) we may rewrite the collision kernel as

$$B(z,x) = \text{const.} z^{\lambda} b(x), \tag{1.6}$$

with $b(\cdot)$ an angular collision kernel that will be specified later on, and $\lambda = \dfrac{s-5}{s-1}$. Potential may in fact be classified in relation of the exponential $s \in \mathbb{R}, s > 2$ as follows

i) Coloumb potentials: $s = 2$

ii) Soft potentials: $s < 5$

iii) Maxwell potentials: $s = 5$

iv) Hard potentials: $s > 5$.

It is straightforward to observe how in the Maxwell case, i.e. $s = 5$, the collision kernel $B(z,x)$ simplifies to

$$B(z,x) = \text{const.} b(x), \tag{1.7}$$

A.2 The space homogeneous case

Although the first proof of existence and uniqueness of solution for the Boltzmann equation dates back to Carleman [49], it has been object of active research of the last decades. Any detailed list of contribution would be incomplete, among other a particular relevance assumed the Italian and French school of kinetic theory, see for example the works of Cercignani, Desvillettes, Lions, Pulvirenti, Toscani, Villani. A rather strong result has been obtained more recently in [103, 104] for what it may concern existence, uniqueness of global classical solutions, further they proved that the solution of the complete Boltzmann equation are always well-behaved.

In the following we restrict to a simplified version of the Boltzmann equation usually known as *spatially homogeneous Boltzmann equation for Maxwell molecules*, describing a rarefied gas with spatial homogeneous particles driven by a Maxwell potential

$$\begin{cases} \dfrac{\partial f(v,t)}{\partial t} = & \displaystyle\int_{\mathbb{R}^3\times S^2} [f(v^*,t)f(w^*,t) - f(v,t)f(w,t)] \\ & b\left(\dfrac{v-w}{|v-w|}\cdot\sigma\right) u(d\sigma)dw, \\ f(v,0) = & f_0(v), \qquad v\in\mathbb{R}^3, t\geq 0, \end{cases} \tag{2.1}$$

where $u(d\sigma) = U(d\sigma)/4\pi$ with $U(d\sigma)$ the Riemann's measure of the sphere S^2. The angular collision kernel is a general even function $b : [-1,1] \to \mathbb{R}^+$, defined in terms of elliptic integrals and not integrable in $x = 0$.

The usual approach for studying the analytically equation (2.1) relyes on the introduction of some hypotheses on the nature of $b(\cdot)$, here we present some of them:

i) Grad cutoff: $\int_{-1}^{1} b(x)dx < +\infty$,

ii) Weak cutoff: $\int_{-1}^{1} |x|b(x)dx < +\infty$,

iii) Very weak cutoff: $\int_{-1}^{1} |x|^2 b(x)dx < +\infty$

Let us assume the Grad cutoff and impose for all $v \neq w$

$$\int_{S^2} b\left(\frac{v-w}{|v-w|}\cdot\sigma\right) u(d\sigma) = 1,$$

it is possible to show that this latter condition corresponds to impose

$$\int_0^1 b(x)dx = 1.$$

Therefore, we can interpret $b(\cdot)$ as a probability density function and the collision operator $Q(\cdot,\cdot)$ in (2.1) may be written as

$$Q(f,f) = \int_{\mathbb{R}^3\times S^2} f(v^*,t)f(w^*,t)b\left(\frac{v-w}{|v-w|}\cdot\sigma\right)u(d\sigma)dw - f(v,t) \quad (2.2)$$

Further, the collision operatore in (2.2) defines a probability density function [169] and equation (2.1) can now be written as

$$\frac{\partial f(v,t)}{\partial t} = Q^*(f,f)(v,t) - f(v,t). \quad (2.3)$$

It is possible to show the following result

Theorem A.2.1. *Let us consider the case of spatial homogeneous Boltzmann equation for Maxwell molecules with the initial distribution $f_0(x,v) = f_0(v)$, we assume also the Grad cutoff. For each $t > 0$ an unique function $f(v,t)$ almost surely exists such that*

i) the function $v \longmapsto f(v,t)$ is a probability density

ii) $f(v,t)$ is solution of (2.1) for every $t \geq 0$ and a.s. in $v \in \mathbb{R}^3$.

Moreover if $\int_{\mathbb{R}} |v|^2 f_0(v)dv < +\infty$ then momentum and energy are conserved, i.e.

$$\int_{\mathbb{R}^3} vf(v,t)dv = \int_{\mathbb{R}^3} vf_0(v)dv, \qquad \forall t > 0, \qquad \text{(Momentum)}$$

$$\int_{\mathbb{R}^3} |v|^2 f(v,t)dv = \int_{\mathbb{R}^3} |v|^2 f_0(v)dv, \qquad \forall t > 0. \qquad \text{(Energy)}$$

Proof. Let us define for each $t \geq 0$ and $v \in \mathbb{R}^3$ the function $g(v,t) = e^t f(v,t)$, therefore equation (2.3) corresponds to

$$\begin{cases} \dfrac{\partial g(v,t)}{\partial t} & = e^{-t}Q^*(g,g)(v,t) \\ g(v,0) & = f_0. \end{cases} \quad (2.4)$$

Further, we define for each $t \geq 0$ a time-dependent function $\tau(\cdot)$ through the Cauchy problem

$$\begin{cases} \tau' = e^{-t} \\ \tau(0) = 0, \end{cases} \quad (2.5)$$

and a function $h(v,\tau(t)) = g(v,t)$. Explicit solution of (2.5) is $\tau(t) = 1 - e^{-t}$, $\tau \in [0,1]$. Hence, equation (2.4) may be rewritten in terms of $h(\cdot,\cdot)$ as follows

$$\begin{cases} \dfrac{\partial h(v,\tau)}{\partial \tau} & = Q^*\left(h,h\right)(v,\tau) \\ \tilde{h}(v,0) & = \tilde{f}_0(v). \end{cases} \quad (2.6)$$

Now we observe that the map

$$\tau \longmapsto (v \longmapsto h(v,\tau))$$

is analytic in the interval $(-\delta,\delta)$, $\delta>0$, with respect to the Fréchet derivative. Then $h(\cdot,\cdot)$ may be written in terms of the sum

$$h(v,\tau)=\sum_{n=0}^{+\infty}\tau^n A_n(v), \tag{2.7}$$

where $A_n(v)$ have to be determined. In what follows we determine explicitly $A_n(v)$ for each $n\geq 0$: for $n=0$

$$A_0(v)=f_0(v) \tag{2.8}$$

and for $n>0$, from the definition of $h(\cdot,\cdot)$ in equation (2.7) we have

$$\begin{aligned}\sum_{n=1}^{+\infty} n\tau^{n-1}A_n(v) =& Q^*\left(\sum_{i=0}^{+\infty}\tau^i A_i,\sum_{j=0}^{+\infty}\tau^i A_j\right)\\ =&\sum_{i,j=0}^{+\infty}\tau^{i+j}Q^*(A_i,A_j),\\ =&\sum_{k=0}^{+\infty}\sum_{j=0}^{k}\tau^k Q^*(A_{k-j},A_j)\\ =&\sum_{k=0}^{+\infty}\tau^k\left(\sum_{j=0}^{k}Q^*(A_{k-j},A_j)\right),\end{aligned}$$

and we obtain

$$\sum_{k=0}^{+\infty}(k+1)\tau^k A_{k+1}=\sum_{k=0}^{+\infty}\tau^k\left(\sum_{j=0}^{k}Q^*(A_{k-j},A_j)\right),$$

which gives

$$A_{k+1}=\frac{1}{k+1}\sum_{j=0}^{k}Q^*(A_{k-j},A_j). \tag{2.9}$$

The term A_0 defines a probability density function as well as $A_1=Q^*(f_0,f_0)$, hence by induction A_{k+1} is a probability density for all $k\in\mathbb{N}$ and the density solution of (2.3) may be written as

$$f(v,t)=\sum_{n=0}^{+\infty}e^{-t}(1-e^{-t})^n A_n(v). \tag{2.10}$$

For all $t \geq 0$ the series (2.10) almost surely converges with respect the variable $v \in \mathbb{R}^3$ and the function

$$v \longmapsto f(v,t)$$

defines a density.

In order to prove the conservation of momentum and energy we write (2.3) in weak form, for each test function $\phi \in C_b(\mathbb{R}^3)$ we have

$$\frac{d}{dt}\int_{\mathbb{R}^3}\phi(v)f(v,t)dv = \int_{\mathbb{R}^3}\phi(v)Q^*(f,f)(v,t)dv - \int_{\mathbb{R}^3}\phi(v)f(v,t)dv. \quad (2.11)$$

Being $T_\sigma : (v,w) \to (v^*,w^*)$ a linear operator with $det(Jac(T_\sigma)) = 1$ and $T_\sigma \circ T_\sigma = \mathbb{1}$, see [56, 79] we have

$$\begin{aligned}\int_{\mathbb{R}^3}\phi(v)Q^*(f,f)(v,t)dv = \\ \int_{S^2}\left[\int_{\mathbb{R}^6}\phi(v^*)f(v)f(w)dvdw\right]b\left(\frac{v-w}{|v-w|}\cdot\sigma\right)u(d\sigma) = \\ \int_{S^2}\left[\int_{\mathbb{R}^6}\phi(w^*)f(w)f(v)dwdv\right]b\left(\frac{v-w}{|v-w|}\cdot\sigma\right)u(d\sigma).\end{aligned} \quad (2.12)$$

Since

$$\begin{aligned}v^* + w^* = v + w, \\ |v^*|^2 + |w^*|^2 = |v|^2 + |w|^2,\end{aligned} \quad (2.13)$$

it is a simple computation to verify that first and second order moments are conserved, in fact if $\phi(v) = v$

$$\begin{aligned}\int_{\mathbb{R}^3} vQ^*(f,f)(v,t)dv = \\ \frac{1}{2}\int_{S^2}[(v^*+w^*)f(v,t)f(w,t)]b\left(\frac{v-w}{|v-w|}\cdot\sigma\right)u(d\sigma)dw = \\ \frac{1}{2}\left[\int_{\mathbb{R}^3} vf(v,t)dv + \int_{\mathbb{R}^3} wf(w,t)dw\right]\end{aligned} \quad (2.14)$$

and similarly for $\phi(v) = v^2$ we have

$$\begin{aligned}\int_{\mathbb{R}^3}|v|^2Q^*(f,f)(v,t)dv = \\ \frac{1}{2}\int_{S^2}[(|v^*|^2+|w^*|^2)f(v,t)f(w,t)]b\left(\frac{v-w}{|v-w|}\cdot\sigma\right)u(d\sigma)dw = \\ \frac{1}{2}\left[\int_{\mathbb{R}^3}|v|^2f(v,t)dv + \int_{\mathbb{R}^3}|w|^2f(w,t)dw\right]\end{aligned} \quad (2.15)$$

□

We defined in the poof of the latter result the so-called *Wild's sum*, let us formalize this object in the following definition.

Definition A.2.1 (Wild's sum)**.** *If the density function $f(v,t)$ is solution of the space homogeneous Boltzmann equation for Maxwell molecules (2.3), then it can be written as*

$$f(v,t) = e^{-t}\sum_{n=0}^{\infty}(1-e^{-t})^{n-1}A_{n-1}(v), \tag{2.16}$$

where

$$A_k = \begin{cases} f_0(v), & k=0, \\ \dfrac{1}{k}\displaystyle\sum_{j=0}^{k-1} Q^*(A_{k-1-j}, A_j)(v) & k = 1,2,\dots, \end{cases} \tag{2.17}$$

and

$$Q^*(p,q) = \int_{\mathbb{R}^3\times S^2} p(v^*)q(w^*)b\left(\frac{v-w}{|v-w|}\cdot\sigma\right)u(d\sigma)dw. \tag{2.18}$$

A further structural property for the Wild's sum is described by the next result.

Proposition A.2.2. *Under the same hypotheses of Theorem A.2.1 we have*

$$\begin{aligned} \int_{\mathbb{R}^3} vA_n(v)dv &= \int_{\mathbb{R}^3} vf_0(v)dv, \\ \int_{\mathbb{R}^3} |v|^2A_n(v)dv &= \int_{\mathbb{R}^3} |v|^2f_0(v)dv \end{aligned} \tag{2.19}$$

Proof. By induction. □

A.3 The Boltzmann equation for measures

In order to give the Boltzmann equation for measures we must extend the definition of $Q^*(\cdot,\cdot)$ by introducing a new collision operator, denoted by $\mathcal{Q}^*[\cdot,\cdot]$, and depending on measures. We observe first that a general collision operator in weak form reads

$$\int_{\mathbb{R}^3}\phi(v)Q^*(p,q)(v)dv = \int_{\mathbb{R}^3\times\mathbb{R}^3\times S^2}\phi(v^*)p(v)q(w)b\left(\frac{v-w}{|v-w|}\sigma\right)u(d\sigma)dvdw, \tag{3.1}$$

where the terms $p(v)dv = \mu$ and $q(w)dw = \nu$ are probability measures. In the spatial homogeneous case with Maxwell potential we may write equation (2.3) in weak form as

$$\frac{d}{dt}\int_{\mathbb{R}^3} f(v,t)\phi(v)dv = \int_{\mathbb{R}^3}\phi(v)Q^*(f,f)(v)dv - \int_{\mathbb{R}^3} f(v,t)\phi(v)dv, \tag{3.2}$$

and in terms of measures we have

$$\frac{d}{dt}\int_{\mathbb{R}^3}\phi(v)\mu(dv,t) = \int_{\mathbb{R}^3\times\mathbb{R}^3\times S^2}\phi(v^*)b\left(\frac{v-w}{|v-w|}\cdot\sigma\right)\mu(dv,t)\mu(dw,t)u(d\sigma) - \int_{\mathbb{R}^3}\phi(v)\mu(dv,t) \tag{3.3}$$

Definition A.3.1. *We define weak solution of the Boltzmann equation for measures (3.3) with initial datum the probability measure μ_0 the family of probability measures $\{\mu(\cdot,t)\}_{t\geq 0}$ over $\left(\mathbb{R}^3,\mathcal{B}_{\mathbb{R}^3}\right)$ such that:*

i) $\mu(\cdot,0)=\mu_0(\cdot)$

ii) $t\longmapsto\int_{\mathbb{R}^3}\phi(v)\mu(dv,t)\in\mathcal{C}^0\left([0,+\infty)\right)\cap\mathcal{C}^1\left([0,+\infty)\right)$ *for each test function* ϕ.

iii) the space homogeneous Boltzmann equation for measures (3.3) is satisfied for each test function ϕ *and* $t\geq 0$.

Now we must investigate the convergence in distribution of the operator $\mathcal{Q}^*[\mu,\nu](dv)$.

Definition A.3.2. *We define $\mathcal{Q}^*[\mu,\nu]$ as the weak limit*

$$\mathcal{Q}^*[\mu,\nu](dv) = w-\lim_{n\to+\infty}Q^*(p_n,q_n)(v)dv, \tag{3.4}$$

where p_n,q_n are approximating densities such that $p_n\rightharpoonup p$, $q_n\rightharpoonup q$.

In the following we prove that such limit exists and that it does not depend by the considered approximating sequence. Let μ_n,ν_n be the measures induced by the densities p_n and q_n respectively, that is $\mu_n=p_ndv$ and $\nu_n=q_ndw$.

For each $n\geq 0$, the the formulation of the collision operator $Q^*(p_n,q_n)$ in weak form reads

$$\int_{\mathbb{R}^3}\phi(v)Q^*(p_n,q_n)dv = \int_{\mathbb{R}^3\times\mathbb{R}^3}\left(\int_{S^2}\phi(v^*)b\left(\frac{v-w}{|v-w|}\cdot\sigma\right)u(d\sigma)\right)p_n(v)q_n(w)dvdw. \tag{3.5}$$

In particular, let us consider for all $(v,w)\in\mathbb{R}^3\times\mathbb{R}^3$, $v\neq w$

$$\int_{S^2}\phi(v^*)b\left(\frac{v-w}{|v-w|}\cdot\sigma\right)u(d\sigma),$$

which can be extended as follows

$$H_\phi(v,w)=\begin{cases}\displaystyle\int_{S^2}\phi(v^*)b\left(\frac{v-w}{|v-w|}\cdot\sigma\right)u(d\sigma) & \text{if } v\neq w\\ \phi(v) & \text{if } v=w.\end{cases} \tag{3.6}$$

We observe that $H_\phi(v,w)$ defines a bounded and continuous function and we have

$$\int_{\mathbb{R}^3} \phi(v) Q^*(p_n,q_n)(v)dv = \int_{\mathbb{R}^3\times\mathbb{R}^3} H_\phi(v,w) \underbrace{p_n(v)q_n(w)dvdw}_{\mu_n\otimes\nu_n(dvdw)}. \tag{3.7}$$

Further, if

$$\mu_n = p_n\ dv \Rightarrow \mu$$
$$\nu_n = q_n\ dw \Rightarrow \nu,$$

we have $\mu_n \otimes \nu_n \Rightarrow \mu\otimes\nu$. Thanks to the Lévy's Continuity Theorem, see for example [120], we have that μ_n converges in distribution toward μ if and only if $\hat{\mu}_n(\xi) \to \hat{\mu}(\xi)$ a.s., where $\hat{\mu}(\xi)$ is the Fourier transform of the probability measure μ. We can prove now for each test function ϕ the a.s. convergence

$$\int_{\mathbb{R}^3\times\mathbb{R}^3} H_\phi(v,w)p_n(v)q_n(w)dvdw \to \int_{\mathbb{R}^3\times\mathbb{R}^3} H_\phi(v,w)\mu\otimes\nu(dvdw). \tag{3.8}$$

Observe that $Q^*(p_n,q_n)$ is a bounded operator, hence the following limit exists for each $\xi\in\mathbb{R}$

$$\lim_{n\to\infty}\int_{\mathbb{R}^3} e^{i\xi v} Q^*(p_n,q_n)(v)dv = A(\xi). \tag{3.9}$$

In order to meet the hypotheses of the Lévy's Theorem we prove that $A(\xi)$ is continuous in $\xi=0$. We consider a sequence $\xi_k\to 0$ and we show that $A(\xi_k)\to A(0)$. If $\xi_k\to 0$ it follows that

$$\phi_k(v) = e^{i\xi_k v} \xrightarrow{k\to+\infty} 1$$

and we have

$$\int_{\mathbb{R}^3\times\mathbb{R}^3} H_{\phi_k}(v,w)\mu(dv)\nu(dw) \xrightarrow{k\to+\infty} \int_{\mathbb{R}^3\times\mathbb{R}^3} H_1(v,w)\mu(dv)\nu(dw), \tag{3.10}$$

begin $|H_{\phi_k}|\le 1$, and $H_{\phi_k}(v,w)\to H_1(v,w)$ from the definition of H_ϕ, which completes the proof.

Let us investigate more in details the Fourier transform of the operator introduced in the Definition A.3.1

$$\hat{\mathcal{Q}}[\mu,\nu](\xi) = \int_{\mathbb{R}^3\times\mathbb{R}^3\times S^2} e^{i\xi v^*} b\left(\frac{v-w}{|v-w|}\cdot\sigma\right)\mu(dv)\nu(dw)u(d\sigma). \tag{3.11}$$

Thanks to the definition of post-collisional velocity v^* introduced in (1.4) we have that

$$e^{i\xi v^*} = e^{i\xi[v+((w-v)\cdot\sigma)\cdot\sigma]} \tag{3.12}$$

and we obtain

$$\hat{\mathcal{Q}}[\mu,\nu](\xi) = \int_{\mathbb{R}^3\times\mathbb{R}^3} \left(\int_{S^2} e^{i\xi v} e^{i\xi\sigma[(w-v)\cdot\sigma]} b\left(\frac{v-w}{|v-w|}\cdot\sigma\right) u(d\sigma) \right) \mu(dv)\nu(dw), \tag{3.13}$$

where the integral over S^2 can be written, for each fixed $\xi \neq 0$, $v, w \in \mathbb{R}^3$ and $v \neq w$, as

$$\int_{S^2} e^{\frac{i\xi\sigma}{|\xi|}\frac{[(w-v)\cdot\sigma]}{|w-v|}|\xi||w-v|} b\left(\frac{v-w}{|v-w|}\cdot\sigma\right) u(d\sigma), \tag{3.14}$$

also known as *Bobylev's trick*. Define then the unit vectors τ and ω as follows

$$\tau = \frac{\xi}{|\xi|} \qquad \omega = \frac{v-w}{|v-w|}. \tag{3.15}$$

The integral in equation (3.14) assumes the form

$$\int_{S^2} e^{i(\tau\cdot\sigma)(\omega\cdot\sigma)|\xi||v-w|} b\left(\omega\cdot\sigma\right) u(d\sigma).$$

Let us consider now a rotation of σ along the $z-$axis, hence

$$\int_{S^2} e^{i(\tau\cdot\sigma)(\omega\cdot\sigma)|\xi||v-w|} b\left(\omega\cdot\sigma\right) u(d\sigma) = \int_{S^2} e^{i(\omega\cdot\sigma)(\tau\cdot\sigma)|\xi||w-v|} b(\tau\cdot\sigma) u(d\sigma)$$

and we obtain

$$\int_{S^2} e^{i\left(\frac{v-w}{|v-w|}\cdot\sigma\right)\left(\frac{\xi}{|\xi|}\cdot\sigma\right)|\xi|\ |v-w|} b\left(\frac{\xi}{|\xi|}\cdot\sigma\right) u(d\sigma) = \int_{S^2} e^{i((v-w)\cdot\sigma)\xi\cdot\sigma} b\left(\frac{\xi}{|\xi|}\cdot\sigma\right) u(d\sigma).$$

From equation (3.13) we have

$$\begin{aligned}
\hat{\mathcal{Q}}[\mu,\nu](\xi) &= \int_{\mathbb{R}^3\times\mathbb{R}^3\times S^2} e^{i\xi v} e^{i\xi\sigma[w-v]\cdot\sigma} b\left(\frac{v-w}{|v-w|}\cdot\sigma\right) \mu(dv)\nu(dw)u(d\sigma) \\
&= \int_{\mathbb{R}^3\times\mathbb{R}^3\times S^2} e^{i\xi v} e^{i\xi\sigma[(w-v)\cdot\sigma]} b\left(\frac{\xi}{|\xi|}\cdot\sigma\right) \mu(dv)\nu(dw)u(d\sigma) \\
&= \int_{S^2} \left[\int_{\mathbb{R}^3\times\mathbb{R}^3} e^{i\xi v - i(\xi\cdot\sigma)(v\cdot\sigma)} e^{i(\xi\cdot\sigma)(w\cdot\sigma)} \mu(dv)\nu(dw) \right] b\left(\frac{\xi\cdot\sigma}{|\xi|}\right) u(d\sigma)
\end{aligned} \tag{3.16}$$

and thanks to the Fubini's Theorem we obtain

$$\int_{\mathbb{R}^3} e^{i[\xi-(\xi\cdot\sigma)\cdot\sigma]\cdot v} \mu(dv) = \hat{\mu}\left(\xi - (\xi\cdot\sigma)\cdot\sigma\right). \tag{3.17}$$

Finally, the Fourier transform of the collisional operator for a couple of measures (μ,ν) can be rewritten as follows

$$\hat{\mathcal{Q}}[\mu,\nu](\xi) = \int_{S^2} \hat{\mu}(\xi - (\xi\cdot\sigma)\sigma)\hat{\nu}((\xi\cdot\sigma)\sigma) b\left(\frac{\xi\cdot\sigma}{|\xi|}\right) u(d\sigma). \tag{3.18}$$

This latter expression is known as *Bobylev's formula*.

Example 3. *Let us consider*

$$\hat{\sigma} = (\sin\varphi\cos\theta, \sin\varphi\sin\theta, \cos\varphi), \qquad \varphi \in [0,\pi], \theta \in [0, 2\pi]. \tag{3.19}$$

The object $\hat{\sigma}$ may be written in terms of the orthonormal basis of $\mathbb{R}^3$: $\left\{\hat{a}, \hat{b}, \dfrac{\xi}{|\xi|}\right\}$ as

$$\hat{\sigma} = \sin\varphi\cos\theta\ \hat{a} + \sin\varphi\sin\theta\ \hat{b} + \cos\varphi\ \frac{\xi}{|\xi|}. \tag{3.20}$$

Then the (3.18) corresponds to

$$\begin{aligned}\hat{\mathcal{Q}}[\mu,\nu](\xi) = \int_0^{2\pi}\int_0^{\pi} \hat{\mu}\left(\xi - \hat{\sigma}(\varphi,\theta)|\xi|\cos\varphi\right) \\ \hat{\nu}(\hat{\sigma}(\varphi,\theta)|\xi|\cos\varphi) b(\cos\varphi)\frac{\sin\varphi d\varphi d\theta}{4\pi},\end{aligned} \tag{3.21}$$

and assuming that the measures μ, ν are of the radial type, that is $\hat{\mu}(\xi) = \hat{\eta}(|\xi|)$, and $\hat{\nu}(\xi) = \hat{\xi}(|\xi|)$, where η, ξ are probability measures over $(\mathbb{R}, \mathcal{B}(\mathbb{R}))$, we have

$$\mathcal{Q}[\mu,\nu](\xi) = \int_0^{\pi} \hat{\eta}(|\xi|\sin\varphi)\xi(|\xi|\cos\varphi)\frac{b}{2}(\cos\varphi)\sin\varphi d\varphi. \tag{3.22}$$

Bibliography

[1] D. Acemoglu and O. Asuman, *Opinion dynamics and learning in social netowkrs*, Dynamic Games and Applications, 1 (2011), pp. 3–49.

[2] S. M. Ahn and S. Y. Ha, *Stochastic flocking dynamics of the Cucker–Smale model with multiplicative white noises*, Journal of Mathematical Physics, 51 (2010), pp. 103301, 17.

[3] R. Albert and A.-L. Barabàsi, *Statistical mechanics of complex networks*, Reviews of Modern Physics, 74 (2002), p. 47.

[4] G. Albi, D. Balagué, J. A. Carrillo, and J. von Brecht, *Stability analysis of flock and mill rings for second order models in swarming*, SIAM Journal on Applied Mathematics, 74 (2014), pp. 794–818.

[5] G. Albi, M. Bongini, E. Cristiani, and D. Kalise, *Invisible control of self–organizing agents leaving unknown environments*, SIAM Journal on Applied Mathematics, 76 (2016), pp. 1683–1710.

[6] G. Albi, M. Herty, and L. Pareschi, *Kinetic description of optimal control problems and applications to opinion consensus*, Communications in Mathematical Sciences, 13 (2015), pp. 1407–1429.

[7] G. Albi and L. Pareschi, *Selective model–predictive control for flocking systems*, arXiv: 1603.05012.

[8] ——, *Binary interaction algorithms for the simulation of flocking and swarming dynamics*, SIAM Journal on Multiscale Modeling & Simulation, 11 (2013), pp. 1–29.

[9] ——, *Modeling of self-organized systems interacting with a few individuals: from microscopic to macroscopic dynamics*, Applied Mathematics Letters, 26 (2013), pp. 397–401.

[10] G. Albi, L. Pareschi, G. Toscani, and M. Zanella, *Recent advances in opinion modeling: control and social influence*, in Active Particles, Volume 1, Advances in Theory, Methods, and Applications,

N. Bellomo, P. Degond, and E. Tadmor, eds., Modeling and Simulation in Science, Engineering and Technology, Birkhäuser, Basel, 2017.

[11] G. Albi, L. Pareschi, and M. Zanella, *Boltzmann-type control of opinion consensus through leaders*, Philosophical Transactions of the Royal Society of London A: Mathematical, Physical and Engineering Sciences, 372 (2014), p. 20140138.

[12] ——, *On the optimal control of opinion dynamics on evolving networks*, in System Modelign and Optimization. Proceedings of the 27th IFIP TC7 Conference, CSMO 2015 Sophia Antipolis, France, vol. 494 of IFIP AICT Series, IFIP, Springer, 2015.

[13] ——, *Uncertainty quantification in control problems for flocking models*, Mathematical Problems in Engineering, 2015 (2015).

[14] ——, *Opinion dynamics over complex networks: kinetic modelling and numerical methods*, Kinetic and Related Models, 10 (2017), pp. 1–32.

[15] L. A. Amaral, A. Scala, M. Barthélemy, and H. E. Stanley, *Classes of small–world networks*, Proceedings of the National Academy of Sciences, 97 (2000), pp. 11149–11152.

[16] D. Armbruster and C. Ringhofer, *Thermalized kinetic and fluid models for re–entrant supply chains*, SIAM Journal on Multiscale Modeling & Simulation, 3 (2005), pp. 782–800.

[17] A. Aydogdo, M. Caponigro, S. McQuade, B. Piccoli, N. P. Duteil, F. Rossi, and E. Trélat, *Interaction network, state space and control in social dynamics*, Birkhäuser, Basel, 2017, ch. Active Particle Volume 1, Theory, Methods, and Applications.

[18] B. Bahrami, K. Olsen, P. E. Latham, A. Roepstorff, G. Rees, and C. D. Frith, *Optimally interacting minds*, Science, 329 (2010), pp. 1081–1085.

[19] D. Balagué, J. A. Carrillo, and Y. Yao, *Confinement for repulsive–attractive kernels*, Discrete and Continuous Dynamical Systems - Series B, 19 (2014), pp. 1227–1248.

[20] A.-L. Barabàsi and R. Albert, *Emergence of scaling in random networks*, Science, 286 (1999), pp. 509–5012.

[21] A.-L. Barabàsi, R. Albert, and H. Jeong, *Mean–field theory for scale–free random networks*, Physica A: Statistical Mechanics and its Applications, 272 (1999), pp. 173–187.

[22] A. B. T. Barbaro, J. A. Cañizo, J. A. Carrillo, and P. Degond, *Phase transitions in a kinetic flocking model of Cucker–Smale type*, SIAM Journal on Multiscale Modeling & Simulation, 14 (2016), pp. 1063–1088.

[23] A. B. T. Barbaro and P. Degond, *Phase transition and diffusion among socially interacting self–propelled agents*, Discrete and Continuous Dynamical Systems - Series B, 19 (2014), pp. 1249–1278.

[24] A. Barrat, M. Barthélemy, and A. Vespignani, *Dynamical processes on complex networks*, Cambridge University Press, Cambridge, 2008.

[25] E. Ben-Naim, *Opinion dynamics, rise and fall of political parties*, Europhysics Letters, 69 (2005), p. 671.

[26] E. Ben-Naim, P. L. Krapivsky, and S. Redner, *Bifurcations and patterns in compromise processes*, Physica D: Nonlinear Phenomena, 183 (2003), pp. 190–204.

[27] A. Bensoussan, J. Frehse, and P. Yam, *Mean Field Games and Mean Field Type Control Theory*, Springer Briefs in Mathematics, Springer, New York, 2013.

[28] M. Bessemoulin-Chatard and F. Filbet, *A finite volume scheme for nonlinear degenerate parabolic equations*, SIAM Journal on Scientific Computing, 34 (2012).

[29] A. Blanchet and G. Carlier, *From Nash to Cournot–Nash equilibria via the Monge–Kantorovich problem*, Philosophical Transactions of the Royal Society of London A: Mathematical, Physical and Engineering Sciences, 372 (2014), p. 20130398.

[30] R. Bogacz, E. Brown, J. Moehlis, P. Holmes, and J. D. Cohen, *The physics of optimal decision making: a formal analysis of models of performance in two-alternative forced-choice task*, Psychological Review, 113 (2006), p. 700.

[31] F. Bolley, J. A. Cañizo, and J. A. Carrillo, *Mean–field limit for the stochastic Vicsek model*, Applied Mathematics Letters, 25 (2012), pp. 339–343.

[32] M. Bongini, M. Fornasier, F. Fröhlich, and L. Haghverdi, *Sparse stabilization of dynamical systems driven by attraction and avoidance forces*, Network and Heterogeneous Media, 9 (2014), pp. 1–31.

[33] M. Bongini, M. Fornasier, and D. Kalise, *(UN)conditional consensus emergence under perturbed and decentralized feedback controls*, Discrete and Continuous Dynamical Systems - Series A, 35 (2015), pp. 4071–4094.

[34] C. M. Bordogna and E. V. Albano, *Dynamic behavior of a social model for opinion formation*, Physical Review E - Statistical, Nonlinear, and Soft Matter Physics, 76 (2007), p. 061125.

[35] D. Borra and T. Lorenzi, *Asymptotic analysis of continuous opinion dynamics models under bounded confidence*, Communications on Pure and Applied Analysis, 12 (2013), pp. 1487–1499.

[36] S. Boscarino, F. Filbet, and G. Russo, *High order semi–implicit schemes for time dependent partial differential equations*, Journal of Scientific Computing, 68 (2016), pp. 975–1001.

[37] L. Boudin, R. Monaco, and F. Salvarani, *Kinetic model for multidimensional opinion formation*, Physical Review E - Statistical, Nonlinear, and Soft Matter Physics, 81 (2010), p. 036109.

[38] L. Boudin and F. Salvarani, *A kinetic approach to the study of opinion formation*, Mathematical Modelling and Numerical Analysis, 43 (2009), pp. 507–522.

[39] C. Brugna and G. Toscani, *Kinetic models of opinion formation in the presence of personal conviction*, Physical Review E, 92 (2015), p. 052818.

[40] C. Buet, S. Cordier, and V. D. Santos, *A conservative and entropy scheme for a simplified model of granular media*, Transport Theory and Statistical Physics, 33 (2004), pp. 125–155.

[41] C. Buet and S. Dellacherie, *On the Chang and Cooper numerical scheme applied to a linear Fokker–Planck equation*, Communications in Mathematical Sciences, 8 (2010), pp. 1079–1090.

[42] M. Burger, J. A. Carrillo, and M.-T. Wolfram, *A mixed finite element method for nonlinear diffusion equations*, Kinetic and Related Models, 3 (2010), pp. 59–83.

[43] M. Burger, M. D. Francesco, P. A. Markowich, and M.-T. Wolfram, *Mean–field games with nonlinear mobilities in pedestrian dynamics*, Discrete and Continuous Dynamical Systems - Series B, 19 (2014), pp. 1311–1333.

[44] E. F. Camacho and C. B. Alba, *Model predictive control*, Advanced Textbooks in Control and Signal Processing, Springer – Verlag London, 2007.

[45] R. H. Cameron and W. T. Martin, *Transformations of Wiener integrals under translations*, Annals of Mathematics, 45 (1944), pp. 386–396.

[46] M. Caponigro, A. C. Lai, and B. Piccoli, *A nonlinear model of opinion formation of the sphere*, Discrete and Continuous Dynamical Systems - Series A, 35 (2015), pp. 4241–4266.

[47] G. Carbone and I. Giannoccaro, *Model of human collective decision–making in complex environments*, The European Physical Journal B-Condensed Matter and Complex Systems, 88 (2015), pp. 1–10.

[48] P. Cardaliaguet, *Notes on mean field games*. P.-L. Lions' lectures at Collége de France, 2010.

[49] T. Carleman, *Problèmes mathématiques dans la théorie cinétique des gaz*, Publ. Sci. Inst. Mittag-Leffler. 2, Almqvist & Wiksells Boktryckeri Ab, Uppsala, 1957.

[50] J. A. Carrillo, A. Chertock, and Y. Huang, *A finite–volume method for nonlinear nonlocal equation with a gradient flow structure*, Communications in Computational Physics, 17 (2015), pp. 233–258.

[51] J. A. Carrillo, Y.-P. Choi, and M. Hauray, *The derivation of swarming models: mean–field limit and Wasserstein distances*, in Collective dynamics from bacteria to crowds, vol. 553, Springer, 2014, pp. 1–46.

[52] J. A. Carrillo, M. Fornasier, J. Rosado, and G. Toscani, *Asymptotic flocking dynamics for the kinetic Cucker–Smale model*, SIAM Journal on Mathematical Analysis, 42 (2010), pp. 218–236.

[53] J. A. Carrillo, M. Fornasier, G. Toscani, and F. Vecil, *Particle, kinetic, and hydrodynamic models of swarming*, in Mathematical Modeling of Collective Behavior in Socio–Economic and Life Sciences, G. Naldi, L. Pareschi, and G. Toscani, eds., Modeling and Simulation in Science, Engineering and Technology, Birkhäuser, Boston, 2010.

[54] J. A. Carrillo, R. J. McCann, and C. Villani, *Kinetic equilibration rates for granular media and related equations: entropy dissipation and mass transportation estimates*, Revista Matemàtica Iberoamericana, 19 (2003), pp. 971–1018.

[55] J. A. Carrillo, L. Pareschi, and M. Zanella, *Monte Carlo–stochastic Galerkin algorithms for mean–field models*, In progress, (2017).

[56] C. Cercignani, *The Boltzmann Equation and its Applications*, vol. 67 of Applied Mathematical Sciences, Springer, 1988.

[57] C. Cercignani, R. Illner, and M. Pulvirenti, *The mathematical theory of diluite gases*, vol. 106 of Applied Mathematical Sciences, Springer – Verlag New York, 1994.

[58] C. Chainais-Hillairet, A. Jüngel, and S. Schuchnigg, *Entropy-dissipative discretization of nonlinear diffusion equations and discrete Beckner inequalities*, ESAIM Mathematical Modelling and Numerical Analysis, 50 (2016), pp. 135–162.

[59] A. Chakraborti and B. K. Chakrabarti, *Statistical mechanics of money: how saving propensity affects its distribution*, The European Physical Journal B-Condensed Matter and Complex Systems, 17 (2000), pp. 167–170.

[60] J. S. Chang and G. Cooper, *A practical difference scheme for Fokker–Planck equation*, Journal of Computational Physics, 6 (1970), pp. 1–16.

[61] L. Chi, *Binary opinion dynamics with noise on random networks*, Chinese Science Bulletin, 56 (2015), pp. 3630–3632.

[62] H. Choi, M. Hinze, and K. Kunisch, *Instantaneous control of backward–facing step flows*, Applied Numerical Mathematics, 31 (1999), pp. 133–158.

[63] Y.-P. Choi, S.-Y. Ha, and Z. Li, *Emergent dynamics of the Cucker–Smale flocking model and its variants*, Preprint arXiv, (2016).

[64] R. M. Colombo, M. Herty, and M. Mercier, *Control of the continuity equation with a non local flow*, ESAIM: Control, Optimization and Calculus of Variations, 17 (2011), p. 353:379.

[65] R. M. Colombo and N. Pogodaev, *Confinement strategies in a model for the interaction between individuals and a continuum*, SIAM Journal on Applied Dynamical Systems, 11 (2012), pp. 741–770.

[66] S. Cordier, L. Pareschi, and G. Toscani, *On a kinetic model for a simple market economy*, Journal of Statistical Physics, 120 (2005), pp. 253–277.

[67] I. Couzin, J. Krause, N. Franks, and S. Levin, *Effective leadership and decision–making in animal groups on the move*, Nature, 433 (2005), pp. 513–516.

[68] R. Cremona, J.-P. Fouque, and L.-H. Sun, *Mean field games and systemic risk*, Communications in Mathematical Sciences, 13 (2015), pp. 911–933.

[69] E. Cristiani, B. Piccoli, and A. Tosin, *Multiscale modeling of granular flows with application to crowd dynamics*, SIAM Journal on Multiscale Modeling & Simulation, 9 (2011), pp. 155–182.

[70] ——, *Multiscale Modeling of Pedestrian Dynamics*, vol. 12 of MS&A: Modeling, Simulation and Applications, Springer International Publishing, 2014.

[71] F. Cucker and S. Smale, *Emergent behavior in flocks*, IEEE Transactions on Automatic Control, 52 (2007), pp. 852–862.

[72] A. Das, S. Gollapudi, and K. Mungala, *Modeling opinion dynamics in social networks*, in Proceedings of the 7th ACM International conference on Web search and data mining, ACM, 2014.

[73] P. Degond, M. Herty, and J.-G. Liu, *Meanfield games and model predictive control*, Preprint arXiv, (2014).

[74] P. Degond, J.-G. Liu, S. Motsch, and V. Panferov, *Hydrodynamic models of self-organized dynamics: derivation and existence theory*, Methods and Applications of Analysis, 20 (2013), pp. 89–114.

[75] P. Degond, J.-G. Liu, and C. Ringhofer, *Evolution of wealth in a nonconservative economy driven by local Nash equilibria*, Philosophical Transactions of the Royal Society of London A: Mathematical, Physical and Engineering Sciences, 372 (2014), p. 20130394.

[76] ——, *Large–scale dynamics of mean-field games driven by local Nash equilibria*, Journal of Nonlinear Science, 24 (2014), pp. 93–115.

[77] B. Després, G. Poëtte, and D. Lucor, *Robust uncertainty propagation in systems of conservation laws with the entropy closure method*, in Uncertainty Quantification in Computational Fluid Dynamics, H. Bijl, D. Lucor, S. Mishra, and C. Schwab, eds., vol. 92 of Lecture Notes in Computational Science and Engineering, Springer International Publishing, 2010.

[78] G. Dimarco and L. Pareschi, *Numerical methods for kinetic equations*, Acta Numerica, 23 (2014), pp. 369–520.

[79] E. Dolera, *On the computation of the spectrum of the linearized Boltzmann collision operator for Maxwellian molecules*, Bollettino della Unione Matematica Italiana, 4 (2011), pp. 47–68.

[80] M. Dolfin and M. Lachowicz, *Modeling opinion dynamics: how the network enhances consensus*, Network and Heterogeneous Media, 10 (2015), pp. 877–896.

[81] B. Düring, A. Jüngel, and L. Trussardi, *A kinetic equation for economic value estimation with irrationality and herding*, Kinetic and Related Models, 10 (2017), pp. 239–261.

[82] B. Düring, P. Markowich, J. F. Pietschmann, and M.-T. Wolfram, *Boltzmann and Fokker–Planck equations modelling opinion formation in the presence of strong leaders*, Proceedings of the Royal Society of London A: Mathematical, Physical and Engineering Sciences, 465 (2009), pp. 3687–3708.

[83] B. Düring, D. Matthes, and G. Toscani, *A Boltzmann–type approach to the formation of wealth distribution curves*, Rivista di Matematica della Università di Parma, 8 (2009), pp. 199–261.

[84] B. Düring and M.-T. Wolfram, *Opinion dynamics: inhomogeneous boltzmann-type equations modelling opinion leadership and political segregation*, Proceedings of the Royal Society of London A: Mathematical, Physical and Engineering Sciences, 471 (2015), p. 20150345.

[85] H. J. Einhorn and R. M. Hogarth, *Confidence in judgement: persistence of the illusion of validity*, Psychological Review, 85 (1978), pp. 395–416.

[86] S. M. Fleming and H. C. Lau, *How to measure metacognition*, Frontiers in Human Neuroscience, 8 (2014), p. 443.

[87] M. Fornasier, J. Haskovec, and G. Toscani, *Fluid dynamic description of flocking via Povzner–Boltzmann equation*, Physica D: Nonlinear Phenomena, 240 (2011), pp. 21–31.

[88] M. Fornasier, B. Piccoli, and F. Rossi, *Mean–field sparse optimal control*, Philosophical Transactions of the Royal Society of London A: Mathematical, Physical and Engineering Sciences, 372 (2014), p. 20130400.

[89] M. Fornasier and F. Solombrino, *Mean–field optimal control*, ESAIM: Control, Optimization and Calculus of Variations, 20 (2014), pp. 1123–1152.

[90] M. D. Francesco and M. D. Rosini, *Rigorous derivation of nonlinear scalar conservation laws from follow-the-leader type models via many particle limit*, Archive for Rational Mechanics and Analysis, 217 (2015), pp. 831–871.

[91] G. Furioli, A. Pulvirenti, E. Terraneo, and G. Toscani, *The grazing collision limit of the inelastic Kac model around a Lévy-type equilibrium.*, SIAM Journal on Mathematical Analysis, 44 (2012), pp. 827–850.

[92] ——, *Fokker–Planck equations in the modeling of socio–economic phenomena*, Mathematical Models and Methods in Applied Sciences, 27 (2017), pp. 115–158.

[93] S. Galam, *Rational group decision making: a random field ising model at T=0*, Physica A: Statistical Mechanics and its Applications, 238 (1997), pp. 66–80.

[94] S. Galam, Y. Gefen, and Y. Shapir, *Sociophysics: a new approach of sociological collective behaviour*, Journal of Mathematical Sociology, 9 (1982), pp. 1–13.

[95] S. Galam and J.-D. Zucker, *From individual choice to group decision–making*, Physica A: Statistical Mechanics and its Applications, 287 (2000), pp. 644–659.

[96] I. Gallagher, L. Saint-Raymond, and B. Texier, *From Newton to Boltzmann: Hard Spheres and Short-range Potentials*, Zurich Lectures in Advanced Mathematics, European Mathematical Society, 2013.

[97] M. Gerritsma, J.-B. van der Steen, P. Vos, and G. Karniadakis, *Time–dependent generalized polynomial chaos*, Journal of Computational Physics, 229 (2010), pp. 8333–8363.

[98] H. Goldstein, *Classical Mechanics*, Addison-Wesley Press, Inc., Cambridge, Mass., 1st ed., 1951.

[99] F. Golse, *The Boltzmann equation and its hydrodynamic limits*, Handbook of Differential Equations: Evolutionary Equations, 2 (2006), pp. 159–301.

[100] J. Gómez-Serrano, C. Graham, and J.-Y. L. Boudec, *The bounded confidence model of opinion dynamics*, Mathematical Models and Methods in Applied Sciences, 22 (2012), pp. 1–46.

[101] L. Gosse, *Computing Qualitatively Correct Approximations of Balance Laws. Exponential-Fit, Well-Balanced and Asymptotic-Preserving*, SEMA SIMAI Springer Series, Springer, 2013.

[102] S. Gottlieb, C. W. Shu, and E. Tadmor, *Strong stability–preserving high–order time discretization methods*, SIAM Review, 43 (2001), pp. 89–112.

[103] P. T. Gressman and R. M. Strain, *Global classical solutions of the Boltzmann equation with long-range interactions*, Proceedings of the National Academy of Sciences, 107 (2010), pp. 5744–5749.

[104] ——, *Global classical solutions of the Boltzmann equation without angular cut-off*, Journal of the Americal Mathematical Society, 24 (2011), pp. 771–847.

[105] G. Grimm, M. J. Messina, S. E. Tuna, and A. R. Teel, *Model predictive control: for want of a local control lyapunov function, all is not lost*, IEEE Transactions on Automatic Control, 50 (2005), pp. 546–558.

[106] L. Grüne, *Analysis and design of unconstrained nonlinear MPC schemes for finite and infinite dimensional systems*, SIAM Journal on Control and Optimization, 48 (2009), pp. 1206–1228.

[107] L. Grüne, J. Pannek, M. Seehafer, and K. Worthmann, *Analysis of unconstrained nonlinear MPC schemes with time varying control horizon*, SIAM Journal on Control and Optimization, 48 (2010), pp. 4938–4962.

[108] S. Y. Ha, K. Lee, and D. Levy, *Emergence of time–asymptotic flocking in a stochastic Cucker–Smale system*, Communications in Mathematical Sciences, 7 (2009), pp. 453–469.

[109] S.-Y. Ha and E. Tadmor, *From particle to kinetic and hydrodynamic descriptions of flocking*, Kinetic and Related Models, 1 (2008), pp. 415–435.

[110] J. M. Harrison and M. I. Taksar, *Instantaneous control of Brownian motion*, Mathematical of Operations Research, 8 (1983), pp. 439–453.

[111] N. Harvey, *Confidence in judgement*, Trends in Cognitive Sciences, 1 (1997), pp. 78–82.

[112] N. Harvey and I. Fisher, *Taking advice: Accepting help, improving judgment, and sharing responsibility*, Organizational Behavior and Human Decision Processes, 70 (1997), pp. 117–133.

[113] R. Hegselmann and U. Krause, *Opinion dynamics and bounded confidence, models, analysis and simulation*, Journal of Artificial Societies and Social Simulation, 5 (2002).

[114] D. Helbing, S. Lämmer, and J.-P. Lebacque, *Optimal Control and Dynamic Games: Applications in Finance, Management Science and Economics*, Springer US, 2005, ch. Self-Organized Control of Irregular or Perturbed Network Traffic, pp. 239–274.

[115] M. Herty and C. Ringhofer, *Feedback controls for continuous priority models in supply chain management*, Computational Methods in Applied Mathematics, 11 (2011), pp. 206—213.

[116] M. Herty, S. Steffensen, and L. Pareschi, *Mean–field control and Riccati equations*, Network and Heterogeneous Media, 10 (2015), pp. 699–715.

[117] M. Herty and M. Zanella, *Performance bounds for the mean-field limit of constrained dynamics*, Discrete and Continuous Dynamical Systems - Series A, 37 (2017), pp. 2023–2043.

[118] H. Hotelling, *Stability and competition*, Economic Journal, 39 (1929), pp. 41–57.

[119] Y. Huang and A. Bertozzi, *Asymptotics of blowup solutions for the aggregation equation*, Discrete and Continuous Dynamical Systems - Series B, 17 (2012), pp. 1309–1331.

[120] J. Jacod and P. Protter, *Probability Essentials*, Universitext, Springer-Verlag, Berlin, 2000.

[121] A. Jadbabaie and J. Hauser, *On the stability of receding horizon control with a general terminal cost*, IEEE Transactions on Automatic Control, 5 (2005).

[122] M. Kac, *Foundations of kinetic theory*, in Proceedings of Third Berkeley Symposium on Mathematical Statistics and Probability, University of California Press, Berkeley and Los Angeles, 1956, pp. 171–197.

[123] A. D. I. Kramer, J. E. Guillory, and J. T. Hancock, *Experimental evidence of massive scale emotional contagion through social networks*, Proceedings of the National Academy of Sciences, 111 (2014), pp. 8788–8789.

[124] J. Kruger and D. Dunning, *Unskilled and unaware of it: how difficulties in recognizing one's own incompetence lead to inflated self-assessments*, Journal of Personality and Social Psychology, 77 (1999), pp. 1121–1134.

[125] M. Lallouache, A. S. Chakrabarti, A. Chakraborti, and B. K. Chakrabarti, *Opinion formation in the kinetic exchange models: spontaneous symmetry breaking transition*, Physical Reviews E, 82 (2010), p. 056112.

[126] L. D. Landau and E. M. Lifshitz, *Mechanics*, vol. 1 of Course of Theoretical Physics, Vol. 1. Translated from the Russian by J. B. Bell, Pergamon Press, Oxford-London-New York-Paris; Addison-Wesley Publishing Co., Inc., Reading, Mass., 1960.

[127] E. W. Larsen, C. D. Levermore, G. C. Pomraning, and J. G. Sanderson, *Discretization methods for one–dimensional Fokker–Planck operators*, Journal of Computational Physics, 61 (1985), pp. 359–390.

[128] J.-M. Lasry and P.-L. Lions, *Mean field games*, Japanese Journal of Mathematics, 2 (2007), pp. 229–260.

[129] D. Luenberger, *Optimization by vector space methods*, John Wiley & Sons Inc., New York, 1969.

[130] T. Lux and M. Marchesi, *Scaling and criticality in a stochastic multi–agent model of a financial market*, Nature, 397 (1999), pp. 498–500.

[131] A. Mahmoodi, D. Bang, K. Olsen, Y. A. Zhao, Z. Shi, K. Broberg, S. Safavi, S. Han, M. N. Ahmadabadi, C. D. Frith, A. Roepstorff, G. Rees, and B. Bahrami, *Equality bias impairs collective decision-making across cultures*, Proceedings of the National Academy of Sciences, 112 (2015), pp. 3835–3840.

[132] D. Maldarella and L. Pareschi, *Kinetic models for socio–economic dynamics of speculative markets*, Physica A: Statistical Mechanics and its Applications, 391 (2012), pp. 715–730.

[133] D. Q. Mayne and H. Michalska, *Receding horizon control of nonlinear systems*, IEEE Transactions on Automatic Control, 35 (1990), pp. 814–824.

[134] D. Q. Mayne, J. B. Rawlings, C. V. Rao, and P. O. M. Scokaert, *Constrained model predictive control: stability and optimality*, Automatica, 36 (2000), pp. 789–814.

[135] H. Michalska and D. Q. Mayne, *Robust receding horizon control of constrained nonlinear systems*, IEEE Transactions on Automatic Control, 38 (1993), pp. 1623–1633.

[136] ——, *Moving horizon observers and oserver–based control*, IEEE Transactions on Automatic Control, 40 (1995), pp. 995–1006.

[137] M. Mohammadi and A. Borzì, *Analysis of the Chang–Cooper discretization scheme for a class of Fokker–Planck equations*, Journal of Numerical Mathematics, 23 (2015), pp. 271–288.

[138] S. Motsch and E. Tadmor, *A new model for self-organized dynamics and its flocking behavior*, Journal of Statistical Physics, 144 (2011), pp. 923–947.

[139] ——, *Heterophilious dynamics enhances consensus*, SIAM Review, 56 (2014), pp. 577–621.

[140] C. Mudde, *Populist Radical Right Parties in Europe*, Cambridge University Press, Cambridge, 2007.

[141] M. R. D. nad Y. L. Chuang, A. L. Bertozzi, and L. S. Chayes, *Self–propelled particles with soft–core interactions: patterns, stability and collapse*, Physical Review Letters, 96 (2006), p. 104302.

[142] G. Naldi, L. Pareschi, and G. Toscani, eds., *Mathematical Modeling of Collective Behavior in Socio–Economic and Life Sciences*, Birkhäuser, Boston, 2010.

[143] M. E. J. Newman, *The structure and function on complex networks*, SIAM Review, 45 (2003), pp. 167–256.

[144] L. Pareschi and G. Russo, *An introduction to Monte Carlo methods for the Boltzmann equation*, ESAIM Proceedings, 10 (2001), pp. 35–75.

[145] L. Pareschi and G. Toscani, *Interacting Multiagent Systems. Kinetic Equations and Monte Carlo Methods*, Oxford University Press, 2013.

[146] ——, *Wealth distribution and collective knowledge: a Boltzmann approach*, Philosophical Transactions of the Royal Society A: Mathematical, Physical and Engineering Sciences, 372 (2014), p. 20130396.

[147] L. Pareschi, P. Vellucci, and M. Zanella, *Kinetic models of collective decision–making in the presence of equality bias*, Physica A: Statistical Mechanics and its Applications, 467 (2017), pp. 201–217.

[148] L. Pareschi and M. Zanella, *Structure preserving schemes for mean–field equations of collective behavior*, in Proceedings of the XVI International Conference on Hyperbolic Problems.

[149] L. Pareschi and M. Zanella, *Structure preserving schemes for nonlinear Fokker–Planck equations and applications*, Preprint arXiv, (2017).

[150] S. Patterson and B. Bamieh, *Interaction–driven opinion dynamics in online social networks*, in Proceedings of the First Workshop on Social Media Analytics, ACM New York, 2010, pp. 98–110.

[151] P. Pettersson, G. Iaccarino, and J. Nordström, *A stochastic Galerkin method for the Euler equations with Roe variable transformation*, Journal of Computational Physics, 257 (2014), pp. 481–500.

[152] I. Poulakakis, L. Scardovi, and N. E. Leonard, *Coupled stochastic differential equations and collective decision making in the two-alternative forced-choice task*, Proceedings of the 2010 American Control Conference, (2010), pp. 69–74.

[153] W. Quattrociocchi, G. Caldarelli, and A. Scala, *Opinion dynamics on interacting networks: media competition and social influence*, Scientific Reports, 4 (2014), p. 4938.

[154] C. Reynolds, *Flocks, herds, and schools: A distributed behavioral model*, in Proceedings of the 14th Annual Conference on Computer Graphics and Interactive Techniques, SIGGRAPH 1987, 1987, pp. 25–34.

[155] L. Saint-Raymond, *Hydrodynamic Limits of the Boltzmann Equation*, vol. 1971 of Lecture Notes in Mathematics, Springer Berlin Heidelberg, 2009.

[156] H. L. Scharfetter and H. K. Gummel, *Large signal analysis of a silicon read diode oscillator*, IEEE Transactions on Electronic Devices, 16 (1969), pp. 64–77.

[157] P. Sen and B. K. Chakrabarti, *Sociophysics: An introduction*, Oxford University Press, 2013.

[158] E. D. Sontag, *Mathematical Control Theory: deterministic finite dimensional systems*, vol. 6, Springer Science & Business Media, 2013.

[159] S. H. Strogatz, *Exploring complex networks*, Nature, 410 (2001), pp. 268–276.

[160] Y. Sun, *Mean square consensus for uncertain multiagent systems with noises and delays*, Abstract and Applied Analysis, 2012 (2012).

[161] S.Wongkaew and A.Borzí, *Modeling and control through leadership of a refined flocking system*, Mathematical Models and Methods in Applied Sciences, 2 (2015), pp. 255–282.

[162] K. Sznajd-Weron and J. Sznajd, *Opinion evolution in closed community*, International Journal of Modern Physics C, 11 (2000), pp. 1157–1165.

[163] G. Tadmor, *Receding horizon revisited: an easy way to robustly stabilize an LTV system*, System Control Letters, 18 (1992), pp. 285–294.

[164] G. Toscani, *Kinetic models of opinion formation*, Communications in Mathematical Sciences, 4 (2006), pp. 481–496.

[165] ——, *Continuum models in wealth distribution*, Rendiconti Lincei - Matematica e Applicazioni, (to appear).

[166] F. Vazquez, P. L. Krapivsky, and S. Redner, *Constrained opinion dynamics: freezing and slow evolution*, Journal of Physics A: Mathematical and General, 36 (2003), p. L61.

[167] T. Vicsek, A. Czirok, E. Ben-Jacob, I. Cohen, and O. Shochet, *Novel type of phase transition in a system of self–driven particles*, Physical Review Letters, 75 (1995), pp. 1226–1229.

[168] C. Villani, *On a new class of weak solutions to the spatially homogeneous Boltzmann and Landau equations*, Achive for Rations Mechanics and Analysis, 143 (1998), pp. 273–307.

[169] ——, *A review of mathematical topics in collisional kinetic theory*, Handbook of Mathematical Fluid Dynamics, 1 (2001).

[170] ——, *Optimal transport. Old and New*, vol. 338 of Grundlehren der Mathematischen Wissenschaften [Fundamental Principles of Mathematical Sciences], Springer-Verlag, Berlin, 2009.

[171] D. J. Watts and S. H. Strogatz, *Collective dynamics of 'small–world' networks*, Nature, 393 (1998), pp. 440–442.

[172] G. Weisbuch, *Bounded confidence and social networks*, The European Physical Journal B-Condensed Matter and Complex Systems, 38 (2004), pp. 339–343.

[173] G. Weisbuch, G. Deffuant, and F. Amblard, *Persuasion dynamics*, Physica A: Statistical Mechanics and its Applications, 353 (2005), pp. 555–575.

[174] S. Wongkaew, M. Caponigro, and A. Borzì, *On the control through leadership of the hegselmann–krause opinion formation model*, Mathematical Models and Methods in Applied Sciences, 25 (2015), pp. 255–282.

[175] Y.-B. Xie, T. Zhou, and B.-H. Wang, *Scale–free networks without growth*, Physica A: Statistical Mechanics and its Applications, 387 (2008), pp. 1683–1688.

[176] D. Xiu, *Numerical Methods for Stochastic Computations*, Princeton University Press, 2010.

[177] D. Xiu and G. E. Karniadakis, *The Wiener–Askey polynomial chaos for stochastic differential equations*, SIAM Journal on Scientific Computing, 24 (2002), pp. 614–644.

[178] C. Yates, R. Erban, C. Escudero, I. Couzin, J. Buhl, I. Kevrekidis, P. Maini, and D. Sumpter, *Inherent noise can facilitate coherence in collective swarm motion*, Proceedings of the National Academy of Sciences of the United States of America, 106 (2009), pp. 5464–5469.

[179] H. Zhou, W. Zhou, and W. Zeng, *Flocking control of multiple mobile agents with the rules of avoiding collision*, Mathematical Problems in Engineering, 2015 (2015).

Acknowledgements

I wish to thank my PhD supervisor Prof. Lorenzo Pareschi who continuously taught me during these years and for his fruitful talks, often over of a cup of coffee. Thanks to his guidance I could attend schools and workshops, meeting and sharing ideas with important members of the scientific community worldwide.

Special thanks to Prof. Michael Herty, Prof. José Antonio Carrillo and Prof. Shi Jin who kindly welcomed me in their institutions for my visiting periods in RWTH Aachen University, Imperial College and University of Wisconsin Madison respectively. They gave me the possibility to work on extremely stimulating issues.

Thanks to all my good friends, mathematicians and not. Your warmth helped me to feel like at home in all my pilgrimages.

At last I would like to thank my beloved family for their continuous and immeasurable support during all these years.